DEEP LEARNING AND KNOWLEDGE REPRESENTATION IN BRAIN-INSPIRED SPIKING NEURAL NETWORKS FOR BRAIN-COMPUTER INTERFACES

A thesis submitted to Auckland University of Technology in partial fulfilment of the requirements for the degree of Doctor of Philosophy

By

K V D C Kaushalya Kumarasinghe

School of Engineering, Computer and Mathematical Sciences

July 2021

Supervisors

Prof. Nikola Kasabov

Prof. Denise Taylor

Attestation of Authorship

I hereby declare that this submission is my own work and that, to the best of my knowledge and belief, it contains no material previously published or written by another person nor material which to a substantial extent has been accepted for the qualification of any other degree or diploma of a university or other institution of higher learning.

Signature of candidate

Acknowledgements

As my PhD journey comes to its end, it is my pleasure to acknowledge many people without whom this study would never have been possible.

Firstly, a huge thanks go to my supervisors Prof. Nikola Kasabov and Prof. Denise Taylor, who have provided expert knowledge, insight, guidance, continuous support, and motivation for conducting this research. I greatly appreciate the freedom you have given me to work on something that I am truly motivated for pursuing. Thank you very much for your guidance, insightful comments and encouragement and as well as raising the hard questions which incented me to widen my research from various perspectives. Its been a great privilege to work with both of you.

I would like to express my sincere gratitude to Associate Professor David White and Dr Imran Niazi for reviewing my PhD research proposal. Your valuable inputs, fruitful discussions and constructive feedback have helped to shape this research in many ways. I am also grateful to Dr Neelava Sengupta and Assistant Professor Enmei Tu for their valuable effort in constructing the generic NeuCube framework, which laid the foundation for this research. I would also like to thank my collaborators Dr Mahonri Owen and Dr Chi Kit Au from the University of Waikato for their contributions.

A massive thanks go to my loving husband for his continuous support and encouragement. Thank you very much Asela for being by my side throughout

this whole journey. Without your support, this would never have been a reality. I would also like to thank my loving daughter, Senuli, for all the happiness, joy and hope you brought to our world. Your innocent smiles helped me to stay motivated even during the most challenging situations of this journey. Thank you very much for being such a good little baby during the past two years, and making it possible for me to complete what I started.

My sincere gratitude goes to my parents for bringing me into this world, raising me and giving me a good education. Without your endless support, this could never be possible. PhD is always a challenging journey which I could never succeed without patience, persistence and resilience. Thank you so much for nurturing these attitudes in my life. They really gave me the strength to embrace my failures and learn from them. I believe this thesis is something that you both can be proud of.

A huge thank you goes to my beloved brother, Prabhash, for inspiring me and being a true role model for my life. I am so much grateful for your support, guidance and for encouraging me to set ambitious aims and believing that I could achieve them. Since the day you taught me to write my first source code, you have been there for me whenever I needed support and helped me through the ups and downs of this PhD journey. I wish your PhD journey will be an exciting and enjoyable one too. I would also like to thank my loving sister-in-law, Harshi, for your encouragement, motivation and kind words. We are so lucky to have as our family member.

I am immensely grateful to Brittany, Thisara, June and Gary for your valuable effort in proofreading this thesis. A special thanks go to all my colleagues at the Knowledge Engineering and Discovery Research Institute and the Rehabilitation Innovation Centre at the Auckland University of Technology for the fruitful discussions, support, encouragement and all the fun we have had in the last

four years. Thank you very much for listening to my ideas and giving me constructive comments for shaping my research. My sincere gratitude goes to all the administrative staff of AUT, especially to Joyce, Karishma, Jenney, Jessica and all staff members of the Graduate Research School for their continuous administrative support.

This acknowledgment is incomplete without a mention of my high school Biology teacher, Mrs Ilendra. Thank you very much for giving me the first motive while you were teaching an inspiring lesson on the human nervous system about fifteen years ago. That was the starting point of this long journey. I thank you for being such an amazing teacher and for all your great lessons that enlighten my life in many aspects.

My sincere gratitude goes to all the academic staff of the Faculty of Information Technology at the University of Moratuwa. Particularly, I would like to thank Dr Lochandaka and Mr Withanage for their advice and encouragement to pursue PhD studies.

Last but not least, I would also like to thank all my friends and family here in New Zealand and back in Sri Lanka for their continuous encouragement, motivation and support for achieving this milestone of my life.

Dedication

To all courageous minds

who are ambitious to turn their disabilities into an ability

To those who believe in science

To turn the impossibilities into a reality

To my loving parents

who brought me into this world, raised me and gave me a good education

To all my teachers

who inspired me, enlighten me and helped me to reach my ambitious goals

To those heroes

who sacrificed their lives to leave us a peaceful tomorrow

And to everybody else

who make this world a beautiful place...

Abstract

Brain-Computer Interfaces aim at decoding neural commands from neurological signals and translate them into machine commands for manipulating digital devices. It provides a way of bypassing affected neural pathways in people with movement impairments. A growing body of literature on non-invasive Brain-Computer Interfaces for motor recovery and restoration highlights the need for improving the machine learning methods that decode neural activity from EEG signals. The low accuracy in decoding movements of the same limb, less biological plausibility, lack of interpretability, high prediction latency, low degree of freedom are some of the significant drawbacks in existing machine learning models used in restorative Brain-Computer Interfaces.

This thesis proposes a Brain-Inspired Spiking Neural Network (BI-SNN) model for incremental learning of spike sequences from stochastic data streams as a promising step towards developing intelligent machines for Brain-Computer Interfaces. The proposed BI-SNN is a generic SNN architecture that can be applied for the predictive modelling of spatio-temporal data streams. Here it was applied to construct an interpretable neural decoder which can incrementally learn spike sequences from Electroencephalography signals. The thesis suggests that the proposed Spiking Neural Network approach results in a better neural decoder compared to the traditional machine learning approaches used by restorative BCIs in multiple aspects. The thesis proposes two spike-based learning algorithms that

extended the generic NeuCube SNN framework to address seven research questions. A series of experiments were performed to address these research questions and to benchmark the model performance with multiple machine learning models.

In the first study, the thesis demonstrates the feasibility of proposed eSPANNet learning algorithm to learn complex spike sequences from stochastic data streams. As an evolving model, the eSPANNet does not require certain predefined parameters related to network architecture, such as the number of neurons in the hidden layer, as it evolves neurons if needed. In the second study, the thesis presents a theoretical framework, algorithmic pipeline and associated software for representing and extraction of deep knowledge from Spiking Neural Networks for enhancing the interpretability of SNN. In the third study, the thesis integrates the proposed learning algorithms with the generic NeuCube SNN framework for constructing a novel Brain-Inspired Brain-Computer Interface.

The thesis revealed that the integration of eSPANNet with the NeuCube SNN architecture could gain a higher accuracy than the standalone sensor-space eSPANNet architecture. The study benchmarked the performance of the proposed learning algorithms and showed a statistically significant improvement in prediction accuracy than several machine learning methods. The thesis has shown the feasibility of extracting neural information that contributes to controlling a wide range of motor parameters such as muscle activity and joint kinematics from Electroencephalography using the proposed BI-SNN in healthy people.

In conclusion, this approach has shown the potential to construct an interpretable neural decoder which can incrementally learn to predict complex movements in real-time from Electroencephalography. This study is one of the first attempts to examine the feasibility of finding neural correlates of muscle activity and kinematics from Electroencephalography using a brain-inspired computational paradigm.

Publications

- **Kumarasinghe, K.**, Kasabov, N., & Taylor, D. (2020). Deep learning and deep knowledge representation in Spiking Neural Networks for Brain-Computer Interfaces. Neural Networks, 121, 169-185. doi: https://doi.org/10.1016/j.neunet.2019.08.029

- **Kumarasinghe, K.**, Kasabov, N., & Taylor, D., Brain-Inspired Spiking Neural Networks for Decoding and Understanding Muscle Activity and Kinematics from Electroencephalography Signals during Hand Movements, Sci Rep 11, 2486 (2021). doi: https://doi.org/10.1038/s41598-021-81805-4, URL:https://www.nature.com/articles/s41598-021-81805-4

- **Kumarasinghe, K.**, Kasabov, N., & Taylor, D., Evolving Spike Pattern Association Neural Networks and Applications for Non-invasive Brain-Computer Interfaces - IEEE Transactions on Biomedical Engineering (under review)

- **Kumarasinghe, K.**, Taylor, D., & Kasabov, N. (2019, July). eSPAN-Net: Evolving Spike Pattern Association Neural Network for Spike-based Supervised Incremental Learning and Its Application for Single-trial Brain-Computer Interfaces. In 2019 International Joint Conference on Neural Networks (IJCNN). IEEE. doi: 10.1109/IJCNN.2019.8852213

- **Kumarasinghe, K.**, Owen, M., Taylor, D., Kasabov, N., & Kit, C. (2018, May). FaNeuRobot: A Framework for Robot and Prosthetic Control Using the NeuCube Spiking Neural Network Architecture and Finite Automata Theory. In 2018 IEEE International Conference on Robotics and Automation (ICRA). IEEE. doi: 10.1109/ICRA.2018.8460197

- Sengupta, N., Ramos, J. I. E., Tu, E., Marks, S., Scott, N., Weclawski, J., Gollahalli, A.R., Doborjeh, M.G., Doborjeh, Z.G., **Kumarasinghe, K.** and Breen, V. (2018). From von Neumann Architecture and Atanasoffs ABC to Neuro-Morphic Computation and Kasabov's NeuCube: Principles and Implementations. In Learning Systems: From Theory to Practice (pp. 1-28). Springer, Cham.

- Doborjeh, M. G., Doborjeh, Z. G., Gollahalli, A. R., **Kumarasinghe, K.**, Breen, V., Sengupta, N., Ramos, J.I.E., Hartono, R., Capecci, E., Kawano, H. and Othman, M., (2018). From von Neumann Architecture and Atanasoff's ABC to Neuromorphic Computation and Kasabov's NeuCube. Part II: Applications. In Practical Issues of Intelligent Innovations (pp. 17-36). Springer, Cham.

Contents

List of Tables

List of Figures

List of Abbreviations

- AD : Anterior deltoid
- AI : Artificial Intelligence
- ALS : Amyotrophic lateral sclerosis
- ANN : Artificial Neural Networks
- ANOVA : Analysis of variance
- AUC : area under curve
- B : Brachioradialis
- BCI : Brain-Computer Interface
- BI-BCI : Brain-Inspired Brain-Computer Interface
- BI-SNN : Brain-Inspired Spiking Neural Networks
- BMI : Brain-Machine Interface
- BSA : Bens Spiker Algorithm
- CDBN : Convolutional Deep Belief Network
- CED : common extensor digitorum
- CNN : Convolutional Neural Networks
- DBN : Deep Belief Network
- deSNN : dynamic evolving Spiking Neural Network
- DT : Decsion Trees
- ECoG : Electrocorticography
- EEG : Electroencephalography

- ELM : Extreme Learning Machine
- EMG : Electromyography
- ERP : Event Related Potential
- ErrP : Error-related Potential
- ERS : Event Related Synchronisation
- eSPANNet : evolving Spike Pattern Association Neural Network
- FD : Flexor Digitorum
- FDI : First Dorsal Interosseous
- FEF : Frontal Eye Field
- FES : Functional Electric Stimulation
- FIR : Finite Impulse Response
- fMRI : functional Magnetic Resonance Imaging
- FNR : False Negative Rate
- FPR : False Positive Rate
- GAL : Grasp and Lift
- GLM : Generalised Linear Model
- GPU : Graphical Processing Unit
- ICA : Independent Component Analysis
- ILC : Iterative Learning Control
- ITA : Inferior Temporal Area
- kNN : k Nearest Neighbor
- LDA : Linear discriminant analysis
- LFP : Local Field Potentials
- LIF : Integrate-and-Fire neuron
- LSL) : Lab Streaming Layer
- LSTM : Long short-term memory

- LTD : Long-Term Depression
- LTP : LongTerm Potentiation
- MEG : Magnetoencephalography
- MI : Motor Imagery
- MLP : Multi Layer Perceptron
- MNI : Montreal Neurological Institute
- MRCP : Movement-Related Cortical Potential
- MW : Moving-Window (MW)
- PCA : principal component analysis
- PMC : Primary Motor Cortex
- PSC : Primary Somatosensory Cortex
- PSTH : Peri Stimulus Time Histogram
- RBM : Restricted Boltzmann Machines
- RMSE : Root Mean Square Error
- RNN : Recurrent Neural Networks
- RQ : Research Question
- SAA : Somatosensory Association Area,
- SF : Step-Forward (SF)
- SMA : Supplementary Motor Area,
- SNN : Spiking Neural Networks
- SNR : Signal to Noise Ratio
- SPAN : Spike Pattern Association Neuron
- SSVEP : Steady-state visual evoked potential
- STDP : Spike Time Dependent Plasticity
- STDP : Spike Time Dependent Plasticity
- SVM : Support Vector Machine

- TB : Threshold-Based
- TPR : True Positive Rate
- V1 : Primary Visual Cortex
- V2 : Secondary Visual Cortex
- VLSI : Very large-scale integration
- WA : Wernicke's area

Chapter 1

Introduction

"Artificial intelligence is the science of making machines do things that would require intelligence if done by men"

Marvin Minsky - A co-founder of the field of Artificial Intelligence, one of the leading contributors of early neural networks, and the theories of human and machine cognition

Chapter Overview

This thesis presents a Brain-Inspired Spiking Neural Network model for constructing an interpretable neural decoder for Brain-Computer Interfaces for incremental learning of spike sequences extracted from Electroencephalography signals. The thesis argues that the proposed Spiking Neural Network approach results in a better neural decoder compared to the traditional machine learning approaches for non-invasive Brain-Computer Interfaces. This chapter introduces the research problem, background, motivation and rationale of the research. The chapter then describes the aim and objectives of the thesis and the research questions addressed by the thesis. Then, a brief overview of the research is described. Finally, the

primary outcomes, contributions and outputs of the research delivered by this thesis are presented at the end of this chapter.

1.1 Motivation

Neurological signals such as Electroencephalography (EEG), Electrocorticography (ECoG), and functional Magnetic Resonance Imaging (fMRI) indicate the neural responses of the brain's neural network that elicit in response to sensory, motor or cognitive events. Brain-Computer Interfaces (BCI) aim at decoding the neural activity from neurological signals and translate it into machine commands for manipulating digital devices. Development of accurate, efficient and effective neural decoders that are capable of decoding continuous sensory, motor and cognitive events from neurological signals is a fundamental problem in developing Brain-Computer Interface systems.

The statistics from the World Health Organization show that every six seconds, someone in the world becomes physically disabled due to a stroke (The Internet Stroke Center, n.d.). Every year, there are about 9000 new stroke cases in New Zealand, and about 60000 New Zealanders live with the consequences of stroke (Stroke Foundation NZ, n.d.). About ten million people on the earth suffer from the consequences of limb amputation (WHO, 2017). Many are disabled and need support for carrying out the activity in their daily living.

BCI's can be used to control digital devices through the users' thoughts decoded from neurological signals without direct physical contact with the device. Thus, BCI enables manipulation of assistive devices such as exoskeletons, prosthetic limbs, or wheelchairs through the mental commands of the user. It has previously been shown that BCI is a promising intervention to improve motor recovery after stroke (Taylor et al., 2015). BCI is a potential approach for improving the quality of life of motor-impaired people.

Efforts have recently started to translate BCI-based rehabilitation technologies from laboratory to real-world applications (Mak & Wolpaw, 2009; Reardon, 2016).

Compared to the invasive neurological signals such as Electrocorticography and Local Field Potentials, Electroencephalography monitors the neural activity of the brain non-invasively, less expensively and under a minimal risk. Compared to other non-invasive recording methods such as functional Magnetic Resonance Imaging, EEG monitors the brain activity at a higher temporal resolution. Therefore, EEG demonstrates a higher potential for implementing neural decoders for BCI applications which suits for every-day life.

The human brain is organised according to different areas that are specialised to perform specific tasks. The brain dynamics during a cognitive task, such as grasping an object, is distributed across multiple areas of the brain in a spatio-temporal manner, rather than being isolated to a specific brain area (Roland, 1984; Milner et al., 2007). To date, conventional electroencephalography-based non-invasive BCI decoders have demonstrated the feasibility of decoding several cognitive tasks by using the response of a specific brain area for an observed stimulus. For instance, Movement Related Cortical Potentials (MRCP), which can be observed from the motor cortex, have been used by BCI's for neurorehabilitation (I. Daly et al., 2018; Lisi et al., 2018; Jochumsen et al., 2015). The Error-related Potentials (ErrP) which are likely to be generated in the Anterior Cingulate Cortex and the Dorsolateral Prefrontal Cortex (Chavarriaga & Millán, 2010; Holroyd et al., 2004; Hester et al., 2005) have been used for error correction and adaptation in assistive BCI's. Several studies have reported the feasibility of using ErrPs to manipulate assistive robots (Perrin et al., 2010). Another example is the use of evoked potentials such as the p300 EEG potentials recorded from the occipital lobe in assistive BCI's that aid communication for language-impaired people.

Neurological disorders such as stroke and spinal cord injury can result in movement impairments, and Brain-Computer Interfaces can assist or restore those affected motor functions. The goal of assistive BCIs such as wheelchairs and

communication support devices controlled through BCI is to replace the lost motor functions. The accurate multi-class classification that improves the degrees of freedom of the assistive control and quick prediction are the main challenges for assistive BCIs. On the other hand, restorative BCIs such as neuroprosthesis, Functional Electric Stimulation and robotic exoskeletons controlled through BCI, aims at recovering the affected movements. They facilitate motor re-learning by strengthening the affected neural pathways and building alternative pathways by inducing neuroplasticity of the brain (Bauer & Gharabaghi, 2017; Gharabaghi, 2016).

An integrated involvement of the mechanical elements of the limb and the associated neural circuitry that is responsible for related sensory, motor and cognitive functions, contribute to the execution of movements in animals. The feasibility of revealing the complex brain dynamics that represent the underlying sensory, motor and cognitive processes in the brain that generate complex functional movements is challenging. It is even more challenging to develop methods to effectively use such knowledge for predictive modelling of the dynamic behaviour from neurological signals. However, if successfully harnessed, such computational models will improve the state-of-the-art in restorative Brain-Computer Interfaces.

The computational models that can decode precise neuro-muscular relationships from EEG signals will enhance the restorative BCI applied in neurorehabilitation and prosthetic control. Several recent studies report the feasibility of extracting neuro-muscular interactions from EEG signals during functional upper limb movements (Pirondini et al., 2017; Yoshimura et al., 2017; Artoni et al., 2016). These studies evidence the feasibility of extracting neural activity from EEG signals useful to control and manipulate objects through non-invasive BCIs.

The traditional approach for constructing neural decoders for BCI's consist of several steps such as pre-processing the neurological signals, feature extraction

and selection (Koprinska, 2009), predict neural activity through classification, clustering or regression analysis and generating control commands to manipulate the intended digital device through BCI. The common feature extraction methods used in BCI are Power Spectrum Density analysis, Common Spatial Pattern Analysis, Independent Component Analysis, Riemannian Geometry, EEG source localisation-based methods, wavelet transformation (Vargic et al., 2015; Y.-H. Liu et al., 2013; R. Upadhyay et al., 2013; Lan et al., 2010). Convolutional Neural Networks, Support Vector Machine, Linear Discriminant Analysis, k-Nearest Neighbour are commonly used to predict neural activity from the extracted features (Trofimov et al., 2012; Y. Zhang, Liu et al., 2017). These human-engineered Artificial Intelligence systems contradict what is already known about information processing in the animal brain. They cannot evolve, learn incrementally or adapt to changes in the environment, require large amounts of labelled data to train, yet can fail catastrophically even with small variations of the input. The complex machine learning models used for decoding neural activity into machine commands in BCI can significantly increase prediction latency and limit their feasibility for real-time prediction. Most of the current machine learning methods that decode neural activity from neurological signals perform batch learning and do not have the ability of incremental and adaptive learning. These limitations influence the development of a Brain-Inspired Artificial Intelligence (BI-AI) approaches to address the weaknesses in current AI systems.

1.2 Research Problem

The development of computational models that can precisely decode the neuro-muscular relationships from EEG signals in real-time is a significant problem in developing neural decoders for restorative Brain-Computer Interfaces. The low

spatial resolution and the volume conductance effect of EEG limit the feasibility of distinguishing less spatially distributed neural activity of the brain, such as different movements of the same limb (Edelman et al., 2015). To address the above limitation, the conventional neural decoders that utilise the sensorimotor rhythms of electroencephalography signals generate distinct neural commands through Event-Related Synchronisation and Event-Related Desynchronisation that evoke as a result of moving different parts of the body. However, this approach results in un-naturalistic control in restorative BCIs due to the cognitive disconnection between the targeted and intended action.

The lack of interpretability of computational models used for decoding neural activity is another limitation in many BCIs that use less-interpretable machine learning approaches such as Support Vector Machine (SVM), Linear Discriminant Analysis (LDA), Generalised Linear Models (GLM), Independent Component Analysis (ICA), and deep Convolutional Neural Networks (CNN). These approaches result in BCIs that often behave as 'black boxes'. They do not allow opportunities to extract new knowledge for a better understanding of the cognitive processes when interacting with the BCIs. Besides, the lack of interpretability limits the feasibility of using known knowledge of the cognitive processes in neuroscience for improving computational models.

Through neurorehabilitation, it is expected that the patients will incrementally learn to regain the affected movements. Changes to the neuronal activation patterns during neurological recovery was reported in several brain connectivity analysis studies (Canuet et al., 2015; Ochoa et al., 2014; Westlake & Nagarajan, 2011). Therefore, the supportive computational technologies used in such neurorehabilitation settings such as BCI should be able to adapt to these physiological changes that happen during neurorehabilitation (Cella et al., 2014). On the other hand, to optimise motor learning, the patient's voluntary involvement in the task

should be enhanced by carefully controlling the amount of support during the neurorehabilitation task (Freeman et al., 2012; Grimm et al., 2016). The ability to learn incrementally and adaptively are essential for machine learning methods applied in rehabilitation applications.

Multiple clinical studies have shown promising outcomes of using Brain-Computer Interface technology to induce functional recovery after stroke. A systematic review presented in (Bai et al., 2020) highlighted that the use of BCIs has significant immediate effects on improving hemiparetic upper extremity function in patients after stroke. The review also pointed out that BCIs combined with functional electrical stimulation can result in a better functional recovery than other neurofeedback approaches. The increased recovery of affected movements using BCI interventions coupled with FES may be attributed to the activation of the cortical network related to motor control. Further, the review has also indicated that the attempted movements appear more effective than imagined movements. It is essential to perform extensive randomised control trials and clinical-based trials with BCI-based interventions to prove the immediate and long-term effects of the intervention. BCI-based interventions need to be translated into smaller, lightweight, wireless devices. There is a need for enhancing the ability to personalise the technology to improve the translational aspects of the intervention. These improvements can lead to the development of portable clinical or home-based personalised intervention protocols (Remsik et al., 2016).

1.3 Rationale

Computational approaches that mimic the biological processes of living nervous systems have provided new insights into Artificial Intelligence. Recent literature reveals several brain-inspired computational models that aim to model complex

brain dynamics, leading to a better understanding of information representation and processing in the brain, and computationally interpret the natural mechanisms of learning and adaptation in animals in Artificial Intelligence systems (N. K. Kasabov, 2014; Markram, 2006, 2012; Furber, 2016; Hawkins et al., 2019; Reimann et al., 2017).

Artificial Neural Networks (ANN), as a sub-set of AI, present mathematical and computational representation of neurons and neural network of the brain. Deep Convolutional Neural Networks are successfully applied for prediction in AI systems (LeCun et al., 2015; Goodfellow et al., 2016); however, they result in static vector-based learning of input data. These vector-based models use fixed structures of neurons that require many layers of classic hierarchical abstraction to achieve a statistically significant accuracy. The lack of interpretability of knowledge gained through learning and the less capability for reasoning makes them vulnerable to failures (Deng, 2018).

Many machine learning methods require a large amount of training data to build an accurate machine learning model. Humans, on the other hand, are fast learners. Humans can learn quickly using few training samples and through a less number of repetitions in most situations. Although machine learning has become a rapidly growing approach for problem-solving in every-day life, this contradiction is a barrier to embed human-like intelligence in machines. Spiking Neural Networks as the third generation of ANN, more closely model the behaviour of a living nervous system as it considers both spatial and temporal aspects of input data for building the computational model. Brain-inspired machine learning models such as Spiking Neural Networks, which are inspired by how the animal brain processes information, represents knowledge, learn through experience and adapts over time through errors and rewards, provides a new approach to eliminate these limitations in conventional machine learning methods.

Neuroprosthesis can also be a small implant placed on the partially injured neural pathways (proximally injured and distally intact pathways) in the limbs to aid the communication between the cortex and peripheral neuromuscular pathways. Different control strategies can be utilised to control the neuroprosthesis, such as open-loop/feedforward, close-loop/feedback or adaptive control (Wright et al., 2016).

The open-loop control only generates commands to produce the expected output by the neuroprosthesis. This control strategy does not utilise a mechanism to measure the error (difference between the expected and actual output). Therefore open-loop control can not optimise the model in order to minimise the error. Many studies that demonstrated the feasibility of the Brain-Computer Interface to manipulate neuroprosthesis utilise the open-loop control strategy. However, different parts of the human body operate through complex closed-loop control. It is also possible that the control may be under multiple loops that govern different physiological aspects of the body at different time scales. Therefore, it is essential to incorporate the closed-loop control in neuroprosthesis.

The closed-loop control requires the inclusion of sensors in the system under control. The closed-loop systems produce the command for controlling the neuroprosthesis, but they also utilise the sensors to measure the actual output in response to the control command. Therefore, closed-loop systems have a mechanism to evaluate the difference between actual and expected output and optimise the model to minimise the error.

The proposed Brain-Inspired Brain-Computer Interface is a promising approach to establishing the bi-directional information flow for neuroprosthetic control to enable closed-loop control. The thesis shows that the proposed BI-SNN can accurately predict the relationship between the brain activity measured non-invasively through EEG signal and the activity of the end-effector, such as the

activity of individual muscles that contribute to generate the output of the end-effector. This corresponds to the forward path of the closed-loop control. At the same time, the model can also utilise information travel from the peripheral to the central nervous system, such as the information from the sensory receptors, which corresponds to the feedback path of the closed-loop control.

1.4 Aim and Objectives of the Research

1.4.1 Aim

This thesis proposes a novel Brain-Inspired Spiking Neural Network (BI-SNN) model for incremental learning of spike sequences from spatio-temporal data. It enables the discovery of polychronising spiking neuron populations that are correlated with the predicted task using spike-time based learning rules. The proposed BI-SNN is a generic SNN architecture that can be applied for the predictive modelling of spatio-temporal data streams. Here it is applied to predict muscle activity and kinematics from EEG during the various human activity, which is useful for restorative Brain-Computer Interfaces.

1.4.2 Objectives

The research set-up the following objectives to achieve the above aim.

1. Develop a spike-based learning method for incremental learning of spike sequences from electroencephalography signals for online event prediction

2. Develop a knowledge representation framework to evaluate the feasibility of the NeuCube SNN architecture to map spiking activity from EEG sensor-space into the structural and functional regions of interest in the brain

3. Develop a method to extract neural trajectories from Brain-Inspired SNN architectures to improve the interpretability of the machine learning model and increase understanding of the information representation in the model as deep spatio-temporal rules

4. Extend the generic NeuCube SNN framework by integrating the proposed spike sequence learning and knowledge representation algorithms to improve the evolution of polychronising spiking neuron populations for spike sequence learning

5. Conduct a comparative analysis of the proposed Brain-Inspired Spiking Neural Network with the other state-of-the-art machine learning methods commonly used in BCI for benchmarking the performance of the proposed method

6. Develop prototypes and conduct proof-of-concept studies to demonstrate in principle the applicability of the proposed Brain-Inspired Brain-Computer Interface in real-world restorative BCI applications

The proposed research intends to address several limitations in the current restorative BCI research such as the less prediction accuracy, less interpretability, long temporal averaging of input data that limit the feasibility of real-time prediction and the batch-learning based training of the neural decoder that increase the calibration time of BCI.

1.5 Research Questions

The thesis addresses the following research questions. A detailed description on each research question is presented in section 4.2.

1.5.1 Generic research questions for online event prediction from spatio-temporal data

The proposed Brain-Inspired Spiking Neural Network is a generic method which can be used for predictive modelling of spatio-temporal data streams. The research addresses the following generic research questions (RQs).

- RQ1: How can the Spike Pattern Association Neuron (SPAN) be extended to develop an incremental spike sequence learning model for online event prediction from spatio-temporal data streams?
- RQ2: How can the network architecture of the eSPANNet learning model be improved to enhance its convergence and the prediction performance when learning from non-stationary stochastic data streams such as Electroencephalography?
- RQ3: Based on the abilities of SNN for deep learning, can SNNs be used to construct an interpretable machine learning model that represents deep knowledge as spatio-temporal rules?

1.5.2 Specific research question for addressing the limitations of non-invasive BCI for motor recovery and restoration

This thesis applies the proposed generic learning algorithms to construct a novel Brain-Inspired Brain-Computer Interface that can address several limitations in the current restorative BCIs for neurorehabilitation and prosthetic control. The proposed learning algorithms that address the above generic research questions will be applied to multiple case-studies.

- RQ4: How does the eSPANNet learning model compare with the static rate-based machine learning methods (such as the Convolutional Neural Networks and Support Vector Machine) and as well as the sequence learning-based machine learning methods (such as the Recurrent Neural Networks, linear regression and SVM-based regression) for predicting movement intention from EEG signals?

- RQ5: How can the NeuCube SNN architecture be improved in order to enable continuous control of a prosthetic hand from EEG signals?

- RQ6: Does the Brain-Inspired Spiking Neural Network model that integrates the eSPANNet with the NeuCube SNN architecture result in higher prediction accuracy than the pure eSPANNet learning model for predicting continuous movements from EEG signals?

- RQ7: How do the Brain-Inspired Spiking Neural Networks and the non-Brain-Inspired machine learning models compare in terms of their ability for sequence prediction, interpretability, and incremental learning to predict complex movements from EEG signals useful for motor recovery and restoration through Brain-Computer Interfaces?

1.6 Overview of the Research

The 'population vector' model initially proposed and experimentally validated by Georgopoulos (A. P. Georgopoulos et al., 1983) describes how the neurons in the motor cortex are trained to perform movements in different directions. It was observed that each neuron in the population demonstrated a preferred direction of movement, and the firing rate of the neurons was increased when the corresponding stimulation was presented. Using the principles of Evolving

Connectionist Systems (ECoS), this research proposes a novel computational model inspired by the concept of population vectors in the brain. It presents a spike-based supervised and incremental learning model to learn polychronising spiking neuron populations in Brain-Inspired Spiking Neural Network architectures. The thesis evaluates the feasibility of the proposed Brain-Inspired SNN to decode neural correlates of muscle activity and kinematics from EEG signals. The proposed research aims at developing a novel type of neural decoder for Brain-Computer Interfaces that enable incremental learning to detect polychronising spiking neuron populations.

This research is based on the generic NeuCube Spiking Neural Network framework (N. Kasabov, 2012; N. K. Kasabov, 2014; N. Kasabov et al., 2016; N. K. Kasabov, 2018) for mapping, learning, predicting, interpreting and understanding brain dynamics from spatio-temporal brain data. The NeuCube consists of a reservoir of spiking neurons placed in a 3-dimensional space according to a brain atlas. The SNN approximately maps the encoded spiking activity from sensor-space into regions of interest in the brain represented by spiking neural clusters placed in the 3-dimensional space. The reservoir of spiking neurons evolve through spike-time based learning rules (Gerstner et al., 1996; Markram & Tsodyks, 1996). The thesis shows the feasibility of such spatio-temporal distribution to map the EEG channel activity from sensor-space into structural and functional regions of interest in the brain.

The research extends the Spike Pattern Association Neuron (SPAN) model (Mohemmed, Schliebs & Kasabov, 2011; Mohemmed, Schliebs, Matsuda & Kasabov, 2011; Mohemmed & Kasabov, 2012; Mohemmed, Lu & Kasabov, 2012; Mohemmed, Schliebs et al., 2012; Mohemmed et al., 2013) and proposes a spike-based incremental spike sequence learning model called evolving Spike Pattern Association Neuron. This model aims to learn complex spatio-temporal spike

sequences from streaming data. SPAN is a spiking neuron model which can emit spikes at the desired time point. It can associate arbitrary spike trains allowing the processing of spatio-temporal information encoded in the precise temporal order of spikes. eSPANNet is integrated as the output layer of NeuCube SNN architecture to enable incremental learning of spike sequences. The integration of the eSPANNet as the output layer of the NeuCube enables the association of temporally correlated spiking activity in distinct brain areas with the output layer of the BI-SNN. The research was conducted under the following three stages.

1.6.1 Stage 1: Development of learning algorithms

This stage of the research aims at designing and constructing brain-inspired machine learning algorithms to address the highlighted limitations of the non-invasive Brain-Computer Interfaces. The thesis proposes the following three generic spike-based learning methods.

1. The eSPANNet computational model is proposed as a spike-based generic learning model for online event prediction from spatio-temporal data streams. The proposed model extends the traditional batch learning of the SPAN.

2. The knowledge representation algorithm is proposed as a spike-based generic method for the extraction of deep knowledge in Brain-Inspired Spiking Neural Network architectures and enhance the interpretability of the machine learning model.

3. The above generic methods are integrated with the NeuCube SNN framework to develop the Brain-Inspired SNN architecture that constructs an interpretable machine learning model for predictive modelling of spatio-temporal brain data. It enables incremental learning of complex spike sequences and constructs a novel type of Brain-Inspired neural decoder.

1.6.2 Stage 2: Proof of concept and the development of software prototypes

This stage of the research aims at implementing the proposed generic algorithms as software prototypes. Proof of concept studies will be conducted to verify in principle the practical potential of the proposed theoretical concepts and learning algorithms. The learning algorithms were implemented using MATLAB programming language on a conventional personal computer. The embedded system that translates the neural activity into machine commands for controlling rehabilitation devices is implemented using the Arduino programming language. The proof of concept studies are conducted using publicly available datasets,

1. to demonstrate the feasibility of accurate and incremental learning of spike sequences by the eSPANNet computational model and,

2. to evaluate the feasibility of extracting deep knowledge in Brain-Inspired Spiking Neural Network architectures as neural trajectories represented in the form of deep spatio-temporal rules.

1.6.3 Stage 3: Experimental Validation

This stage aims at experimentally validating the proposed Brain-Inspired Brain-Computer Interface. The proposed BI-SNN is experimentally validated using publicly available datasets, and appropriate statistical tests are performed to evaluate the statistical significance of the results. The thesis also presents a preliminary study on online controlling of a prosthetic hand through the proposed SNN-based Brain-Computer Interface approach.

1.7 Structure of the thesis

This thesis contains ten chapters structured under four main sections. Figure 1.1 depicts the structure of the thesis and the interconnections of the chapters (the bird's eye view of the thesis).

1.7.1 Section 1: Overview

This section consists of three chapters that present an overview of the research. The first chapter presents an overview of the thesis. A comprehensive literature review on the restorative BCI, the challenges, limitations and future research directions of non-invasive BCI applied for motor recovery and restoration is presented in the second chapter. Chapter 3 presents a detailed description of brain-inspired computational methods with a particular focus on their applications in constructing neural decoders for BCI. The chapter also presents an overview of the proposed Brain-Inspired Brain-Computer Interface. Chapter 4 describes the overview of the proposed methodology.

1.7.2 Section 2: Proposed generic methods and algorithms for Spiking Neural Networks

The second section of the thesis consists of three chapters that present the proposed spike-based generic methods for constructing interpretable, spike-based incremental learning model for online event prediction from spatio-temporal data. Chapter 5 introduces the evolving Spike Pattern Association Neural Network (eSPANNet). It presents the evolving SNN architecture and the learning algorithms for constructing the model. The chapter also presents a proof of concept study of the eSPANNet using a publicly available dataset.

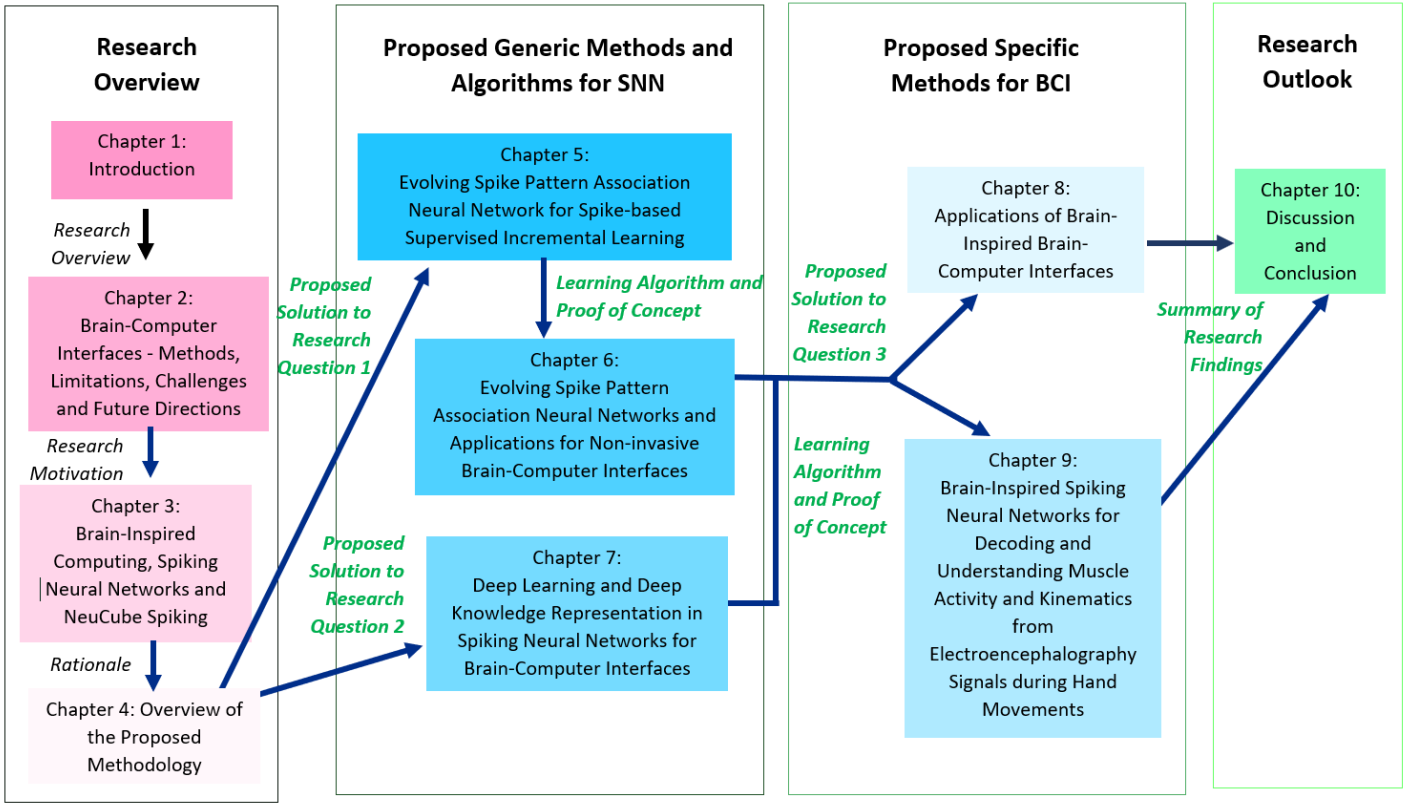

Figure 1.1: Structure of the thesis (bird's eye view) and the interconnections among the chapters

Chapter 6 extends the eSPANNet network architecture and presents a case study on movement intention from EEG signals. The proposed generic algorithms for knowledge representation and extraction in Brain-Inspired Spiking Neural Network architectures is presented in chapter 7.

1.7.3 Section 3: Proposed Brain-Inspired methods for restorative Brain-Computer Interfaces

This section consists of two chapters that present a Brain-Inspired Brain-Computer Interface (BI-BCI) for addressing the limitations in current BCI research highlighted in the second chapter. A proof of concept study on evaluating the feasibility of the proposed spike-based BCI for prosthetic control is presented in chapter 8. Chapter 9 presents the proposed BI-BCI that integrates the proposed knowledge representation algorithms and the spike-based incremental sequence learning model with the generic NeuCube SNN framework. The chapter also presents the experimental validation of the proposed BI-BCI through a case study on predicting muscle activity and hand kinematics during grasp and lift movements.

1.7.4 Section 4: Outlook

The final section of the thesis presents a summary of the findings and outcomes of the research. Chapter 10 presents a general discussion of the research, scientific contributions of the research, the limitations of the research, the research outcomes and concludes the findings.

1.8 Contributions of the Research

This research makes the following contributions.

1.8.1 Identification of the limitation in existing restorative BCI research

The thesis presents a comprehensive literature review on the restorative Brain-Computer Interfaces that utilise electroencephalography signals to decode movements applicable in motor recovery and restoration interventions. The thesis highlights several challenges specific to decoding neural activity in restorative BCIs from EEG and emphasis on the necessary improvements in machine learning methods used for decoding neural activity in order to address those limitations.

1.8.2 Development of learning algorithms

This thesis delivers two generic learning algorithms for spike-based supervised learning for online event prediction from spatio-temporal data streams. The proposed algorithms enable incremental learning of spike-sequences and enhance the interpretability of the machine learning model compared to the conventional less-interpretable 'black-box' type machine learning models. These generic methods construct a novel type of Brain-Computer Interface for addressing the highlighted limitations of the existing restorative BCI research.

1.8.3 Implementation of software prototypes of the proposed computational models

The thesis presents the implementation of the proposed generic methods and software prototypes of the proposed Brain-Inspired Brain-Computer Interface system using the MATLAB programming language.

1.8.4 Experimental validation through case studies

This research validates the proposed computational models through several case studies using publicly available neurological datasets. The thesis also presents a laboratory-based preliminary study on validating the feasibility of the proposed BI-BCI for online control of a prosthetic hand.

1.8.5 Knowledge dissemination through scientific publications, demonstrations and talks

The findings of this research are disseminated through the following media.

Journals

- **Kumarasinghe, K.**, Kasabov, N., & Taylor, D. (2020). Deep learning and deep knowledge representation in Spiking Neural Networks for Brain-Computer Interfaces. Neural Networks, 121, 169-185.doi:https://doi.org/10.1016/j.neunet.2019.08.029

- **Kumarasinghe, K.**, Kasabov, N., & Taylor, D., Brain-Inspired Spiking Neural Networks for Decoding and Understanding Muscle Activity and Kinematics from Electroencephalography Signals during Hand Movements, Scientific Reports 11, 2486 (2021). doi: https://doi.org/10.1038/s41598-021-81805-4, URL:https://www.nature.com/articles/s41598-021-81805-4

- **Kumarasinghe, K.**, Kasabov, N., & Taylor, D., Evolving Spike Pattern Association Neural Networks and Applications for Non-invasive Brain-Computer Interfaces, IEEE Transactions on Biomedical Engineering (under review)

Conference Proceedings

- **Kumarasinghe, K.**, Taylor, D., & Kasabov, N. (2019, July). eSPAN-Net: Evolving Spike Pattern Association Neural Network for Spike-based Supervised Incremental Learning and Its Application for Single-trial Brain-Computer Interfaces. In 2019 International Joint Conference on Neural Networks (IJCNN). IEEE.doi:10.1109/IJCNN.2019.8852213

- **Kumarasinghe, K.**, Owen, M., Taylor, D., Kasabov, N., & Kit, C. (2018, May). FaNeuRobot: A Framework for Robot and Prosthetic Control Using the NeuCube Spiking Neural Network Architecture and Finite Automata Theory. In 2018 IEEE International Conference on Robotics and Automation (ICRA). IEEE.doi:10.1109/ICRA.2018.8460197

Demonstrations

- A video demonstration on controlling a prosthetic hand described in the conference paper - 'FaNeuRobot: A Framework for Robot and Prosthetics Control Using the NeuCube Spiking Neural Network Architecture and Finite Automata Theory' presented at the IEEE International Conference on Robotics and Automation (ICRA) 2018 is available from the following URL. https://www.youtube.com/watch?v=cLqtUoBjJWs&t=18s

Book Chapters

- Sengupta, N., Ramos, J. I. E., Tu, E., Marks, S., Scott, N., Weclawski, J., Gollahalli, A.R., Doborjeh, M.G., Doborjeh, Z.G., **Kumarasinghe, K.** and Breen, V. (2018). From von Neumann Architecture and Atanasoffs ABC to Neuro-Morphic Computation and Kasabov's NeuCube: Principles and Implementations. In Learning Systems: From Theory to Practice (pp. 1-28).

Springer, Cham.

- Doborjeh, M. G., Doborjeh, Z. G., Gollahalli, A. R., **Kumarasinghe, K.**, Breen, V., Sengupta, N., Ramos, J.I.E., Hartono, R., Capecci, E., Kawano, H. and Othman, M., (2018). From von Neumann Architecture and Atanasoff's ABC to Neuromorphic Computation and Kasabov's NeuCube. Part II: Applications. In Practical Issues of Intelligent Innovations (pp. 17-36). Springer, Cham.

Talks

- Towards Finding the ABC's of 'Brainish' - Finalist of the AUT Three-Minutes Thesis (3MT) Competition 2020 (A video of the three minutes talk is available from the following URL: https://www.youtube.com/watch?v=FSzlgw_MYC0)

1.9 Summary of the chapter

This chapter presented an overview of the proposed research. The chapter began with a brief description of the motivation, research problem addressed by the thesis and the rationale for conducting this research. The thesis aims to deliver an interpretable Brain-Inspired Spiking Neural Network for incremental learning of spike sequences for online event prediction from spatio-temporal data streams. The chapter stated the six objectives set up to achieve the above aim. The chapter then outlined the seven research questions addressed by the thesis and presented an overview of the proposed research methodology. Next, the chapter described the three stages of the research aimed at developing the learning algorithms, implementing the proposed learning algorithms as software prototypes and conducting experimental validation of the proposed learning algorithms

using EEG datasets. The chapter then presented the structure of the thesis and the interconnections of the chapters. Finally, the chapter outlines the main contributions of the thesis.

Chapter 2

Brain-Computer Interfaces – Brain-Inspired Methods, Limitations, Challenges and Future Directions

"A scientist in his laboratory is not a mere technician: he is also a child confronting natural phenomena that impress him as though they were fairy tales."

Marie Curie, a pioneering researcher on radioactivity, the first woman to win a Nobel Prize, the first person and the only woman to win the Nobel Prize twice and also the only person to win a Nobel Prize in two different sciences

Chapter Overview

The previous chapter presented an overview of the thesis, including rationale and motivation of the research, the research questions addressed by the thesis, a brief description of the research methodology and main contributions of this research. This chapter will emphasise on the limitations in the non-invasive Brain-Computer Interfaces that utilise electroencephalography signals applied in motor recovery and restoration applications. The chapter begins with a general introduction to Brain-Computer Interfaces and the applications of BCI. Then, the recent developments in constructing neural decoders are critically examined, including their limitations and challenges. The chapter next outlines several future directions for restorative Brain-Computer Interface research. Finally, the chapter concludes with several suggestions to the machine learning approaches used to construct neural decoders for restorative BCI.

2.1 Introduction

Nature has inspired many technological innovations over the years. In 1780, an accidental observation of a movement in a dead frog struck by an electric impulse inspired Luigi Galvani's discovery of bioelectricity in animals (Tudor et al., 2005). Following the discovery of the Galvanic current, in 1809, Luigi Rolando stimulated the surface of the cortex in the brain for the first time (Sironi, 2011). These experiments led to the discovery of cerebral localisation in the brain (Marshall & Fink, 2003). In 1875, Richard Caton reported the observation of electric impulses from the surfaces of living brains, proving that the brain produces an intrinsic electrical activity which can be recorded from the cerebral surface of the brain. Caton's experiments set up the foundation for Hans Burger to discover electroencephalography, a method for recording brain waves in 1924 (Haas, 2003).

Later, it was shown that apart from monitoring the neural activity in the brain, EEG could also be transformed into electrical impulses that could be used to control electronic devices. Jacques Vidal reported the first experiment and a digital device was controlled using brain waves extracted from EEG in 1973 (Vidal, 1973). He introduced the term 'Brain-Computer Interface' for this type of communication. Electroencephalography non-invasively monitors the neural activity of the brain. Empirical studies provide evidence on decoding various human behaviours from neurological signals. Brain-Computer Interface detects mental commands from neurological signals and translates them into machine commands. BCI enables users to control external digital devices such as exoskeletons, computers, wheelchairs, prosthetic limbs, cognitive games and communication support devices through the user's mental commands without direct physical interaction with the device. Therefore BCI is a promising intervention to improve the quality of life of motor-impaired people.

Based on the purpose, BCI-base rehabilitation technologies can be divided into two categories as restorative BCI and replacive BCI. The restorative BCIs intend to restore the affected movements through intuitive manipulation of restorative neuroprosthesis such as exoskeletons, Functional Electrical Stimulation, prosthetic limbs. Neuroprosthetics aims to restore the affected motor function by strengthening the affected neural pathways or building alternative pathways through motor learning. In this regard, neurorehabilitation with neuro-feedback supports to restore the affected movements through repetitive exercises (Bauer & Gharabaghi, 2017; Gharabaghi, 2016). Often in modern rehabilitation settings, Functional Electrical Stimulation, robotic exoskeletons and virtual reality are coupled with these treatments to gain better recovery of the motor functions. The replacive BCI, on the other hand, intend to replace the lost functionalities such as communication and navigation through intuitive manipulation of assistive devices. The applications of replacive BCI include navigation using mind-controlled assistive wheelchairs and communication through mind-controlled spelling devices through BCI. The goal of assistive neuroprosthesis such as wheelchairs and communication aid devices controlled through BCI's is to replace the lost motor functions. The accurate multi-class classification that increases the degrees of freedom of the assistive control and short prediction latency are the main challenges for assistive BCI. The review focuses on previous studies related to processing and analysis of EEG signals for implementing neural decoders for restorative BCI.

2.2 Focus of the Review

The focus of this review is to critically examine previous research on Brain-Computer Interfaces that utilise EEG signals to predict multidimensional limb movements which are helpful to motor recovery and restoration in rehabilitation.

The research articles were filtered using the 'Scopus' database using the keywords such as, 'Brain Computer Interface', 'Brain-Computer Interface', 'BCI' , 'Brain Machine Interface', 'EEG', 'electroencephalogram', 'electroencephalograph', 'electroencephalography'. (Search Query: TITLE-ABS-KEY (("Brain Computer Interface" OR "Brain-Computer Interface" OR "BCI" OR "Brain-Computer Interfaces" OR "Brain Machine Interface" OR "Brain-Machine Interface") AND ("EEG" OR "electroencephalogram" OR "electroencephalograph" OR "electroencephalography")))

2.2.1 Inclusion and exclusion criteria

This review critically examines previous studies on improving machine learning approaches that were applied to predict movements in restorative BCI. The research articles focused on predicting other Event-Related Potentials such as p300, Steady State Visual Evoked Potentials, Evoked Potentials, Visual Evoked Potential, Evoked Visual Response, visual oddball task are excluded from this review. The neurological signals other than EEG such as ECoG, MEG, fMRI, LFP, multi-electrode arrays, single-unit recording are also excluded from the review. Since the current literature review focuses on the state-of-the-art in restorative Brain-Computer Interfaces applied in neurorehabilitation and prosthetic control for motor recovery and restoration, previous research of other BCI application areas such as the assistive systems for communication and navigation, neuromarketing, vigilance level estimation to assist drivers, affective computing, epileptic state detection, cognitive games and entertainment are also excluded from the review.

A growing body of BCI literature on sensorimotor rhythm-based neural decoders have used three different strategies to originate BCI commands as executed, attempted and imagined (Ang et al., 2010; Muralidharan et al., 2011; Jochumsen et

al., 2015) movements that generate Movement Related Cortical Potentials (MRCP). These movements result in Event-Related Synchronisation and Desynchronisation in the brain that generates distinct control commands. The populations of neurons that correspond to movements in different parts of the body are spatially distributed in sensory and motor areas of the brain. A majority of studies that utilise MRCP are focused on the movements of different parts of the body such as left hand, right hand, feet and tongue to enable multidimensional control through BCI as such movements cause spatially distinguishable patterns in MRCP. However, this approach does not suit for restorative BCIs as they intend to restore the affected motor functions of the same limb. Therefore, this literature review focuses on machine learning methods that intend to predict different movements of the same limb.

2.3 Overview of Brain-Computer Interfaces

2.3.1 Invasive and non-invasive Brain-Computer Interfaces

Figure 2.1 represents different types of neurological signals that monitor the neural activity of the brain (source: Leuthardt et al., 2009). Brain-Computer Interfaces can be divided into two main categories as invasive BCI and non-invasive BCI according to the invasiveness of the neurological signal used for monitoring the brain activity. The invasive BCI utilises electrodes that are placed inside the brain such as Electrocorticography, Lead-Field Potentials, microelectrode arrays to monitor the neural activity of the brain. The non-invasive BCI utilises electrodes that are placed on the skin surface, which do not require invasive procedures to monitor the neural activity of the brain. Electroencephalography, Magneto-encephalography, and functional Magnetic Resonance Imaging are examples of

non-invasive neurological signals.

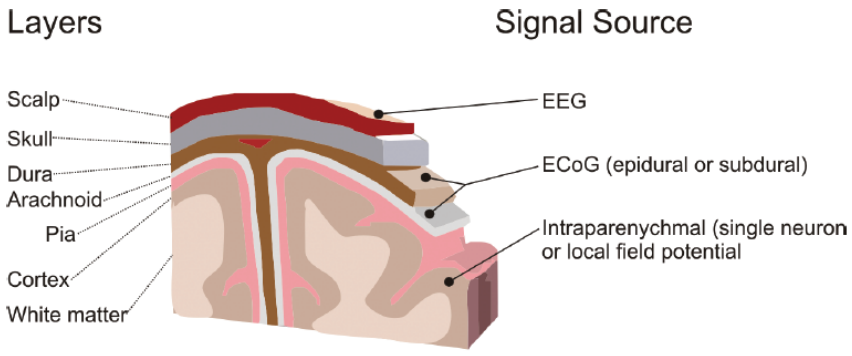

Figure 2.1: Different types of neurological signals that measure neural activity of the brain (source: Leuthardt et al., 2009)

2.3.2 BCI paradigms

A set of well-established concepts, protocols, and procedures used to develop Brain-Computer Interfaces are known as a BCI paradigm. Some of the commonly used BCI paradigms are the p300, Steady-State Visually Evoked Potentials (SSVEP), Motor Imagery, and visual and auditory odd-ball BCI paradigms. According to the origin of the stimuli, these BCI paradigms can be divided into two categories as endogenous and exogenous paradigms (Han et al., 2019). The exogenous BCI paradigms depend on external stimuli such as sound or flickering digital displays to elicit distinct patterns in brain activity. The BCIs that use evoked potentials such as p300 and SSVEP based BCI belong to exogenous BCI paradigms. The endogenous BCI paradigms utilise self-regulated brain activity such as Motor Imagery, Motor Execution and Error-related Potentials. The endogenous BCI paradigms do not require an external cue to generate distinguishable neural activity patterns.

2.3.3 Single-trial Brain-Computer Interfaces

For real-time control of BCI applications, online event prediction is essential yet challenging due to the non-stationarity of EEG signals. A BCI which performs online prediction without averaging the brain data across multiple trials is known as a 'single-trial' BCI. Due to the high trial-to-trial, session-to-session and subject-to-subject variability in EEG, several approaches have managed to extract essential EEG features by temporal averaging across multiple trials. It is known as the 'grand average' of EEG. This approach maximises the significant statistical features of the EEG signal but reduces the information transfer rate of the BCI due to the long temporal averaging. Thus taking the 'grand average' as an EEG feature to predict neural activity increases the prediction latency of BCI and limits its feasibility to real-time prediction.

2.4 Applications of Brain-Computer Interfaces

BCI is applied in a wide range of application areas such as neurorehabilitation, prosthetic control, communication and navigation in assistive systems, neuromarketing and entertainment. Brain-Computer Interface provides a way of by-passing the affected functionalities of the brain in people with neurological disorders. Therefore, BCI can assist a wide range of neurological disorders such as paralysis (Ang & Guan, 2013; Muralidharan et al., 2011; Soekadar et al., 2015; Jiang et al., 2015), Amyotrophic Lateral Sclerosis (Kasahara et al., 2012; Sorbello et al., 2017), Spinal Cord Injury (Wei et al., 2009), Parkinson's disease (Broccard et al., 2014), Dystonia (Hashimoto et al., 2014), cerebellar ataxia (Ying et al., 2011) and amputation (Azizi, 2013; Prathibha et al., 2017). Neuroprosthetics aims at assisting or restoring the affected motor functions in people with movement impairments. The technological advancements in rehabilitation engineering witness several promising

interventions for effective recovery in people with motor-impairments. Brain-Computer Interface is one of these interventions that shows promising evidence of motor recovery or substitution in people with movement impairments.

2.5 Restorative Brain-Computer Interfaces

Intense rehabilitation therapies through an extensive amount of repetitive exercises have shown success in gaining motor recovery up to a certain extent in stroke patients suffering from movement impairments. However, they are time-consuming, cost and labour intensive, require the support of a one-to-one interaction and assistance of a rehabilitation therapist and have to be performed mostly in clinical settings using complicated and expensive equipment. These practical challenges limit the accessibility of sufficient intensity and dose of rehabilitation therapy for many stroke survivors (Gao et al., 2013). There is a significant demand in integrating technological advancements to rehabilitation practices for effective and efficient delivery of rehabilitation therapies.

Studies have shown that Brain-Computer Interface is a promising intervention for stroke rehabilitation (Taylor et al., 2015; Soekadar et al., 2015; Ang & Guan, 2013; Mattia et al., 2016; Y. Zhang, Prasad et al., 2017). J. J. Daly and Wolpaw (2008) point-out four important factors for the development of new BCI methods in neurological rehabilitation. These include first to understand the characteristics and possible use of brain signals from previous animal studies. Secondly, to recognise the activity-dependent plasticity and its influence on determining the functional effects of disease and trauma. Thirdly, development of powerful, low-cost hardware and software programs for recording and real-time online analysis of brain signals. Finally, to enhance the societal interest and appreciation for people with motor disabilities.

Ang and Guan (2013) present a review of the methodology and clinical studies on stroke rehabilitation through Brain-Computer Interfaces. The BCI intervention for neurorehabilitation provides two aspects of support for rehabilitation and recovery. First, BCI restores intuitive multi-dimensional control of the affected limb through intuitive manipulation of rehabilitation devices such as robotic exoskeletons (Ang et al., 2010) or muscle stimulation through Functional Electrical Stimulation for assisting daily activities. Secondly, studies have shown that BCI mediated rehabilitation therapies are more effective in inducing neuroplasticity than the traditional exercise-based therapies (Muralidharan et al., 2011; Soekadar et al., 2015). Thus, BCI enhances motor re-learning and motor recovery by boosting the activity of residual neural circuits in stroke patients.

The integration of robotic technologies with neurorehabilitation enable the rehabilitation more accessible for many stroke survivors and are promising interventions to facilitate rehabilitation therapies event at patient's household environments. The use of BCI technology for controlling robotic exoskeletons enables patients to use their movement intention to control the exoskeleton during therapies. Recent literature presents several studies on BCI-activated exoskeletons for motor recovery (Xiao et al., 2014; Ang & Guan, 2013; Noda et al., 2012). Ang et al. (2010) shows the efficacy of robotic feedback integrated motor-imagery BCI for upper extremity motor recovery after stroke. Gao et al. (2013) presents a rehabilitation system that integrates BCI with a robotic orthosis for motor recovery. The system performs online detection of movement intention through motor imagery EEG signals and provides an adaptive mechanism to determine the level of assistance using real-time neurofeedback.

Functional Electrical Stimulation (FES) is an approach used in neurorehabilitation to restore or improve motor functions of a paralysed limb. It applies a small electrical pulse to paralysed muscles. Usually, the amount of electrical stimulation

is determined by the neurorehabilitation therapist based on the observations. Several studies have shown that in order to gain a better recovery of the movement during repetitive attempts, the electrical stimulation provided by the FES should be carefully controlled based on the feedback from the task. Several computational approaches have been applied to adjust the amount of support by FES to move an impaired limb during successive neurorehabilitation tasks.

Studies have shown the feasibility of using Iterative Learning Control (ILC) to adjust the parameters of the FES to enhance voluntarily involvement of the patient during the task (Freeman, 2014; P. Müller et al., 2017). Studies have reported the improvement of learning upper limb movement trajectory with the support of a robotic exoskeleton (Sampson et al., 2016) and virtual reality environment (Freeman, 2015; Meadmore et al., 2014) with ILC mediated electrical stimulation. Zhao et al. (2016) present a Steady State Visually Evoked Potential based BCI integrated with FES for upper extremity rehabilitation. The approach translates the movement intention detected by the SSEVP-based BCI to trigger relevant electrodes in FES.

Integrating BCI with Functional Electrical Stimulation systems enable linking movement intention directly with the associated muscle activity and provides a mechanism to by-pass the affected neural pathways (Bhattacharyya et al., 2016; Jiang et al., 2015). Previous studies have provided evidence that a properly timed neuromuscular electrical stimulation improves the cortical excitability and induce neuroplasticity in the brain (Ethier et al., 2015; Jochumsen et al., 2016). In (Jiang et al., 2015), the authors present an evaluation of rehabilitation in post-stroke hemiplegia patients through a BCI-FES rehabilitation system. The study confirms significant activation of the affected brain areas and also the efficacy of improving the affected motor areas of the cortex. These studies confirm the improvements in motor recovery through BCI-FES rehabilitation interventions. Ortner et al. (2012);

Anopas et al. (2013); Wairagkar et al. (2016); Muñoz et al. (2014) integrated BCI with virtual reality-based rehabilitation systems. These studies provide evidence of the importance of using the patient's voluntarily movement intention detected through motor imagery EEG for inducing neural plasticity.

2.5.1 Proof of concept studies on healthy participants

The current BCI studies that aim to apply for motor recovery mainly designed for detecting movement intention from EEG for activating the rehabilitation device such as FES, exoskeleton or virtual reality system. Many can only generate a single degree of freedom movements. Park et al. (2013) reports the performance of movement intention prediction from EEG in five healthy participants through the Fisher discriminant classification. The BCI predicts the movement intention of executed and imagined pronation and supination movements for controlling the rehabilitation device. The authors report a classification accuracy of 78% and 70% while reducing the false alarm rate to 10% and 17% for executed and imagined movements, respectively. The reported average time for movement intention detection was 842 ms which denotes limited feasibility of real-time prediction.

Savić et al. (2013) report a cue-based BCI for triggering three different types of grasps. A set of predefined stimulation patterns of an FES rehabilitation system was used to generate palmar, lateral, and precision grasps according to the movement intention detected from EEG. The study used an online frequency band-power estimation of the mu frequency band was used for detecting the movement intention from four healthy participants, and the authors report the mean accuracy of 89%. Tavella et al. (2010) reports the development of a non-invasive asynchronous BCI for generating hand opening and closing to perform power grasp of a prosthetic hand. The BCI was tested on four healthy participants.

In the authors show the feasibility of reducing BCI calibration time by setting up the classifier to detect MI using active and passive hand movements. Ethier et al. (2015) suggest that the recovery of movements through FES might be enhanced by modulating the stimulations with the patient's voluntary movement intention through a BCI integrated with the FES rehabilitation system. The authors highlight the need for better understanding of complex neuromuscular interactions for effective use of BCI mediated FES rehabilitation therapies.

2.5.2 Studies on evaluating the clinical efficacy of the BCI intervention in people with movement impairments

Several clinical studies and case reports confirm the efficacy of the BCI intervention for motor recovery. In M. Li et al., 2014, authors present evidence on enhanced motor recovery through motor imagery based BCI training in stroke rehabilitation. Ang and Guan (2015) show the efficacy of motor recovery in stroke survivors through BCI. The enhance neurological recovery in several randomised control trials through BCI-FES rehabilitation system is presented in Osuagwu et al., 2015; Pichiorri et al., 2013; Lee et al., 2010; Muralidharan et al., 2011; H. G. Tan et al., 2011. A pilot study on treating dystonia through BCI based neurofeedback training is presented in (Hashimoto et al., 2014). The case study has shown the feasibility of suppressing exaggerated brain activity by providing feedback on the ongoing cortical excitability in dystonia patients. Several randomised control trial on post-stroke rehabilitation (Frolov et al., 2017; Bhagat et al., 2016) show the improvements in motor recovery through the integration of BCI intervention coupled with exoskeleton assisted rehabilitation therapy for enhancing motor recovery.

Yilmaz et al. (2013) reported significant changes in the Movement Related

Cortical Potentials after BCI intervention. Five chronic stroke patients with no residual finger extension ability performed online BCI training coupled with the physiotherapy during one month. The MRCP extracted from EEG showed a significantly decreased peak amplitude and significantly delayed MRCP onset over the Cz channel during attempts to moving the paralysed hand after the BCI intervention. In contrast, no such difference between the pre and post-intervention was observed in the healthy hand which indicates the changes in MRCP may be due to the less mental effort and shorter planning time required for executing the movement after the intervention.

Previous studies have evident the improvements in motor recovery, balance and walking in stroke patients through motor imagery BCI interventions in lower limb rehabilitation (Sun et al., 2011; Mahadevappa et al., 2013; Xu et al., 2014). Mahadevappa et al. (2013) present a BCI-based self-adaptive approach for estimating the stimulation strength of the FES to support hemiplegic patients to achieve foot dorsiflexion. The approach utilises the mean delta frequency band and the peak alpha frequencies as features to predict the appropriate stimulation strength through regression analysis.

The above studies evident the significance of BCI interventions for motor recovery and restoration. The process of translating neural activity into machine commands through a BCI generally follow the following steps.

1. Acquisition of neurological signals that represent the neural activity of the brain

2. Pre-processing and filtering artefacts

3. Feature extraction and feature selection

4. Supervised or unsupervised learning to predict activity from neurological

signals

5. Translation of predicted neural commands into machine commands to manipulate objects

Pre-processing of EEG signals includes band-pass filtering to extract significant EEG frequency bands, notch filtering to eliminate specific noises such as the electromagnetic interference that occurs around the frequency of 50-60 Hz. Pre-processing also filters the EEG artefacts such as eye blinks and eye movements, movements of the jaw or tongue, activity of the neck and other nearby muscles, breathing and heartbeat of the person. A commonly used artefact removal approach is the Independent Component Analysis. ICA is a matrix factorisation method that aims at decomposing the EEG channel activity into uncorrelated and statistically independent components. Then the artefact-free EEG signal is reconstructed by removing the Independent Components that are contaminated by artefacts.

Next, the EEG features are extracted from the pre-processed EEG signals. Power Spectrum Density analysis, Independent Component Analysis, time-frequency (spectrogram) analysis, Common Spatial Pattern Analysis, Minimum Norm Estimation, autocorrelation and Riemannian geometry are some of the common approaches for feature extraction in BCI. Finally, neural activity is predicted from the extracted features through a suitable supervised (classification or regression analysis) or unsupervised (clustering) machine learning approach. Support Vector Machine (Lei et al., 2017), Linear Discriminant Analysis and Artificial Neural Networks (Sánchez-Cossío et al., n.d.) are the commonly used classifiers for predicting neural activity from EEG in BCI.

The thesis suggests that the Spiking Neural Networks, as a Brain-Inspired Machine Learning approach, constructs an interpretable neural decoder that

can incrementally learn to predict complex movements from EEG signals. The thesis compares and contrasts the proposed brain-inspired system and the traditional machine learning approaches that were used to construct BCI decoders. The following section presents a methodological review of the current Artificial Neural Network-based brain-inspired machine intelligence approach for decoding movements from EEG.

2.6 Methodological review of Artificial Neural Network-based methods for decoding neural activity in BCI

Artificial Neural Networks are computational models that are inspired by biological neural networks in living beings. They are good at discovering hidden relationships between input and output, in particular when it is hard to find explicit mathematical equations that describe such relationships. There are three generations during the evolution of ANN. The Perceptron or the threshold gates which generate a binary output using a threshold that does not use a non-linear activation function belongs to the first generation of NN. The second generation of neural networks such as Multi-layer Perceptron (MLP) applies non-linear activation functions on the weighted sum of the synaptic input. Spiking Neural Networks as the third generation of neural networks more closely model the computation take place in biological neural networks. The remainder of this section presents a brief methodological review of ANN-based approaches for non-invasive BCI followed by a particular focus on previous studies on brain-inspired neural decoders for non-invasive restorative BCI.

2.6.1 Methodological Review of ANN-based Approaches for BCI

Previous studies on ANN-based neural decoders for non-invasive BCI have employed different ANN-based methods such as Convolutional Neural Networks, Recurrent Neural Networks (RNN), Restricted Boltzmann Machine (RBM), Deep Belief Networks (DBN), Extreme Learning Machine (ELM), Spiking Neural Networks and Multi-Layer Perceptron for predicting mental commands from EEG. Here we present a brief methodological review of these approaches during the past ten years.

Convolutional Neural Networks

Convolutional Neural Networks is a type of deep neural networks which can retrieve a hierarchical feature representation from raw data using multiple layers of neurons with one or many convolution layers. CNN's are inspired by the connectivity structure of the visual cortex in animals for visual information processing and demonstrated success in machine learning from visual data such as images and videos. In addition, studies have also shown the applicability of CNN to predict human behaviour from EEG useful in rehabilitation applications.

Sakhavi et al. (2015); Tabar, Yousef Rezaei and Halici (2016); J. Liu et al. (2015); Mao et al. (2017) presented several studies on evaluating CNN-based BCI decoders for predicting mental commands from EEG. CNN, as automatic feature learners have the ability to discover significant features from raw data. Therefore, CNNs can replace the traditional feature engineering process of BCI, which consist of explicit feature extraction and selection steps (Tabar, Yousef Rezaei and Halici, 2016; J. Liu et al., 2015; Mao et al., 2017). A CNN architecture that uses both static and dynamic energy features during Event-Related Synchronisation and

Desynchronisation is presented in (Sakhavi et al., 2015). Energy dynamics of the EEG signals carry important discriminating features which are not significant in commonly used static energy-based features. The authors report a significant increase in performance by considering both static and dynamic energy features using CNN compared to static energy-based classifiers such as SVM for predicting left hand, right hand, foot and tongue motor imagery tasks.

A CNN based feature learning combined with stack autoencoder for classifying three-class motor imagery is presented in (Tabar, Yousef Rezaei and Halici, 2016). J. Liu et al. (2015) present a high-level feature representation of multiclass motor imagery EEG called 'deep motor features' using multi-scale deep CNN. This approach resulted in higher classification accuracy from relatively less amount of training data. However, since the study is limited only for a single subject, it is not appropriate to generalise the results. Mao et al. (2017) present a CNN approach trained on raw EEG for predicting driver fatigue. The authors report higher classification accuracy and short training time on a dataset collected from 100 subjects.

CNN, exhibit several advantages compared to the other machine learning approaches that decode movements from EEG. CNN can learn significant features from raw data, use both dynamic and static features for classification and perform accurate predictions compared to static feature-vector based classifiers. However, CNN's are limited by the long training time and the requirement of selecting the most appropriate neural network architecture and parameters for optimal results. The network architecture and parameters have a significant impact on classification performance and finding the most appropriate architecture and parameters is a computationally expensive and time-consuming task (Sakhavi et al., 2015; J. Liu et al., 2015).

Restricted Boltzmann Machine and Deep Belief Networks

Restricted Boltzmann Machines are a type of stochastic generative deep learning neural network limited only to two layers of neurons called visible layer and hidden layer. RBMs have the ability to learn an internal representation of data.Scherer et al. (2013) and Gandhi et al. (2014) present restricted Boltzmann machine approach for predicting mental tasks from EEG. Gandhi et al. (2014) present a Restricted Boltzmann Machine based deep learning approach for the EEG features extracted from Fast Fourier Transformation and Wavelet Package Decomposition. The authors report statistically significant performance compared to state-of-the-art methods. The authors also investigate the feasibility of session to session and subject to subject transfer of knowledge through transfer learning. The study reports a successful transfer of knowledge between multiple sessions in individual subjects, although the subject to subject transfer was inefficient. The authors also claim the robustness of the proposed approach.

Multiple-RBM's stacked on each other and trained using backpropagation is called a Deep Belief Network.Ren and Wu (2014) present a Convolutional Deep Belief Network (CDBN) for EEG feature learning. Results highlight the ability of CDBN for feature learning compared to state-of-the-art feature extraction methods, particularly with limited labelled data. A comparison between two neural networks based classifiers, Deep Belief Networks and Stacked Auto Encoders for predicting the eye state classification is presented in (Narejo et al., 2016).

Extreme Learning Machines

Extreme Learning Machines are feed-forward neural networks with single or multiple layers of hidden units with randomly assigned or inherited parameter values of hidden units which do not tune through training. P. Tan et al. (2016)

show ELM's result in higher classification accuracy and mutual information transfer compared to LDA and SVM. In (Ding et al., 2015), the authors present a multi-layer Deep Extreme Learning Machine approach. This network architecture claims the advantages of accurate prediction through deep learning and as well as fast and efficient learning in ELM's. However, the main limitation of this approach is the requirement of employing the most appropriate network architecture and parameters for optimal results. The time and resource-intensive pre-processing and feature extraction process of this approach is also a challenge for real-time processing.

Duan et al. (2014, 2016) present a voting-based ELM coupled with PCA and LDA for EEG feature selection. The results suggest that the voted ELM results in a better classification performance compared to average ELM and SVM. Also, the voted ELM is the least human intervene machine learning approach compared to the other methods evaluated by the study. (Bashashati et al., 2017) presents a Neural Network Random Conditional Fields approach for extracting temporal correlation of EEG. The approach results in higher Area Under the Curve (AUC) compared to the dynamic classification models such as Hidden Markov Models and Conditional Random Fields and static SVM based classifier.

Recurrent Neural Networks

Unlike the feed-forward neural networks discussed so far, RNN's contain recurrent synaptic connections which can process input sequences and generate sequences of outputs. Thus, RNN-based neural decoders of BCI can benefit from the time-domain dynamic EEG features compared to static vector-based neural decoders that use SVM, LDA and MLP as classifiers.

Echo State Networks, which is a subset of Recurrent Neural Networks that

contain winner-take-all readouts neurons for predicting intended movement direction from EEG, is presented in (Kim & Jeong, n.d.). Gandhi et al. (2011) describe a Recurrent Quantum Neural Network architecture that addresses the noisy and nonstationary nature of EEG signals. The authors evaluate several RNN architectures for predicting Grasp-and-Lift (GAL) events from EEG (An, 2016). M. Li et al. (2016) integrate a Discrete Wavelet Transform with RNN with Long Short-Term Memory (LSTM) gating units for predicting motor imagery tasks from EEG. Forney and Anderson (2011) present a generative machine learning model for mental task classification from EEG using Elman Recurrent Neural Networks. The authors show that the proposed RNN can forecast EEG with lower Root Mean Square Error. An adaptive neuro-fuzzy inference system integrated with RNN for mental task prediction from EEG is presented in (Morales-Flores et al., 2013). The authors show that a fully connected RNN results in higher classification accuracy than Elman Recurrent Networks. Popov and Fomenkov (2016) present a Recurrent Convolutional Neural Network architecture for multiclass classification, which takes the advantages of both Recurrent and Convolutional Neural Networks. The authors suggest that a recurrent convolutional layer can results in a higher classification performance compared to a standard convolutional layer.

Multi-Layer Perceptron

In addition to the deep learning methods discussed above, previous studies have also used Multi-Layer Perceptron for classifying mental commands from EEG. Unlike the deep learning neural networks, MLP's are not capable of discovering significant features from raw data. Therefore, it is essential to use appropriate feature extraction and selection method before classification by the MLP to achieve a significant classification performance.

Hamedi et al. (2014) present an MLP with Radial bias function to classify

three-class motor imagery data using Integrated multi-channel EEG and Root Mean Square features. A hierarchical neuro-fuzzy hybrid model for improved classification performance compared to MLP and ensemble of adaptive neuro-fuzzy inference systems is proposed in (Barbosa et al., 2009). In (Turnip et al., 2010), the authors compare a backpropagation neural network classifier with LDA.Hema C. R., Paulraj M. P., Nagarajan R. Sazali Yaacob (2009) reports a marginal increment in classification accuracy by MLP-based neural classifier compared to a fuzzy classifier for predicting five mental tasks using band power EEG features. Martišius et al. (2013) present a modified Voted Perceptron algorithm compatible with the real-time prediction that consumes less training time. Anh et al. (2016) suggests that an ANN-based approach for classifying different mental states using spectral features is better than several other classifiers such as k-NN, Naive Bayesian, Support Vector Machine, and Linear Discriminant Analysis.

In (Liyanage et al., 2009), authors present a study on using Common Spatial Pattern features to train an ANN. The authors have also used Particle Swarm Optimisation for feature selection before classification by ANN. Several studies have reported the improvements in prediction accuracy by applying an appropriate feature selection method such as PCA before classification by MLP (Kottaimalai et al., 2013; Anh et al., 2016). However, PCA does not always guarantee a better classification since the best discriminating components may not lie in the most significant principal components (J. Liu et al., 2015).

Plechawska-Wojcik et al. (2016) present a control structure containing multiple neural networks and automated approach for selecting the best classifiers. In (Nakayama et al., 2010), the authors describe a Multiple Multi-Layer Neural Networks (MLNNs) architecture with Gram-Schmidt orthogonalisation to improve the features. Although the authors report a higher classification accuracy compared to other conventional methods, searching the most suitable network architecture

from multiple combinations of MLPs is a crucial yet computationally expensive step to achieve a good classification accuracy. Liyanage et al. (2009) present the feasibility of evolutionary training of an Artificial Neural Network with Genetic algorithms to find the optimal structure for the neural network.

Neuromorphic Platforms

Neuromorphic platforms are Very Large Scale Integration (VLSI) systems with analogue electronic circuits inspired by the massively parallel connectivity structures in the living nervous systems. Integrating deep learning with neuromorphic computational platforms such as SpiNNaker (Furber et al., 2014) and TrueNorth (Merolla et al., 2014) can massively impact on increasing the accuracy, speed and biological plausibility in neural decoders for BCI. Neuromorphic processors can process spiking information in a massively parallel manner compared to conventional processors and thus capable of real-time information processing.

Nurse et al. (2016); Mashford, Benjamin S and Yepes, A Jimeno and Kiral-Kornek, Isabell and Tang, Jianbin and Harrer (2017); Boi et al. (2016) present deep neural network architectures compatible with neuromorphic platforms that consume significantly less power compared to traditional microprocessors. Nurse et al. (2016) present a CNN architecture compatible with the TrueNorth neuromorphic platform and demonstrate higher classification accuracy on predicting left vs right-hand squeezing patterns from EEG. A Spiking Neural Network that is compatible with the TrueNorth neuromorphic platform for EEG classification is presented in (Mashford, Benjamin S and Yepes, A Jimeno and Kiral-Kornek, Isabell and Tang, Jianbin and Harrer, 2017). The authors demonstrate state-of-the-art classification accuracy using a modified backpropagation training method.

Spiking Neural Networks

N. Kasabov (2012); N. K. Kasabov (2014) proposed a novel 3-D evolving Spiking Neural Network architecture called NeuCube for modelling, predicting and understanding spatio-temporal brain data. It is inspired by the structural and functional organisation of the brain's neural network. Several case studies confirm the feasibility of the NeuCube SNN architecture for predicting cognitive tasks from EEG (N. Kasabov & Capecci, 2015; N. Kasabov et al., 2016, 2017; Doborjeh et al., 2018). The experimental results suggest that the NeuCube SNN architecture not only results in a higher classification performance from non-invasive brain data compared to conventional machine learning methods but also results in an interpretable Artificial Intelligence system that can provide a knowledge representation of the biological processes that generated the data. NeuCube and its applications in stroke and neurorehabilitation robots is patented under N. K. Kasabov et al., 2016.

Boi et al. (2016) report a modular BCI compatible with neuromorphic platforms using SNN to facilitate bidirectional control through BCI. The SNN was built using online Spike Time Dependent Plasticity (STDP) learning rule. Tayeb et al. (2017) present an SNN implemented in a SpiNNaker neuromorphic processor to classify motor imagery tasks from EEG. The classifier resulted in comparable classification accuracy, although the study was limited to data from a single participant, which reduces its ability to generalise the obtained results. Although the accuracy of the SNN was slightly lower than that of SVM implemented on a conventional processor, the study provides new insights into a novel type of neural decoder for Brain-Machine Interface due to its brain-inspired architecture, short processing time and less power consumption. The feasibility of online closed-loop control of a BCI that using SNN that uses a Kalman filter is presented in (Adam Moser & York, 2008).

The system was tested on two rhesus monkeys, and the SNN based implementation of Kalman filter resulted in comparable performance compared to its standard implementation. The study explored the feasibility of translating the neural decoding algorithms into Spiking Neural Network-based architectures so that they can be executed on low power consuming neuromorphic processors instead of conventional microprocessors that suffer from the von Neumann bottleneck (K. Roy et al., 2019).

2.6.2 Artificial Neural Networks based neural decoders for restorative BCI applications

Movement-Related Cortical Potentials is a type of Event-Related Potential (ERP) that occur up to two seconds before the onset of a voluntary movement. MRCP is an indication of the cortical processes that happen during a voluntary movement such as planning, preparation and execution of the movement. Sensorimotor rhythms of EEG are the cortical activities related to motor and sensory information processing extracted from EEG signals. A BCI, which utilises this sensorimotor information is called a sensorimotor rhythm-based BCI and plays a significant role in BCI for neurorehabilitation and prosthetic control. This section of the thesis focuses on critically evaluating the previous studies on neural decoders that use sensorimotor rhythms of EEG to predict different movements for restorative BCI.

Previous studies witness the applicability of sensorimotor-based Brain-Computer Interfaces for applications in communication and control, motor recovery, navigation, motor substitution and entertainment in assistive and rehabilitation technologies. The control paradigms used in such BCI systems can be divided mainly into two categories. The first category uses either imagined or executed movements of different parts of the body such as left hand, right hand, feet and

tongue to generate control commands. The second category employees different movements of the same limb to activate the BCI. For instance, the prediction of self-paced grasp and lift movements of the right hand.

According to the sensory and motor homunculus of the human body, sensation and motor control of the different parts of the body are spatially mapped in the brain's cortex. Thus, the activation of different parts of the body generates discriminative spatial patterns that can be used to generate distinct control commands. For instance, prediction of movements in left-hand vs right-hand from EEG construct a binary classifier while the prediction of multiple movements such as the movements in left-hand, right-hand, foot and tongue construct a multiclass classifier.

A graphical representation of the sensory and motor homunculus is depicted in figure 2.2 (source: (Nguyen & Duong, 2019)).

Most of the studies reported in the literature were applied on multiple participants (T. Li et al., 2013; Tabar, Yousef Rezaei and Halici, 2016; Gandhi et al., 2011, 2014; R. Roy et al., 2012; Kumar et al., 2017; P. Tan et al., 2016; Ren & Wu, 2014; Sakhavi et al., 2015; Hamedi et al., 2014; Scherer et al., 2013; Tayeb et al., 2017; T. Li et al., 2013; Djamal, Esmeralda Contessa and Suprijanto, Suprijanto and Setiadi, 2016) while few studies were limited to a single participant (Nurse et al., 2016; Liyanage et al., 2009; Duan et al., 2014; J. Liu et al., 2015; M. Li et al., 2016). Some approaches have used specific feature extraction methods such as Common Spatial Pattern Analysis (T. Li et al., 2013; Kumar et al., 2017; Sakhavi et al., 2015; Liyanage et al., 2009), Discrete Wavelet Transformation (R. Roy et al., 2012; M. Li et al., 2016), Fourier Transformation (Ren & Wu, 2014; P. Tan et al., 2016; Scherer et al., 2013), band power and energy entropy (Hamedi et al., 2014; P. Tan et al., 2016; Tayeb et al., 2017), dimensionality reduction such as Principal Component Analysis (Ren & Wu, 2014; Tayeb et al., 2017; Duan et al.,

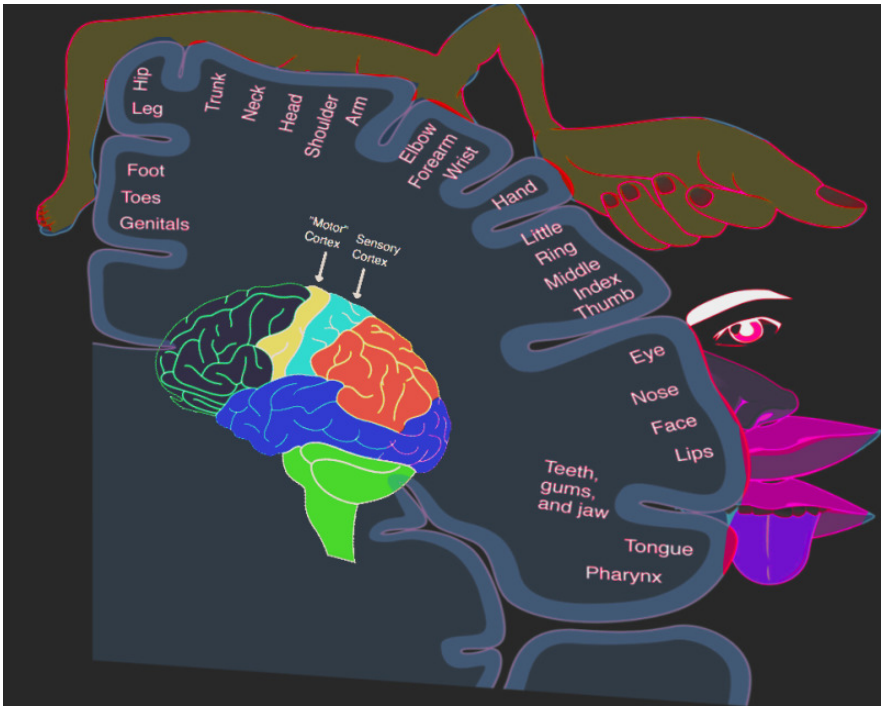

Figure 2.2: Sensory and motor homunculus of the human brain that indicate a representation of spatial and proportional cortical mapping of sensation and motor control of different body parts (Nguyen & Duong, 2019)

2014) and feature selection using Linear Discriminant Analysis (Duan et al., 2014) before classification. In contrast, several studies reported the feasibility of CNN (Tabar, Yousef Rezaei and Halici, 2016; J. Liu et al., 2015; Nurse et al., 2016), SNN (Tayeb et al., 2017), and RNN(Gandhi et al., 2011, 2014) to learn significant features from raw EEG without using explicit feature engineering methods. Tayeb et al. (2017) present a Spiking Neural Network implemented in the SpiNNaker neuromorphic processor.

Although these methods have shown the state-of-the-art performance in terms of the accuracy and speed, the classification tasks were focused on detecting movements of different parts of the body that generate distinct ERD/ERS spatial patterns. However, this approach is not appropriate for restorative BCIs as it causes a cognitive disconnection between the BCI user and the rehabilitation device.

The second BCI category has aimed at decoding different movements of the same limb to activate the BCI. This strategy is more compatible with restorative BCI. The goal of restorative BCI is to predict different movements of the affected or amputated limb. Most of them have used executed movements rather than imagined movements. Many studies have used non-invasive EEG (Djamal, Esmeralda Contessa and Suprijanto, Suprijanto and Setiadi, 2016; Popov & Fomenkov, 2016; An, 2016; Bashashati et al., 2017; Moubayed & Mcgough, 2017; Kumarasinghe et al., 2018) while few studies have reported the use of invasive brain data (Boi et al., 2016; Adam Moser & York, 2008). Most studies have reported their results by applying the decoding algorithms on multiple human participants (Djamal, Esmeralda Contessa and Suprijanto, Suprijanto and Setiadi, 2016; Popov & Fomenkov, 2016; An, 2016; Bashashati et al., 2017; Moubayed & Mcgough, 2017; Kumarasinghe et al., 2018) while few studies were on animals (Boi et al., 2016; Adam Moser & York, 2008). The classification task of such studies includes prediction of self-paced index finger flexion and extension (Bashashati et al., 2017; Moubayed & Mcgough, 2017), hand opening and closing (Kumarasinghe et al., 2018), centre-out-reaching and back (Adam Moser & York, 2008), grasping, closing and relaxing (Djamal, Esmeralda Contessa and Suprijanto, Suprijanto and Setiadi, 2016) and grasp and lift tasks (Popov & Fomenkov, 2016; An, 2016).

The first and second generations of neural networks such as Multi-Layer Perceptron have applied different feature extraction methods such as Autoregressive Modelling (Djamal, Esmeralda Contessa and Suprijanto, Suprijanto and Setiadi, 2016), signal power estimation (Moubayed & Mcgough, 2017) and feature selection methods such as Sequential Forward Floating Search (Moubayed & Mcgough, 2017) on raw EEG before classification. However several deep neural network architectures such as SNN (Boi et al., 2016; Adam Moser & York, 2008), CNN (Popov & Fomenkov, 2016) and RNN (An, 2016) have built the computational

model directly on raw EEG without utilising a separate feature engineering processes. In (Adam Moser & York, 2008), the authors report an implementation of a classifier on a neuromorphic chip. Boi et al. (2016) claim the compatibility of the simulated implementation on neuromorphic platforms.

A summary of neural network-based approaches for predicting different movements of the same limb using sensorimotor rhythms is presented in table 2.1. These studies evident that BCI is a successful intervention for inducing neural plasticity and permit motor recovery in people with movement impairments. EEG is a less expensively approach for monitoring the neural activity of the brain under a minimal risk. Moreover, its' high temporal resolution permits decoding of movement in real-time. However, a primary concern of EEG-based BCI intervention in motor recovery is, up to what extent EEG signals can provide useful information useful for neurorehabilitation interventions. Can EEG be used for decoding complex functional movements for manipulating objects?

The low spatial resolution of EEG limits the practical usefulness of EEG-based restorative BCI. Recent developments in restorative BCI have heightened the need for advanced machine learning methods that can predict complex movements from EEG. There is a growing body of literature that claim several limitations in machine learning and data analytics methods used for predicting movements from EEG signals useful for restorative BCIs. The next section of this chapter highlights several critical limitations in state-of-the-art machine learning methods used for decoding movements in restorative BCIs.

Table 2.1: A Summary of Artificial Neural Networks-based studies on predicting movements of the same limb from EEG

Motor task	**Participants**	**Feature extraction & selection**	**Prediction**	**Significant findings**	**Reference**
Center out reach and back	2 rhesus monkeys	Kalmann filter	SNN	Demonstrates the feasibility of low-power fully-implanted prostheses using the SNN-based BCI decoder implemented on the neuromorphic chip	Adam Moser & York, 2008
Control the movement of an object	1 rat	No separate feature extraction method	SNN with online Spike Time Dependent Plasticity (STDP)	Compatible with neuromorphic platforms and facilitate bidirectional control through BCI	Boi et al., 2016
Grasping, loosing and relaxing of right hand	4 healthy humans	Autoregressive (AR) modeling	MLP	Increased classification accuracy using the adaptive BP compared to conventional BP	Djamal, Esmeralda Contessa and Suprijanto, Suprijanto and Setiadi, 2016
Grasp and lift movements	12 healthy humans	No separate feature extraction method	Recurrent CNN	CNN discover significant features from raw EEG. Improved classification performance using the recurrent convolutional layer compared to standard convolution layer.	Popov & Fomenkov, 2016
Grasp and lift movements	12 healthy humans	No separate feature extraction method	RNN	Emphasis the selection of most suitable RNN network architecture for achieving the best performance	An, 2016

Continued over page ...

Table 2.1: A Summary of Artificial Neural Networks-based studies on ... *(continued)*

Motor task	**Participants**	**Feature extraction & selection**	**Prediction**	**Significant findings**	**Reference**
Self-paced light switch using right index finger	4 healthy humans	band power of EEG filter bank containing 8-12Hz and 16-24Hz frequency bands	NN Conditional Random Fields	As a dynamic classifier, Neural Networks Conditional Random fields results in higher AUC than the HMM, Conditional Random Fields and SVM	Bashashati et al., 2017
Self-paced flexion and extension of the left index finger	11 healthy humans	Extraction of μ, β, lower γ bands, then over-sampled using unsupervised deep generative neural networks. Sequential Forward Floating Search (SFFS) was used for feature selection	LDA	Oversampling results in higher movement onset detection accuracy after temporal smoothing	Moubayed & Mcgough, 2017
Closing and opening of the right hand	2 healthy humans	No separate feature extraction methods	NeuCube Spiking Neural Network architecture trained through unsupervised (STDP) and then supervised (dynamic evolving SNN (deSNN)) learning and automated using a Finite Automata	SNN enables discovery of significant features from raw EEG. Integration of finite automata with SNN improves classification accuracy and robustness of online control	Kumarasinghe et al., 2018

2.7 Research limitations of the machine learning methods for decoding neural activity from EEG in restorative Brain-Computer Interfaces

2.7.1 Lack of studies that investigate the performance in predicting complex movements from EEG in motor-impaired people

Although there has been a growing interest in recent literature for advancing the machine learning algorithms used to decode complex movements from EEG (Farid et al., 2010; Gao et al., 2013), a less attention was paid to evaluate their effectiveness in decoding movements in people with movement impairments. This limitation is prominent in cutting-edge brain-inspired approaches for decoding neural activity from EEG in restorative BCI. Table 2.1 summarises recent advancements in brain-inspired methods for decoding movements from EEG. Most of these methods were tested on multiple subjects (T. Li et al., 2013; Tabar, Yousef Rezaei and Halici, 2016; Gandhi et al., 2011, 2014; R. Roy et al., 2012; Kumar et al., 2017; P. Tan et al., 2016; Ren & Wu, 2014; Sakhavi et al., 2015; Hamedi et al., 2014; Scherer et al., 2013; Tayeb et al., 2017; T. Li et al., 2013; Djamal, Esmeralda Contessa and Suprijanto, Suprijanto and Setiadi, 2016) except few studies are limited only for a single subject (Nurse et al., 2016; Liyanage et al., 2009; Duan et al., 2014; J. Liu et al., 2015; M. Li et al., 2016). All these studies were conducted on a healthy participant without any movement impairments. Also, many studies were performed using a small sample size which reduces the statistical power of

the empirical findings.

Many differences can be observed when performing the same functional movement by healthy and paretic people. For instance, a paretic person puts more effort and process a higher amount of cognitive workload to achieve a movement compared to a healthy person. Also, a paretic person may use compensatory strategies which can result in significant changes in joint kinematics compared to the same functional movement performed by a healthy person(Cirstea & Levin, 2000; Hussain et al., 2018).

Studies have shown that these differences are also reflected in the neural activity of the brain (Rossiter et al., 2014; Hsu et al., 2016). Hsu et al. (2016) compare the neural activity in the sensory and motor areas of the brain in healthy people and stroke patients while the participants were performing repeated finger movements. The authors reported changes in alpha and beta brain waves when the finger movement rate was increased in healthy participants. The increment in alpha and beta activity of the brain may indicate the increased cognitive workload when moving the finger at a higher movement rate. A similar effect was also observed when increasing the finger movement rate in the un-affected hand of stroke patients. In contrast, the increase in movement rate of the finger in the paretic hand of stroke patients did not demonstrate changes in the alpha and beta brain activity at different finger movement rates. These observations imply the comparatively higher cognitive workload required for performing movements in a paretic limb compared to the movements in a non-paralysed limb.

To date, only a limited number of studies have evaluated the performance decoding movements from EEG signals in people with movement impairments. Those studies were restricted for only movement intention detection from EEG and can only facilitate a single degree of freedom control of the impaired limb through BCI. Also, non of these methods were brain-inspired machine learning

approaches and therefore considerably contradict with how the animal brain process information for learning and adaptation. Therefore the lack of experimental evidence of the prediction performance, effectiveness and efficacy on decoding complex movements from EEG in paralysed patients by the cutting-edge brain-inspired machine learning algorithms is one of the major limitations in the current restorative BCI literature (Verplaetse et al., 2016).

2.7.2 Lack of interpretability of the machine learning models used in BCI

The commonly used machine learning models for feature extraction and learning in non-invasive restorative BCIs consist of conventional machine learning methods. Some of them are Independent Component Analysis, Support Vector Machine, Generalised Linear Models, Linear Discriminant Analysis, Riemannian geometry, and EEG source localisation. These methods considerably contradict what is already known about information processing in the animal brain. They cannot evolve, learn incrementally or adapt to changes in the environment, require large amounts of labelled data to train, yet can fail catastrophically even with small variations of the input.

The lack of interpretability of computational models used for decoding neural activity is a significant limitation in many BCIs that use less-interpretable machine learning approaches. These approaches result in BCIs that often behave as 'black boxes' (Hong et al., 2010). They do not allow opportunities to extract new knowledge for a better understanding of the cognitive processes when interacting with the BCIs (Tung et al., 2015). This lack of interpretability limits the feasibility of using known knowledge of the cognitive processes in neuroscience for improving the computational model. Further, the lack of interpretability limits the feasibility

of using the known knowledge of the cognitive process in neuroscience for improving the machine learning model.

2.7.3 Limited ability to perform real-time predictions due to high prediction latency

High latency in predicting movements from EEG is another limitation in current restorative BCIs. The ability to decode neural activity from single trials EEG with a short latency is an essential requirement for restorative BCIs (Xu et al., 2016). Although the complex learning algorithms have demonstrated the state-of-the-art performance in terms of the prediction accuracy, their complexity results in a higher computational processing power consumption compared to the simple learning algorithms (Skomrock et al., 2018).

Previous research has established the impact of the temporal averaging on the prediction latency in BCIs. Several studies highlight the trade-off between the true-positive rate and the latency of movement intention detection (Skomrock et al., 2018; Xu et al., 2016). Improving the true-positive rate of BCI may cause undesirable impacts on prediction latency or vice versa. Xu et al. (2016) study the impact of the repetitive or the ballistic motor imagery movements on predicting movement intention in healthy participants. Also, the authors investigate the impact of different EEG processing techniques such as time-series analysis and sub-band power estimation on the movement intention prediction from motor imagery EEG. Therefore the high prediction latency of the computational models is another limitation in current restorative BCI literature.

2.7.4 Low information transfer rate and less accuracy in single-trial prediction

A growing body of literature on decoding movements from EEG evident the limitation of the low information transfer rate of BCI. Gao et al. (2013) present a BCI system that results in an average information transfer rate of 0.5 bits per second. This information transfer rate implies an approximately two-second delay after the cue in predicting movement intention from MI-EEG.

The non-stationarity of EEG signals reduce the accuracy of decoding neural activities in BCI systems. Due to the high trial-to-trial, session-to-session and subject-to-subject variability of the signal, several approaches have managed to achieve higher accuracy by taking the average across multiple epochs. This approach maximises the significant statistical features of the EEG signal by eliminating the random noise and therefore improves the prediction accuracy. However, for temporal averaging, the BCI decoder has to wait until it collects a sufficient amount of input data to compute the temporal average. Thus, although the temporal average improves the prediction accuracy, it can also reduce the information transfer rate of the BCI, which limits its feasibility of real-time prediction.

2.7.5 Less accuracy in decoding multi-dimensional movements of the same limb

The conventional neural decoders that utilise the sensorimotor rhythms of electroencephalography generate distinct neural commands through Event-related Synchronisation, and Desynchronisation evoked as a result of moving different parts of the body. For instance, when moving the left hand, the contralateral side (right hemisphere) of the brain shows a significant decrease in EEG power.

Many BCI systems have utilised this natural phenomenon to generate distinct control commands either using imagined or executed movements of different body parts. Although this approach increases the degree of freedom in BCI control, this paradigm results in un-naturalistic control when applied to neurorehabilitation due to the cognitive disconnection between the targeted and intended action. Development of computational models that can decode precise neuro-muscular relationships from EEG will enhance restorative Brain-Computer Interfaces for motor recovery and restoration.

Accurate decoding of precise neuro-muscular interactions that result in multi-dimensional functional hand movements has been demonstrated using invasive neurological signals (Chadwick et al., 2011). However, many non-invasive studies applied in clinical rehabilitation settings have a limited ability to extract precise neuro-muscular interactions from EEG that result in multi-dimensional limb movements. The BCI presented in (Hortal et al., 2015) only detect the start and end of gait by detecting the movement intentions from EEG. Bundy et al. (2012) demonstrate the feasibility of single-dimensional control of a rehabilitation device by stroke patients through overt and imagined movement intentions. These studies were evident that the neural decoders applied in clinical applications to date mainly capable of detecting movement intentions rather than the precise neuro-muscular relationships from EEG. Therefore, these traditional machine learning approaches are limited by less degree of freedom control of the affected limb (Yoshioka et al., 2011).

The clinical studies on restorative BCI interventions to date have not yet demonstrated the feasibility of decoding the dynamics of muscle activity, kinematics and kinesthetics from EEG. Therefore the efficacy of BCIs that decode multi-dimensional movements from EEG in neurorehabilitation has not yet been investigated and remains unclear.

2.8 Current challenges in decoding movements from EEG in motor recovery and restorative BCI interventions

2.8.1 Poor spatial resolution and the 'volume conductance' effect of EEG

Compared to the other neurological signals that monitor the neural activity of the brain such as Electrocorticography, Local Field Potential and functional Magnetic Resonance Imaging, EEG monitors the neural activities non-invasively, at a higher temporal resolution, less expensively and under a minimal risk. Therefore, EEG shows higher potential in BCI applications which suites for every-day life. However, being a non-invasive neurological signal, EEG suffers from the 'volume conductance effect' (Rutkove, 2007) which distorts the original electric potential as a result of travelling from its origination to the skin surface of the head including grey matter, white matter, dura, skull and skin. The statistical features such as co-variance, correlation, spectral features and features from the time-frequency domain for online EEG classification results low accuracy and often fail during online EEG classification (Klonowski, 2009; N. Li et al., 2016).

2.8.2 Motor re-learning causes evolving changes in the neurological signals over time that cause concept drifts in neural decoders

Neurorehabilitation aims to restore the impaired movements by inducing the neuroplasticity of the brain. The repetitive exercises indicate promising results for motor recovery in neurorehabilitation. The successful repetitive attempts

of motor re-learning cause behavioural changes during and after rehabilitation therapies. Some of them are the amount of planning, effort and attention required for performing the movement as the patient involvement in the rehabilitation practices. Studies have shown that motor re-learning also result in changes in the neurological signals that evolve during motor recovery.

Through neurorehabilitation, it is expected that the patients incrementally learn to regain the affected movements. Changes to the neuronal activation patterns during neurological recovery was reported in several brain connectivity analysis studies (Canuet et al., 2015; Ochoa et al., 2014; Westlake & Nagarajan, 2011). These studies provided evidence that the neural activities in stroke patients demonstrate significant changes before and after the BCI-based neurorehabilitation interventions. Yilmaz et al. (2013) shows significant decreases in peak MRCP amplitude and as well as delayed onset of MRCPs after the neurorehabilitation therapies. This implies that the patients required less mental effort and planning as a result of motor re-learning. Savic et al. (2014) also indicate a higher variability of post-intervention Motor Evoke Potentials, providing evidence on the ongoing changes in the motor cortex during rehabilitation therapies.

Due to the changes in neural activity patterns during neurorehabilitation interventions, the traditional neural decoders that have fixed classification boundaries are unable to adapt to the plastic changes in the brain activity during long-term rehabilitation sessions. As the patient incrementally learns to regain the affected movements, the non-adaptive neural decoders that utilise statistical features of the EEG signal for predicting neural activities of the brain often fail due to this concept drifts in EEG (Chowdhury et al., 2017; Ang & Guan, 2016). Y. Zhang, Prasad et al. (2017) highlights the importance of adaptively finding EEG channels that contain important information during longitudinal experiments. The computational approaches used in restorative BCIs should be equipped with the

ability to adapt to these physiological changes as the patient become more familiar with the rehabilitation task (Cella et al., 2014). Also, to optimise motor learning, the patient's voluntary involvement in the task should be enhanced by carefully controlling the amount of support during the neurorehabilitation task (Freeman et al., 2012; Grimm et al., 2016). It is important to embed incremental and adaptive learning in the machine learning approach that decodes movements from EEG in restorative BCI, to match this adaptability in biological neural networks.

2.8.3 Variability of electroencephalography features

The non-stationarity of EEG signals results in high variability in the statistical features of EEG signals over time. This variability is significant across different individual participants, session, and even individual trials (Han & Im, 2014). Non-stationarity of EEG causes significant trial-to-trial and subject-to-subject variability. Taking the grand average over multiple trials is a classical approach for eliminating the variability of the signal. However, the grand average only provides an average activity of brain over multiple trials and does not indicate any dynamic and behavioural variability observed during single-trial analysis (K.-R. Müller et al., 2008). Thus grand average has a less significance for online EEG classification (Arieli et al., 1996).

Mainen and Sejnowski (1995) discuss the reliability of spike timing in neocortical neurons and shows precise spike timing of individual neurons for a variable input current. They show that the intrinsic variability of neurons is arising from multiple inputs to the neuron received from the other neurons of the population through synaptic connections. Tessadori et al. (2012) studies the variability of spike trains in cortical neurons for developing Brain-Computer Interfaces. They argue that a large component of variability comes from the synchronous inputs produced by

signals arriving from multiple sources. Two causes of the variability in EEG are,

- The external physical factors originated from the data collection devices and method
- The internal physiological factors originated by the intrinsic variability of spiking activity of neurons in the brain.

Many previous studies on EEG classification only address the first component of the variability through different forms of filters influenced by the principles in digital signal processing. However, the neurobiological basis of this variability is poorly understood and understudied in the context of BCI mainly when applied to BCI for neurorehabilitation, where the patient incrementally learns to regain the affected movements.

2.8.4 Decoding precise neuro-muscular relationships from EEG that can generate complex functional movements

The sensory and motor homunculus indicates that the neuronal populations which are responsible for motor control and sensation of a particular part of the body, such as the right upper limb, are spatially located in a tiny cortical area of the brain, because of this spatial density, different movements of the same limb results in less spatially distinguishable patterns in neural activity. It is more challenging when decoding such movements from EEG signals due to the poor spatial resolution (Burle et al., 2015), low signal-to-noise ratio and the volume conductance effect (Rutkove, 2007) of EEG. Therefore, decoding complex functional movements that require extraction of neural correlates of muscle activity and joint kinematics from EEG is a significant challenge in non-invasive BCI.

2.8.5 Real time prediction

Due to the low signal to noise ratio and high variability of the EEG features across different trials, sessions, and participants, the machine learning algorithms used for decoding movements often use temporal averaging to eliminate random noise. In addition, the complex machine learning algorithms that depend on a significant amount of pre-processing, feature extraction and selection to extract significant EEG features that permit accurate prediction. These two approaches have demonstrated a sufficient level of accuracy in decoding movements from EEG. However, long temporal averaging and high computational complexity of the machine learning algorithms increases the prediction latency of the neural decoder and limits the feasibility of real-time control through BCI (Chou et al., 2015; Niazi et al., 2011; Ibáñez et al., 2017). There is a trade-off between the prediction accuracy and the prediction latency in BCI. The optimisation of prediction accuracy without compromising the latency of prediction and vice versa is a key challenge in BCI.

2.8.6 Enabling naturalistic motor control through self-paced BCI

The asynchronous BCI paradigms enable the BCI users to perform an intended action at the desired time and result in self-paced movements through the BCI. The asynchronous BCI generate more naturalistic motor control as the users do not have to wait for an external cue to initiate the movement. However, a majority of the existing body of research on restorative BCI follows a synchronous BCI paradigm where the BCI users were instructed to perform the intended action in response to an external cue. Such cue-base synchronised BCI paradigms do not fully represent a natural form of motor control through a BCI as the user have to

wait for an external cue to initiate the movement.

With the presence of a visual or auditory cue, the sensory information of the external stimuli is propagated through the dorsal and ventral pathways of the brain which consists of the cortical areas responsible for recognising and processing the cue (van Polanen & Davare, 2015; Goodale et al., 2005). A neural decoder used in synchronised BCI can benefit from these additional significant EEG features that emerge in response to the external cue, which is not directly related to planning and executing the intended movement. In contrast, the EEG signals obtained during a self-paced movement represent the neural activity mainly related to planning and executing a self-paced movement. To succeed, the neural decoder of a self-paced BCI should be able to extract movement intentions of the user from neurological signals without any extra information (Müller-Putz et al., 2006). Decoding self-paced movements is more challenging than the cued movements as the neural decoder should extract precise neuro-muscular relationships from EEG related to planning, execution and coordination of different body parts that contribute to the movement.

2.8.7 Less understanding about the natural mechanisms of the brain that give rise to human cognitive abilities

The human brain has a remarkable potential that emerges as a result of learning, adaptation, memory formation, recognition and recalling abilities in humans. However, compared to the complexity of the natural mechanisms that give rise to these abilities, less is know about the underlying biological processes of the brain that generate them. Neuroscience aims at understanding the neural circuitry, electrochemical processes of signal transmission mechanisms in the neural circuits and patterns of neural activity that produce different animal behaviours and thought

processes. Computational neuroscience as a subset of neuroscience investigates the natural computational mechanisms that give rise to these behaviours and attempt to quantify and derive mathematical relationships that represent them as computational elements in electronic systems.

Previous studies have shown changes in neural activity of the brain after lesions (Wei et al., 2009) and as well as during motor recovery (Yilmaz et al., 2013; Savic et al., 2014). However, a little is known about the neurobiological impact of the lesion itself and its nearby brain areas in repairing and restoring the affected movements. Research to date on decoding movements from EEG signals in restorative BCI has not yet adequately utilised the neural mechanisms of motor control and motor re-learning that has already been explained in neuroscience (Y. Zhang, Prasad et al., 2017). A majority of machine learning algorithms that were used to decode movements from EEG behave as mere function approximators that intend to quantify the relationship between the input and output variables.

One of the substantial challenges of machine learning methods used by restorative BCI is that the fundamentals that construct these machine learning methods do not provide sufficient support for incorporating the natural mechanisms of neural computing. They do not pay much attention to the neurobiological basis that gave rise to different Event-Related Potentials in EEG used as features for prediction in BCI. This multi-disciplinary field of research requires integrating the expertise from many areas of research, including neuroscience, health, artificial intelligence, electronics, digital signal processing, behavioural analysis in order to improve restorative Brain-Computer Interfaces. Development of a computational platform that can integrate all these multi-disciplinary expertise is one of the significant challenges in BCI research.

2.9 Future research directions of restorative Brain-Computer Interfaces

Despite the success in decoding movements from EEG useful for motor recovery and restoration in the growing body of BCI literature, several questions remain to be answered. This section highlights several future directions to improve the machine learning methods used by restorative BCIs.

2.9.1 Develop methods for better understanding of brain dynamics

A better understanding of brain dynamics that represent complex cognitive processes in the brain would be helpful to improve movement decoding from EEG. More information on how the underlying cognitive processes impact the neural responses observed through EEG would help to establish a greater degree of accuracy and interpretability in BCI. Previous studies on decoding movements from EEG for neurorehabilitation interventions have established the significance of brain activity in sensory and motor cortices. The ERD and ERS observed from the EEG electrodes that monitor these cortical areas such as the C3, C4, and Cz channels have demonstrated their significance in decoding movement intention (Jochumsen et al., 2015).

In addition, studies have also reported the involvement of the cortical regions beyond the sensorimotor areas of the brain in predicting movement intention. Özdenizci et al. (2017) reports the involvement of the Parieto-Occipital (PO) and Fronto-Parietal (FP) areas of the cortex during movement intention. The authors suggest the use of the beta wave strength of the Parieto-Occipital region at rest as a significant feature for movement intention prediction. The study

also claims changes in the pre-trial beta wave strength in the Fronto-Parietal regions during movements. Bundy et al. (2012) shows the feasibility of utilising the ipsilateral (same side of the body) motor signals obtained from the unaffected hemisphere of hemiplegic stroke survivors for predicting movement intentions of the paralysed hand from EEG. Formaggio et al. (2016) analyse the topographical distribution of ERD or ERS and as well as the task-related coherence during lower limb movements in healthy participants. The study intends to enhance the understanding of oscillatory activity and functional interactions of different brain areas during lower limb robot-assisted rehabilitation. Biasiucci et al. (2011) present a spatio-temporal analysis of EEG topographic in stroke patients during upper limb movements. These topographies represent EEG microstates which may imply the plastic changes in the associated neural network while providing neurofeedback for enhancing motor recovery. These findings highlight the importance of investigating the potential of neural activity beyond the sensory and motor areas of the brain during BCI interventions that intend to gain motor recovery.

The traditional approaches that use the static energy-based features such as SVM, MLP, LDA have a limited ability to capture complex spatio-temporal dynamics (Forney & Anderson, 2011; M. Li et al., 2016). Further research is required to implement machine learning algorithms that can extract spatio-temporal brain dynamics that emerge as a result of different brain areas coordinate and collaborate to execute functional movements in humans. Future research should explore the effectiveness of the extracted brain dynamics to improve movement decoding.

2.9.2 Improve the biological plausibility of the computational models that analyse the neural activity of the brain without compromising the prediction performance

The biological plausibility plays a significant role in embedding intelligence in machines. On one hand, the human brain represents the greatest form of intelligence so far we have come across. So, imitating its natural mechanisms that give rise to human intelligence may be a promising step towards developing intelligent machines. On the other hand, it enhances the understanding of the information processing in the brain and provides new inspirations on improving the existing intelligence systems. However, the precise natural mechanism that gives rise to human intelligence through various human abilities such as learning, adaptation, memorising, and recognition in humans remains under-explored. Further modelling work will be required in order to integrate these natural mechanisms in computational systems.

Improving the biological plausibility of the machine learning methods that decode movements from EEG is a promising approach towards addressing the limitations of traditional methods used in the existing BCI research. The future research on transferring the traditional batch learning-based algorithms into incremental and adaptive learning algorithms will address several challenges in restorative BCI. For instance, adaptive learning will enable the machine learning models to self-regulate their internal representation of the relationship between input and output variables of the model using the current response produced by the computational model. The neural decoder will have the ability to learn from its own mistakes as humans do. Also, they will facilitate the auto-calibration of the neural decoder and deliver plug-and-play BCI systems.

From the rehabilitation point of view, adaptive learning of the neural decoders also supports optimising the assistance ('assistance-as-needed') to patients during therapies and eliminate the risk of slacking when the assistance is too supportive (Grimm et al., 2016). Several studies have shown the feasibility of employing reinforcement learning to make the computational approach used in a neuroprosthesis adaptable to the environment (Bauer & Gharabaghi, 2017). Jagodnik et al. (2016) and Grimm et al. (2016) present reinforcement learning-based adaptive learning controllers to adjust the amount of assistance in different neurorehabilitation settings.

In the context of restorative BCI, further research should be undertaken to explore how neural responses of different brain areas that collaboratively involved in executing movements. These neural responses can be used to inform self-regulation in the machine learning model used by BCI in response to the plastic changes that emerge during motor re-learning. For instance, Error-related Potentials represent natural cortical responses that represent feedback and error correction in response to human actions. Future research can investigate the effects of Error-related Potentials on influencing self-regulation in neural decoders. To achieve this goal, improving the biological plausibility of the neural decoder by integrating the natural mechanisms that enable learning, adaptation, memory formation and recalling in living nervous systems should be appropriately integrated into digital systems.

2.9.3 Enable automatic feature learning in neural decoders in contrast to the conventional hand-crafted feature engineering

In contrast to the conventional feature engineering approaches that include multiple hand-coded steps such as prepossessing, feature extraction, dimensionality reduction, and feature selection, future research would aim at enabling automatic feature learning from raw input data. Automatic feature learning will also eliminate the need for manual feature engineering that require a considerable amount of human intervening, which becomes more challenging in huge datasets.

Deep neural networks applied in movement decoding from EEG have shown the ability to learn discriminative features from raw data. They eliminate the need for hand-crafted EEG features. However, the size of the data set and as well as the quality of data have a significant impact on achieving a desirable classification performance in deep learning (Nurse et al., 2016). Although complex classification algorithms such as neural networks that utilise explicit feature engineering processes have shown a higher classification accuracy, they result in a considerable delay during online prediction due to high computational cost and prediction latency. Therefore, it is equally important to optimise the complexity of deep learning methods through simple network architectures that do not consume a large amount of processing power in digital systems (Boi et al., 2016; Martišius et al., 2013; Hamedi et al., 2014).

The human brain, that processes a massive amount of information within a fraction of a second while consuming an ultra-low amount of computational power is a great inspiration to address the limitations caused by the von Neumann bottleneck in traditional computer architectures. Further research could also be conducted to develop biologically plausible automatic feature learners that are

compatible with neuromorphic platforms. The success in this research direction will combine the best of both approaches by integrating the massively parallel information processing ability in neuromorphic architectures and as well as the accurate prediction delivers by deep neural networks.

2.9.4 Integrate neurofeedback of motor control with the conventional uni-directional BCIs to enable bi-directional closed-loop motor control through BCI

Motor control is a bi-directional perception-action loop that consists of transiting over different cognitive states such as movement intention, action, feedback and perception. Many BCI studies have mainly concentrated on decoding information from EEG that are useful to predict movement intention and execution in motor control. There has been less attention on integrating feedback and perception of the action in neural decoders. Future research would focus on the development of bi-directional closed-loop BCIs that integrates neurofeedback with the conventional uni-directional BCI control to enable both action and perception during motor control.

2.9.5 Develop hybrid BCI systems by integrating multiple multi-model information sources to improve prediction accuracy

The motor circuit of the brain consists of cortical areas such as the visual and motor cortex and as well as deep brain areas such as basal ganglia. In addition, the spinal cord and peripheral nerves also contribute to executing movements in humans. Figure 2.3 graphically represents the neural circuit of motor control in

humans (Scott, 2004). Each sub-network in this neural circuit plays a vital role in performing the movement.

It is also important to note that there exists a short circuit from the periphery to the cerebellum to the brainstem and back to muscles that can work faster and independently from the cortical circuit. This circuit has been underestimated in the existing BCI application. The cerebellum involves automated and semi-automated repetitive motor movements like walking. NeuCube has an architecture that supports the involvement of both the cerebellum and cerebrum activity. However, there are practical limitations to incorporate the cerebellum activity within the model. The conventional EEG measurement systems do not contain dedicated electrodes to measure cerebellum activity. The electrodes that monitor the occipital lobe (i.e. Oz, O1, O2, O3, O4) can partially pick the cerebellum activity due to its proximity. However, they may be mixed up with brain activity related to vision originate from the occipital lobe. Also, due to the head and neck movements, there are many EEG artefacts when monitoring cerebellum activity using EEG. Further studies are required to evaluate the feasibility of effectively utilising this short circuit for automated and semi-automated motor movement recovery and rehabilitation with BCI.

It is evident that beyond the sensory and motor cortices, many parts of the human nervous system contribute to executing a movement. However, non-invasive recordings of brain activity such as EEG do not carry neural activity of all these components of the neural circuit. Previous studies have emphasised the importance of integrating different information sources that represent useful information related to motor control for accurate and robust BCI control.

A hybrid-BCI use multiple data sources in addition to EEG signals, such as audio and visual data, electrophysiological signals such as Electromyography, Electrooculography that provide additional information to facilitate accurate,

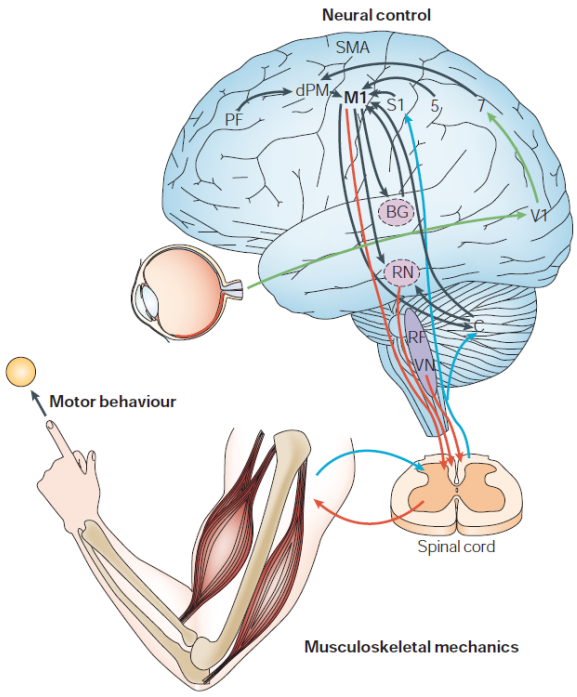

Figure 2.3: A graphical representation of the neural circuit of motor control in humans (Scott, 2004)

robust and multi-dimensional control through BCI. These sources are exhibit multi-model and multi-dimensional form of information and therefore integrating them into a single computational model that can process all this information is challenging.

2.10 Discussion and motivation of the research

Brain-Computer Interfaces monitor neural activity of the brain and translate them into machine commands. This technology enables control of digital devices through mental commands extracted from brain waves of the BCI user. Studies have shown promising results on motor recovery in people with movement impairments through restorative BCI interventions. This chapter critically examined previous research on decoding movement useful for restorative Brain-Computer Interfaces

with a particular focus on the limitations, challenges and future directions of the machine learning algorithms used for decoding movements from EEG.

Overall, these studies highlight the need for improving the machine learning method to extract precise neuro-muscular relationships from EEG signals. In all the studies reviewed here, the less biological plausibility, less interpretability, high prediction latency, low degree of freedom are recognised as significant drawbacks. The human brain, as the highest form of intelligence known to us, is a powerful inspiration to develop intelligent machines. Human-engineered machine learning methods used in these studies largely contradict what is already known about information processing in the animal brain. They have a limited ability to evolve, learn incrementally or adapt to changes in the environment similar to humans. These methods require large amounts of labelled data to train, yet can fail catastrophically even with small variations of the input. Together these studies provide important insights into the brain-inspired machine learning methods and architectures to decode movements in restorative BCI.

Spiking Neural Networks as the third generation of Artificial Neural Networks, more closely model the behaviour of a living nervous system as it considers both spatial and temporal aspects of input data for building the computational model. This thesis presents a Brain-Inspired Spiking Neural Network model to address the above limitations in current BCI literature. BI-SNN enables precise spike timing in spiking neural populations using spike-time based learning rules and provides a promising direction for building a new type of BCI called Brain-Inspired Brain-Computer Interfaces (BI-BCIs).

2.11 Summary of the chapter

This chapter presented a review of recent advancements in decoding mental commands from EEG signals in Brain-Computer Interfaces for motor recovery and motor restoration. A general overview of the Brain-Computer Interfaces, including different types of BCIs and the common BCI paradigms presented in the literature, was described at the beginning of the chapter. Next, different applications of BCI were discussed with a particular focus on restorative Brain-Computer Interfaces that applied to gain motor recovery and restoration. The chapter outlined several proof-of-concept studies on healthy participants and as well as multiple clinical studies of EEG-based BCI interventions in people who suffer from movement impairments such as paralysis. The chapter then presented a detailed methodological review of the brain-inspired Artificial Neural Networks based methods for decoding movements from EEG. It highlighted the limitations of decoding complex movements from EEG that are useful for motor recovery by these cutting-edge brain-inspired methods. Then, the chapter presented several challenges in decoding such movements from EEG useful for BCI interventions aimed at gaining motor recovery. The chapter proposed multiple future directions to improve the machine learning algorithms used for decoding movements from EEG. The chapter concluded with a general discussion that emphasised the motivation for conducting the research proposed by this thesis.

2.12 Contributions

1. The chapter presented an overview of the Brain-Computer Interface technology and critically analysed previous research on decoding various movements

from Electroencephalography signals in restorative Brain-Computer Interfaces

2. The chapter presented a methodological review of the recent trends in Artificial Neural Networks based neural decoders to construct restorative Brain-Computer Interfaces

3. The chapter highlighted several critical limitations of the existing machine learning approaches and challenges to decode movements from EEG signals in BCI interventions which aim to achieve motor recovery

4. The chapter identified several future directions to improve the state-of-the-art in restorative Brain-Computer Interfaces

5. The chapter highlights the significance of a biologically plausible brain-inspired machine learning approach to address the limitations of traditional neural decoders used by current restorative Brain-Computer Interfaces

Chapter 3

Brain-Inspired Computing, Spiking Neural Networks and the NeuCube Spiking Neural Network Architecture

> "There is no scientific study more vital to man than the study of his own brain. Our entire view of the universe depends on it."
>
> *Francis Crick - A molecular biologist, biophysicist, and neuroscientist best known for his work with James Watson which led to the identification of the double helix structure of DNA*

Chapter Overview

The previous chapter highlighted the limitations of the current non-invasive BCI research applied in neurorehabilitation. The chapter emphasised the need for a brain-inspired computational approach to address the limitations in the

existing neural decoders. This chapter will present an overview of brain-inspired computing, Spiking Neural Networks, and the NeuCube Spiking Neural Network architecture. The chapter will first establish the foundation of brain-inspired computing by providing a brief overview of the biological processes in living nervous systems that give rise to the transmission of action potentials and the evolution of synaptic plasticity in biological neural networks. Furthermore, a brief description of brain-inspired computing and its evolution will be presented with a particular focus on the third generation of Artificial Neural Networks called Spiking Neural Networks. The chapter will briefly introduce neural coding and describe different spike encoding methods to extract spiking events from temporal data. The chapter will also describe several spiking neuron models that computationally model the passive membrane potential of a living neuron. This will be followed by a brief description of the spike-based supervised, unsupervised, and reinforcement machine learning approaches. Finally, a brief description of the NeuCube Spiking Neural Network architecture and the different processes associated with analysing data using the NeuCube framework will be discussed.

3.1 Introduction

The brain is organised in several areas which are specialised to perform specific tasks. For instance, the neurons in the visual cortex are trained for visual information processing, while the neurons in the motor cortex are specialised to execute movements. These different areas of the brain coordinate and collaborate to execute cognitive tasks.

Neurons and synapses form the fundamental computational elements of the brain. An average human brain approximately contains a hundred billion individual neurons and a thousand trillion synaptic connections that interconnect these neurons to form the neural network of the brain. Figure 3.1 A shows an image of the pyramidal neurons in the cerebral cortex (source: *Neuron*, 2012). A typical neuron consists of three parts, the dendrites, the soma (cell body) and a single axon as shown in figure 3.1 B (source: staff, 2018). A neuron receives input signals through dendrites or soma and transmits the output signals away from the neuron through the axon.

Neurons transmit signals as short electric pulses called action potentials or spikes. The action potentials are generated as a result of an electrochemical process that changes the electric potential of the neuron. The neuron's cell membrane maintains a voltage gradient across its membrane called the resting potential (-70mV). The cell membrane of a neuron contains small poses known as voltage-gated ion channels that allow the transmission of ions across the cell membrane of the neuron. The voltage-gated channels are closed when the membrane potential is near the resting potential and gradually start to open with the rising of the membrane potential. This causes the opening of the voltage-gated sodium channels that let positively charged sodium ions flow into the cell, further increasing the electric potential of the neuron (see figure 3.1 C - source: *Action*

Potential, 2013). The starting of an action potential is marked by this increase of the electric potential called depolarisation.

Transmission of ions into the cell that contains a sufficient amount of positive electric charges within a short period that increases the membrane potential over a certain threshold level enables more voltage-gated ion channels to open rapidly and contributes to generating an action potential or spike. The rapid inflow of sodium channels reverses the polarity of the cell membrane and results in closing the voltage-gated sodium channels. The sodium ions are then actively transported back out of the cell membrane. Furthermore, the voltage-gated potassium channels open at this stage and bring back the membrane potential into the resting state potential by sending the potassium channels out of the cell membrane. This period is called the refractory period of an action potential; where the neuron is unable to emit a spike even though it receives input spikes. After the refractory period, the membrane potential is set back to its resting state potential, and the neuron is ready to generate an action potential in response to the incoming input spikes. Figure 3.1 D shows the changes in membrane potential during different stages of an action potential (source: *Action potential*, 2020).

The action potentials are transmitted from one neuron to another through the conjunctions between neurons called synapses. As a post-synaptic neuron receives multiple input spikes from the pre-synaptic neuron, these electric potentials are summed together in the post-synaptic neuron. The pre-synaptic electric pulses which cause a sufficient amount of positive charge to reach the spike threshold causes emission of a spike in the post-synaptic neuron. Once a spike is emitted, the membrane potential is repolarised and then gradually set to its resting potential.

The figure shows the response of a single neuron in the somatosensory neocortex of a Wistar rat to a constant somatic input current (data obtained from Gerstner & Naud, 2009). As the intensity of the input current increases, the neuron fires

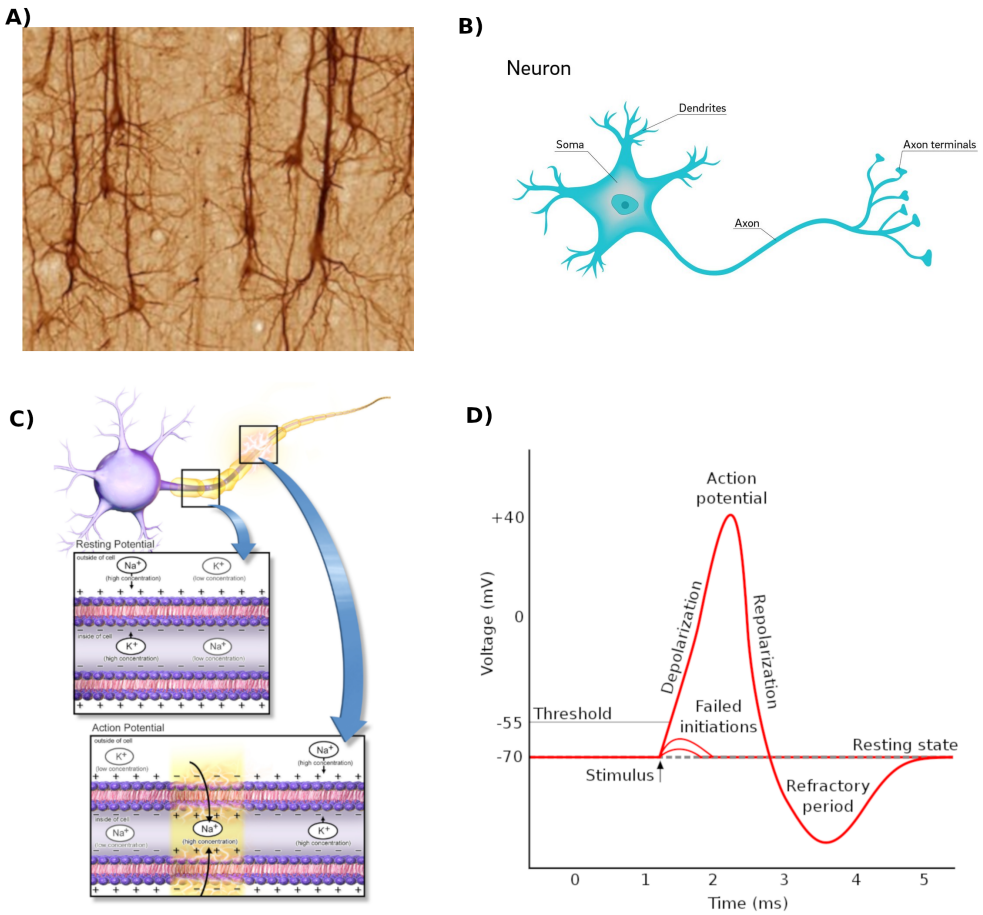

Figure 3.1: Fundamental components of the brain's neural network and the basic steps in its' signal transmission mechanism A) An image of pyramidal neurons in the cerebral cortex (source: (*Neuron*, 2012)) B) Illustration of different parts of a neuron (source: (staff, 2018)) C) Mechanisms of ion transmission across the neuron membrane during the propagation of an action potential (source: (*Action Potential*, 2013)) D) Different stages of an action potential and changes of the membrane potential during these stages (source: (*Action potential*, 2020))

spikes at a higher firing rate as a result of receiving more positive charges that depolarise the cell membrane rapidly.

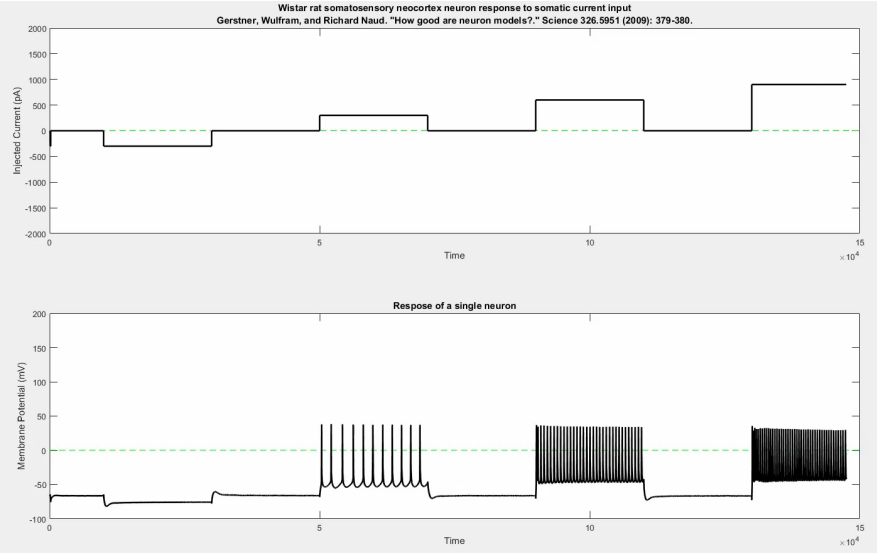

Figure 3.2: Response of a single neuron in the somatosensory neocortex of a Wistar rat to a constant somatic input current (data source: (Gerstner & Naud, 2009))

The conjunction between two neurons that allow communication between neurons via an electro-chemical process is known as a synapse. Action potentials are passed from one neuron to another through synaptic connections forming neural pathways in the brain. The strength of synaptic connections between neurons are changed over time resulting in evolving connections in the brain network. This is known as the plasticity of the brain that shapes the ability of learning and adaptation in animals. With training, the brain develops new neural pathways that can be activated from relevant stimuli. Neuroplasticity is the brain's ability to form and reorganise synaptic connections over time. Neuroplasticity is a key feature of the brain's neural network that results in its incredible capability to evolve through life-long and adaptive learning. From a computational neuroscience perspective, neuroplasticity is defined as the ability to increase or decrease the synaptic efficiency between two neurons according to the firing time of these

pre-and post-synaptic neurons. Such adaptation of nerve cells during learning was explained by the Hebb's postulate (Hebb, 1949), which later became the basis for the synaptic learning rule in many artificial neural network algorithms.

3.2 Brain-Inspired Computing

Inspired by the natural computational mechanisms in the biological neurons and synapses, neuromorphic computing (K. Roy et al., 2019) initially started to interpret such features in digital systems using silicon transistors. Later on, this research field emerged into the development of largescale neuromorphic chips that facilitate both hardware and algorithmic support to implement complex and massively parallel brain-inspired computing architectures. Many recent studies explore the feasibility of spike-based computational models that are implemented on or compatible with neuromorphic computational platforms to deliver scalable, energy-efficient, and biologically plausible machine intelligence systems. The computational approaches that are inspired by the biological processes of a living nervous system have provided new insights into artificial intelligence. Recent literature reveals several brain-inspired computational models that aim to provide a better understanding of information representation, processing, learning, and adaptation in the brain.

3.2.1 A Simple Electronic Circuit for Modeling the Membrane Potential of a Neuron

The electrical behaviour of the passive cell membrane of a neuron can be modelled using a simple electronic circuit that contains a resistor and a capacitor (R-C Circuit) as shown in figure 3.3 (source: Gerstner et al., 2014). A short electric

pulse is injected into the circuit by keeping the switch on for a short period. As more electric pulses receive, the electric potential of the circuit is increased and exponentially reduced with the absence of electric pulses.

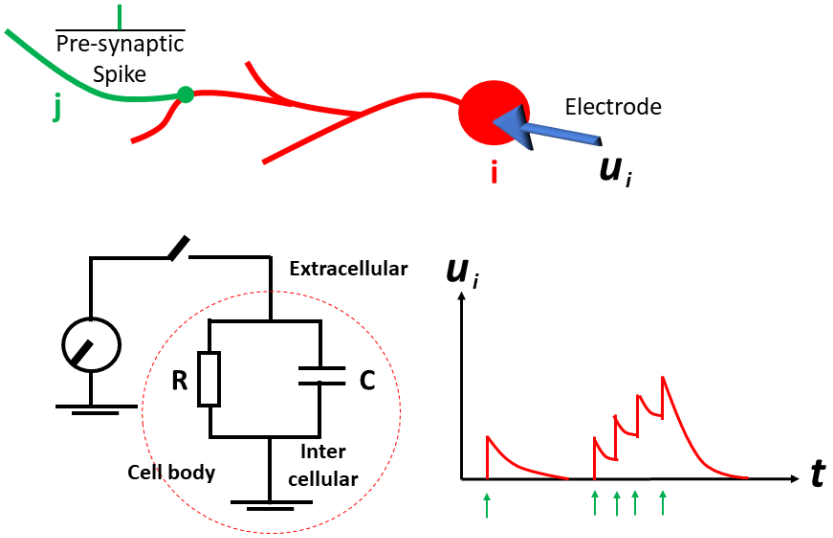

Figure 3.3: An electronic circuit for modelling the behaviour of passive cell membrane of a neuron

The response of the RC circuit for time-dependent arbitrary input current can be mathematically derived, which forms the basis of the Leaky Integrate and Fire neuron model discussed later in this chapter. Figure 3.4 contains an R-C Circuit that models the behaviour of the passive neuron membrane. In addition to the resistor and the capacitor, the circuit also contains a battery to provide the notion of the resting membrane potential (U_{Rest}).

As shown in figure 3.4, the total current injected $I(t)$ will be split into two part as the current flow through the capacitor I_C and the current flow through the resistor I_R. So the total current (I(t)) is given by the equation 3.1.

$$I(t) = I_C(t) + I_R(t) \tag{3.1}$$

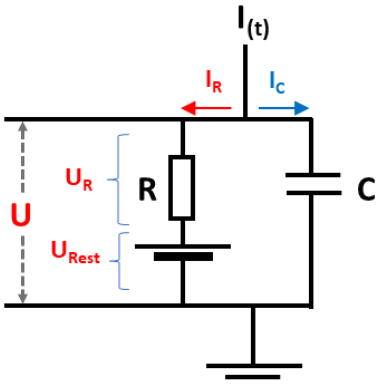

Figure 3.4: Deriving the behaviour of the passive neuron membrane using the R-C circuit

The capacitance of the capacitor is defined as the total charge stored in the capacitor (Q) divided by the total voltage across the capacitor (U) (equation 3.2 and 3.3).

$$C = \frac{Q}{U} \tag{3.2}$$

$$Q = CU \tag{3.3}$$

Likewise, the current (I) is defined as the charge over a unit period of time. By substituting equation 3.3, the current through the capacitor is given by the equation 3.4.

$$I_C = \frac{\mathrm{d}}{\mathrm{d}t}Q = C\frac{\mathrm{d}U}{\mathrm{d}t} \tag{3.4}$$

The total voltage difference U equals the summation of the voltage across the resistor (U_R) and the voltage across the battery (U_{rest}) (refer equation 3.5).

$$U = U_{Rest} + U_R \tag{3.5}$$

From 'Ohm's' law, the voltage across the capacitor is defined by equation 3.6.

$$U_R = RI_R \tag{3.6}$$

By substituting equation 3.6 with equation 3.5, a mathematical representation of the electrical behaviour of the passive membrane can be derived according to equation 3.10.

$$U - U_{Rest} = RI_R \tag{3.7}$$

$$I_R = \frac{1}{R}(U - U_{Rest}) \tag{3.8}$$

$$C\frac{\mathrm{d}U}{\mathrm{d}t} = -\frac{1}{R}\left[U - U_{Rest}\right] + I\left(t\right) \tag{3.9}$$

$$R * C\frac{\mathrm{d}U}{\mathrm{d}t} = -\left[U - U_{Rest}\right] + R * I\left(t\right) \tag{3.10}$$

The resistance of the resistor (R) and the capacitance of the capacitor (C) are constants. A new variable τ is defined to denote R*C which stands for the time constant of the membrane (equation 3.11). Therefore, equation 3.10 can be rewritten as equation 3.12.

$$R * C = \tau \tag{3.11}$$

$$\tau\frac{\mathrm{d}U}{\mathrm{d}t} = -\left[U - U_{Rest}\right] + R * I\left(t\right) \tag{3.12}$$

The membrane potential of the neuron in response to a time-varying synaptic input can be mathematically expressed using the linear differential equation presented in 3.12. This mathematical model is referred to as the Leaky Integrate and Fire (LIF) spiking neuron model.

3.3 Neural Coding

Neural coding is a fundamental issue in computational neuroscience. A long-lasting argument was the mean firing rate carries the information is referred to as rate coding. However, based on behavioural studies that investigated the reaction time in animals, it was evident that the animals can produce response so quickly and the mean firing rate obtained through a long temporal averaging is too slow to explain these fast reactions.

Many recent studies have shown the importance of temporal coding for encoding information in biological neural circuits. This is contradictory to the previous idea that the firing rate of a neuron encodes the essential information. Several animal studies have reported the importance of precise and reliable spike timing in the cortex. Hires et al. (2015) shows the encoding of information in L4 neurons in the somatosensory cortex during active tactile sensation. The analysis shows a low spiking rate in neurons all the time except several milliseconds before the onset of touch stimuli. Mainen and Sejnowski (1995) provide evidence on the reliability of spiking of an individual neuron is by isolating it from the network. The isolated neuron from the neocortex shows precise spike timing of individual neurons for a variable input current multiple trials. The findings suggest that the variable nature of spiking arises due to the interaction with other neurons of the population and inputs received through synaptic connections from neurons in the network.

3.4 Spike encoding

Neurons receive information as short electric pulses called spikes. Spiking neurons intend to computationally model the spike-driven behavior of living nervous

systems that gives rise to different biologically plausible features such as learning, memory formation, and adaptation in Spiking Neural Networks. The temporal input data streams that contain real-values need to be first converted into discrete binary spike sequences to be processed by the spiking neurons. This process is known as spike encoding.

It is important to ensure that the event-related information in the original input data stream is preserved during this encoding process. A successful spike encoding approach will allow fast information processing and reduce the power consumption of the computational system due to the discrete nature of information processed by the system. Also, an effective spike encoding method will represent a way of compressing the content in the original signal and reduce the memory consumption of SNN-based computational models. Petro et al. (2020) presents a comprehensive description and a comparative analysis of multiple spike encoding algorithms. This section briefly describes several spike encoding methods commonly used in SNNs.

3.4.1 Threshold-based Encoding algorithm

The Threshold-Based (TB) encoding method forms one of the simplest forms of spike encoding approaches. As a result of this simplicity, its main advantage is the ability to deliver fast encoding, which fulfils one of the requirements for real-time information processing in SNNs. The temporal difference between the consecutive observations (d) in the input stream (x) is obtained to compute the encoding threshold (refer equation 3.13).

$$d = \sum_{t=2}^{n} |x\,(t-1) - x(t)| \tag{3.13}$$

The mean value ($mean$) and the standard deviation (std) of the computed

temporal differences are calculated to compute the encoding threshold. The standard deviation is first multiplied by a predefined variable referred to as the encoding factor (c) and then added to the mean value of the computed temporal differences to obtain the encoding threshold (see equation 3.14).

$$th = mean(d) + c \cdot std(d) \tag{3.14}$$

The sign of the threshold value can be used to form both positive (th_+) and negative (th_+) encoding thresholds as per equation 3.15.

$$th_+ = th; \;\; th_- = -th \tag{3.15}$$

Depending on the polarity (sign) of the temporal difference, the TB encoding method can extract both positive and negative spikes from the input signal. If the current temporal difference is larger than the positive threshold, a positive spike is generated, and if it is smaller than the negative threshold, a negative spike is produced. Otherwise, no spike event is added to the current time interval of the spike train (refer equation 3.16).

$$s(t) = \begin{cases} 1 & if \quad d(t) >= th_+ \\ -1 & if \quad d(t) <= th_- \\ 0 & otherwise \end{cases} \tag{3.16}$$

3.4.2 Bens Spiker Encoding algorithm

Stimulus estimation is another approach commonly used for estimating spike sequences from analogue signals. Its primary goal is to approximate the actual response of a biological neuron through linear filtering. The Bens Spiker Algorithm (BSA) proposed in (Schrauwen & Van Campenhout, 2003) is one of the stimulus

estimation based spike encoding method commonly used in SNNs. In such an encoding paradigm, the estimated stimulus s_{est} can be formulated as equation 3.17 where x_t denotes the spike train of the neuron and h_t is the impulse response of the linear filter.

$$s_{est} = (h * x)(t) = \int_{-\infty}^{+\infty} x(t-\tau)h(\tau)\, d\tau = \sum_{k=1}^{N} h(t-t_k) \tag{3.17}$$

The spike train of the neuron $x(t)$ can be written as equation 3.18 where t_k represents the firing time of the neuron.

$$x(t) = \sum_{k=1}^{N} \delta(t-t_k) \tag{3.18}$$

BSA encoding first creates a Finite Impulse Response (FIR) filter. At every time interval (τ), the BSA encoding computes two types of error metrics. The first error is calculated by deducting the filter coefficients from the subsequent signal values as per equation 3.19.

$$e_1(\tau) = \sum_{k=0}^{M} abs(s(k+\tau) - h_k) \tag{3.19}$$

The second error is calculated without subtracting the filter coefficients as per equation 3.20.

$$e_2(\tau) = \sum_{k=0}^{M} abs(s(k+\tau)) \tag{3.20}$$

For spike encoding, if the $e_1(\tau)$ is smaller than $e_2(\tau) - th_{BSA}$, a spike event is generated and deduce the filter from the input. Otherwise, no spike event is generated (refer equation 3.21 where th_{BSA} denotes the encoding threshold of BSA)

$$s(\tau)\begin{cases}1 & if \quad e_1(\tau) < (e_2(\tau) - th_{BSA}) \\ 0 & otherwise\end{cases} \tag{3.21}$$

Studies have shown the feasibility of the BSA encoding algorithm to encode different types of signals such as audio and electroencephalography signals into spike trains. Verstraeten et al. (2005) evaluated the performance of the BSA encoding algorithm to encode audio signals into spike trains to recognise isolated spoken digits using a Liquid State Machine. The study was further extended in (Schrauwen et al., 2007) to explore the construction of a digital hardware architecture based on a Liquid State Machine that performs speech recognition of isolated digits. Nuntalid et al. (2011) applied BSA to encode electroencephalography signals into spike trains to classify auditory and visual stimulus from EEG using an evolving probabilistic Spiking Neural Network.

3.4.3 Other spike encoding methods

Apart from the spike encoding algorithms mentioned above, there are several other encoding methods proposed in the literature to extract spike sequences from data streams. Step-Forward (SF) encoding utilises a moving baseline with a predefined encoding threshold. Moving-Window (MW) spike encoding utilises a baseline of the signal as the average of earlier signal intensities within a predefined time window which enables MW encoding to be robust to noises in the input signal up to a certain extent. The NeuCube Spiking Neural Network framework facilitate spike encoding using TB, BSA, SF, and MW encoding algorithms (N. Kasabov et al., 2016). Recently proposed GAGamma encoding algorithm (Sengupta & Kasabov, 2017) not only facilitates accurate pattern recognition in fMRI signals but also efficiently compress the original data for cost-effective data storage and

transmission.

Spike encoding plays a vital role in SNNs. One of the major drawbacks is the information lost during the encoding process. Therefore, it is essential to carefully choose a suitable encoding method that is compatible with the signal characteristics and as well as to appropriately optimise the parameters of the encoding algorithms to minimise information loss.

3.4.4 Optimisation of spike encoding methods

Petro et al. (2020) presents a systematic analysis of the Threshold-Based, Step-forward, Moving-Window, and Bens Spiker encoding algorithms. The authors quantitatively and qualitatively analysed these encoding methods and presented a recommendation for the selection and optimisation of spike encoding methods. The recommendations include, firstly the authors suggesting carefully considering the characteristics of the original signal for selecting an appropriate encoding method. Secondly, optimising the parameters of the encoding algorithm using a suitable error calculation method that indicates the difference between the actual and reconstructed signals. Petro et al. (2020) evaluated multiple statistical measures such as the Signal-to-Noise Ratio (SNR), Root Mean Square Error (RMSE), and R-squared (R^2). SNR is the ratio between meaningful input power and background noise power. In the analysis, the noise power of the signal is derived as the power difference between the original and reconstructed signals. RMSE is the standard deviation of the prediction errors and indicates the distance between the actual and predicted values of a statistical model. R^2 is a statistical measure that indicates the variance of a dependent variable that is derived through regression of one or many independent variables. Thirdly, validating the encoding method by comparing the original signal and the encoded spike trains.

3.5 Evolution of Brain-Inspired computing and Spiking Neural Networks

Artificial Neural Networks are computational models that are inspired by biological neural networks in living beings. They are exceptional at discovering hidden relationships between inputs and outputs; in particular when it is hard to find explicit mathematical equations that describe such relationships. There are three generations during the evolution of ANN. The Perceptron or threshold gates which generate a binary output using a threshold belongs to the first generation of ANN. Perceptron does not use a non-linear activation function for output prediction. The second generation of neural networks such as Multi-layer Perceptron applies non-linear activation functions on the weighted sum of the synaptic input. Spiking Neural Network, as the third generation of neural networks more closely model the computation that takes place in biological neural networks.

All forms of sensory inputs such as sound, smell, light are first transformed into action potentials or spikes before being processed by the neurons for learning or recalling. Being the third generation of Artificial Neural Networks, Spiking Neural Networks consider the spiking nature of neurons. Spiking neurons capture the most crucial dynamics of information processing in the animal brain as such models consider encoding of information in terms of the spikes and memory as the strength of synaptic connections. The remainder of this section presents an overview of the computational elements that construct Spiking Neural Networks.

Being the third generation of Artificial Neural Networks, Spiking Neural Networks considers the spiking nature of neurons. Therefore, Spiking Neural Networks captures the most crucial dynamics of information processing in the animal brain as it considers encoding of information in terms of the spikes or action potentials

and memory as the strength of synaptic connections. SNN combines several computational models that mathematically describe the spiking nature of a neuron and properties of a neural network such as synapses and synaptic plasticity, resulting in a biologically plausible model of human learning.

3.6 Spiking Neuron Models

With the ever-growing interest in understanding the computation in neural circuits for describing such computations in individual neurons and neural populations, several spiking neuron and synaptic models are being emerged. Each model models certain aspects of information processing in the brain. For instance, the Integrate and Fire model, Spike Response Model, and Hodgkin–Huxley model describe information processing at the neuronal-level as a result of the current passed through the ion channels in the neuron membrane. The long term goal of computational neuroscience is to understand the neural dynamics better and describe the behaviour of neural circuits in the same manner compared to electronic circuits. The following section briefly describes several commonly used spiking neuron models in SNN (N. Kasabov, 2013; Gerstner et al., 2014).

3.6.1 Leaky Integrate and Fire neuron model

As described in the previous section 3.3.1, the dynamic behaviour of a neuron can be described as an integration process that gradually increases the membrane potential of the postsynaptic neuron from its resting potential as a result of receiving input spikes, associated with a mechanism that generates a post-synaptic spike when the membrane potential crosses its firing threshold. This type of neuron model is known as the 'Integrate-and-Fire' (IF) neuron model. The Integrate-and-Fire neuron model does not attempt to model the shape or the biophysical

mechanisms of an action potential. Instead, it considers the generation of action potentials as precisely-timed events that carry the information (Gerstner et al., 2014).

There are two main modules in an Integrate-and-Fire neuron model. First, it contains a summation module that describes the elevation of the membrane potential from its resting state potential as a result of receiving input spikes $u_i(t)$. It can be represented in a form of a linear differential equation presented in equation 3.12. The membrane potential exponentially decays to its resting membrane potential with the absence of input spikes. The membrane time constant τ defined in equation 3.11 characterises the timing of this exponential decay. The criteria for firing time $t^{(f)}$ is given by equation 3.23 where ϑ is the firing threshold of the neuron.

$$f^{(f)} : u\left(t^{(f)}\right) = \vartheta \tag{3.22}$$

Each time the membrane potential hits the threshold, the variable u is reset from ϑ to ur. For t>t(f) the behaviour of the membrane potential is again represented by 3.12 until the membrane potential reaches its next threshold crossing. This type of model that combines the leaky integration and the resting state of a neuron is called the 'Leaky Integrate-and-Fire' model.

3.6.2 Hodgkin–Huxley neuron model

The LIF neuron model describes the essential properties of the passive membrane. It is an efficient model. However, it is less biophysically plausible since it does not represent the biophysical mechanisms of the neuron membrane such as the sodium and potassium ion pumps in the cell membrane that let the neuron to maintain a resting potential. Hodgkin–Huxley experimented with the properties

of the neuron membrane using the giant axon of the squid and came up with a more biologically plausible neuronal model called the 'Hodgkin–Huxley' model (Hodgkin & Huxley, 1952).

Hodgkin and Huxley showed that the resting potential of a neuron is caused by the difference in ion concentration between inside and outside a neuron. The ion pumps in the neuron membrane contribute to this difference in ion concentration. They found three sources that contribute to the ion current of a neuron; the sodium, potassium, and leak (mainly by the Chloride ions) current.

$$f^{(f)} : u\left(t^{(f)}\right) = \vartheta \tag{3.23}$$

The Hodgkin–Huxley model can be represented as the following electronic circuit that contains a capacitor, and multiple resistors placed in parallel (source: (Gerstner et al., 2014)).

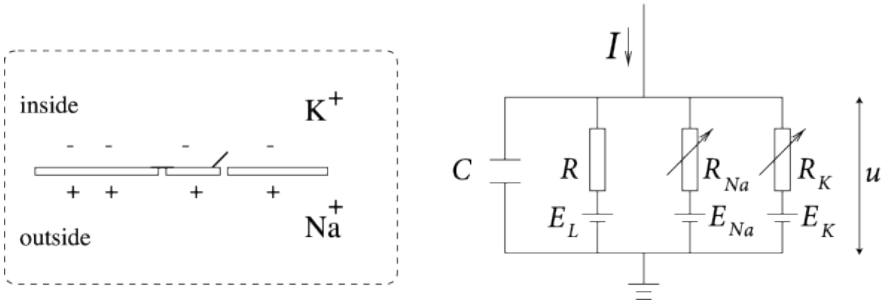

Figure 3.5: Schematic diagram for the Hodgkin-Huxley model

Therefore, the total current $I(t)$ can be represented as the summation of current through the capacitor $I_c(t)$, the current generated by the potassium ions ($I_K(t)$), the current generated by the sodium ions ($I_{Na}(t)$) and the leaky current $I_l(t)$ as equation 3.24.

$$I\left(t\right) = I_C\left(t\right) + I_K\left(t\right) + I_{Na}\left(t\right) + I_l\left(t\right) \tag{3.24}$$

The two resistors that represent the sodium (R_{Na}) and potassium (R_K) currents contain a variable resistance variable depending on the degree of conductance of the corresponding ion channel. If the ion channels are opened, they represent a comparatively high conductance (low resistance) of the channel. If the channel is closed, there is a high resistance for ion transmission. The batteries represent the difference of potential between the inside of the neuron and the extracellular area. This difference occurs as a result of active ion transportation across the membrane. The active transportation of ions generates a difference in ion concentration inside and outside of the cell. g_K, g_{Na} and $g + l$ represent the maximum conductance of potassium, sodium, and leak channels. Hodgkin and Huxley experimentally evaluated the effective resistance of an ion channel in response to the time and voltage. The relationships were then mathematically expressed by the induction of additional 'gating' variables m, n, and h. The gating variables represent the probability of an ion channel is open at a particular time.

Following equation 3.25 summaries the Hodgkin and Huxley model.

$$\sum_k I_k = g_{Na} m^3 h \left(u - E_{Na}\right) + g_K n^4 h \left(u - E_K\right) + g_l \left(u - E_l\right) \tag{3.25}$$

3.6.3 Izhikevich model

The Hodgkin and Huxley model present a biologically plausible model of a neuron. However, in terms of the computational cost, the model exhibits less efficiency. On the other hand, the Integrate-and-Fire neuron model is more efficient than the Hodgkin and Huxley model, but it is less biologically plausible. Eugene Izhikevich presented a spiking neuron model that contains represent the biophysical mechanisms of the Hodgkin and Huxley type (biophysical) models and as well as maintaining the computational efficiency of the LIF type models

(Izhikevich, 2003, 2004).

The Izhikevich neuron model mathematically defines the membrane potential of a neuron using four variable a, b, c, and d as per the following three equations (Izhikevich, 2003) where v is the membrane potential, and u is the membrane recovery variable which respectively denotes the activation and inactivation of potassium and sodium currents. Equation 3.28 resets the membrane potential v and the recovery variable u after the membrane potential reached its peak value of +30mV.

$$v^{'} = 0.04v^2 + 5v + 140 - u + I \tag{3.26}$$

$$u^{'} = a(bv - u) \tag{3.27}$$

$$\textbf{if } v \geq +30\, mV, \textbf{ then } \begin{cases} v & \leftarrow c \\ u & \leftarrow u + d \end{cases} \tag{3.28}$$

3.7 Synaptic Plasticity

Synaptic plasticity of the brain is known to be the fundamental mechanism of learning, memory formation, and evolution of neural circuits in animals. This is extensively studied in neuroscience for quantifying the biophysical mechanisms of plasticity and as well as on investigating its role in learning, adaptation, and memory formation. From a computational neuroscience perspective, synaptic plasticity is defined as the ability to increase or decrease the synaptic efficiency between two neurons according to the firing time of the pre-and post-synaptic neurons. The Hebb's postulate (Hebb, 1949) represent the most fundamental inspiration of the synaptic plasticity, which later became the basis for many

synaptic learning rules. The Hebb's postulate describes the evolution of the strength of a synaptic connection between two neurons as; "When an axon of cell A is near enough to excite cell B or repeatedly or persistently takes part in firing it, some growth process or metabolic change takes place in one or both cells such that A's efficiency, as one of the cells firing B, is increased." (Hebb, 1949)

3.7.1 Neuromodulation and neuroplasticity

Neuromodulation is the physiological process that alters (modulate) nerve activity by delivering neuromodulatory agents (i.e. dopamine, serotonin, histamine) directly to a target area to regulate the nerve activity. It utilises a specific form of stimulation such as electric, pharmaceutical or optical stimulus. The effects of neuromodulation can last from a few milliseconds to several minutes. Some of the neuromodulatory effects are the alteration of intrinsic firing activity, increase or decrease voltage-dependent currents, alter synaptic efficacy (*Neuromodulation*, 2021). Neuroplasticity is the learned ongoing functional response of the neurons following the termination of a stimulus that causes neuromodulation.

Both the neuromodulation and neuroplasticity is a learning phenomenon for the neurons. However, neuromodulation occurs during the stimulation. It is the learned functional response to a stimulus during the presence of the stimulus. Neuroplasticity can be any adaptation activity related to the functional and/or structural characteristics of the nervous system.

3.8 Spike-based Unsupervised Learning

3.8.1 Spike Time Dependent Plasticity

Based on the principals of Hebbian learning, the spike-based learning models that consider the timing information of temporally correlated spike sequences have led to the development of Spike Time Dependent Plasticity learning models (Gerstner et al., 1996; Kempter et al., 1999; Roberts, 1999; Abbott & Nelson, 2000). Such models can be seen as a spike-based generalisation of Hebbian learning. (Markram & Sakmann, 1995; Markram et al., 1997) reports the first experimental results on the induction of Long-Term Potentiation (LTP) and Long-Term Depression (LTD) of spike sequences at a ten-millisecond time scale. Several studies provide evidence that the change of synaptic efficiency in the brain is correlated to the timing of pre and post-synaptic activities of a neuron (Froemke & Dan, 2002; Rao & Sejnowski, 2001). A comprehensive review of the spike timing-based phenomenological models of synaptic plasticity is given in (Morrison et al., 2008).

STDP modifies the synaptic weight between two neurons based on the firing time of pre and post neurons. Strengthening of the synaptic efficiency is known as Long Term Potentiation, while weakening is known as Long Term Depression. During the learning process, STDP determines the synaptic weight between two neurons based on the arrival time of spikes to pre and post-synaptic neurons. According to STDP learning, repetitive spikes arriving at the post-synaptic neuron few discrete time intervals earlier than the post-synaptic spikes lead to Long-term Potentiation. Repetitive spikes arrive after the post-synaptic spike results in Long-term Depression (Sjöström & Gerstner, 2010). The difference of synaptic weight (δw) plotted as a function of the relative timing of pre and post-synaptic spikes ($t_{pre} - t_{post}$) indicates the STDP learning window as as shown in figure

3.6 (source: (Sjöström & Gerstner, 2010)). The difference of the STDP learning window specific to different synapses and cell types (i.e. neocortex layer 5 and layer 2/3 of the hippocampus, retinotectal synapses in Xenopus tadpoles, etc.) is reported in (Bi & Poo, 2001; Abbott & Nelson, 2000).

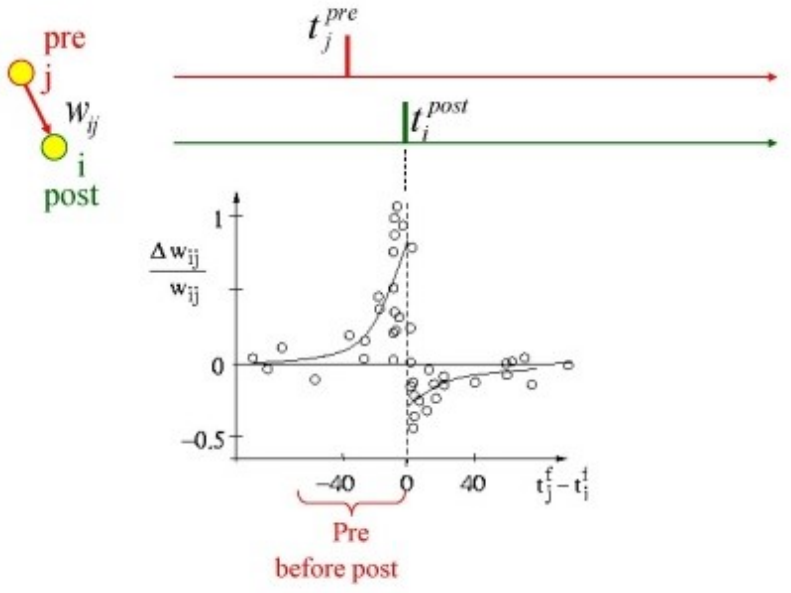

Figure 3.6: Spike-Timing Dependent Plasticity learning window that shows the synaptic weight update with respect to the relative timing of the pre and post-synaptic spikes (source: Sjöström & Gerstner, 2010)

The STDP learning rule quantifies the synaptic weight update of the presynaptic neuron j, δw_j according to the relative timing of the pre synaptic (i) spike arrival and the firing time of the post synaptic (j) spikes. The pre-synaptic spike arrival is denoted as t_j^f and the firing time of the post-synaptic neuron is indicated by t_i^n where $f = 1, 2, 3....$ The total synaptic weight update δw_j is given by equation 3.29 where $W(x)$ denotes the STDP learning window (refer figure 3.6) given by the equation 3.30.

$$\Delta w_j = \sum_{f=1}^{N} \sum_{n=1}^{N} W\left(t_i^n - t_j^f\right) \tag{3.29}$$

$$W(x) = \begin{cases} A_+ exp(-x/\tau_+) & \textbf{for} \quad x > 0 \\ -A_- exp(x/\tau_-) & \textbf{for} \quad x < 0 \end{cases} \tag{3.30}$$

3.9 Spike-based supervised learning

The common learning goal of all the supervisory methods in SNN is to find the weight vector w between pre and postsynaptic neurons for a given input spike sequence $S_{in}(t)$ and the desired output spike pattern of the postsynaptic neuron $S_d(t)$, such that the actual spike sequence $S_{out}(t)$ is similar to the expected output spike pattern $S_d(t)$ (Kasinski & Ponulak, 2006). The precision and reliability of spike trains have inspired several SNN models and influenced to map this physiological phenomenon in a supervised learning context. Different learning algorithms such as SpikeProp (Bohte et al., 2002), Remote Supervised Method (ReSuMe) (Kasinski & Ponulak, 2006), Spike Time Dependent Plasticity-based methods (Paugam-Moisy et al., 2006), Tempotron (Gutig & Sompolinsky, 2006), Linear Algebra-based methods and Spike Pattern Association Neuron (SPAN) (Mohemmed, Schliebs & Kasabov, 2011; Mohemmed & Kasabov, 2012; Mohemmed, Lu & Kasabov, 2012; Mohemmed, Schliebs et al., 2012; Mohemmed et al., 2013) have been proposed as supervised learning methods for spiking neural networks.

3.9.1 Spike Pattern Association Neuron

A common issue in spike-based supervised learning in SNN is that due to the discrete nature of spike sequences, the common mathematical operations that enable supervised learning in Artificial Neural Networks can not be easily and directly applied to spike sequences. The Spike Pattern Association neuron model addresses this limitation by transforming the discrete input, desired and actual

spike sequences into continuous signals using a kernel function. This transformation allows the application of common mathematical operations used in supervised learning on these spike sequences and reduces the complexity of computing the learning error.

In temporal coding, it is assumed that only the timing of each spike carries the information and the other attributes of a spike train such as the shape of a spike do not carry significant information. Therefore, measures of the distance between two spikes trains are indicators of the similarity between two arbitrary spike trains and can be used as a tool to compare the degree of similarity or dissimilarity between spike trains. The Victor–Purpura distance (Victor & Purpura, 1996), van Rossum distance (Rossum, 2001) and Schreiber et al. similarity measure (Schreiber et al., 2003) are some of the widely used measures to compute spike synchrony (Kreuz, 2011).

SPAN learning algorithm makes use of a measure similar to the van Rossum distance to compute the learning error. van Rossum distance between two spike sequences as for each spike is convoluted using an exponential kernel function as per equation 3.31.

$$\tilde{s}(t) = e^{-(t-t_i)/\tau_R}; (t > t_i) \tag{3.31}$$

where t_i is the spike time.

The van Rossum distance D_R between the two convoluted spike sequences $f(t)$ and $g(t)$, can be calculated using equation 3.32.

$$D_R(\tau_R) = \frac{1}{\tau_R} \int_0^\infty [f(t) - g(t)]^2 \, dt \tag{3.32}$$

The time constant τ_R characterises the scale of the timing of the exponentials for spike convolution. In spike-based supervised learning, this type of distance measure

that indicates the similarity between two spike trains is a suitable mechanism to compute the difference between the expected and actual spike sequences (error) at each training iteration. Such a learning error can be optimised by adjusting the synaptic weights between the input and output neurons. The error calculation of supervised learning in the SPAN learning algorithm utilises a similar measure as the van Rossum distance.

SPAN is a spiking neuron model that can learn to associate arbitrary spike trains allowing the processing of spatio-temporal information encoded in the precise temporal order of spikes. The synaptic weights between the input and output neurons are updated iteratively by minimising this learning error in order to emit output spikes at a desired time. Such type of spike sequence learning allows the association of arbitrary input and output spike sequences. A brief description of the derivation of the SPAN learning rule is presented below.

The SPAN learning algorithm is based on the spike-based interpretation of the Widrow-Hoff/Delta learning rule that uses the training error as an input for its objective function for training. This training error is defined as the difference between the expected and actual output produced after each training iteration. During learning the weights are updated in such a way that it reduces the training error.

The Widrow-Hoff rule for the i^{th} synapse of a neural network is defined as equation 3.33.

$$\Delta w = \lambda x_i \left(y_d - y_{out}\right) = \lambda x_i \Delta_i \qquad \lambda \in \mathbb{R} \tag{3.33}$$

x_i denotes the input through the i^{th} synapse, y_d is the desired output for the learning task, y_{out} is the actual output after training and λ is the learning rate. However, if x_i, y_d, and y_{out} are considered as spike trains, due to the sparse nature

of spike trains, the difference between two spike trains does not provide a proper error landscape which can be minimised by gradient descent. Although it is possible to consider spike count as a measurement of training error, this does not capture the dynamic changes of spike trains with respect to its temporal order. This limitation has been addressed by SPAN by transforming the discrete spike trains into a continuous signal using a convolution function $k(t)$.

$$\tilde{x}_i(t) = \sum_{t_i^f \in F_{in}} k\left(t - t_i^f\right) \tag{3.34}$$

$$\tilde{y}_d(t) = \sum_{t_d^g \in F_d} k\left(t - t_d^g\right) \tag{3.35}$$

$$\tilde{y}_{out}(t) = \sum_{t_{out}^h \in F_{out}} k\left(t - t_{out}^h\right) \tag{3.36}$$

$$\tilde{s}(t) = \sum_f \delta\left(t - t^f\right) \tag{3.37}$$

t^f is the firing time of a spike and $\delta(.)$ is the Dirac delta function $\delta(x) = 1$ if $x = 0$ and 0 otherwise. Thus the spike-based representation of Widow-Hoff learning rule can be derived as,

$$\Delta w_{i,m}(t) = \lambda \tilde{x}_i(t)\left(\tilde{y}_d(t) - \tilde{y}_{out}(t)\right) \tag{3.38}$$

$$\Delta w_{i,m} = \lambda \int_0^\infty \Delta w_i(t)\, dt \tag{3.39}$$

$$\Delta w_{i,m} = \lambda \left(\frac{e}{\tau}^2 \left[\sum_g \sum_f \left(\left| t_i^f - t_d^g \right| + \tau \right) e^{-\frac{\left| t_i^f - t_d^g \right|}{\tau}} - \sum_h \sum_f \left(\left| t_i^f - t_{out}^h \right| + \tau \right) e^{-\frac{\left| t_i^f - t_{out}^h \right|}{\tau}} \right] \right) \tag{3.40}$$

λ is the learning rate, τ is the time constant of the kernel function, t_i, t_d and t_{out} are the times of input, desired and actual spikes. f, g and h denotes the indexes of input, desired and actual spikes.

The equation 5.10 provides the weight update rule of the Spike Pattern Association Neuron model. SPAN has been used for classification through spike pattern association in several previous studies. Mohemmed, Schliebs and Kasabov (2011); Mohemmed and Kasabov (2012); Mohemmed, Schliebs et al. (2012) proposed and experimentally validated the SPAN learning rule using a computer-generated dataset. The studies also present a comparison of the learning performance between SPAN and ReSuMe synaptic learning model (Kasinski & Ponulak, 2006). Mohemmed and Kasabov (2012) showed the feasibility of incremental learning of SPAN synaptic learning rule for handwritten digital character recognition. Mohemmed et al. (2013) constructed a Spiking Neural Network that contains multiple Spike Pattern Association Neurons for learning multiple spatio-temporal patterns.

3.9.2 Dynamic Evolving Spiking Neural Networks

Rank-order learning was introduced in (Thorpe & Gautrais, 1998) that permits fast, one-pass learning of static patterns in SNNs. It assumes that the most crucial bits of information of an input spike sequence arrive earlier than the other spikes. Rank-order coding assigns priorities to the input spikes based on their

arrival. The basics of Rank-order learning have been utilised in evolving Spiking Neural Networks (eSNN) to enable a fast, one-pass data-driven mechanism for spike sequence learning.

An evolving Spiking Neural Network can evolve in an online manner based on the incoming input spike trains. However, the rank-order learning through eSNN suffers from the following limitation. In rank-order learning, the eSNN updates the synaptic weights only once based on the order of the first spike. Although this approach may be appropriate for learning from static data, it is not efficient in learning from complex spatio and spectro-temporal data. To learn from such dynamic data streams, the synaptic weights obtained through the rank-order learning based on the first spike of a particular synapse needs to be further updated based on the spikes that arrive after the first spike through the same synapse.

The dynamic evolving Spiking Neural Network (deSNN) model utilises the principles of both rank-order and Spike-Driven Synaptic Plasticity learning to address the above limitation in pure rank-order based learning. It enables learning of dynamic synapses through the spike-time based learning. Dynamic evolving Spiking Neural Network learning model is a spike-based supervised learning algorithm for evolving Spiking Neural Networks that utilise the principles of rank-order coding (N. Kasabov et al., 2013). In addition to the rank-order learning in eSNN, the deSNN utilises an additional parameter called 'drift' which can further fine-tune the synaptic weights obtained through rank-order learning based on the timing of the spikes that arrive through that synapse after the first spike. The evolved synapses of the SNN can be clustered based on the strength of the synaptic weights to extract meaningful structural and functional representations of input data (Soltic & Kasabov, 2010). The details of constructing the deSNN classifier are described below.

deSNN learning

For each input spike pattern that contains an M-dimensional feature vector, a new output neuron is created in the eSNN, and the synaptic weights between the input and the assigned output neuron are evolved through rank-order learning. deSNN learning assigns synaptic weights based on the order of incoming spikes from the corresponding input synapse as shown in equation 3.41 where P_i denotes the output neuron i, $w_{i,j}$ is the synaptic weight between the input neuron j ($j = 1, 2, \ldots M$)and the output neuron i.

$$w_{i,j} = \alpha \cdot mod^{\,order(j,i)} \tag{3.41}$$

Here, the parameters α and mod defines the learning rate and the modulation factor that defines the significance of the first spike in deSNN learning, respectively.

After the synaptic weight $w_{j,i}$ is initialised based on the time of the first spike arrival of that synapse as per equation 3.41, deSNN further fine-tunes the synaptic weight according to the Spike Driven Synaptic Plasticity and dynamically updates the synaptic weight based on the proceeding spikes. If there is a spiking event at time t, the initial synaptic weight obtained through rank-order learning is further increased by a small amount using the positive drift parameter and if there is no spike at the time interval t, the synaptic weight is further decreased by using the negative drift parameter as per the equation 3.42.

$$\Delta w_{j,i}(t) = e_j(t) \cdot D \tag{3.42}$$

If there is a successive spike at time interval t, the value of $e_j(t)$ is equals to 1. Otherwise, $e_j(t)$ equals to -1 to denote the decrease in synaptic weight of the dynamic synapse. Likewise, during deSNN learning, all dynamic synapses can

update their synaptic weights in parallel at each time interval of t corresponds to an input spike sequence.

deSNN classification

During prediction, deSNN emits an output spike in the output neuron according to equation 3.43, if the Post Synaptic Potential (PSP) is higher than a pre-defined threshold $PSP_{i,th}$.

$$PSP_{i,max} = \sum_{j} mod^{\,order(j,i)} \tag{3.43}$$

The threshold is calculated as per equation 3.44 where C represent the fraction of the maximum Post Synaptic Potential used for calculating the threshold.

$$PSP_{i,th} = C \cdot PSP_{i,max} \tag{3.44}$$

The feasibility of learning complex spatio-temporal and spectro-temporal patterns by deSNN learning algorithm has been demonstrated in several studies. N. Kasabov et al. (2013) presents several case-studies on evaluating the feasibility of deSNN for moving object recognition, and EEG pattern recognition. deSNN is the most common supervised learning method in the NeuCube Spiking Neural Network architecture which constructs brain-inspired computational models for mapping, learning, predicting and understanding of spatio-temporal brain data (N. K. Kasabov, 2014; N. Kasabov et al., 2016; N. K. Kasabov, 2018).

3.10 Spike-based reinforcement learning

Reward-modulated learning is another form of learning in animals that allow gaining a new skill, learning a new behaviour, or achieving a specific goal that is

guided through the rewards and punishments received in response to an exploration of each feasible action. Animals learn different skills, tasks, or behaviours through rewards or punishments received as the animal explores different feasible actions that reinforce the learning of a desired behaviour. In machine learning, such type of learning behaviour is known as reinforcement learning.

Many conventional experimental protocols that investigate the synaptic plasticity in animal brain demonstrate a form of Hebbian learning where co-activation of two neurons permit the strengthening of synaptic connections. In such a learning paradigm, two main parameters contribute to the evolution of synaptic strength. They are the firing time of the pre and post-synaptic neurons. Although studies have shown a third factor - the involvement of neuromodulators such as dopamine in specific brain areas that construct the rewarding mechanism in animal learning, only a few brain-inspired learning algorithms have computationally modelled such that reward modulated behaviour is biologically plausible machine learning models. This third factor that gives the notion of the rewarding mechanism in living nervous systems has enabled the computational models to reinforce the desired behaviour through reward (or punishment) as a result of exploring the possible actions. This section provides a brief overview of the recently proposed spike-based reinforcement learning algorithms.

Dopamine-dependent Spike Time Dependent Plasticity has been proposed to model a biologically plausible learning rule that gives the notion of reward-based learning in animals by integrating a rewarding signal with the traditional Hebbian type Spike Time Dependent Plasticity learning in SNNs (Legenstein et al., 2008). One of the approaches proposed to integrate the notion of learning from reward is gradient descent (Xie & Seung, 2004). Another approach is the reward-modulated Spike Time Dependent Plasticity which extends the classic STDP that depends on the co-activation of pre and post-synaptic neurons (Florian,

2007; Izhikevich, 2007; Legenstein et al., 2008). Another approach is the Temporal Difference learning which integrates an actor-critic model that supports spike-based reinforcement learning in SNNs (Suri & Schultz, 2001). A brief review of the spike-based reinforcement learning approaches reported in the literature is presented in (Vasilaki et al., 2009).

3.11 NeuCube Brain-inspired-Spiking Neural Network Architecture

Based on the mathematical models of neurons and learning, a novel evolving spatio-temporal SNN model of the brain known as NeuCube has been developed (N. Kasabov, 2012; N. K. Kasabov, 2014; N. Kasabov et al., 2016; N. K. Kasabov, 2018). By combining anatomical and physiological information, NeuCube provides a better understanding of how activities emerge and learning occurs at a network level. In (N. Kasabov, 2012; N. K. Kasabov, 2014) a Brain-inspired-Spiking Neural Network (BI-SNN) architecture was introduced and illustrated called NeuCube (Fig. 3.7). This section briefly describes the NeuCube structure and functions (see also(N. K. Kasabov, 2018) for further information). The Brain-inspired SNN architecture called NeuCube, that is structured according to a 3D brain template (N. K. Kasabov, 2014) and use spike-time learning rules such as Spike Time Dependent Plasticity, has been demonstrated to manifest deep learning from brain data (Doborjeh et al., 2018), from vision data (Paulun et al., 2018) and from environmental data (N. Kasabov et al., 2016; N. K. Kasabov, 2018). The first part of the following section briefly explains the existing NeuCube SNN framework, while the next part describes the implementation of the above theoretical framework for deep knowledge representation using SNN in the existing

NeuCube SNN framework.

In NeuCube, a 3D SNN structure is spatially organised to map a 3D brain template (Evans et al., 2012), such as Tailarach atlas(Dervin, 1990), Montreal Neurological Institute (MNI) atlas(Collins, 1994), or other. The main purpose of the SNNCube is to transform the compressed spike representation from input data into a higher-dimensional space and enable the polychronisation effect of spiking neural networks.

Learning in a NeuCube model is a two-phase process, including unsupervised learning in the 3D SNNcube and consecutive supervised learning for classification or regression purposes if this is required by the task. Spike trains are entered into the SNNcube, and as a result of the STDP or other spike-time learning rules, deep trajectories of connections are formed that represent different patterns of activity in the SNNcube. These patterns are then learned in a supervised way and classified in an output classifier (e.g. deSNN (N. Kasabov et al., 2013)) as illustrated in Fig.3.7.

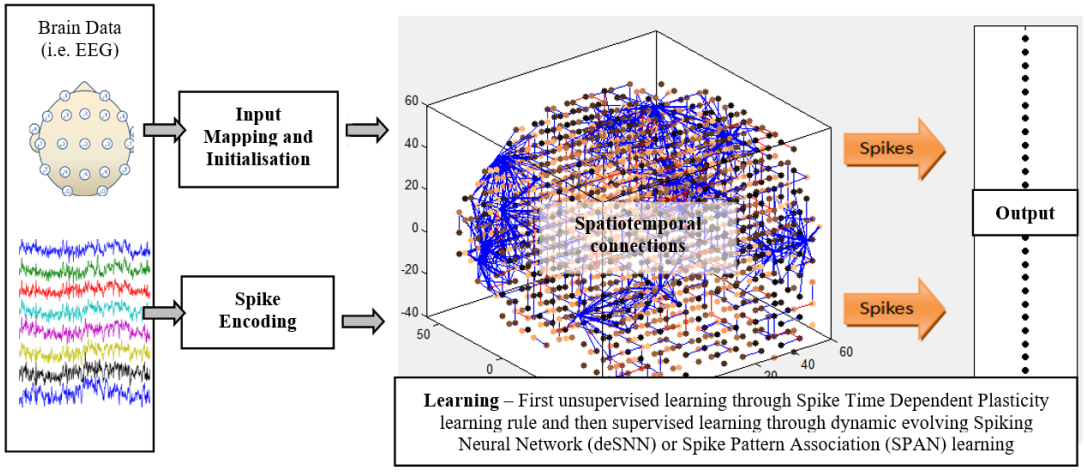

Figure 3.7: Deep learning in time-space in the BI-SNN NeuCube

3.11.1 Spike encoding

First, the input signals are encoded into spike trains using a spike encoding algorithm, such as the threshold-based encoding algorithm (Chan et al., 2007; N. Kasabov et al., 2017), the Bens Spikes algorithm (BSA) (Schrauwen & Van Campenhout, 2003), the Population Rank Coding (Bohte, 2004) and other(N. Kasabov et al., 2016).

3.11.2 Input mapping and network initialisation

A 3D SNN Cube is pre-structured to map structural and functional areas of the modelled temporal or spatio-temporal data (N. K. Kasabov, 2014; Tu et al., 2017). The reservoir of spiking neurons in the NeuCube is pre-structured in the 3D space according to a brain atlas. Each spiking neuron of the reservoir corresponds to a small 3D area of the brain (e.g. approximately 1 cm^3). The Talairach brain atlas annotates the 3-dimensional space of the brain in 1 mm^3 resolution including the hemisphere, lobe, tissue type (i.e. grey matter/white matter), and cell type (i.e. Brodmann area) of each brain region. The initial synaptic connections in the SNN reservoir are initialised by assigning random weights using the small-world connectivity principle (Braitenberg & Schüz, 2013; Bullmore & Sporns, 2009).

Since the EEG mapping of the NeuCube SNN architecture is based on the Talairach brain atlas, which contains the 3D coordinates of both cerebellum and cerebrum, the proposed Brain-Inspired Brain-Computer Interface architecture can represent both cerebrum and cerebellum activity together in the model. Therefore, the model can utilise the brain's independent circuitry that connects the periphery, cerebellum, and brainstem during automated or semi-automated motor actions.

Learning in a NeuCube framework is a two-phase process that includes unsupervised learning followed by supervised learning for classification or regression.

3.11.3 Unsupervised learning using Spike Time Dependent Plasticity

Unsupervised learning in NeuCube applies spike-time based learning rules such as Spike Time Dependent Plasticity (eq. 3.30) on the input spike sequences received from the input neurons. The learning process results in evolving synaptic connections in the reservoir based on the relative timing of the spiking activity between pre and post-synaptic neurons. The goal of the learning rule is to enable the spiking neurons in the SNNCube to integrate temporally correlated inputs from spatially distributed neural clusters and then transform them into a meaningful output. The STDP learning causes Long-term Potentiation (LDP) when a spiking neuron receives repetitive pre-synaptic spikes arrive at few discrete time intervals earlier than the post-synaptic spikes. The repetitive spikes appear few discrete time intervals after the post-synaptic spike results in Long-term Depression (LTD).

The NeuCube framework utilises a modified version of the STDP learning rule to generate an evolving connectionist structure from input spike sequences (Sengupta, 2018). In contrast to the conventional STDP learning, the modified STDP used in the NeuCube updates the synaptic weights between pre-and post-synaptic neurons only when a spiking neuron emits a spike. The synapses are not updated when a neuron receives a spike. Further, when a neuron fires, the modified STDP learning rule updates both pre-and post-synaptic connections. The STDP learning permits the spiking neurons in the NeuCube reservoir to associate temporally correlated input spike sequences and then transform them into a meaningful output.

3.11.4 Supervised learning in the SNNcube

When a trained SNN Cube is recalled on spatio-temporal input data, deep functional patterns can be revealed as a sequence of spiking activity of spiking

neurons in the SNNcube. Such patterns are defined by the learned structural patterns of connections. When the same or similar input data is presented to a trained SNN model, the functional patterns are revealed as the neuronal activity is propagated through the connectionist structure. The spike-based supervised learning algorithms such as deSNN (N. Kasabov et al., 2013) is used to predict the class labels from the spiking activity of the NeuCube SNN reservoir.

3.12 Summary of the chapter

This chapter presented an overview of brain-inspired computing, Spiking Neural Networks, and the NeuCube Spiking Neural Network architecture. At the beginning of the chapter, a brief description of the underlying neurological processes that contribute to the signal transmission and the evolution of synapses in living nervous systems was presented. Then the chapter introduced brain-inspired computing, in particular the evolution of Artificial Neural Networks. Then the chapter mainly focused on the third generation of Artificial Neural Networks called Spiking Neural Networks. A brief introduction to neural coding and various spike encoding methods that extract spiking activity from various types of signals were discussed in the chapter. Then, several spiking neurons and synaptic learning models that computationally model different electrochemical processes of the brain that give rise to the generation and transmission of action potentials were discussed. The chapter next described different spike-based learning approaches related to supervised, unsupervised, and reinforcement machine learning paradigms. A description of the NeuCube Spiking Neural Network architecture for modelling, analysing, and understanding spatio-temporal data was presented, and different steps related to analysing data using the NeuCube SNN framework were briefly described. Finally, the chapter presented a brief overview of the proposed research

to construct a Brain-Inspired Brain-Computer Interface and the contribution of the forthcoming chapters for constructing different components of the proposed BI-SNN architecture.

3.13 Contributions

1. The chapter presented an overview of the underlying biological processes that give rise to transmission of action potentials and evolution of synaptic plasticity in a living nervous system

2. The chapter highlighted the significance of a neuromorphic computational approach to address the weakness in traditional machine learning approaches

3. The chapter reviewed related literature on Spiking Neural Networks as a biologically plausible machine learning approach to online event prediction from spatio-temporal brain data

3.14 Related publications

- Sengupta, N., Ramos, J. I. E., Tu, E., Marks, S., Scott, N., Weclawski, J., Gollahalli, A.R., Doborjeh, M.G., Doborjeh, Z.G., **Kumarasinghe, K.** and Breen, V. (2018). From von Neumann Architecture and Atanasoffs ABC to Neuro-Morphic Computation and Kasabov's NeuCube: Principles and Implementations. In Learning Systems: From Theory to Practice (pp. 1-28). Springer, Cham.

- Doborjeh, M. G., Doborjeh, Z. G., Gollahalli, A. R., **Kumarasinghe, K.**, Breen, V., Sengupta, N., Ramos, J.I.E., Hartono, R., Capecci, E., Kawano, H. and Othman, M., (2018). From von Neumann Architecture and Atanasoff's

ABC to Neuromorphic Computation and Kasabov's NeuCube. Part II: Applications. In Practical Issues of Intelligent Innovations (pp. 17-36). Springer, Cham.

Chapter 4

Overview of the Proposed Methodology

> "To raise new questions, new possibilities, to regard old problems from a new angle, requires creative imagination and marks real advance in science. "
>
> *Albert Einstein - The greatest scientist of the twentieth century and one of the supreme intellects of all time*

Chapter Overview

The previous chapter presented a review of Spiking Neural Networks and the NeuCube Spiking Neural Network architecture for enabling Brain-Inspired Artificial Intelligence in digital systems. This chapter will present an overview of the proposed Brain-Inspired Spiking Neural Network model which has the potential to address multiple limitations in the existing neural decoders of non-invasive BCI highlighted in chapter 2. First the chapter will present a brief overview of the proposed Brain-Inspired Spiking Neural Network model. Next, the chapter

will describe the research questions addressed by the thesis. Finally, the chapter will present a brief overview of the public datasets used for the experimental validation of the proposed model. The chapter will also describe the contributions, interconnections and dependencies of each forthcoming chapter for constructing different components of the proposed BI-SNN architecture.

4.1 Introduction

This thesis presents a novel brain-inspired learning model to decode and understand neural activity of the brain from Electroencephalography signals. The proposed methodology intends to address multiple limitations in the existing machine learning approaches used in the state-of-the-art restorative BCI applications. It is based on the third generation of Artificial Neural Networks called Spiking Neural Networks, which has the potential to computationally model the behaviour of a living nervous system than the other Artificial Neural Network approaches. The SNNs can represent both time and space in the machine learning model, and therefore has the advantages over the pure spatial or temporal learning. The proposed BI-SNN is a generic SNN architecture that can be applied for the predictive modelling of spatio-temporal data streams. Here, it will be evaluated through multiple case-studies related to restorative Brain-Computer Interface applications.

The proposed SNN-based approach intends to achieve incremental learning of spiking neuron populations to associate input spikes sequences with the corresponding desired behaviour using the principles of Evolving Connectionist Systems. The population vector model which describe how the neurons in the motor cortex are trained to perform movements towards the desired direction has inspired the proposed Brain-Inspired Spiking Neual Network model. This methodology intends to address three limitations in the current restorative BCI – the less accuracy in decoding continuous movements of the same limb from EEG, lack of interpretability of neural decoders, and less ability of the machine learning model to learn incrementally and adapt to the changes in neural activity which occur as a result of motor re-learning. The proposed BI-SNN is a promising approach for constructing a Brain-Inspired Brain-Computer Interface.

4.2 Research Questions

The thesis presents two generic learning algorithms and integrates them with the NeuCube SNN architecture for constructing the proposed Brain-Inspired Spiking Neural Network model. The thesis will address the following generic research questions.

4.2.1 Generic Research Questions for Online Event Prediction from Spatio-temporal data

RQ1: How can the Spike Pattern Association Neuron (SPAN) be extended to develop an incremental spike sequence learning model for online event prediction from spatio-temporal data streams?

Non-stationarity, non-linearity and noise of time series are common challenges for analysis and predictive modelling of biomedical signals. Temporal averaging could maximise significant statistical features of the signal by eliminating the random noise to improve the prediction accuracy. However, it significantly reduces the information transfer rate as the machine learning model has to recurrently wait until it receives a sufficient amount of data to compute the average. The ability to online (single-trial) event prediction within a short latency is an essential requirement for real-time time-series forecasting models. This research question focuses on extending the existing Spike Pattern Association Neuron model to develop a spike-based incremental learning algorithm for online event prediction from spatio-temporal data streams.

Learning in the existing Spike Pattern Association Neuron model is limited to batch learning of expected spike sequences that contain only one spike; the feasibility of incremental learning of complex spike sequences using the SPAN learning

model remains under-investigated. This research question aims at addressing this limitation. The research question will be answered through the development of the proposed spike-based supervised learning model, called evolving Spike Pattern Association Neural Network (eSPANNet). The construction of the learning model will be described in chapter 5. The chapter will present a series of experiments from E1.1 - E1.3 (section 5.4.1, 5.4.2 and 5.4.3) to answer this research question.

The eSPANNet model will be compared with both Artificial Neural Networks based methods such as Convolutional Neural Networks and Recurrent Neural Networks and as well as the non-brain-inspired multi-class classifiers namely, k-Nearest Neighbors, Support Vector Machine, Decision Trees and Discriminant analysis, and several ensemble-based methods such as AdaBoost, RUSBoost, Bagging and Subspace. eSPANNet will be evaluated as a classifier and a regression analysis method and compared with the above machine learning methods under different performance measures such as the accuracy, sensitivity, specificity, F1 Score, False Positive Rate, False Negative Rate, prediction latency, correlation and cross-correlation coefficients. The feasibility of incremental learning will be evaluated by examining the change of the true positive rate during eSPANNet training process.

RQ2: How can the network architecture of the eSPANNet learning model be improved to enhance its convergence and the prediction accuracy when learning from non-stationary stochastic data streams such as Electroencephalography?

Non-invasive neurological signals such as Electroencephalography are unable to measure the neural activity at a scale of individual neurons. Instead, EEG indicates the accumulated activity of neural populations that may contain thousands of neurons. A typical biological neural network exhibits more complex spike patterns

than the simple pre and post-synaptic spike pairs studied in traditional protocols that characterise the synaptic plasticity of the brain (Faugeras et al., 2009). The stochasticity of input spike trains is a challenge for convergence in spike-time based learning rules and the reliability of spike responses for predictive modelling using Spiking Neural Networks. When learning from stochastic spike sequences, the timing of the first spike of an input spike sequence has a significant impact on the convergence of the SPAN learning to a global optimum. The random spike trains arrive earlier than the desired time point causes the SPAN learning rule to trap in local minima instead of converging to its global optimal.

Non-invasive neural signals such as Electroencephalography exhibit a greater level of non-stationarity and low signal-to-noise ratio compared to invasive neurological signals such as Electrocorticography. After the proof of concept of the eSPANNet learning model for incremental spike sequence learning from invasive Electrocoticography signals, this research question will investigate how the network architecture of eSPANNet be improved to enhance the convergence and prediction accuracy when learning from stochastic data streams such as EEG. The study will evaluate its performance for event prediction using non-invasive brain data from multiple participants. This research question will be addressed in chapter 6. Section 6.5.1 will propose and compare two network architectures to evaluate how eSPANNet can be improved to enhance its convergence and prediction accuracy when learning from stochastic data streams.

RQ3: Based on the abilities of SNN for deep learning, can SNNs be used to construct an interpretable machine learning model that represents deep knowledge as spatio-temporal rules?

This research question aims at improving the interpretability of Spiking Neural Networks. The research question will be addressed through the proposed knowledge

representation framework for Brain-Inspired SNNs which will be prsented in chapter 7. The study will present a theoretical framework and its implementation for extracting deep spatio-temporal rules from Brain-Inspired SNN architectures. The study will investigate the feasibility of interpreting deep knowledge in SNNs as deep spatio-temporal rules. Section 7.4.4 will evaluate the feasibility of obtaining topological patterns, and underlying neural trajectories during cognitive events from EEG signals.

4.2.2 Specific research question for addressing the limitations of non-invasive BCI for motor recovery and restoration

The thesis will address the following research questions which are specific to restorative Brain-Computer Interfaces that utilise non-invasive Electroencephalography signals.

RQ4: How does the eSPANNet learning model compare with the static rate-based machine learning methods (such as the Convolutional Neural Networks and Support Vector Machine) and as well as the sequence learning-based machine learning methods (such as the Recurrent Neural Networks, linear regression and SVM-based regression) for predicting movement intention from EEG signals?

The early MRCPs which is also known as Bereitschaftspotentials or readiness potentials that occur before the onset of a movement represent the neural activity of the brain correspond to planning and preparation for executing a voluntary movement. They can be used to decode the intention to perform a voluntary movement from neurological signals which are useful for restorative Brain-Computer

Interface interventions for prosthetic control and neurorehabilitation. This research question will apply the eSPANNet learning algorithm on a case-study on predicting movement intentions from EEG signals presented in chapter 6. The study will evaluate and benchmark the performance of predicting movement intentions to perform a grasp and lift movement from EEG signals using the eSPANNet learning model. This research question will be addressed in section 6.5.1 and 6.5.2.

RQ5: How can the NeuCube SNN architecture be improved in order to enable continuous control of a prosthetic hand from EEG signals?

The research question will investigate how the existing NeuCube SNN framework be improved in order to decode sequential hand open and close movements from EEG signals to control an upper-limb prosthesis. This research question aims at improving the SNN algorithm by integrating finite automata with the NeuCube SNN and the development of a BCI prototype software that enables online control of the prosthetic limb. The research question will be addressed through the proposed FaNeuRobot framework presented in chapter 8. The proposed framework will integrate the SNN with finite automata to model the state-based behaviour of forearm flexor and extensor muscles during hand opening and closing movements. Section 8.4.2 will present a proof-of-concept of the proposed framework for answering this research question.

RQ6: Does the Brain-Inspired Spiking Neural Network model that integrates the eSPANNet with the NeuCube SNN architecture result in higher prediction accuracy than the pure eSPANNet learning model for predicting continuous movements from EEG signals?

This research question evaluates whether the integration of eSPANNet learning model as the output classifier of the NeuCube SNN architecture results in a higher

prediction performance compared to the learning in pure eSPANNet model. The research question will be addressed in chapter 9. Section 9.3.1 compares the performance between the pure eSPANNet and the eSPANNet integrated with the NeuCube SNN architecture to answer this research question.

RQ7: How do the Brain-Inspired Spiking Neural Networks and the non-Brain-Inspired machine learning models compare in terms of their ability for sequence prediction, interpretability, and incremental learning to predict complex movements from EEG signals useful for motor recovery and restoration through Brain-Computer Interfaces?

This research question will be answered through the development of the proposed Brain-Inspired Brain-Computer Interface that integrates the proposed spike-based learning algorithms in the Brain-Inspired Spiking Neural Networks. The proposed computational model constructs a novel type of neural decoder for restorative BCIs that addresses several limitations of the current BCI systems. This research question will be addressed in chapter 9. Section 9.3.2 - 9.3.6 present a series of experiments to answer this research question.

4.3 Brain-Inspired Spiking Neural Networks for Brain-Computer Interfaces

This section presents a brief overview of the proposed methodology. The proposed methodology will extend the Spike Pattern Association Neuron (Mohemmed, Schliebs, Matsuda & Kasabov, 2011) and the generic NeuCube SNN framework (N. K. Kasabov, 2014; N. Kasabov et al., 2016; N. K. Kasabov, 2018) for constructing the proposed Brain-Inspired Brain-Computer Interface model. Figure 4.1

illustrates the architecture and major steps of the proposed SNN model. Learning in BI-SNN includes spike encoding, input mapping, network initialisation, and unsupervised learning through Spike-Time Dependent Plasticity learning. These steps are specific to predictive modelling of spatio-temporal data using the NeuCube SNN framework. The thesis proposes a novel knowledge representation framework for brain-inspired SNN architectures as a generic method for enhancing the interpretability of the SNN which will be discussed in chapter 7. This framework is integrated with the generic NeuCube SNN architecture for improving the interpretability of the proposed BI-SNN. The framework permits the extraction of anatomical clusters that represent neural activity in different regions of interest in the brain.

4.3.1 Novelty

The novelty of the proposed methodology includes the improved interpretability, feasibility of incremental learning, ability to learn spike sequence and support for online processing and real-time prediction. The proposed eSPANNet, as an ANN-based supervised learning model, is not limited to a fixed structure of spiking neurons. It does not require specific predefined parameters such as the number of neurons in the hidden layer, as it evolves neurons if needed.

The BI-SNN is more interpretable than the generic NeuCube framework as it contains the required algorithms and software support for knowledge representation and extraction. The proposed BI-SNN enhances the explainability of the learning and model predictions. The proposed model can interpret the learning in SNN under different spatial and temporal granularity levels which are not feasible with the generic NeuCube SNN architecture.

Also, by integrating eSPANNet as the output classifier of the generic NeuCube

SNN architecture, the model gains the ability to learn a whole spike sequence. This contradicts with the deSNN learning, which mainly depends on the order of the first spike of the output neuron. The deSNN initialises and trains a new neuron as it receives new input spike train. The deSNN learning process puts significant attention to the first spike of the output neuron, but not the whole spike sequence. The class label is determined by comparing with the synaptic weights of existing neurons using kNN. In contrast, the proposed learning model which replaces the deSNN by the eSPANNet predicts a spike sequence as the output. This makes the model more compatible with online prediction and real-time spike sequence analysis.

4.3.2 Overview of the methodology

The BI-SNN model considers the signals from EEG channels as the input to the model (figure 4.1 A) while motor signals which represent a certain motor behaviour such as the muscle activity or upper-limb kinematics are considered as the expected outputs from the BI-SNN model. To model the motor behaviour in a spike-based interpretation, the model converted both input and expected output signals into spike sequences. Here, the input signals are first encoded into spike sequences (figure 4.1 B) using a suitable spike encoding algorithm, such as the threshold-based encoding (Chan et al., 2007; N. Kasabov et al., 2017), the Bens Spikes Algorithm(Schrauwen & Van Campenhout, 2003), or the Population Rank Coding (Bohte, 2004).

The SNN then maps the encoded spiking activity from EEG channels into this 3D space through EEG mapping as shown in figure 4.1 C. The network is initialised according to the small-world connectivity principle (figure 4.1 D). As the input spike trains are fed into this reservoir through input neurons, the SNN

will evolve based on the spike time of pre and post-synaptic neurons according to Spike-Time Dependent Plasticity learning (Gerstner et al., 1996; Markram & Tsodyks, 1996) (figure 4.1 E). The BI-SNN will then cluster the spiking activity based on their anatomical locations (figure 4.1 F) using the proposed knowledge representation framework.

The thesis presents the evolving Spike Pattern Association Neural Network as a generic method for spike-based sequence learning. The proposed BI-SNN model integrates the eSPANNet as the output classification/regression layer with the generic NeuCube SNN architecture. eSPANNet aims at enabling the SNN to incrementally learn the spatio-temporal association between the spiking activity of distinct brain regions with the corresponding motor behaviour (figure 4.1 G). The eSPANNet learning model utilises the polychronisation effect of Spiking Neural Networks(Izhikevich, 2006) to decode neural activity from spatio-temporal brain data. Finally, the BI-SNN will extract the polychronising spiking neural clusters which can generate temporally associated spike sequences correlated with the predicted event as per figure 4.1 H. These predicted spike sequences are decoded back to continuous motor signals. Decoding of motor signals from output spike sequences will utilise the encoding threshold values of each motor signal and the initial state of each motor signal at the beginning of each GAL trial as exemplified in figure 4.1 I. A detailed description of each step related to BI-SNN is presented in the next five chapters of this thesis.

Chapter 5 and 6 will propose and experimentally validate the evolving Spike Pattern Association Neural Network for incremental learning and online event prediction from electroencephalography signals. Chapter 7 will present a knowledge representation framework and the associated algorithmic pipe-line to extract deep spatio-temporal knowledge from the brain-inspired Spiking Neural Network architectures. The overall Brain-Inspired SNN architecture that integrates the

proposed generic methods is described and experimentally validated in chapter 8 and 9. The interconnections and contributions of each chapter for constructing different components of the Brain-Inspired Brain-Computer Interface are highlighted in figure 4.1.

4.4 Experimental validation

The following public datasets will be used for the experimental validation of the proposed research.

BCI Competition IV - dataset 4

This dataset is used in the proof of concept of the eSPANNet learning model which will be presented in chapter 5. The dataset The dataset contains Electrocoticography signals recorded from three healthy participants while performing finger flexion according to a cue presented to the subject. Electrocoticography signals were sampled at 1000Hz and recorded over a 10 min duration in each session (Schalk et al., 2007).

WAY-EEG-GAL (WAY: Wearable interfaces for hAnd function recovery, EEG: Electroencephalography, GAL: Grasp-And-Lift) dataset

The experimental validation of the proposed Brain-Inspired Spiking Neural Network will be performed using this dataset. The WAY-EEG-GAL dataset (Luciw et al., 2014a, 2014b) which is specifically designed to critically examine the information processing in the human brain related to sensation, intention, and action from EEG signals when performing a grasp-and-lift task. The dataset has been collected by following a well-established prototypical paradigm to study precision grasp-and-lift of an object (Westling & Johansson, 1984; Johansson &

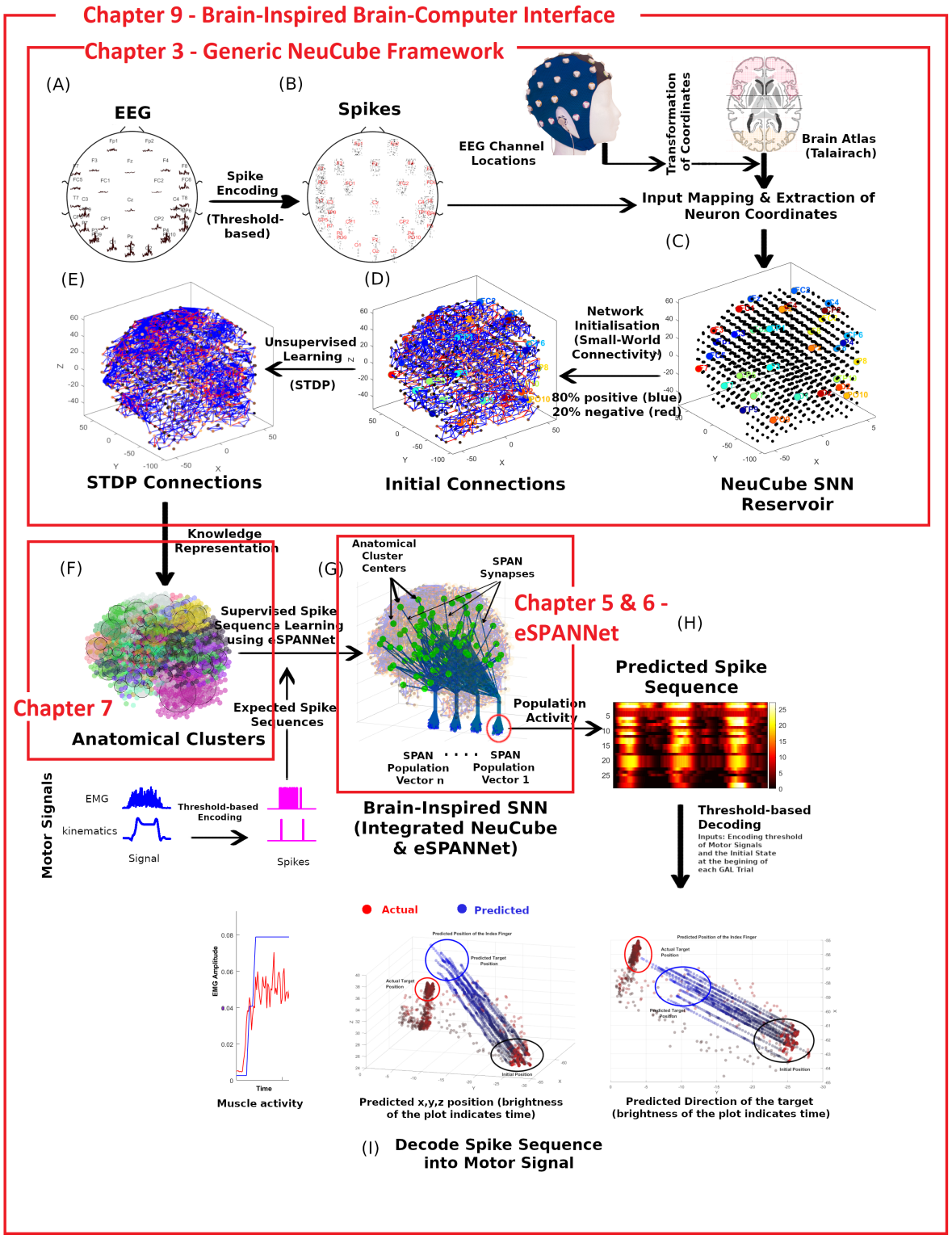

Figure 4.1: Integration of the eSPANNet with the NeuCube SNN architecture and major steps in training a BI-SNN model - A) Filtered EEG B) Spike encoding c) EEG mapping D) Network initialisation E) Unsupervised Spike Time Dependent Plasticity learning F) Extraction of anatomical clusters G) eSPANNet learning H) Predicted spike sequence by the SNN I) Decoding predicted spike sequences into muscle activity and kinematics

Westling, 1988b, 1988a). Twelve healthy participants performed a series of grasp and lift trials of a small object when the object's weight, surface friction, or both, were changed unpredictably between trials. The dataset can be downloaded from (Luciw et al., 2014b) and provides a platform to non-invasively study information processing in the human brain related to sensation, intention, and action in healthy participants during a functional upper limb motor task.

The dataset contains simultaneous EEG, Electromyography (EMG), force and kinematic signals recorded from 12 healthy participants during cued grasp and lift (GAL) movements. The participants performed a series of grasp and lift trials of a small object. During a GAL trial, the participant reached to the object, grasped it using the index finger and thumb, and lifted it a few centimetres up in the air, held it stably for a couple of seconds, and then replaced and released the object. An LED light cued the start and end of a GAL trial.

The dataset contained EMG signals from five sensors that monitored the muscle activity of the Anterior Deltoid (AD), Brachoradial (B), Flexor Digitorum (FD), Common Extensor Digitorum (CED) and First Dorsal Interosseous (FDI) muscles of the right arm at a 4kHz sampling frequency. The EEG, force and kinematic signals were recorded at 500Hz sampling frequency. Two surface contact plates were placed on each side of the object to record the grip force and load force applied on the object during each trial. Data from kinematics sensors was gathered using 3D position sensors placed on the object, wrist, thumb and index finger. Each sensor recorded x,y,z position and azimuth, elevation and roll angles. The signals recorded from multiple devices were synchronised using a sync signal recorded by each device. More information about the data collection protocol can be found in (Luciw et al., 2014a).

4.5 Chapter Summary

This chapter presented an overview of the proposed Brain-Inspired Spiking Neural Network model, which aims at constructing a novel type of interpretable neural decoder for non-invasive Brain-Computer Interfaces. The chapter presented a detailed description of the research questions addressed by the thesis. Next, an overview of the Brain-Inspired Spiking Neural Network model for constructing the proposed Brain-Inspired Brain-Computer Interface was presented. Finally, the chapter presented a short description of the public datasets used for the experimental validation of each study.

4.6 Contributions

1. The chapter proposed a Brain-Inspired Spiking Neural Network model to construct a novel type of Brain-Inspired Brain-Computer Interface for decoding complex upper-limb movements

Chapter 5

Evolving Spike Pattern Association Neural Network for Spike-based Supervised Incremental Learning

"Research is what I'm doing when I don't know what I'm doing"

Wernher von Braun - Pioneer of rocket technology and space science

Chapter Overview

The previous chapter described the research questions addressed by the thesis and a brief overview of the proposed Brain-Inspired Spiking Neural Network model. The next three chapters will present the proposed spike-based generic learning algorithms. The goal of the proposed generic methods is to construct an interpretable machine learning model that can incrementally learn to predict events from temporal, spatio-temporal or spectro-temporal data streams. This

chapter introduces a Spiking Neural Network model named evolving Spike Pattern Association Neural Network for online event prediction from data streams. The goal of eSPANNet is to utilise the polychronization effect of Spiking Neural Networks for spike sequence learning from data streams. The eSPANNet model contains a network of Spike Pattern Association Neurons, a spiking neuron model which can emit spikes at the desired time-point. The learning algorithm utilises the principles of Evolving Connectionist Systems to incrementally learn the association between input and expected output spike sequences. The chapter will describe the eSPANNet incremental learning algorithm and, present a proof of concept study to evaluate its performance for predicting continuous movements from Electrocoticography signals. A discussion on the significance of the proposed learning algorithm is presented at the end of the chapter. A comprehensive analysis which will experimentally validate and benchmark the performance of eSPANNet learning model on Electroencephalography signals will be presented in the next chapter.

5.1 Introduction

Due to the non-stationarity and high trial-to-trial variability, online event prediction from electroencephalography signals is challenging. This issue is significant when it is applied to neurological rehabilitation where the person incrementally learns to regain control of movement. Through neurorehabilitation, it is expected that the patients will incrementally learn to regain the affected movements. Motor relearning causes evolving changes in the neurological signals(Canuet et al., 2015; Ochoa et al., 2014; Westlake & Nagarajan, 2011). It is crucial to facilitate incremental and adaptive learning of the computational approaches used in rehabilitation applications to address this adaptability. This research intends to examine the emerging role of adaptive and incremental learning in the context of Brain-Computer Interfaces.

This chapter proposes a spike-based supervised learning algorithm for spike sequence learning from data streams. The goal of the proposed learning algorithm is utilise the polychronising effect of SNN to learn the polychronising spiking neuron populations which are correlated with the predicted sequence. The proposed BI-SNN is a generic SNN architecture that can be applied for the predictive modelling of spatio-temporal data streams. This chapter will address the following research question.

- **RQ1: How can the Spike Pattern Association Neuron be extended to develop incremental spike sequence learning model for online event prediction from spatio-temporal data streams?**

This chapter presents a novel incremental learning approach for spike sequence learning using Spiking Neural Networks called evolving Spike Pattern Association Neural Network to address the above research question. It is a generic learning

model that can be used for online event prediction from multi-sensory temporal, spatio-temporal or spectro-temporal signals. eSPANNet is a computational model inspired by incremental learning for motor control in living nervous systems. It is inspired by the concept of 'population vectors' which have been experimentally proven by several computational neuroscience studies. This chapter presents a proof-of-concept study on the proposed computational model for single-trial BCI using a public dataset from the fourth BCI competition.

The proposed eSPANNet model will be compared with Artificial Neural Networks based methods such as Convolutional Neural Networks and Recurrent Neural Networks. It will also be compared with multiple non-brain-inspired multi-class classification or clustering methods such as k-Nearest Neighbors, Support Vector Machine, Decision Trees and Discriminant analysis, and several ensemble-based methods such as AdaBoost, RUSBoost, Bagging and Subspace. eSPANNet will be evaluated as a classifier and a regression analysis method and compared with the above machine learning methods under different performance matrices such as the accuracy, sensitivity, specificity, F1 Score, False Positive Rate, False Negative Rate, prediction latency, correlation and cross-correlation coefficients. The feasibility of incremental learning will be evaluated by examining the change of the true positive rate during eSPANNet training process. The novelty of the proposed eSPANNet algorithm is its ability to learn which inputs to focus on as new training samples are received. The model can learn as it performs predictions, and therefore is robust to changes in a biological system.

The chapter has been organised in the following way. The next section presents the eSPANNet learning model. It includes an overview of the theoretical layout of the proposed methodology and mainly looks at implementing the proposed method in a spike-based supervised learning context. The Matlab source codes that implement the eSPANNet learning model as a prototype software are included

in Appendix A. The third section presents a proof of concept followed by its experimental results presented in the fourth section. Finally, the fifth section discusses the implications of the findings. Throughout this thesis, the term 'population vector' (A. P. Georgopoulos et al., 1986) has been used to indicate the response of a group of spiking neurons for a certain input stimulus. The term 'activation time-course' of a neuron has been used to indicate the varying activity of a readout neuron over time.

5.2 Evolving Spike Pattern Association Neural Network

The precision and reliability of spike trains have inspired several SNN models and influenced to model it in a supervised learning context. Different learning algorithms such as SpikeProp (Bohte et al., 2002), Remote Supervised Method (ReSuMe) (Kasinski & Ponulak, 2006), Spike Time Dependent Plasticity-based methods (Paugam-Moisy et al., 2006), Tempotron (Gutig & Sompolinsky, 2006), Linear Algebra-based methods and Spike Pattern Association Neuron (Mohemmed, Schliebs & Kasabov, 2011; Mohemmed & Kasabov, 2012; Mohemmed, Lu & Kasabov, 2012; Mohemmed, Schliebs et al., 2012; Mohemmed et al., 2013) have been proposed as supervised learning methods for spiking neural networks. A detailed description of multiple spike-based supervised learning models was presented in section 3.9.

The eSPANNet is an evolving feed-forward spiking neural network model which extends the Spike Pattern Association Neuron model proposed in Mohemmed, Schliebs & Kasabov, 2011; Mohemmed, Schliebs, Matsuda & Kasabov, 2011; Mohemmed & Kasabov, 2012; Mohemmed, Lu & Kasabov, 2012; Mohemmed,

Schliebs et al., 2012; Mohemmed et al., 2013. The SPAN neuron model will be extended and combined with a computational interpretation of a 'population vector model' to derive a biologically plausible model of motor learning and adaptation in the proposed evolving Spike Pattern Association Neural Network architecture.

SPAN is a spiking neuron model which can learn to associate arbitrary spike trains allowing the processing of spatio-temporal information encoded in the precise temporal order of spikes. A detailed description of the SPAN learning algorithm was presented in section 3.9.1.

5.2.1 Problem formulation

The common learning goal of all spike-based supervised learning methods in SNN is to find the weight vector w between pre and postsynaptic neurons for a given input spike sequence $S_{in}(t)$ and the desired output spike pattern of the postsynaptic neuron $S_d(t)$, such that the actual spike sequence $S_{out}(t)$ is similar to the expected output spike pattern $S_d(t)$ (refer figure 5.1) (Kasinski & Ponulak, 2006).

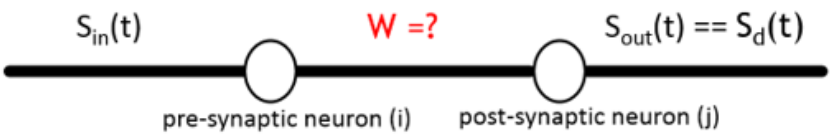

Figure 5.1: Spike-based supervised learning problem

For a labeled training dataset with n number of class labels and, x number of input channels (features), a feed-forward SNN is formed to derive the synaptic weight, w by the proposed supervised learning model. During the time period of Δt from t_1 to t_2, prediction of the output class label $l_{\Delta t}$ from testing spike sequences is performed using the activation time-course of n readout neurons in

the output layer given by $q_{n,t}$. Each readout neuron exhibits a binary state space; $Q_{readout} = \{0, 1\}$, determined by the average post-synaptic spike pattern of the group of readout neurons $q_{n,t}$ during the Δt time period.

$$l_{\Delta t} = f\left(q_{n,t}\right) \tag{5.1}$$

$q_{n,t}$ is n by 1 dimension vector that represent the current spiking state (spike or no spike) of n^{th} readout neurons at a given time. Using a suitable synaptic learning method, the SNN derives the synaptic weight between input and output spiking neuron layers so that for a given input spike pattern, the SNN will learn to emit a desired spike sequence by the corresponding output neuron.

5.2.2 Construction of the learning model

The thesis proposes the eSPANNet learning model to incrementally learn the synaptic weight vector that associate an arbitrary input spike sequence with a desired output spike pattern. eSPANNet is an evolving feed-forward SNN architecture with a hidden layer containing groups of Spike Pattern Association Neurons arranged as population vectors. New spiking neurons are trained to incrementally learn new input patterns following the principles of Evolving Connectionist Systems (N. K. Kasabov, 2007).

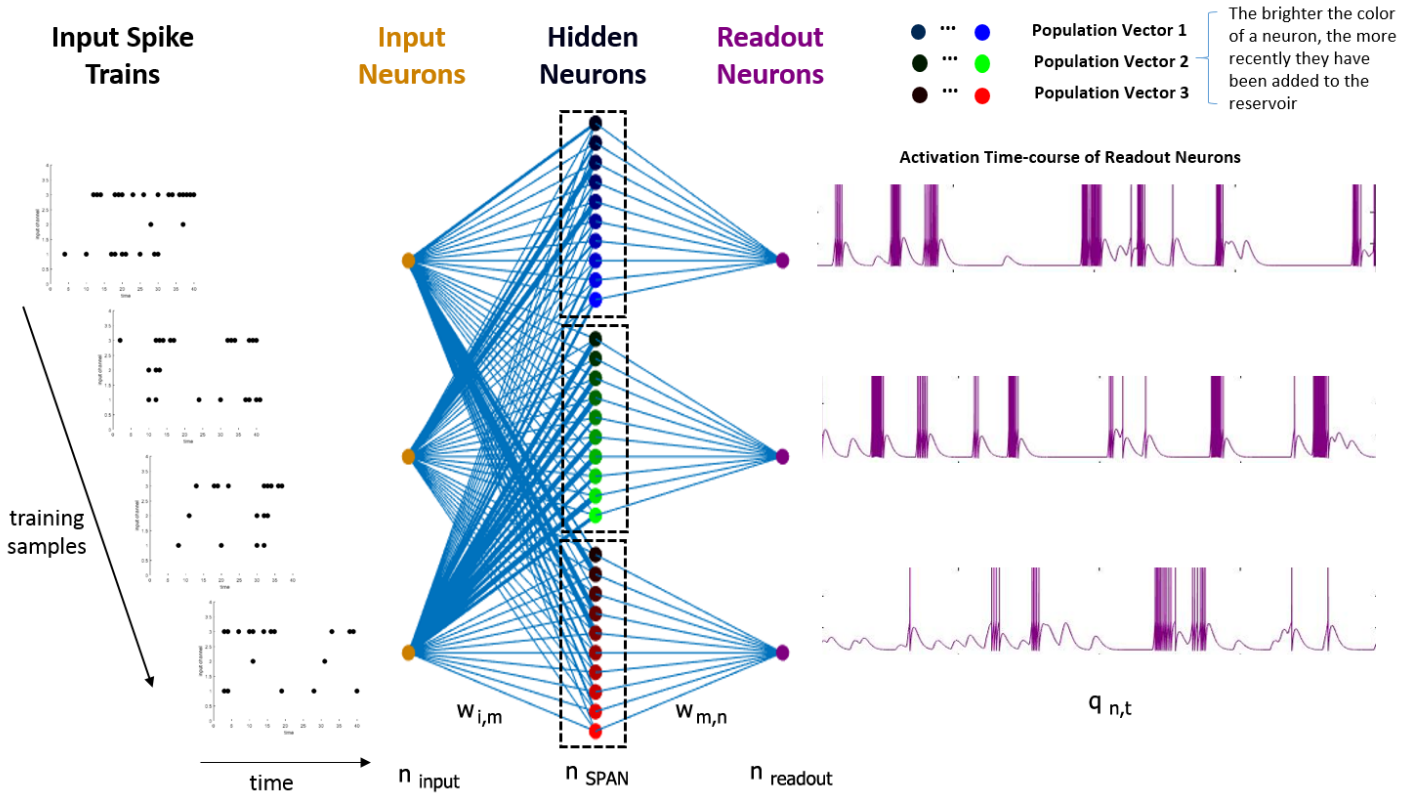

Figure 5.2: Multiple input synapse-based eSPANNet architecture

5.2.3 Network architecture

For a labeled training dataset with n number of class labels and, x number of input channels (features), eSPANNet forms a feed-forward spiking neural network with three layers; input, hidden and output layers. The input layer contains x number of input neurons that feed input spike trains into the hidden layer. The hidden layer contains groups of SPAN's arranged as n number of population vectors. This thesis proposes two different eSPANNet network architectures based on the input layer to hidden layer connectivity principle. The first network architecture contains a layer of input neurons that are fully connected with the neurons of each population vector. Figure 5.2 depicts the multiple input synapse-based eSPANNet network architecture. In the second network architecture each neuron of a particular SPAN population is connected with only one input neuron as describe in the next chapter. Each SPAN is trained using a single training spike sequence received through the corresponding input neuron(s) and validated using the other training and validation spike samples during incremental learning. The output layer contains n number of integrate and fire neurons each associated with the corresponding population vector. Each SPAN that belong to a certain population vector is connected with only one output neuron which receive spikes through all SPANs in that particular SPAN population vector. Each neuron in the output layer acts as a readout neuron where the corresponding class label is predicted according to the behaviour of these readout neurons. Output neuron will determine the corresponding class label using a suitable strategy such as by using the average population activity or majority-voting.

5.2.4 Incremental learning

A bottom up approach will be followed to explain the eSPANNet computational model. State of the n^{th} readout neuron during Δt time period is calculated using $\bar{I_n}$, the synaptic current from the hidden layer neurons of tje n^{th} population vector to n^{th} readout neuron, $F_{n,t}$ postsynaptic spike pattern of the n^{th} population vector during Δt and, th_n the firing threshold of the n^{th} readout neuron.

$$q_{n,t} = g\left(\bar{I}_{n,t}, th_n\right) = \begin{cases} 1 & if \quad \bar{I}_{n,t} \geq th_n \\ 0 & otherwise \end{cases} \tag{5.2}$$

Appendix A.1.1 section includes the Matlab source code for calculating the membrane potential of a Leaky Integrate and Fire neuron utilised in the proposed eSPANNet learning model.

The average synaptic current from the n^{th} population vector to the n^{th} readout neuron at time t, $I_n\bar{(t)}$, is given by synaptic weight $w_{m,n}$ between m^{th} hidden neuron in the n^{th} population vector and the convoluted spike pattern of m^{th} hidden neuron in the n^{th} population vector at time t, $\tilde{s}_{m,n}$,

$$\bar{I}_n(t) = \frac{1}{m}\sum_{i=1}^{m} I_{m,n} = \frac{1}{m}\sum_{i=1}^{m} w_{m,n} \odot \tilde{s}_{m,n}(t) \tag{5.3}$$

The convoluted spike pattern for m^{th} neuron in the n^{th} population vector $(\tilde{s}_{m,n}(t))$ is obtained using a kernel function which convolute the discrete spike sequences into a continuous signal. Similar to previous studies on the Spike Pattern Association Neuron model (Mohemmed, Schliebs & Kasabov, 2011), this research applied the α kernel for spike convolution. If $F_{m,n}$ denotes the set of firing

times of the m^{th} neuron in n^{th} population vector, the convoluted spike pattern ($\tilde{s}_{m,n}(t)$) is obtained by applying the α-kernel as per equation 5.4

$$\tilde{s}_{m,n}(t) = \sum_{t^f_{m,n} \epsilon F_{m,n}} \alpha(t - t^f) \tag{5.4}$$

The α kernel is defined as equation 5.5 where τ_s denotes the synaptic time constant that characterise the exponential decay of the convoluted spike sequence and $\Theta(t)$ represents the Heaviside step function (Mohemmed, Schliebs, Matsuda & Kasabov, 2011).

$$\alpha(t) = e\, \tau_s^{-1}\, t\, e^{-t/\tau_s}\, \Theta(t) \tag{5.5}$$

Appendix A.1.2 presents the Matlab source code of the alpha kernel utilised for spike convolutoin in the proposed eSPANNet learning model.

τ_s characterises the exponential decay of a convoluted spike. Figure B.1 shows the difference in this exponential decay of the same spike in response to distinct synaptic time constant values.

The hidden layer (m) contains groups of SPAN's arranged as n number of population vectors. Firing times of the m^{th} neuron in the n^{th} population vector ($F_{m,n}$) is obtained using the post-synaptic spike pattern of the neuron ($s_{m,n}$) using the synaptic weight between input and hidden layer neurons ($w_{i,m}$), input spike train from the input neuron (x_i) and the firing threshold of the SPANs in the hidden layer ($th_{m,n}$). Therefore, the synaptic current of the neuron m in the SPAN population $I_m(t)$ is obtained using the weighted convoluted spike pattern received by the neuron m from the input neuron i as per equation 5.6.

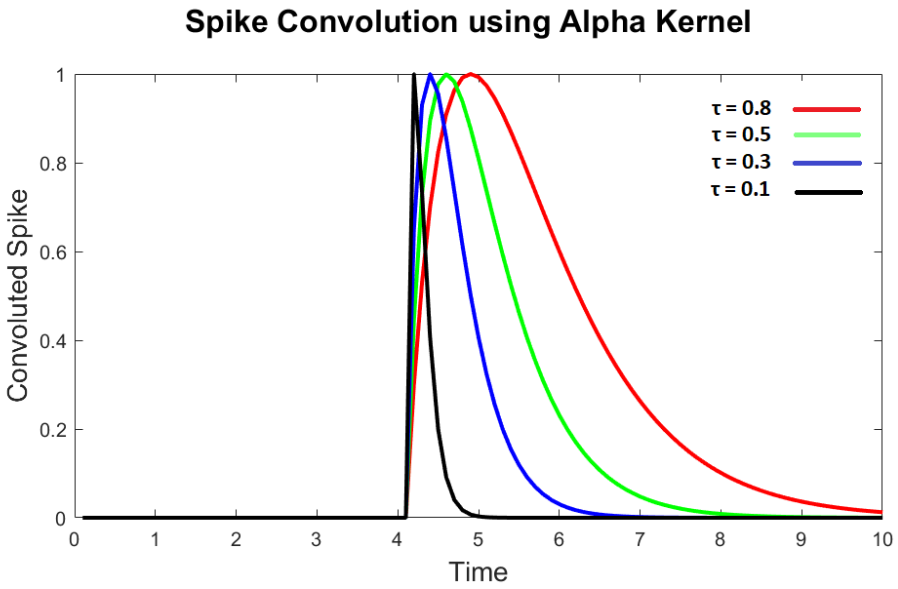

Figure 5.3: Alpha kernel

$$I_m(t) = \sum_i w_{i,m} \sum_f \alpha\left(t - t_i^f\right) \tag{5.6}$$

Here, $f_m(t)$ denotes the firing times of the m^{th} SPAN in the hidden layer marked by the time intervals its membrane potential ($I_m(t)$) reach the firing threshold th_m of the neuron as per equation 5.7.

$$f_m(t) = g\left(I_m(t), th_m\right) = \begin{cases} 1 & if \quad I_m(t) \geq th_m \\ 0 & otherwise \end{cases} \tag{5.7}$$

$w_{i,m}$ is calculated using the synaptic learning rule of the Spike Pattern Association Neuron (Mohemmed, Schliebs & Kasabov, 2011) as per equation 5.10.

$$\Delta w_{i,m}(t) = \lambda \tilde{x}_i(t)\left(\tilde{y}_d(t) - \tilde{y}_{out}(t)\right) \tag{5.8}$$

$$\Delta w_{i,m} = \lambda \int_0^{\infty} \Delta w_i(t)\, dt \tag{5.9}$$

$$\begin{aligned} \Delta w_{i,m} = \lambda \Bigg(\frac{e}{\tau}^2 \Bigg[\sum_g \sum_f \left(\left| t_i^f - t_d^g \right| + \tau \right) e^{-\frac{\left| t_i^f - t_d^g \right|}{\tau}} \\ - \sum_h \sum_f \left(\left| t_i^f - t_{out}^h \right| + \tau \right) e^{-\frac{\left| t_i^f - t_{out}^h \right|}{\tau}} \Bigg] \Bigg) \end{aligned} \tag{5.10}$$

where λ is the learning rate, τ is the time constant of the kernel function, t_i, t_d and t_{out} are the times of input, desired and acutal spikes. f, g and h denotes the indexes of input, desired and actual spikes.

Appendix A.1.3 contains the Matlab source code for calculating the SPAN synaptic weight update in the proposed eSPANNet learning model.

During incremental learning to predict a certain event, eSPANNet will first determine whether there is any SPAN in the corresponding population vector associated with that particular event. If there are no trained SPANs for the current event or if the trained SPANs can not produce the expected spike sequence for a given input spike sequence, a new SPAN is initialised in the corresponding population vector and trained to emit the expected spike sequence at the desired time point(s). As the SNN is exposed to continuous input spike sequences associated with distinct events, eSPANNet will incrementally evolve separate SPAN populations to associate input spike sequences with the corresponding events. Appendix A.1.4 presents the Matlab code corresponds to the incremental learning of eSPANNet.

Algorithm 1 Algorithm for updating the synaptic weight through SPAN learning in eSPANNet

Input:

input spike sequence: timing of the input spike events,

desired spike sequence: timing of the expected spike events,

actual spike sequence: timing of the actual spike events

Parameters:

τ: time constant that characterises the timing of the exponential decay of membrane potential,

λ: learning rate of SPAN

Output:

ΔW = synaptic weight update at current epoch

Process:

if there is at least one actual spikes in the actual spike sequence **then**

    compute difference between actual and input sequences $d_{input,actual}$ as :

    $d_{input,actual} = \sum_h \sum_f \left(\left|t_i^f - t_{out}^h\right| + \tau\right) e^{-\frac{\left|t_i^f - t_{out}^h\right|}{\tau}}$

else if no actual spike **then**

    $d_{input,actual}= 0$

end if

compute desired input difference $d_{input,desired}$ as:

$d_{input,desired}= \sum_g \sum_f \left(\left|t_i^f - t_d^g\right| + \tau\right) e^{-\frac{\left|t_i^f - t_d^g\right|}{\tau}}$

compute synaptic weight update ΔW as:

$\Delta W = \lambda \left(\frac{e}{\tau}^2 \left[d_{input,desired} - d_{input,actual}\right]\right)$

Algorithm 2 Algorithm for eSPANNet incremental learning

Input:

input spike sequence: timing of the input spike events,

desired spike sequence: timing of the expected spike events

Parameters:

max-error: maximum accepted difference between expected and desired spike time

isCorrectResponse = false: flag to train a new SPAN

Output:

SPAN Population Vectors

Process:

for <each streaming window> **do**
    get input and desired spike segment for learning
    if <event in the current desired spike segment> **then**
        get spike response of the current input segment from the corresponding population vector
        for <each event> **do**
            if <not empty population vector> **then**
                for <each anatomical cluster> **do**
                    if <empty cluster> **then**
                        set isCorrectResponse = false
                    else if <not empty cluster> **then**
                        get spike response of the population as:
                        difference between desired and actual spike time
                        $f_m(t) = g\left(I_m(t), th_m\right)$
                        where $I_m\left(t\right) = \sum_i w_{i,m} \sum_f \alpha\left(t - t_i^f\right)$
                        compute the error of each neuron in the population as:
                        if <correct responses> **then**
                            set isCorrectResponse = true
                        else if <incorrect responses> **then**
                            set isCorrectResponse = false
                        end if
                    end if
                end for
            else if <empty population vector> **then**
                set isCorrectResponse = false;
            end if
        end for
        if <isCorrectResponse == false> **then**
            train new spans for each channel
            if <error <= max-error> **then**
                add the trained SPAN to the current population
            end if
        end if
    end if
end for

5.2.5 Network validation

Each SPAN in the hidden layer is trained using a single training sample. As the network is exposed to more training samples, the SPAN will be evaluated based on its spike response for the forthcoming training samples. In addition, a separate validation dataset can also be used to validate each SPAN before evaluating the performance of the eSPANNet on the test dataset to improve the generalization of the eSPANNet learning model. A validation dataset can filter the neurons that can accurately predict class labels using a threshold level. The spike response of the SPAN's that demonstrated a less accuracy during validation will not be considered to determine the class labels of the test dataset. As the SPAN readout populations are evolved, each spiking neuron in the SPAN population is validated using their ability to emit spikes at desired time points for unseen input spike sequences. The eSPANNet only considers the spiking activity of the SPANs, which result in higher accuracy than a predefined threshold level. The threshold level is determined by the number of SPANs in the corresponding population and the maximum prediction accuracy of the SPANs in the population.

5.2.6 Evaluation of eSPANNet model using test data

For each unseen input spike trains, the spike response of each SPAN population will be obtained to determine the corresponding class label. Different strategies such as the average population activity or majority voting can be followed to determine the class label of a particular input spike sequence. Appendix A.1.6 includes the Matlab source code for eSPANNet spike response prediction and determination of class labels.

5.3 Proof of concept of the eSPANNet learning model

This section presents a proof of concept of the proposed eSPANNet learning model. The performance of predicting finger flexion events from Electrocorticography signals by a single healthy participant was used as a preliminary experiment to evaluate the prediction accuracy and incremental learning of eSPANNet. The proof of concept study uses data from a publicly awailable dataset called the 'prediction of finger flexion from Electrocorticography signals' (Schalk et al., 2007; Miller & Schalk, 2008). The dataset was released by the fourth Brain-Computer Interface competition. The dataset contains ECoG signals recorded from three subjects while performing finger flexion according to a cue presented to the subject.

5.3.1 Experimental conditions

The following sections describe the experimental conditions of the ECoG dataset used in this study (Miller & Schalk, 2008).

Subjects

This public dataset contains ECoG signals and the time courses of the flexion of each finger on the hand contralateral to the implanted grid. The three subjects in the dataset were epileptic patients who had electrode grids placed subdurally on the brain's surface for extended clinical monitoring and localisation of seizure foci.

Experimental protocol

The subjects were cued to move a particular finger by displaying the corresponding finger in words (i.e. Thumb) on a computer screen placed at the bed-side. There

were 30 movement stimulus cues for each finger which were interleaved randomly. The subjects typically moved the requested finger 3-5 times during each cue. Each cue lasted two seconds and was followed by a two-second rest period. During the rest period the screen was blank. The data collection lasted 10 minutes for each subject.

Signal recording

Each patient had subdural electrode arrays implanted. Each array contained 48-64 platinum electrodes that were configured in 8x6 or 8x8 arrangements. The electrodes had a diameter of 4 mm (2.3mm exposed), 1 cm inter-electrode distance, and were embedded in silastic. Signals from the electrode grid were amplified and digitised. The general-purpose BCI system (BCI2000) provided visual stimuli to the patient, acquired brain signals from the amplifier, and recorded individual fingers' flexion using a data glove. Electrocorticographic signals were acquired with respect to a scalp reference and ground, bandpass filtered between 0.15 to 200 Hz, and sampled at 1000 Hz.

5.3.2 Previous studies on the dataset

Several experiments on the dataset have been reported in the literature (Liang & Bougrain, 2012; Sanchez et al., 2008). The main goal of all three experiments is to approximate the finger movements from the ECoG signals. The effectiveness of approximation was evaluated using the Pearson correlation coefficient between the approximated finger flexion signal to the actual finger flexion signal recorded using a digital data glove. Here the proposed incremental learning approach was applied for predicting and approximating finger flexion events using the same dataset. In addition to the correlation coefficients, this study also utilises several performance

measures commonly used in machine learning to evaluate the performance of predicting finger flexion events.

5.3.3 Sampling and pre-processing

To simulate data streaming required for a single-trial BCI using this pre-recorded dataset, input and expected output signals were buffered using a buffer with fixed length and overlapping window. They fed input (ECoG signals) and expected output signals (actual finger movements recorded by the data glove) into two separate buffers, namely the input buffer and the expected output buffer. The signal stored in the input buffer was then filtered using a band-pass filter (low-pass cutoff: 120Hz and high-pass cutoff: 180Hz) and rectified. The first 400,000 data-points of the dataset was used for training while the remaining 200000 data-points were used for testing.

Previous studies on ECoG signals indicates several frequency bands related to sensory-motor processes. These include sub-bands (1 to 60 Hz), gamma band (60 to 100 Hz), fast gamma band (100 to 300 Hz), and ensemble depolarisation (300 to 6k Hz) (Liang & Bougrain, 2012; Sanchez et al., 2008). The filtered signal was then used for spike encoding.

There are four main steps for event prediction using eSPANNet as spike encoding, incremental synaptic learning, network validation, and determination of class label based on different criteria such as majority-voting or population activity.

5.3.4 Spike encoding

Temporal, spatio-temporal or spectro-temporal input data streams are first transformed into discrete spike trains using a suitable encoding algorithm such as the

Threshold-Based, Bens Spiker, Step-Forward or Moving-Window spike encoding methods. A detailed description of different spike encoding methods was presented in section 3.4. Spike encoding may performed either on raw or the pre-processed signals. Preprocessing can be utilised to increase the signal-to-noise ratio and enhance the event related information of raw input signals before spike encoding. One of the common approach for preprocessing is to extract the signal power of specific event-related frequency bands through band-pass filtering.

To calculate the encoding threshold a quarter of the training dataset was used initially. These input spike trains are then used for training the spiking neural network. Encoding of input signals into spike trains was performed using the Threshold-Based encoding algorithm (refer section 3.4.1). A fixed threshold θ for all input channels per subject was used for encoding the input signals into spike trains. If the band-pass filtered and rectified input signal through i_th input channel is $x_i(t)$, the encoding threshold θ_i is given by,

$$\theta_i = \bar{x_i} + a \cdot \sqrt{(x_i - \bar{x_i})^2/(N-1)} \tag{5.11}$$

where, $\bar{x_i}$ is the mean of the signal from all channels during the training session and a is an experimental factor determined by maximizing the correlation between temporal changes of the input and expected spike rates.

5.3.5 Incremental synaptic learning

As new training samples are received, the onset of finger flexion movements is detected from the signals stored in the expected output buffer. When a new finger flexion event is detected, if the current network is unable to predict the output class label accurately using equation 5.1, a new neuron is trained using the SPAN synaptic learning rule (equation 5.10). Depending on which finger it is,

this neuron will be added to the relevant population vector (equation 5.2). The readout neuron of the population vector is trained to emit spiking at the onset of the movement.

The difference in spike timing between the actual and expected spike times of the SPAN was considered as the spike time error. Therefore, if the spike time error is less than a predefined threshold level, the new neuron is added to the corresponding population vector. Otherwise, the response of that neuron is not considered when evaluating the network performance on test data. When the next sample is received, it is given to the current network, and the response of the readout neurons are obtained. If the spike time error is greater than the defined maximum error level (i.e. 5 % from the total sample duration) a new SPAN will be trained as per equation 5.10 to produce a spike at the expected spike time. Likewise, the neural network is evolved over time based on the response of the readout neurons to the incoming input spike trains.

5.4 Results

5.4.1 E1.1: Classification performance of eSPANNet

The performance of the eSPANNet as a classification method was evaluated using the following performance measures and compared with other state-of-the-art multiclass classification or clustering methods namely, Support Vector Machine, Decision Trees, Discriminant analysis and k-Nearest Neighbors. It was also compared with several ensemble-based methods such as AdaBoost, RUSBoost, Bagging and Subspace. In this multiclass classification problem, the performance of predicting each class label was calculated as one-vs-rest approach and ranked according to the descending order. The results are presented in figure 5.4 - 5.11.

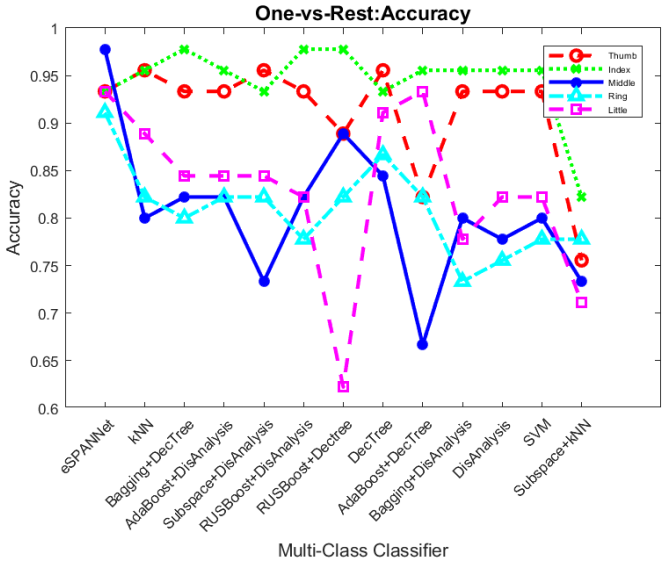

Figure 5.4: Comparison of classification performance - one-vs-rest accuracy on classifying finger flexion events of the thumb (red), index (green), middle (blue), ring (cyan) and little (magenta) fingers

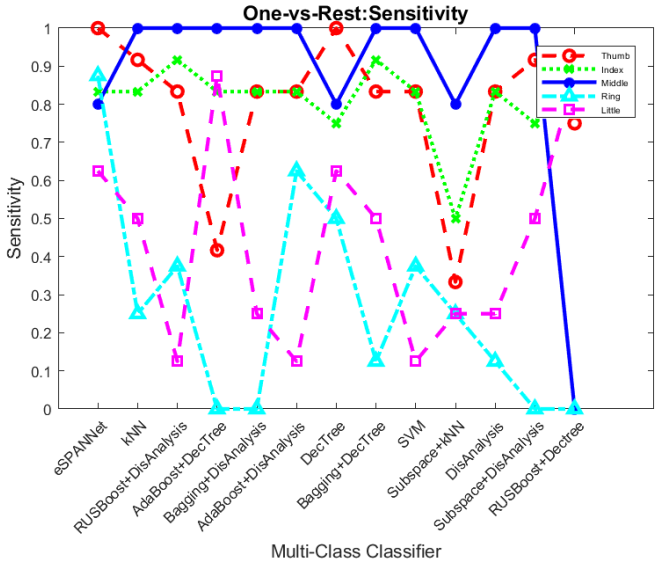

Figure 5.5: Comparison of classification performance - one-vs-rest sensitivity on classifying finger flexion events of the thumb (red), index (green), middle (blue), ring (cyan) and little (magenta) fingers

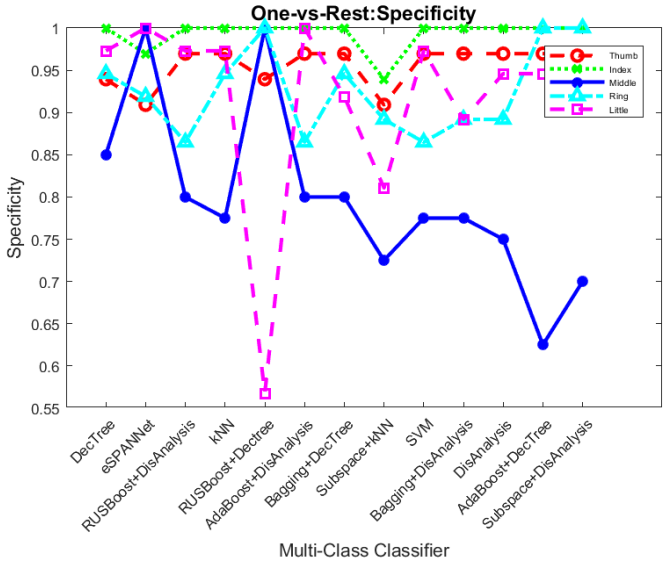

Figure 5.6: Comparison of classification performance - one-vs-rest specificity on classifying finger flexion events of the thumb (red), index (green), middle (blue), ring (cyan) and little (magenta) fingers

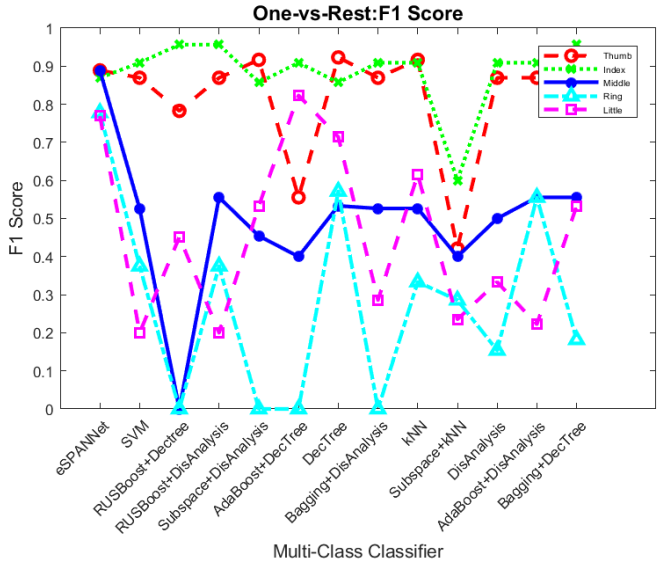

Figure 5.7: Comparison of classification performance - one-vs-rest F1-Score on classifying finger flexion events of the thumb (red), index (green), middle (blue), ring (cyan) and little (magenta) fingers

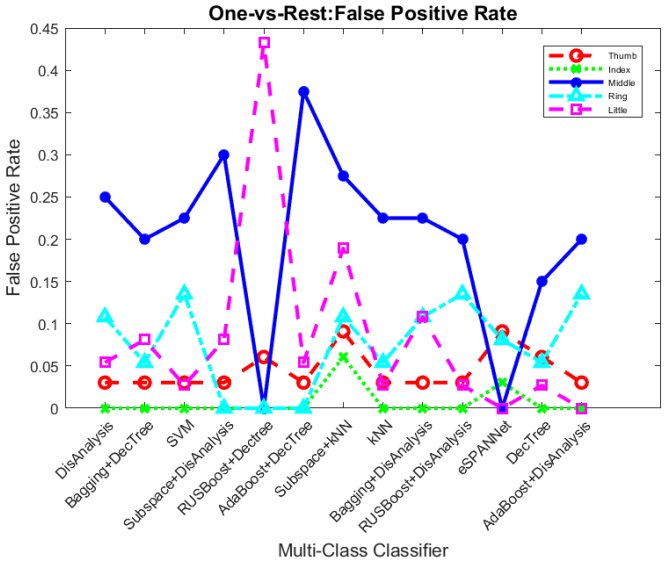

Figure 5.8: Comparison of classification performance - one-vs-rest False Positive Rate on classifying finger flexion events of the thumb (red), index (green), middle (blue), ring (cyan) and little (magenta) fingers

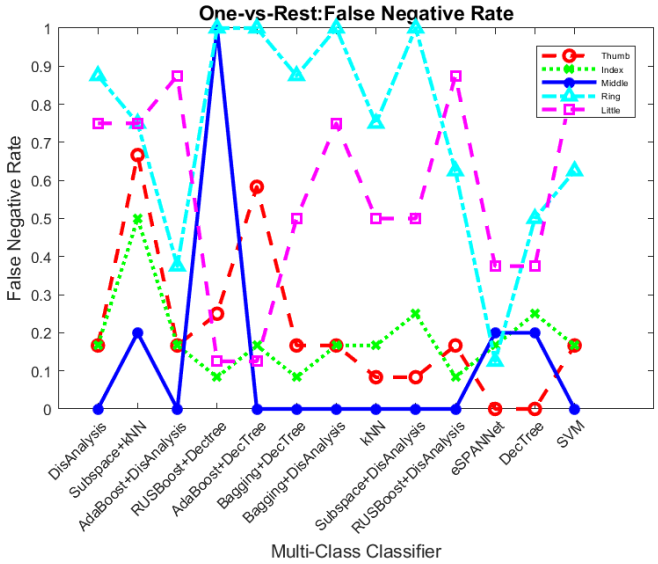

Figure 5.9: Comparison of classification performance - one-vs-rest False Negative Rate on classifying finger flexion events of the thumb (red), index (green), middle (blue), ring (cyan) and little (magenta) fingers

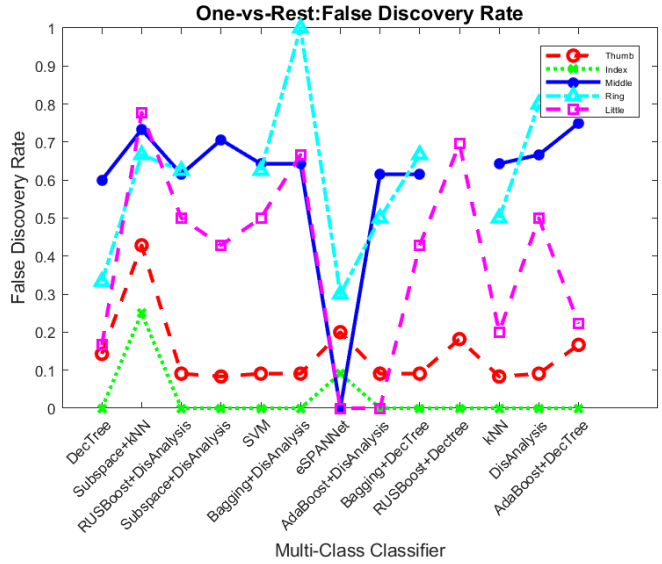

Figure 5.10: Comparison of classification performance - one-vs-rest False Discovery Rate on classifying finger flexion events of the thumb (red), index (green), middle (blue), ring (cyan) and little (magenta) fingers

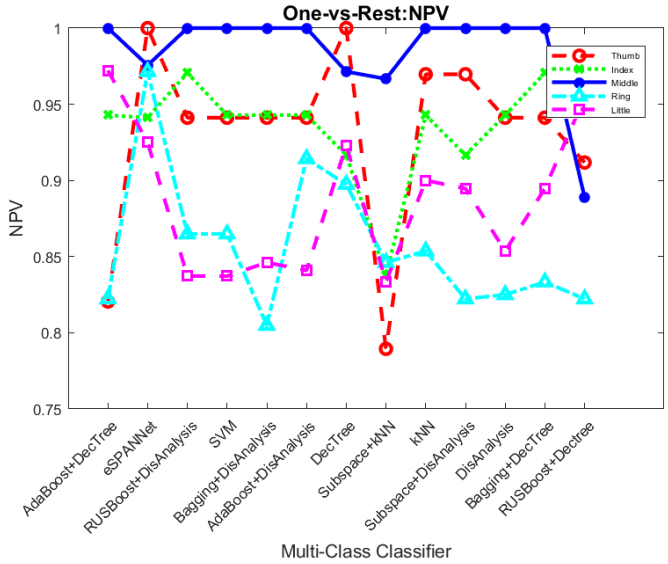

Figure 5.11: Comparison of classification performance - one-vs-rest Negative Predictive Value on classifying finger flexion events of the thumb (red), index (green), middle (blue), ring (cyan) and little (magenta) fingers

eSPANNet resulted in the highest classification accuracy on predicting flexion of the thumb, middle, ring and little fingers while the accuracy of predicting index finger flexion is slightly lower than the other classifiers. eSPANNet resulted in the highest sensitivity in predicting the flexion of thumb and ring fingers while the other fingers also showed a higher classification accuracy than other methods including kNN, AdaBoost and Bagging. The specificity of prediction by eSPANNet remains higher for all finger flexion events while the prediction of the index finger flexion by eSPANNet resulted in the highest specificity. eSPANNet showed a higher F1 score which was higher than many multiclass classification methods. False Positive Rate of the eSPANNet for all fingers remain low. The F1 score of eSPANNet is lower than the other classifiers. False Negative Rate for all fingers except the little finger by eSPANNet remains low, and it is lower than the other classifiers.

5.4.2 E1.2: Performance of reconstructing a continuous signal by eSPANNet

Figure 5.12 presents the finger flexion events predicted from test ECoG data by eSPANNet method. The correlation coefficients between the predicted and actual finger flexion events were obtained for comparative analysis. The results were compared with the approach presented in (Liang & Bougrain, 2012). Figure 5.13 presents the correlation coefficients returned by the two methods using ECoG data from subject 1.

5.4.3 E1.3: Evolving incremental learning of eSPANNet

The learning stage of the eSPANNet was partitioned into time bins (duration = 10 seconds) and continuously evaluated the performance using the TPR and FPR

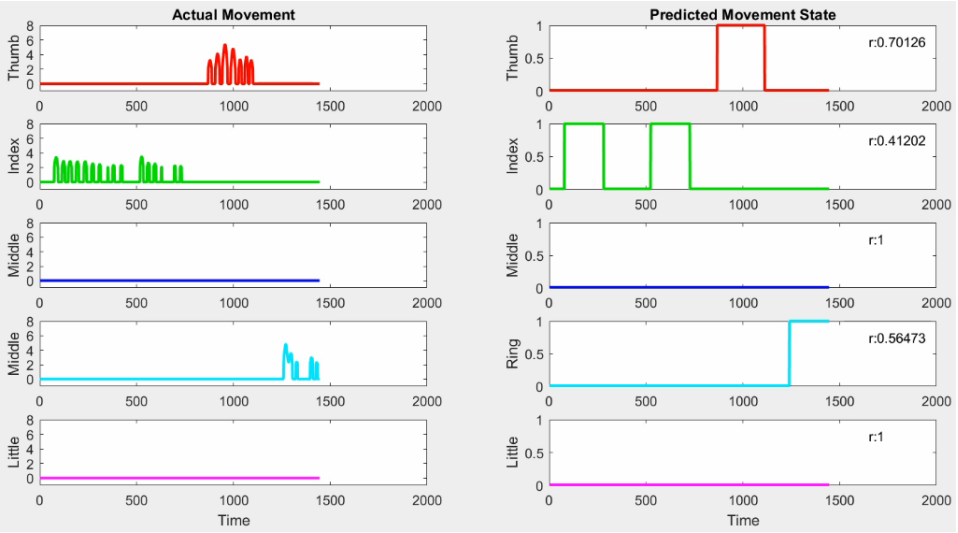

Figure 5.12: Predicted finger flexion state by the eSPANNet

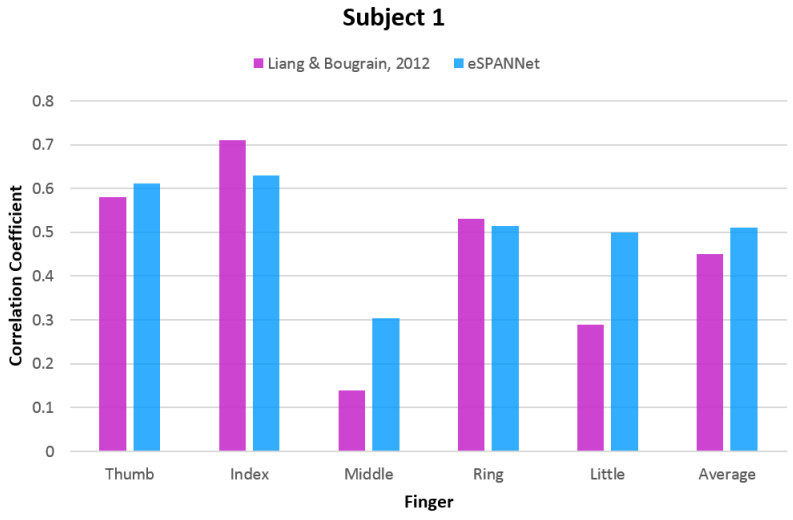

Figure 5.13: Comparison of Correlation Coefficients between the actual and approximated finger movements by eSPANNet

of each time bin to evaluate the incremental learning of eSPANNet. Figure 5.14 presents the evolution of true positive count of eSPANNet that demonstrate the feasibility of incremental learning. The number of True Positives in each time bin was gradually increased as new training samples are presented to the SNN model as shown in 5.14.

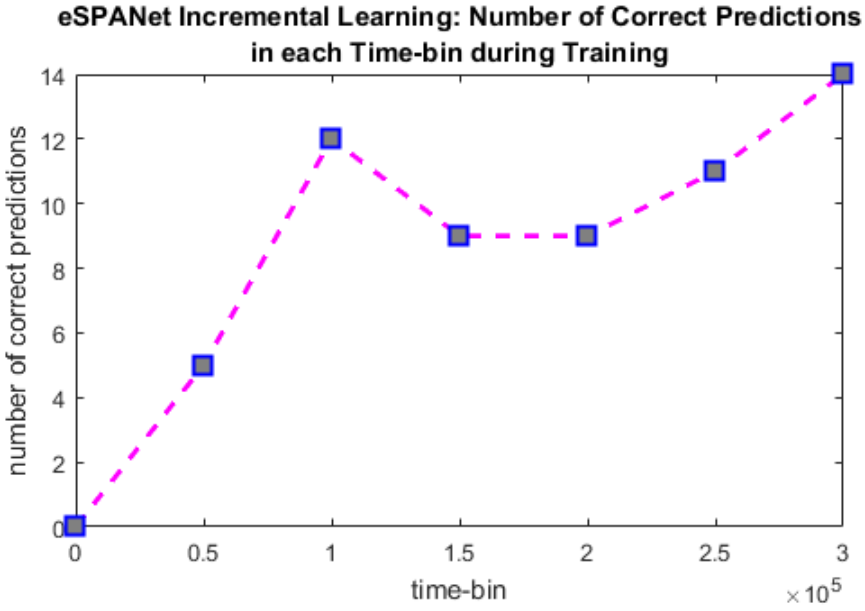

Figure 5.14: Evolution of true positive count during training

5.5 Discussion

Learning in animals is an incremental, adaptive and life-long process that require many repetitive attempts. Enabling such features in machine learning algorithms is a challenge. This chapter presented a spike-based supervised learning method called evolving Spike Pattern Association Neural Network which can learn spike sequences from temporal, spatio-temporal or spectro-temporal data streams. The eSPANNet learning algorithm is designed to learn incrementally from input spike sequences, and it can perform online event prediction. Through the experimental

results, it was shown that the algorithm could learn incrementally to produce precise spike timing in readout neurons. eSPANNet showed the ability to continuously decode the desired output from the input spike sequences, which is essential for many time series analysis systems, including Brain-Computer Interfaces.

5.5.1 Comparative analysis of the learning and classification performance

The proposed approach was experimentally validated using the finger flexion prediction dataset from the fourth BCI competition. The results showed that the eSPANNet as a classifier resulted in higher classification accuracy, sensitivity and F1 score, as well as lower False Positive and False Negative Rates, compared to several classifiers.

Figure 5.15 and 5.16 show the average ranking of each classification method according to the performance measures presented in section 5.4. The mean of each performance measure per each individual class was obtained and then ranked according to the descending order to compute the average rank. The lower ranks indicate a higher performance, while higher ranks indicate a lower performance measure. As shown in figure 5.15, in comparison with the other classification methods, eSPANNet resulted in a lower rank in terms of the accuracy, sensitivity and F1 score. The lower average ranks suggest that eSPANNet resulted in higher accuracy, sensitivity and F1 score in predicting individual finger flexion events.

Generally, eSPANNet showed a lower specificity in predicting individual finger flexion events compared to the other machine learning methods. The lower specificity in predicting finger flexion events by eSPANNet was mainly due to its lower performance in distinguishing finger flexion events by the middle, ring and little fingers. According to the neuromuscular anatomy of the forearm,

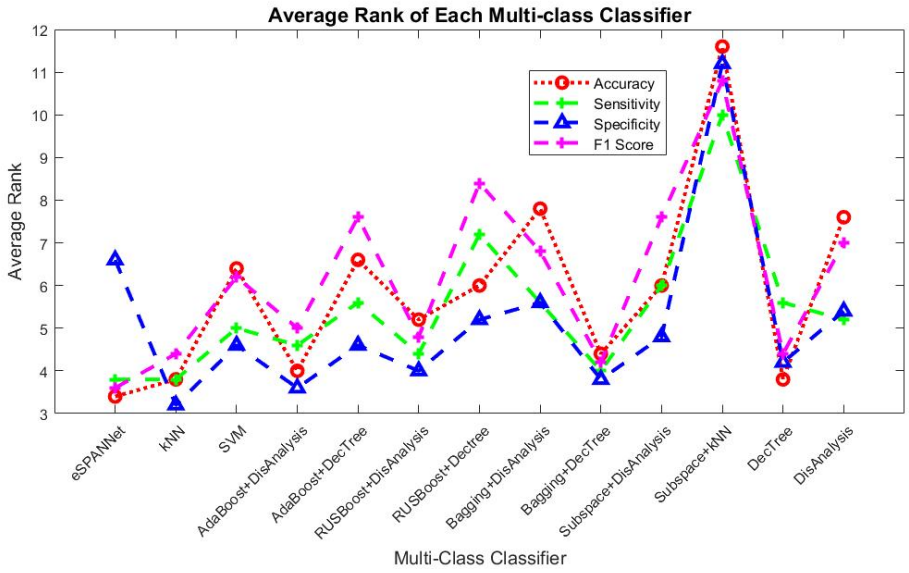

Figure 5.15: Accuracy, Sensitivity and Specificity

middle, ring and little fingers have a closely related nerve supply. Therefore, these three fingers often move together. In this particular case study, this anatomical relationship has caused a less performance in predicting finger flexion events of middle, ring and little fingers. However, distinguishing these movements is not an essential requirement for a restorative BCI that aims at facilitating functional hand movements such as grasping as these three fingers often move together during grasping. Prediction of finger flexion events of these three fingers as a whole group is sufficient for achieving object manipulation through a BCI. Although eSPANNet has shown a lower specificity, it will not result in a significant impact in utilising the eSPANNet algorithm for decoding functional hand movements in restorative Brain-Computer Interfaces.

Figure 5.16 ranked the machine learning methods in terms of their False Positive Rate, False Negative Rate and False Discovery Rate. According to the analysis, all three measures returned a higher average rank compared to the other classifiers. The higher ranking of eSPANNet indicates a lower False Positive, False Negative and False Discovery Rates. Further, as a regression analysis method,

eSPANNet also resulted in a higher correlation and therefore showed a better approximation of the original signal compared to the method proposed by Liang and Bougrain (2012).

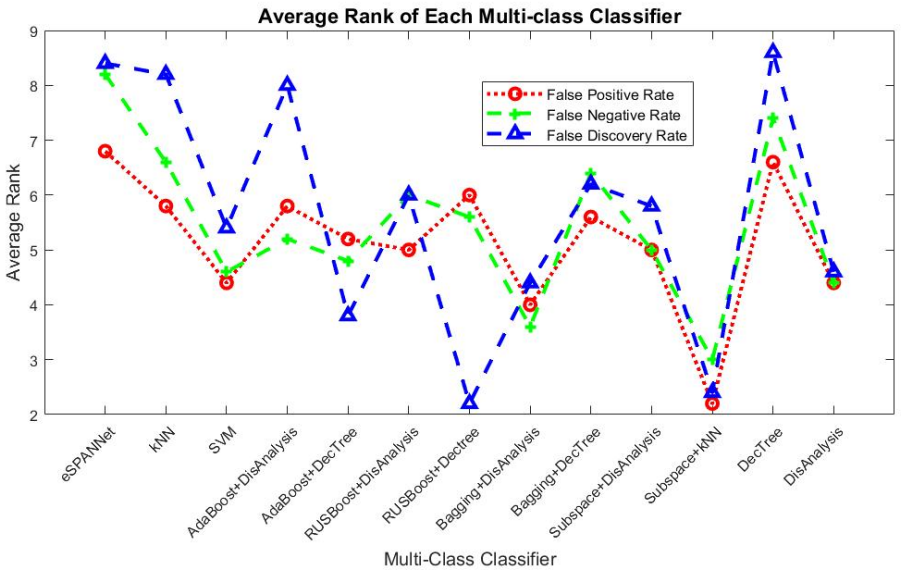

Figure 5.16: FPR, FNR and FDR

In contrast to the traditional batch processing based learning approaches, the proposed eSPANNet learning model could improve the training efficiency as it only considers an adequate amount of training samples. Further, the feedback from the previous learning iterations was used to determine the prediction error and used to adapt the network by suppressing the synapses that cause undesired spiking events. These features enhanced the biological plausibility of the model. The ability to evolve and learn incrementally was only feasible with eSPANNet and was not feasible with other traditional machine learning methods presented in this chapter.

5.5.2 Compatibility with neuromorphic platforms

Neuromorphic computing implements aspects of living nervous systems on electronic circuits. Compared to the silicon processors in conventional computers or embedded systems, neuromorphic computing platforms such as SpiNNaker can produce energy-efficient, fast, biologically plausible computation in machine learning systems. Transferring the computation from conventional embedded systems used by the BCI applications to neuromorphic platforms can advance state-of-the-art in Brain-Computer Interfacing. However, to date, most of the machine learning methods used in BCI's are not compatible with neuromorphic architectures.

This chapter compared eSPANNet with several other classification and regression analysis based methods, and none of them is compatible with neuromorphic platforms. eSPANNet, on the other hand, consists of a group of Leaky-Integrate-and-Fire neurons and trained using spike-time base learning rules. Therefore it is compatible with the neuromorphic architectures compared to the other machine learning methods presented in this chapter. While eSPANNet resulted in a better performance in prediction as a machine learning algorithm, it can also take the advantages of neuromorphic architectures to deliver a biologically plausible, fast and energy-efficient machine learning model.

5.5.3 Limitations

This chapter presented an incremental learning algorithm for Brain-Computer Interfaces using Spiking Neural Networks. Due to the non-stationarity and high trial-to-trial variability of brain data, online classification is challenging for BCI. In particular, it is more challenging in BCIs applied for neurorehabilitation interventions where the person incrementally learns to regain control of movement.

Therefore, classifiers which are unable to adapt for the changes of the signal, fail to achieve good accuracy in such experimental settings. The current research propose a biologically plausible computational model that is inspired by the 'population vectors' in living nervous system to address the variability of neural activity. The model contains a group of Spike Pattern Association Neurons, a spiking neuron model which can emit spikes at the desired time-point.

This proof of concept is limited to data from a single participant. Although the eSPANNet has shown a better performance than the other machine learning methods, due to this limitation, the statistical significance of the results is difficult to determine. The next chapter will present a comprehensive analysis using data from multiple participants to evaluate the performance of the eSPANNet learning model. The next chapter will investigate the feasibility of incremental learning using non-invasive Electroencephalography signals which have a lower signal-to-noise ratio than ECoG signals.

5.6 Significance

The current preliminary analysis shows that eSPANNet results in 1) a higher classification accuracy, sensitivity and F1 score compared to several other multi-class classifiers and, 2) a better approximation of the actual movement compared to several regression analysis based approaches. The novelty of the proposed algorithm is the ability to learn which inputs to focus on in an online manner. The results suggest that the eSPANNet could be a better BCI decoder due to its i) ability to incremental and life-long learning, ii) compatibility with the neuromorphic platforms and, iii) ability to address the non-stationarity of brain data.

eSPANNet, as a generative model, does not require certain predefined parameters to define the network architecture, such as the number of neurons in the hidden layer as it evolves neurons if needed. Its simple network architecture reduces the processing time during training and prediction. eSPANNet is more compatible with neuromorphic platforms compared to conventional methods that are commonly used for online event prediction as eSPANNet is based on more biologically plausible computational elements. eSPANNet, as a temporal learning method, can predict a continuous output as a desired spike time sequence from input spike sequences. Therefore, it is better compatible with real-time processing than spike rate-based methods.

5.7 Summary of the chapter

This chapter introduced a Spiking Neural Network model named evolving Spike Pattern Association Neural Network for online event prediction from data streams. The goal of eSPANNet was to utilise the polychronisation effect of Spiking Neural Networks for spike sequence learning from data streams. The chapter will described the eSPANNet incremental learning algorithm and, presented a proof of concept to preliminary evaluate its performance on predicting movements from neurological signals. A comprehensive study that experimentally validates the eSPANNet learning model using EEG data from multiple participants will be presented in the next chapter.

5.8 Contributions

- This research designed and implemented the evolving Spike Pattern Association Neural Network model which extended the Spike Pattern Association

Neuron model for incremental learning of spike sequences from temporal, spatio-temporal or spectro-temporal data streams.

- The research presented a proof of concept of the eSPANNet learning model to evaluate in principle the feasibility of predicting movements from neurological signals
- The research compared the performance of eSPANNet with multiple machine learning methods

5.9 Related publications

1. **Kumarasinghe, K.**, Taylor, D., & Kasabov, N. (2019, July). eSPANNet: Evolving Spike Pattern Association Neural Network for Spike-based Supervised Incremental Learning and Its Application for Single-trial Brain-Computer Interfaces. In 2019 International Joint Conference on Neural Networks (IJCNN). IEEE.doi:10.1109/IJCNN.2019.8852213

Chapter 6

Evolving Spike Pattern Association Neural Networks for Non-invasive Brain-Computer Interfaces

"Genius is one percent inspiration, ninety-nine percent perspiration."

Thomas A. Edison - America's greatest inventor

Chapter Overview

The previous chapter proposed a feedforward Spiking Neural Network model named evolving Spike Pattern Association Neural Network, for spike sequence learning from temporal, spatio-temporal or spectro-temporal data streams. eSPANNet is a computational model inspired by incremental learning for motor control in living nervous systems. A preliminary proof of concept study was presented in the previous chapter to evaluate its feasiblity for online event prediction, regression,

and incremental learning. This chapter extends the eSPANNet learning model and evaluates its performance on single-trial event prediction in non-invasive Brain-Computer Interfaces. The chapter also comparatively analyse the eSPANNet learning model with several brain-inspired and state-of-the-art non-brain-inspired machine learning methods. Appropriate statistical tests will be applied to evaluate the statistical significance of the results.

6.1 Introduction

The previous chapter proposed the eSPANNet model and demonstrated in principle its feasibility for spike-based incremental learning and online event prediction. The inspiration for the eSPANNet architecture is from the 'population vectors' which have been experimentally proven by several computational neuroscience studies. As a proof-of-concept, eSPANNet was experimentally validated by predicting individual finger flexion events from Electrocorticography signals. The results showed that eSPANNet results in higher classification accuracy, sensitivity and F1 score compared to multiple ensemble-based multi-class classifiers. Further, it could approximate the actual movement better than the linear regression-based method that used amplitude modulation of band-specific ECoG approach presented in (Liang & Bougrain, 2012). The significance of the eSPANNet as a neural decoder is its potential to learn which inputs to focus on from multichannel input signals in an online manner. The proof-of-concept study suggested that eSPANNet may be a better neural decoder for Brain-Computer Interface due to its incremental and life-long learning, compatibility with the neuromorphic platforms and, the ability to address the non-stationarity of brain data.

The previous chapter showed in principle the feasibility of evolving Spike Pattern Association Neural Network to online predict finger flexion events from invasive Electrocorticography signals adaptively and incrementally. However, the preliminary study presented in chapter 5 was limited to a single participant and used invasive ECoG signals to validate the performance of eSPANNet. As an invasive signal, ECoG has a relatively higher signal-to-noise ratio compared to non-invasive neurophysiological signals such as Electroencephalography. This chapter presents a new methodology, based on the eSPANNet architecture, and evaluate its performance for event prediction using non-invasive brain data from

multiple participants. The methodology is experimentally validated using a case study on predicting movement intention from EEG signals.

This chapter will address the following research questions.

- **RQ2: How can the network architecture of the eSPANNet learning model be improved to enhance its convergence and the prediction performance when learning from non-stationary stochastic data streams such as Electroencephalography?**
- **RQ4: How does the eSPANNet learning model compare with the static rate-based machine learning methods (such as the Convolutional Neural Networks and Support Vector Machine) and as well as the sequence learning-based machine learning methods (such as the Recurrent Neural Networks, linear regression and SVM-based regression) for predicting movement intention from EEG signals?**

This chapter introduces a methodology that uses the eSPANNet for predicting movement intentions from EEG signals for non-invasive Brain-Computer Interfaces. The goal of the current study is to enable the eSPANNet neural decoder to learn the association between the input and expected output by adjusting the synaptic connection weights of the SNN. This will enable eSPANNet to learn the temporal association between input and output and therefore will be able to produce precise spike time sequences for the input spike sequences.

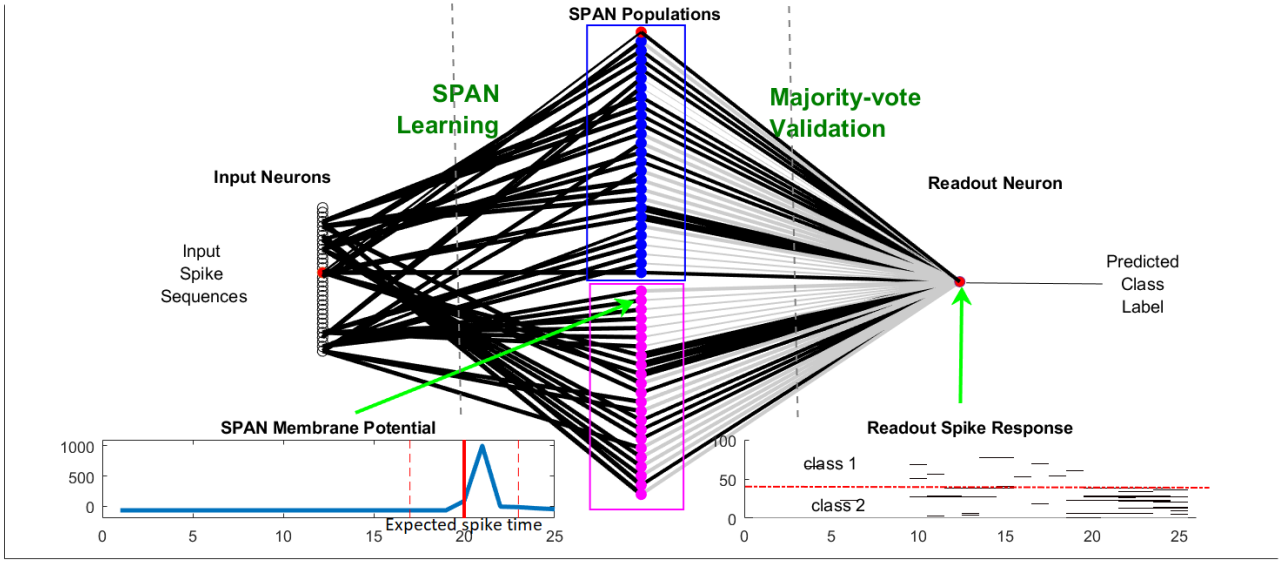

Figure 6.1: A single input synapse-based eSPANNet model trained and validated using movement intention and resting-state EEG signals of data from a single participant. Synaptic learning was performed using SPAN learning rule with training spike sequences. The network was validated using majority-vote of SPAN's for the validation dataset. Grey-coloured synapses between SPAN's and readout neuron returned a lower correct rate than the expected threshold level and therefore not considered when evaluating the performance on the test dataset.

6.2 Stochasticity of spike trains and the convergence of the eSPANNet learning model

Non-invasive neurological signals such as Electroencephalography are unable to measure the neural activity at a scale of individual neurons. Instead, EEG indicates the accumulated activity of neural populations that may contain thousands of neurons. A typical biological neural network exhibits more complex spike patterns than the simple pre and post-synaptic spike pairs studied in traditional protocols that characterise the synaptic plasticity of the brain (Faugeras et al., 2009).

The stochasticity of input spike trains is a challenge for convergence in spike-time based learning rules and the reliability of spike responses for predictive modelling using Spiking Neural Networks. When learning from stochastic spike sequences, the timing of the first spike of an input spike sequence has a significant impact on the convergence of the SPAN learning to a global optimum. The random spike trains arrive earlier than the desired time point causes the SPAN learning rule to trap in local minima instead of converging to its global optimal.

The anatomical studies of the animal brain have witnessed the existence of hierarchically organised sub-cortical structures such as the cortical columns that are specialised to execute specific functions. For instance, the neocortex of the brain can be divided into six distinct layers, each with a specific structure and associated functionality (Greig et al., 2013). The previous animal studies suggest that the neural activity at the populational level may provide a significant contribution to information processing in the brain to execute a cognitive task. In this regards, computationally modelling the collective neuronal dynamics at a scale of neuronal populations will enhance the predictive modelling of brain dynamics.

The models that describe these collective spatio-temporal brain dynamics has

to be different from the models of individual neurons that consist of parameters such as the membrane potential, firing threshold and membrane time constant. Faugeras et al. (2009) emphasis that based on the theories of effective mean-field in statistical physics, to model such dynamics it would be sufficient that the spatial scale to be large enough to include a large amount the neurons and small enough to ensure the homogeneousness of the brain region. Based on this theory, if there are m number of parameters are used to describe the behaviour of a single neuron, it is not necessary to have Nm amount of parameters to represent a mesoscopic description of a neural ensemble containing N number of neurons. Instead, the theory suggests that with the increase of N, the collective neuronal dynamics can be described by effective mean-field, which summarises the effect of interaction using a smaller amount of parameters.

Based on the above viewpoint, here, a new eSPANNet architecture is proposed to ensure the convergence of SPAN learning to a global optimum from stochastic input spike trains extracted from noisy and non-stationary EEG signals. This study will propose a single input synapse based Spike Pattern Association Neurons instead of the fully connected SPANs used in the eSPANNet architecture used in the proof of concept study presented in the previous chapter. Although this study does not provide theoretical proof, the experimental results empirically show that the single input synapse-based SPANs result in higher classification accuracy compared to the fully connected network architecture and thereby have more possibility on learning the optimal synaptic weights for emitting precise spike timing.

6.3 Construction of the neural decoder using eSPANNet learning model for non-invasive BCI

eSPANNet is an evolving feed-forward SNN architecture with a hidden layer containing groups of SPANs arranged as population vectors. The network evolves as new SPANs are trained to incrementally learn spike sequences following the principles of evolving connectionist systems (N. K. Kasabov, 2007). Due to the low signal-to-noise ratio and non-stationarity of EEG the spike sequences extracted from EEG signals exhibits more stochastic nature compared to the Electrocoticography signals analysed in the preliminary experiment of eSPANNet. As described in the previous section, the random spikes arrive prior to the desired time intervals is a problem for convergence of the eSPANNet learning model. The stochastic spikes cause the SPAN learning to reach to a local minimum instead of the global minimum. Therefore, the stochasticity of spike trains reduce the reliability of the spike response produce by a trained eSPANNet.

To address this randomness in spike trains, here a single input synapse base eSPANNet architecture is proposed instead of the fully connected eSPANNet architecture proposed in the proof of concept study of the eSPANNet. It is based on the assumption that if a certain input channel or feature contains a source of a certain event, the spiking activity of that channel the is temporally correlated with the timing of that particular event. The randomness of spike trains can be eliminated through a population of spiking neurons trained to emit spikes at a desired time point as such population can represent a probability distribution. In contrast to SPAN's in the hidden layer being connected with all input neurons, the modified architecture connects each SPAN with only one input

neuron which permits receiving of input spikes through only one synapse. The previous eSPANNet architecture used average population activity for determining the class label. In contrast, here, majority-voting was used to determine the class label. Figure 6.1 presents an exemplified single input synapse-based eSPANNet architecture evolved from EEG signals of a particular participant.

6.3.1 Structure of the Network

A detailed description of the eSPANNet learning model was presented in the previous chapter (refer section 5.2). Here only the relevant information are presented to ensure the clarity of this description. The current case study aims at distinguishing the movement intention from resting state EEG signals. Therefore, it forms a binary classification problem which will be addressed through the proposed eSPANNet model.

For binary classification using a labelled dataset with x number of input channels (features), a feed-forward SNN containing three layers, input, hidden and output is formed which is referred as the evolving Spike Pattern Association Neural Network or eSPANNet. The input layer contains x number of input neurons that feed input spike trains into the hidden layer. The hidden layer consists of groups of SPAN's. Each SPAN is connected to only one input neuron and trained using the input spike train of a single training sample received through that particular input-SPAN synapse. The output layer contains a single output neuron which receive spikes through all neurons in the hidden layer. Output neuron predicts the corresponding class label using majority-voting of SPAN's in the hidden layer.

There are four main steps for event prediction using eSPANNet as spike encoding, synaptic learning, network validation, and determination of class label through majority-voting.

6.3.2 Spike encoding

The power of the band-passed filtered EEG signal was used for spike encoding using the threshold-based spike encoding method. The threshold values for encoding was obtained using the mean and standard deviation of the filtered EEG signal. To encode, first the temporal difference between two consecutive data points of the pre-processed EEG signal is obtained (refer equation 6.1).

$$d = \sum_{t=2}^{n} |x\,(t-1) - x(t)| \tag{6.1}$$

The mean value ($mean$) and the standard deviation (std) of the computed temporal differences are calculated to compute the encoding threshold as per equation 6.2 where c denotes a predefined constant referred as encoding factor.

$$th = mean(d) + c \cdot std(d) \tag{6.2}$$

The sign of the threshold value can be used to form both positive (th_+) and negative (th_+) encoding thresholds. However, since SPAN can not be trained with both positive and negative spikes together at the same time, here the polarity (sign) of the spike train is not considered. Any temporal difference that reach either the positive or negative threshold was marked as a positive spike in the encoded spike train.

If the current temporal difference is larger than the positive threshold, or smaller than the negative threshold, a spiking event is marked in the encoded spike train. Otherwise, no spike event is added to the current time interval of the spike train (refer equation 6.3).

$$s(t) = \begin{cases} 1 & if \quad d(t) >= th_{+} \quad OR \quad d(t) <= th_{-} \\ 0 & otherwise \end{cases} \tag{6.3}$$

6.3.3 Synaptic learning

As the input spikes were fed into the SNN, a new Spike Pattern Association Neuron will be initialised and trained to emit spike at the desired time point. For each class, a separate neuron population was trained using 6.4.

$$\begin{aligned} \Delta w_{i,m} = \lambda \Bigg(\frac{e}{\tau}^2 \Bigg[\sum_g \sum_f \left(\left| t_i^f - t_d^g \right| + \tau \right) e^{-\frac{\left| t_i^f - t_d^g \right|}{\tau}} \\ - \sum_h \sum_f \left(\left| t_i^f - t_{out}^h \right| + \tau \right) e^{-\frac{\left| t_i^f - t_{out}^h \right|}{\tau}} \Bigg] \Bigg) \end{aligned} \tag{6.4}$$

Actual firing time of spiking neurons f_{out} are obtained using the synaptic current, I_m according to equation 6.5 where th_m is the threshold of the neuron.

$$f_{out}\left(I_m(t), th_m\right) = \begin{cases} 1 & if \quad I_m(t) \geq th_m \\ 0 & otherwise \end{cases} \tag{6.5}$$

Synaptic current of the neuron m in the SPAN population is obtained using the weighted convoluted spike pattern observed by the neuron m from the i input neuron as given by equation 6.6.

$$I_m\left(t\right) = \sum_i w_{i,m} \sum_f \alpha\left(t - t_i^f\right) \tag{6.6}$$

Convoluted spike pattern of the neuron m in the n SPAN population is obtained using an α-kernel (equation 6.7).

$$\tilde{s}_{m,n}(t) = \sum_{t^f_{m,n} \epsilon F_{m,n}} \alpha(t - t^f) \tag{6.7}$$

6.3.4 Validation of population vector

The prediction accuracy of each neuron in each population was obtained using the validation dataset. This set filters the neurons which can more accurately predict class labels and the other SPAN's will not be considered for determining the class labels of test data.

6.3.5 Prediction using majority-vote

For each unseen input spike trains, the response of each neuron population was obtained. The class label assigned by each SPAN was obtained. From these class labels, the output neuron computes the majority vote to determine the class label.

6.4 Movement intention prediction from Electroencephalography signals

6.4.1 Experimental conditions

This case study applies the eSPANNet computational model for predicting movement intention during a grasp and lift task. The study used the WAY-EEG-GAL (WAY: Wearable interfaces for hAnd function recovery, EEG: Electroencephalography, GAL: Grasp-And-Lift) dataset (Luciw et al., 2014a, 2014b) which is specifically designed to critically examine the information processing in the human

brain related to sensation, intention, and action from EEG signals when performing a grasp-and-lift task. A detailed description of the dataset was presented in section 4.4.

Subjects

Twelve healthy participants performed a series of grasp and lift trials of a small object when the object's weight, surface friction, or both, were changed unpredictably between trials.

Task

The dataset contains simultaneous EEG, Electromyography (EMG), force and kinematic signals recorded from 12 healthy participants during cued grasp and lift (GAL) movements. The participants performed a series of grasp and lift trials of a small object. During a GAL trial, the participant reached the object, grasped it using the index finger and thumb, and lifted it a few centimetres up in the air, held it stably for a couple of seconds, and then replaced and released the object. An LED light cued the start and end of a GAL trial. Since this is a functional upper limb movement, the participants were gazing at the cue, hand, object, initial position and target position of the object. The participants demonstrated natural coordination among eye, hand, object and target position while performing the grasp and lift movement.

Signal recording

The dataset contained EMG signals from five sensors that monitored the muscle activity of the Anterior Deltoid (AD), Brachoradial (B), Flexor Digitorum (FD), Common Extensor Digitorum (CED) and First Dorsal Interosseous (FDI) muscles of the right arm at a 4kHz sampling frequency. The EEG, force and kinematic

signals were recorded at 500Hz sampling frequency. Two surface contact plates were placed on each side of the object to record the grip force and load force applied on the object during each trial. Data from kinematics sensors was gathered using 3D position sensors placed on the object, wrist, thumb and index finger. Each sensor recorded x,y,z position and azimuth, elevation and roll angles. The signals recorded from multiple devices were synchronised using a sync signal recorded by each device.

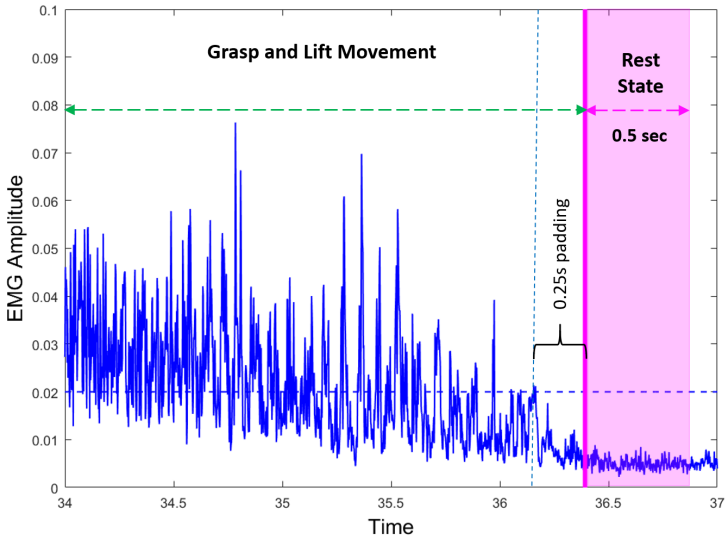

Figure 6.2: Extraction of resting state during a grasp-and-lift trial using the accumulated amplitude the five fore-arm EMG sensors The blue-solid line indicates smoothed and rectified accumulated amplitude of five fore-arm EMG sensors. The blue-dotted line represents the threshold value for detecting movement onset. The movement stopped time is marked by the magenta colored line. EEG signals corresponding to 0.5s from movement stopped time (magenta) was extracted as rest state EEG.

6.4.2 Pre-processing and data extraction

First, the EEG signals were filtered using a band-pass filter with the low-pass cutoff at 12 Hz and high-pass cutoff at 30Hz frequencies. EEG samples during the resting state were extracted using the accumulated amplitude of the five fore-arm

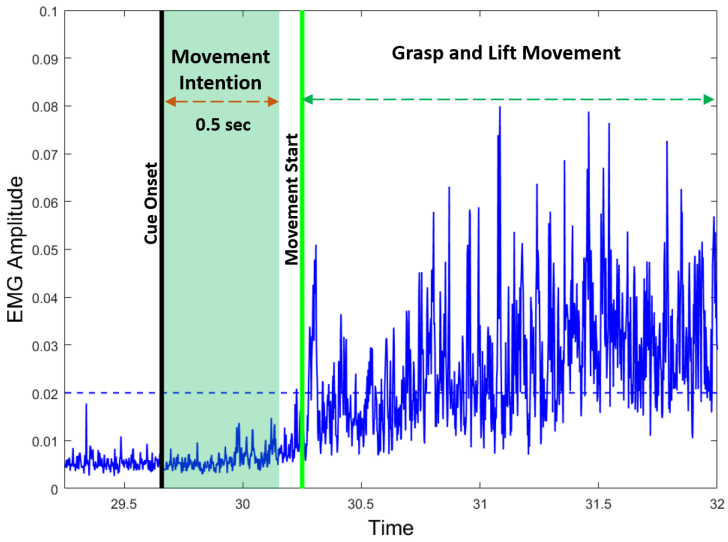

Figure 6.3: Detection of movement intention period after the cue onset of the grasp-and-lift trial. The blue-solid line represent the smoothed and rectified accumulated amplitude of the five fore-arm EMG sensors. The blue-dotted line is the threshold value for detecting movement onset from the rest states. The black line indicates the time LED was switched on to present cue for initiating the movement (cue onset time) and the green line represents the movement onset time. EEG signals corresponding to 0.5s from cue onset time was extracted as movement intention period.

Electromyography sensors. Mean amplitude of the rectified and smoothed EMG signal was used to obtain a subject-specific threshold value which distinguishes the movement and resting states. Resting-state EEG samples were obtained 500 ms from the time the mean EMG signal went below the defined EMG threshold. Figure 6.2 shows extraction of rest EEG from a grasp-and-lift trial using movement stopped time. Blue-solid line indicates the smoothed and rectified accumulated amplitude of five EMG sensors. Blue-dotted line shows the threshold value for detecting movement onset and stopped time. All samples were visually examined to validate the correctness of the defined threshold value. Vertical magenta line indicates movement stopped time as detected by the EMG threshold value. EEG signals corresponding to 500 ms from movement stopped time was extracted as

rest state EEG. Figure 6.3 depicts extraction of movement intention duration from a grasp-and-lift trial using cue onset time. Black vertical line indicates the time LED was switched on to present cue for initiating the grasp and lift trial. Green line indicates the movement onset time detected using the threshold value. EEG signals corresponding to 500ms from cue onset time (black) was extracted as EEG samples correspond to the movement intention state.

6.4.3 Evolution of the eSPANNet learning model

For this case study on predicting movement intention during cued grasp and lift tasks, the EEG signals corresponding to 500ms from cue onset time was extracted as the EEG samples correspond to movement intention. The desired spike time (d_t) for SPAN learning was considered as $d_t = round(N * p)$ where N and p denote the total number of data points in the sample and a predefined percentile, respectively. In this particular case study, p was set to 0.75 which indicates that the SPANs are trained to emit a spike at 375 ms after the cue onset time. However, p is an experimental parameter for eSPANNet computational model which needs to be empirically determined and optimised based on an appropriate performance measure such as the prediction accuracy. As the SNN receive input spike sequences correspond to movement intention, the eSPANNet is incrementally evolved to emit spike at 375 ms from the onset of the cue according to the eSPANNet learning model presented in section 6.3.3.

6.4.4 Comparative analysis

Multiple experiments were conducted to comparatively analyse the performance of the eSPANNet learning model. The first experiment aims at answering the RQ2 of this thesis (refer section 4.2.1 for details). The study will compare the

performance of movement intention detection by the two eSPANNet architectures. The performance will be compared to empirically evaluate the ability to address the stochastic nature of spike trains extracted from EEG signals by each network architecture. For this comparison, the two eSPANNet models were evolved using the same training dataset and evaluated using the same validation dataset. The number of correct movement intention predictions by each eSPANNet architecture was recorded and used to obtain the average correct rate. The Student's t-test was performed to evaluate the statistical significance of the observed difference in the mean correct rates.

The next two experiments are designed to answer RQ4 of this thesis (refer section 4.2.2 for details). The second comparative analysis was performed to compare the performance of the eSPANNet with multiple supervised learning methods. This comparison is mainly divided into two stages. At the first stage, eSPANNet was compared with two rate-based computation models; a Support Vector Machine and a Long-Short Term Memory Recurrent Neural Network; that use static features to train the model. Appendix A.2 and A.2 contains the Matlab source codes used for implementing the CNN and RNN, respectively. The SVM and LSTM models were trained using the spike rate of each input spike sample. The accuracy of detecting movement intention by the two models was compared with the performance of the eSPANNet learning model. At the second stage of the analysis, eSPANNet was compared with multiple machine learning models that aimed at predicting a continuous output from data streams. Multiple regression analysis based methods such as SVM-based regression, Decision Tree-based regression, Linear regression, and as well as a 2D Convolutional Neural Network which is compatible with time-series data were considered for the comparative analysis. Each model was trained using the same training dataset and evaluated using the same validation dataset. One-way ANOVA under the

95% confidence level was applied to evaluate the statistical significance of the differences in average correct rates. Appendix A.2 includes the Matlab source code for determining the statistical significance. The next section will report the obtained results and discuss their interpretations.

6.5 Results and Discussion

6.5.1 E2.1: Comparison between Single and Multi-Input Synapse-based Network Architectures

Table 6.1 presents the correct rates of movement intention prediction by the two network architectures of eSPANNet. All participants showed an above chance-level in terms of predicting the movement intention using both network architectures. The single-input synapse based network architecture resulted in 0.71 mean correct rate and the standard deviation of 0.06. The multi-input synapse architecture cause 0.65 mean correct rate and 0.07 standard deviation. The comparison between the two architectures shows a 6% improvement of the mean correct rate in predicting movement intention using the single input synapse-based network architecture compared to the multiple input synapse-based network architecture. Subject 1 resulted in the highest correct rate of 0.81 while subject 6 was correspond to the lowest correct rate of 0.62 using the single input synapse eSPANNet architecture.

Figure 6.4 shows a box plot that represent the statistical distribution of the obtained results including the minimum, maximum, median, and the first and third quartiles of the correct rates correspond to the participant group. The mean correct rate of the population indicated 0.06 difference in mean correct rate by the two network architectures of eSPANNet. The statistical significance of the observed difference in mean correct rates were evaluated using the paired-sample

Table 6.1: Comparison of the Correct Rate of Movement Intention Prediction by Single and Multi-input Synapse-based Architectures

Subject ID	**Single-Input Synapse Architecture**	**Multi-Input Synapse Architecture**
1	0.81	0.76
2	0.74	0.7
3	0.73	0.7
4	0.77	0.63
5	0.71	0.58
6	0.62	0.59
7	0.68	0.59
8	0.68	0.64
9	0.69	0.6
10	0.72	0.76
11	0.77	0.69
12	0.64	0.61
Average	**0.71 (+/-0.06)**	**0.65 (+/-0.07)**

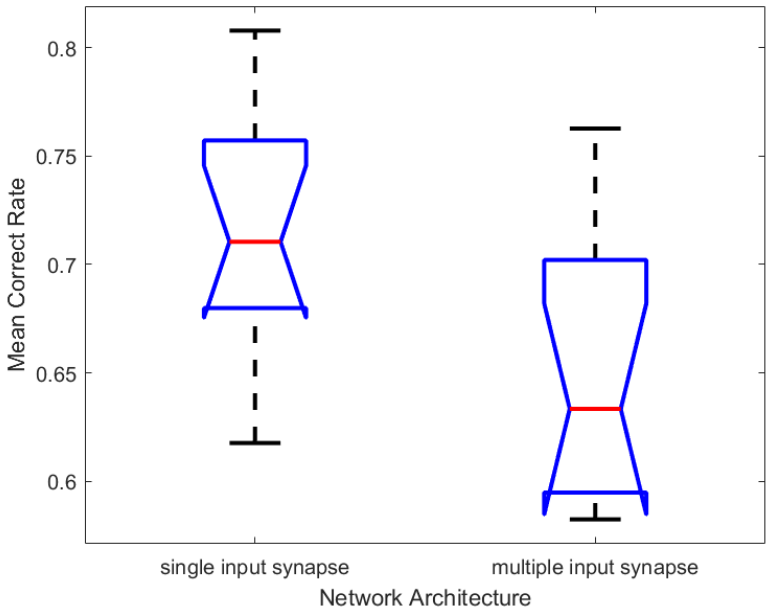

Figure 6.4: Mean correct rates of movement intention prediction by single and multiple input synapse-based network architectures of eSPANNet

t-test for means at the 95% confidence interval (H_0: $\mu_0 = 0$, H_A: $\mu_0 \neq 0$; where H_0 is the null hypothesis, H_A is the alternative hypothesis, and μ_0 is the hypothesised

mean difference, $\alpha = 0.05$). The one-tail paired sample t-test resulted in a p-value of 0.001. As the p-values is smaller than the 0.05 significance level, the t-test rejects the null hypothesis in favour of the alternative hypothesis. The smaller p-value confirms the statistical significance of the mean correct rate obtained through the single-input synapse-based network architecture compared to the fully connected multi-input synapse-based network architecture.

The eSPANNet synaptic learning model has the ability to learn which inputs to focus on in an online manner as the network is exposed to new training samples. The comparison empirically shows that single input synapse-based approach resulted in a higher prediction accuracy compared to the multi-input synapse-based architecture. Although it is not theoretically proved in the thesis, this increment in prediction accuracy may be due to the ability of single input synapse based SPAN learning to eliminate random noise and converge better than the multiple input synapse-base SPANs. In SPAN learning, the spikes receive earlier than the desired spike time can cause the learning rule to reach a local minima instead of converging to it's global minima. When receiving spikes from multiple input synapses, the SPAN neuron model is unable to learn the optimal synaptic weight vector due to the temporally uncorrelated spikes arrive through noisy input synapses. Thus the learning algorithm is unable to reach its global optimal. Therefore the neuron model can not obtain the most appropriate and accurate weight vector between input and output neurons for generating precise spike timing. This issue is more significant when using EEG signals than the ECoG signals used in our previous preliminary study as EEG exhibits a smaller signal-to-noise ratio compared to ECoG signals. However, when receiving input spikes through only one synapse, the SPAN synaptic learning rule can generate the optimal synaptic weight vector that can emit precise spike timing at the desired time point. Therefore the single input synapse based architecture results in a

higher correct rate compared to multiple input synapse based architecture.

6.5.2 E2.2: Comparison with rate-based methods

Table 6.2: Comparison of the Correct-rate of Movement Intention Detection using Spike-rate by SVM and LSTM

Subject ID	**eSPANNet**	**SVM (spike-rate)**	**LSTM (spike-rate)**
1	0.81	0.81	0.8
2	0.74	0.71	0.71
3	0.73	0.74	0.74
4	0.77	0.73	0.77
5	0.71	0.64	0.66
6	0.62	0.71	0.72
7	0.68	0.75	0.77
8	0.68	0.72	0.73
9	0.69	0.61	0.6
10	0.72	0.72	0.75
11	0.77	0.76	0.77
12	0.64	0.68	0.67
Average	**0.71**	**0.72**	**0.72**

Table 6.2 shows the correct rates of detecting movement intention by eSPANNet as a dynamic classifier and by the two static energy based classifiers, SVM and LSTM that used the spike-rate. SVM and LSTM resulted in an average correct rate of 0.72 for all subjects while the average correct rate of eSPANNet was 0.71. The results indicate that subject 1 corresponds to the highest correct rate by all three methods. eSPANNet and SVM resulted in the highest correct rate of 0.81 while LSTM resulted in 0.80. The lowest correct rate by eSPANNet was 0.62 by subject 6 while the lowest of SVM was 0.61 using EEG data of subject 9. The lowest correct rate of all three methods was 0.60 obtained from LSTM using data from subject 9. Figure 6.5 shows the mean correct rates obtained by eSPANNet, SVM and LSTM models.

One-way ANOVA was conducted under the 95% (α = 0.05) confidence level to verify the statistical significance of the obtained results. The statistical test resulted in a relatively larger p-value of 0.87. Since the p-value is larger than the significance level of 0.05, it is not possible to reject the null hypothesis in favour of the alternative hypothesis. The larger p values suggest that the difference in mean correct rates is not statistically significant, while the eSPANNet has some significant advantages when compared to the the two rate-based methods considered for the comparative analysis as explained below.

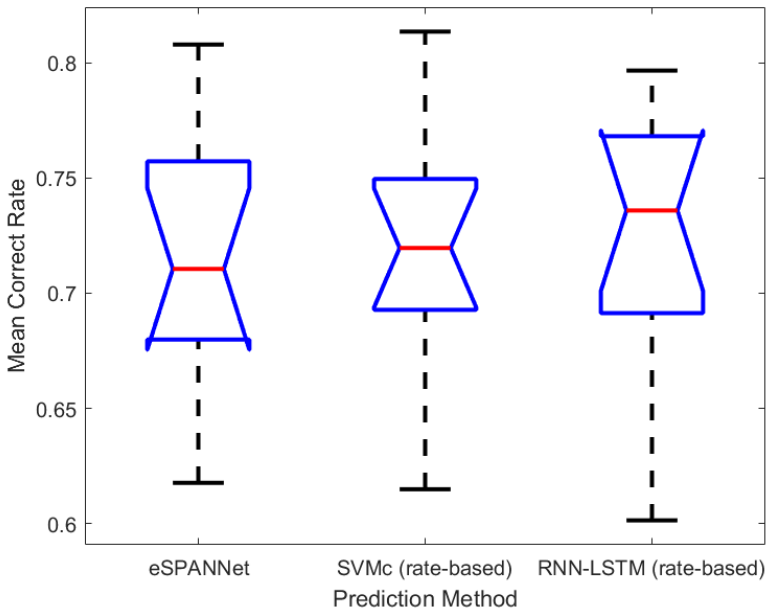

Figure 6.5: The statistical distribution of the mean correct rates of movement intention prediction by single input synapse-based eSPANNet, spike rate-based SVM and LSTM

eSPANNet as a generative model can incrementally evolve to model temporal associations between input and desired spike events without explicit feature engineering steps that require a considerable amount of human intervening. Since the eSPANNet learning model is based on brain-inspired computational elements such as the spiking neuron models and synaptic learning principals, it is more

biologically plausible and compatible with neuromorphic processors than the LSTM and SVM. eSPANNet, as a temporal learning model, can predict the continuous output from input data streams. It does not depend on static energy-based features such as the spike rate and does not require temporal averaging, which reduce the information transfer rate of the prediction model. In contrast, SVM and LSTM that used spike-rate as input features for prediction required to wait until the required amount of input samples are collected iteratively to compute the spike-rate. During online prediction, spike rate-based methods reduce the information transfer rate of a BCI and result in a lower bit-rate compared spike sequence-based methods. These three approaches were similar in terms of the prediction accuracy; however, eSPANNet was more compatible for real-time prediction than the rate-based SVM and LSTM models.

6.5.3 E2.3: Comparison with sequence-based methods

Table 6.3 compares the correct rates of movement intention detection by eSPANNet with four spike sequence-based methods; namely, RNN with LSTM, SVM-based regression, Decision Tree-based regression, linear regression and 2D Convolutional Neural Network. The results show that eSPANNet resulted in the highest mean correct rate, while the CNN (0.67) and linear regression (0.66) returned the second and third-highest correct rates respectively. The SVM-based regression resulted in a mean correct rate of 0.62, while LSTM and DT showed an average correct rage of 0.56. The results suggest that LSTM and DT with spike-sequence resulted in very low mean correct rate, which is much closer to that of random guessing. Figure 6.6 shows a box plot that represents the statistical distribution of the correct rates of the twelve participants by each method. Evaluation of the statistical significance of the observed mean correct rates using one-way ANOVA under the

95% confidence interval resulted in a p-value of 0.0000008. The smaller p-value indicates the statistical significance of the observed difference in mean correct rates. As shown in figure 6.7, the mean correct rate obtained using eSPANNet is statistically significant compared to spike sequence-based LSTM, and as well as the SVM and DT-based regression models. However, the linear regression and the Convolutional Neural Network models resulted in a statistically insignificant mean correct rate.

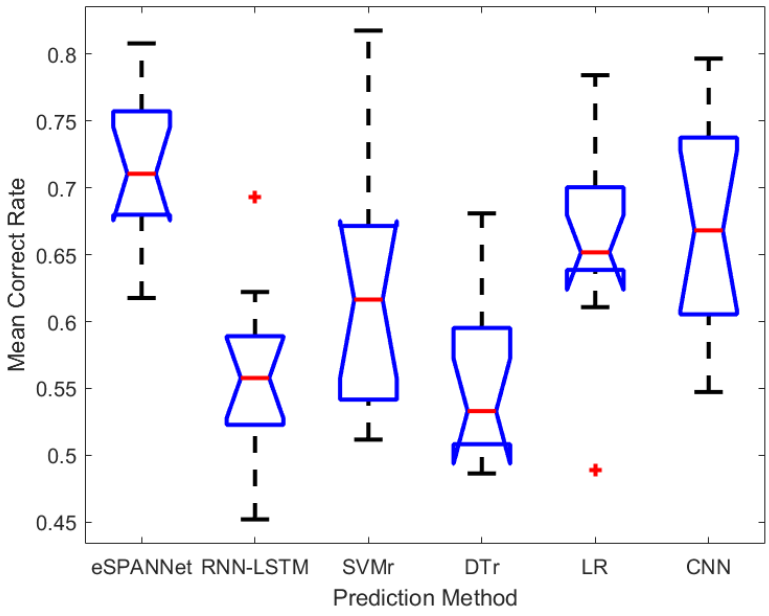

Figure 6.6: The statistical distribution of the mean correct rates of movement intention prediction by single input synapse-based eSPANNet, spike sequence-based CNN, SVM-based Regression, Decision Tree-based Regression and Linear Regression

Table 6.3: Comparison of the Correct Rate of Movement Intention Detection using Spike-sequence by LSTM, SVM, DT and Linear Regression

Subject ID	**eSPANNet**	**LSTM (spike-sequence)**	**SVM-regression (spike-sequence)**	**DT-regression (spike-sequence)**	**Linear-regression (spike-sequence)**	**CNN (spike-sequence)**
1	0.81	0.58	0.68	0.54	0.77	0.80
2	0.74	0.5	0.64	0.68	0.69	0.59
3	0.73	0.45	0.66	0.53	0.68	0.73
4	0.77	0.57	0.61	0.54	0.78	0.74
5	0.71	0.51	0.51	0.53	0.64	0.65
6	0.62	0.56	0.51	0.51	0.65	0.59
7	0.68	0.55	0.53	0.5	0.61	0.62
8	0.68	0.54	0.56	0.59	0.65	0.68
9	0.69	0.53	0.57	0.49	0.64	0.55
10	0.72	0.62	0.7	0.6	0.71	0.7
11	0.77	0.69	0.82	0.66	0.49	0.78
12	0.64	0.6	0.62	0.5	0.65	0.66
average	**0.71**	**0.56**	**0.62**	**0.56**	**0.66**	**0.67**

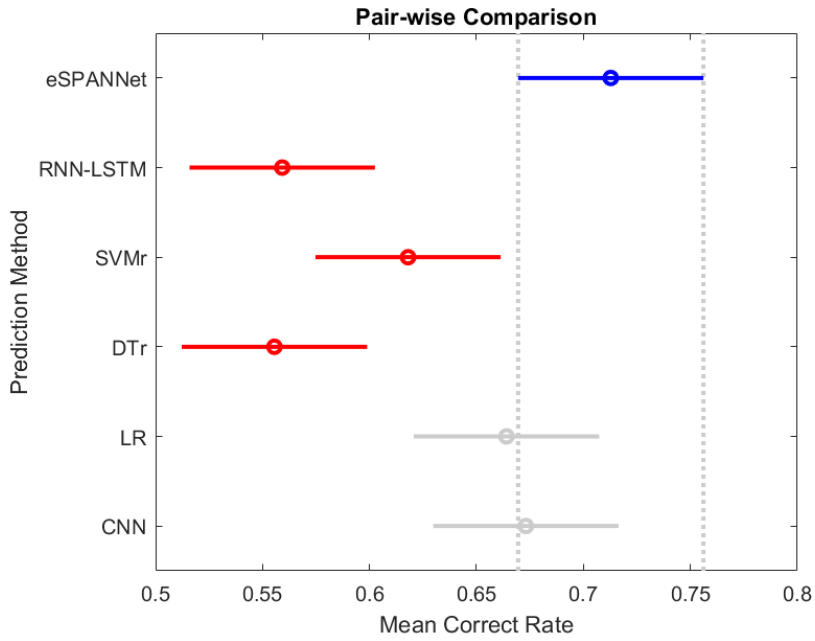

Figure 6.7: Statistical significance of the mean correct rates by spike sequence-based methods using one-way ANOVA (blue: eSPANNet, red: statistically significant difference, gray: statistically insignificant difference)

6.6 Significance

In order to successfully utilise the BCI intervention for motor recovery and motor substitution, it is essential to develop classifiers which can predict different movements of an impaired or an amputated limb. Such predictions are challenging as they should be performed in real-time using less spatially and temporally distinguishable neural activities of the brain. Computational approaches that are inspired by the biological processes of living nervous system such as the deep Spiking Neural Networks provide new insights into artificial intelligence. Previous studies on ANN-based neural decoders for noninvasive BCI has employed different ANN-based methods such as Convolutional Neural Networks, Recurrent Neural Networks, Restricted Boltzmann Machine, Deep Belief Networks, Extreme

Learning Machine, Spiking Neural Networks and Multi-Layer Perceptron. Complex classification algorithms for predicting mental commands from EEG increase the training and prediction time of a BCI decoder. Further, BCI decoders that utilise conventional feature engineering approaches such as prepossessing, feature extraction, dimensionality reduction, and feature selection adds a considerable delay to the prediction time.

Deep neural networks as automatic feature learners can discover significant discriminative features from raw data. Although deep neural network architectures with several convolutional layers exhibit higher classification accuracy, they require higher training and prediction time and computational power as a result of the computational complexity that emerge from such classic hierarchical abstraction. At the same time, finding the most suitable neural network architecture has to be performed empirically as it is hard to determine which architecture suite best for a given classification task.

This chapter presented a novel method based on the eSPANNet SNN model for online event prediction non-invasive Electroencephalography signals. eSPANNet is a feed-forward SNN model which can evolve incrementally. The comparison between the two network architectures of eSPANNet showed a statistically significant improvement when using the single-input synapse-based network architecture than the multiple input synapse-based eSPANNet network architecture. It is emperically shown that this increment in prediction accuracy may be due to the ability of the SPAN learning rule to better converge when receiving inputs through a single input synapse.

This thesis aimed to develop a biologically plausible machine learning model to decode and understand various human behaviour from EEG. The model has incorporated several existing neurocomputational models such as the Spike-Time Dependent Plasticity that describe certain aspects of biological neurons and

neural network. The movement intention EEG represents the brain activity just after observing the cue (stimulus). The resting-state EEG was obtained after the participant completed the task which was about seven seconds after the onset of the cue. From the neurophysiological perspective, the cued grasp and lift movement under consideration might have induced neuromodulation and neuroplasticity of the brain. However, the thesis did not intend to replicate the exact neurophysiological phenomenon of the brain. Instead, the thesis intended to evaluate whether a brain-inspired machine learning approach could improve the prediction accuracy and interpretability of the neural decoder than the conventional non-brain-inspired machine learning models.

In conclusion, eSPANNet, as a generative model, does not require certain predefined parameters related to network architecture, such as the number of neurons in the hidden layer as it evolves neurons if needed. Its simple network architecture reduces the processing time during training and prediction. eSPANNet is more compatible with neuromorphic platforms compared to the other methods such as SVM, LDA and MLP as the network architecture utilises more biologically plausible computational elements. Moreover, eSPANNet as a temporal learning method can predict a continuous spike-time outputs from streaming input sequences. Therefore, it is suitable for real-time processing, in contrast to the rate-based prediction methods. The findings of this study show the feasibility of eSPANNet learning model to construct a neural decoder for non-invasive Brain-Computer Interfaces.

6.7 Summary of the chapter

This chapter extends the eSPANNet learning model and evaluates its performance on single-trial event prediction in non-invasive Brain-Computer Interfaces. The

chapter also comparatively analyse eSPANNet with several brain-inspired and as well as the traditional non-brain-inspired machine learning methods. Appropriate statistical tests are applied to evaluate the statistical significance of the results.

6.8 Contributions

- This research evaluated the performance of eSPANNet learning model to learn complex spike sequences from stochastic data streams.
- The research proposed the single input synapse based eSPANNet network architecture to address the non-stationarity of EEG signals.
- The research experimentally validated the eSPANNet learning model using Electroencephalography signals from multiple healthy participants.
- The current study evaluated the performance on predicting movement intentions from Electroencephalography signals when performing grasp and lift movements by multiple healthy participants.
- This study compared the prediction performance of eSPANNet with multiple rate-based and sequence-based learning models and appropriate statistical tests were conducted to evaluate the statistical significance of the observed differences in model performance.

6.9 Related publications

1. **Kumarasinghe, K.**, Kasabov, N., & Taylor, D., Evolving Spike Pattern Association Neural Networks and Applications for Non-invasive Brain-Computer Interfaces (in preperation to be submitted to IEEE Transactions on Neural Networks and Learning Systems by December 2020)

Chapter 7

Deep Learning and Deep Knowledge Representation in Spiking Neural Networks for Brain-Computer Interfaces

"Mathematics is the language with which God wrote the Universe."

Galileo Galilei - an pioneering astronomer, physicist and engineer who is often referred to as the as the "father of the scientific method"

Chapter Overview

This thesis proposes two spike-based generic methods for constructing interpretable Brain-Inspired Spiking Neural Network model for spike sequence learning from data streams. The previous two chapters proposed and validated one of the proposed generic method named evolving Spike Pattern Association Neural Network. This chapter presents the second spike-based generic method proposed in this thesis.

The proposed learning method aims at representing and extracting deep spatio-temporal knowledge in Brain-Inspired Spiking Neural Network architectures. The current study suggests that such SNN architectures demonstrate the ability to learn and reveal deep in time-space functional and structural patterns from spatio-temporal data. These patterns can be represented as deep knowledge, in a partial case in the form of deep spatio-temporal rules. The chapter will first present a theoretical framework of the proposed knowledge representation algorithm. Then an experimental validation of the proposed learning model will be presented to show the feasibility of the proposed framework for revealing the topological patterns. The proposed framework is a promising direction for building a new type of Brain-Computer Interfaces.

7.1 Introduction

Deep learning in ML is inspired by the human's ability to learn and evolve over time by creating spatio-temporal connections in the brain's neural network. A common organisation of visual information processing can be found in the human brain and computational models of deep learning CNNs. Long networks of connections, that are activated at a millisecond time scale, represent deep knowledge as illustrated on image recognition, speech and language and other cognitive tasks (N. Kasabov & Benuskova, 2004; N. K. Kasabov, 2018). It has already been demonstrated that Spiking Neural Networks can be successfully used as computational models to model not only dynamic data in neuroscience but also other types of temporal data such as seismic, audio and video data (N. K. Kasabov, 2014; Gerstner et al., 2012, 1997; Masquelier et al., 2009; Maass et al., 2002). The ability to produce non-synchronous but precisely timed sequence of spikes that were emitted as a result of strongly connected clusters of spiking neurons is called the polychronisation effect in Spiking Neural Networks (Izhikevich, 2006). Such polychronous groups emerge through synaptic learning such as Spike Time Dependent Plasticity learning when as SNN is exposed to recurrent spatio-temporal stimuli.

This study suggests that Brain-Inspired Spiking Neural Network architectures can learn and reveal deep in time-space functional and structural patterns from Spatio-temporal data. These patterns can be represented as deep knowledge, in a partial case in the form of deep spatio-temporal rules. This is a promising direction for building new types of Brain-Computer Interfaces called Brain-Inspired Brain-Computer Interfaces. This chapter will address the following research question.

- **RQ3: Based on the abilities of SNN for deep learning, can SNNs be used to construct an interpretable machine learning model that represents deep knowledge as spatio-temporal rules?**

Several recent studies point out the less interpritablity of of deep learning models and propose different approaches to improve the interpretability of deep neural networks. Chakraborty et al. (2017) present a review of different attempts for enhancing the interpretability of machine learning models. Ribeiro et al. (2016) proposed Local Interpretable Model-Agnostic Explanations (LIME) framework that can be applied on multiple machine learning algorithms to extract interpretable and human understandable representations of data. A recent 'in-silico' study on the digital reconstruction of a rat neocortical microcircuitry using spiking neurons suggests that the brain learns from stimuli to create new dimensions in a dynamically evolved connectionist structure to provide a missing link between structures and functions over time (Reimann et al., 2017). Convolutional SNN has been developed for audio-visual information processing (Wysoski et al., 2010) and also for predicting cognitive events from neurological signals (Sakhavi et al., 2015; Tabar, Yousef Rezaei and Halici, 2016; J. Liu et al., 2015; Mao et al., 2017). It has been observed that such deep learning ML models can better reveal the complex dynamics of the information processing in the brain than the conventional vector-based ML methods.

Based on the abilities for deep learning, this research explores the feasibility of SNNs to represent deep knowledge from spatio-temporal brain data, learned in a BCI. The study assesses the possibility of articulating and interpreting this knowledge for a better understanding of brain dynamics and the creation of more sophisticated neural decoder for Brain-Computer Interfaces. A theoretical framework and its experimental validation on deep knowledge extraction and representation using SNN are presented. The proposed methodology was applied in a case study to extract deep knowledge of the functional and structural organisation of the brain's neural network during the execution of a Grasp and Lift task. The experimental validation shows that the the proposed approach successfully

extracted the neural trajectories that represent the dorsal and ventral visual information processing streams as well as its connection to the motor cortex in the brain. Deep spatio-temporal rules on functional and structural interaction of distinct brain areas were then used for event prediction in the BCI. The computational framework can be used for unveiling the topological patterns of the brain, and such knowledge can be effectively used to enhance the existing neural decoders for non-invasive Brain-Computer Interfaces.

The findings from this study make several contributions to the existing BCI literature. Firstly, this study shows that the proposed brain-inspired SNN architecture can be effectively used to model the spatio-temporal brain dynamics during cognitive tasks. Secondly, such knowledge can be effectively used not only to predict the cognitive states of the brain to operate a BCI but also to understand the brain dynamics during a cognitive task through the presented BI-BCI. Thirdly, this chapter establishes a methodological framework for effectively merge the already known knowledge about the brain's functionality from neuroscience studies with machine learning research to enhance the interpretability of BCI's. The chapter presents a theoretical framework, its implementation and experimental validation of a brain-inspired SNN-based approach for deep learning and knowledge representation on spatio-temporal data. It also presents a novel brain-inspired methodology to analysing trained SNN models to represent new knowledge and understanding of the underlying cognitive processes that generated the data.

The rest of the chapter is organised as follows. The next section briefly explains the theoretical framework on deep knowledge extraction using the proposed BI-SNN architecture followed by the methodology presented in section 7.3. Section 7.4 states the experimental validation of the proposed methodology. Results are presented in section 7.5 followed by the discussion and significance of the study

presented in section 7.6.

7.2 Theoretical Framework

7.2.1 Definition of Deep Knowledge

Deep knowledge is what the human brain learns and manifests all the time, exemplified by: listening or playing musical pieces, playing a game, visual perception, predicting the movement of a predator, all sorts of cognition, decision making, consciousness, and everything else the brain does.

Deep knowledge as defined in (N. K. Kasabov, 2018), represents an informative spatio-temporal pattern of events that happen in *space* and *time* in their interaction, and this representation can be interpreted and comprehensible through symbolic and/or numerical expressions.

The repetitive sequences of spatio-temporal activities of distinct brain areas, together with their probabilities of being active after one another (referred as the transition probability - $P_{(\{\text{from-state}\},\{\text{to-state}\})}$), form neural trajectories that are deep in space and time. Such trajectories can be retrieved using fuzzy or crisp rules. A hypothetical example is given below and illustrated graphically in figure 7.1 (see (N. K. Kasabov, 2018) for more information).

For a set of events $E_{\text{from-state, to-state}}$, that form a neural trajectory in space S over the time t at a probability of $P_{(\{\text{from-state}\}, \{\text{to-state}\})}$ that trigger a transition from the previous state to the current state through the function $F_{\text{from-state, to-state}}$, a crisp or fuzzy depending on the nature of the membership function that determine the state transitions rule-base can be extracted and represented according to the following format.

$$Q_n = f_{\text{crisp}}(E_{\text{n,t}}, e_{\text{t}})$$

where $E_{n,t}$ is the known neural trajectory of the n number of spatio-temporal patterns over the time t and the e_t is the observed neural trajectory of the test spike sequence.

Each spatial location is defined as a cluster of spiking neurons and acts as a binary unit depending on its activation level. Thus, there are 2^l number of different states where l is the number of different spatial locations. Several parameters can be used to determine the level of activation, such as the average spike rate of the cluster and the number of synaptic connections with significant weight change during Spike Time Dependent Plasticity learning. The event $E_{\text{from-state,to-state}}$ denotes an event that triggers a state transition at time T and can be represented in the following format.

$$E_{from-state,to-state} = (F_{from-state,to-state}, S_{to-state}, T_t, P_{from-state,to-state}) \quad (7.1)$$

where $F_{\text{from-state, to-state}}$ is the function that triggers the state change, $S_{\text{to-state}}$ is the active neural clusters at time T_t and the $P_{\text{from-state, to-state}}$ is the transition probability of the two states.

$P_{(n,t,E_{\text{from-state,to-state}})}$ denotes the transition probability of the n^{th} pattern (Q_n) at the time interval t and obtained using the following equation.

$$P_{(n,t,E_{from-state,to-state})} = \frac{\sum_{S_{from-state}=1}^{S} \sum_{S_{to-state}=1}^{S} (q_{S_{from-state,t-1}} \wedge q_{S_{to-state,t}})}{N} \quad (7.2)$$

where S is the set of neural clusters, q is the activation level of each neural cluster, and N is the number of training samples.

7.2.2 A Hypothetical Example

The above theoretical framework is illustrated by the following hypothetical problem presented below and illustrated graphically in figure 7.1.

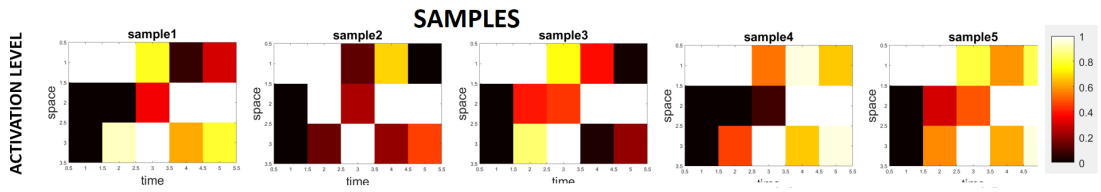

(a) Activation level of the samples over time

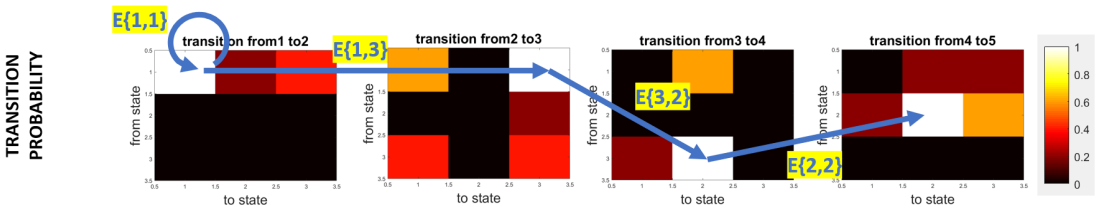

(b) probabilities of transition over time

STATE SPACE AND TRUTH TABLE

State id	L1	L2	L3
S{}	0	0	0
S{3}	0	0	1
S{2}	0	1	0
S{2,3}	0	1	1
S{1}	1	0	0
S{1,3}	1	0	1
S{1,2}	1	1	0
S{1,2,3}	1	1	1

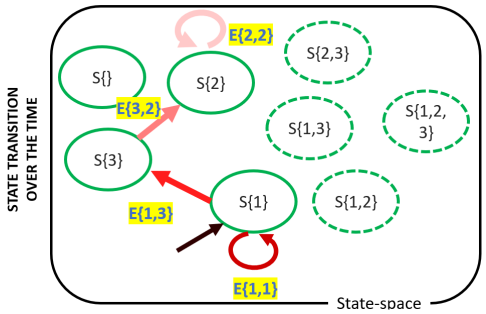

(c) State-space, truth table and state transition over time

Figure 7.1: Hypothetical example

Figure 7.1a depicts the activation level (q) of three neural clusters (S = {S_1, S_2, S_3}) over five time bins (t={t_1, t_2, t_3, t_4, t_5}).

The transition probabilities of each state ($P_{(n,t,E_{from\text{-}state,to\text{-}state})}$) between two adjacent time intervals are presented in figure 7.1b and the neural trajectory of the spike pattern is extracted by applying a transition probability threshold. The extracted trajectory is highlighted in blue color.

Figure 7.1c shows all possible events and the truth table for the hypothetical

problem. The neural trajectory is presented as a sequence of state transitions that happen over time in 7.1c. Each state is labeled using the neural clusters which are active. For instance, S{1} is to indicate the state in which only the S1 is active and S2 and S3 are not active. S{} indicates the state which does not show activity in any of the neural clusters. The brightness of the arrow indicates the relative time of each state transition.

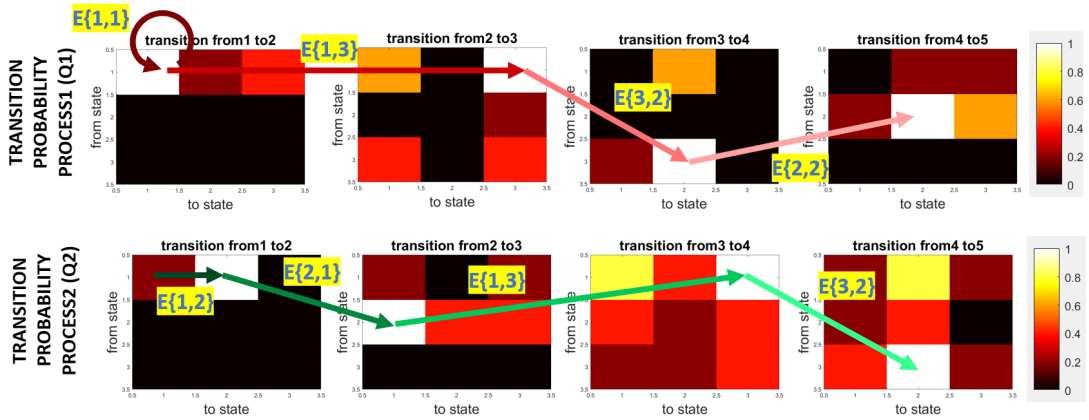

(a) Macrostates and state transition probabilities of two different spatio-temporal spike patterns

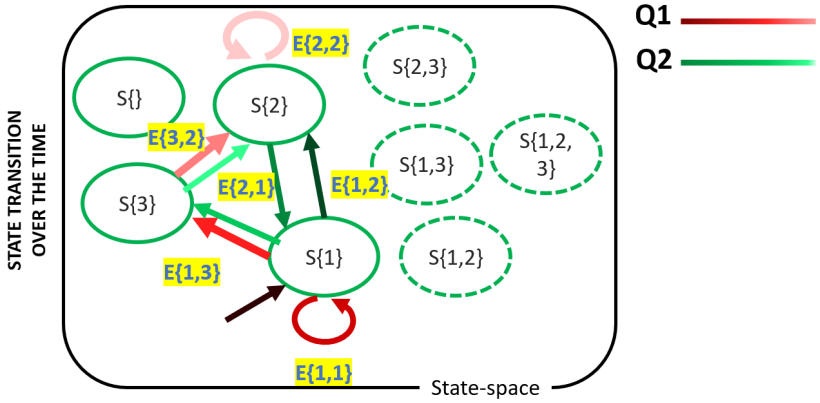

(b) State-space and state transitions of the two spatio-temporal spike patterns

Figure 7.2: Neural trajectories for two different spatio-temporal spike patterns

Therefore, a deep crisp rule related to the events above can be presented in the following form:

$$
\begin{aligned}
&IF(E_{(\{1\},\{1\})}:\ F_{(\{1\},\{1\})},\ S_{\{1\}},\ t_1,\ P_{(\{1\},\{1\})})\\
&\quad AND(E_{(\{1\},\{3\})}:\ F_{(\{1\},\{3\})},\ S_{\{3\}},\ t_2,\ P_{(\{1\},\{3\})})\\
&\quad AND(E_{(\{3\},\{2\})}:\ F_{(\{3\},\{2\})},\ S_{\{2\}},\ t_3,\ P_{(\{3\},\{2\})})\\
&\quad AND(E_{(\{2\},\{2\})}:\ F_{(\{2\},\{2\})},\ S_{\{2\}},\ t_4,\ P_{(\{2\},\{2\})})\\
&THEN(Q\ =\ Q_1)
\end{aligned}
\tag{7.3}
$$

The neural trajectories for two different spatio-temporal spike patterns are highlighted using their transition probability matrices in figure 7.2a. The extracted trajectories are highlighted in red and green colors. Figure 7.2b shows the transitions of each pattern in the state space. Therefore the corresponding label (n) of a given test spike sequence can be determined using,

$$Q_n = f_{crisp}(E_{n,t}, e_t) \tag{7.4}$$

$$Q_n = f_{\text{crisp}}(\begin{bmatrix} E_{1,1} & E_{1,3} & E_{3,2} & E_{2,2} \\ E_{1,2} & E_{2,1} & E_{1,3} & E_{3,2} \end{bmatrix}, \begin{bmatrix} E_{1,2} & E_{2,1} & E_{1,3} & E_{3,2} \end{bmatrix})$$

The above-defined type of knowledge is characterised by the following features. It represents informative patterns of multimodal data, deep in time (theoretically unconstrained) and in space (when dealing with spatio-temporal data). The knowledge is adaptable in an incremental, theoretically 'life-long' way. The knowledge is not restricted by fixed structures. The knowledge is obtained in supervised-, unsupervised or semi-supervised modes. The knowledge can be interpreted for a better understanding of the data and the processes that generated it. The knowledge can be used for early and accurate future event prediction.

Deep knowledge acquired in the human brain is manifested from numerous spatio-temporal events that happen when the spatially distributed neuronal

populations coordinate together to accomplish a common goal. Representation of such deep knowledge depends on the chosen spatial and temporal scale. Each scale has its own significance for information representation. Thus, the selection of a proper spatial and temporal scale is important to solve the problem at hand. Different spatial and temporal scales of knowledge representation emerge the granularity of deep knowledge.

7.2.3 Knowledge Granularity

Groups of events that happen at a similar time in a similar place can be integrated together in larger spatio-temporal clusters, or knowledge 'granules', thus the term deep knowledge granularity. The hierarchical organisations of neuronal activity can be interpreted as 'knowledge granularity'. Being one of the emerging computing paradigms of information processing, granular computing considers a specific type of representational entities called 'granule' that arise as a result of abstraction and knowledge extraction from data. Such collection of complex information entities, together with their associated functionalities, indicate meaningful patterns of information and thus can be used for better understanding of the underlying processes. Optimal spatio-temporal resolution and spatio-temporal depth of the patterns and granularity of knowledge representation for a given task is difficult to define; it very much varies across tasks and problems and is often restricted by the measured data.

The time resolution or temporal depth indicates how deep in time the knowledge is represented. According to the algorithm for extracting active brain areas (algorithm 3), the size of the time bin t_y defines how deep in time the knowledge is represented. This ranges from seconds to milli-seconds level for detecting hand movements from EEG.

The spatial resolution or the spatial depth indicates how deep in space the knowledge is represented. The SNN framework allows the formation of spatial clusters at different anatomical levels according to the brain atlas used for placing the spiking neurons of the hidden layer in the 3-dimensional space. The analysis presented in the chapter considers four levels of spatial depth according to the Talairach Brain Atlas. In a top-down approach, the analysis of neuronal clusters starts from the whole brain network level. At the next level, the spatial resolution is expanded to the hemispheric level. From each hemisphere, the knowledge is further scaled-up to the different lobes of the brain and finally, to the different Brodmann areas in each lobe.

7.3 Deep knowledge representation and extraction in the NeuCube Spiking Neural Network architecture

In N. K. Kasabov (2014) a Brain-inspired-Spiking Neural Network (BI-SNN) architecture was introduced and illustrated called NeuCube (Fig. 3.7). The proposed methodology of the BI-SNN is grounded in a NeuCube-like SNN architecture. A detailed description about the generic NeuCube SNN framework was presented in section 3.11.

7.3.1 Mapping the anatomical neural populations in the brain with the 3D spiking neuron coordinates of the NeuCube

In the brain's organisation, distinct anatomical regions represent defined brain functions. For instance, the neural populations in the Occipital lobe correspond for vision, while the neural populations in the Temporal lobe correspond for hearing. First, this approach integrated a mechanism to map the activities of the spiking neurons in the NeuCube, which are arranged in a 3D space according to a brain template with the defined anatomical regions in the human brain. It was hypothesised that the activities of a neural population in a particular anatomical region could be approximated up to a certain extent by the activities of the spiking neurons in the corresponding 3D space.

In NeuCube, each spiking neuron corresponds to a small 3D area of the brain (e.g. 1 cm^3). The Talairach brain atlas provides spatial information in a 1 mm^3 resolution and is arranged in a hierarchical order. These levels include the hemisphere, lobe, type of tissue (i.e. grey matter/white matter) and cell type (i.e. Brodmann area) of each 1 mm^3 in the 3D space of the brain. By using this hierarchy, each 3D spiking neuron coordinate was annotated with the corresponding anatomical region in the human brain. Therefore the activities of a certain spiking neuron can be associated with the corresponding anatomical region in the human brain.

The NeuCube SNN framework provides a list of brain coordinates extracted from the Talairach brain atlas and approximate mapping of 65 EEG channel locations for initialising the 3-dimensional SNNCube. These coordinates were extracted from the Talairach Daemon which can be accessed through the Talairach Applet or the Talairach Client from the following URL -http://www.talairach.org/

daemon.html (*Talairach Daemon*, n.d.). In addition, the corresponding NIfTI (Neuroimaging Informatics Technology Initiative) files that represent neuroimaging data correspond to the brain coordinates that represent different aspects of can be downloaded from the following URL - http://www.talairach.org/nii/. Although the list of brain coordinates distributed with the NeuCube software is sufficient for conducting a decent level of analysis of spatio-temporal brain dynamics; increasing the number of neurons in the NeuCube, assigning anatomical labels to them, increasing the number of EEG channels or using an EEG coordinate system other than the 10-20 convention is not feasible with the available resources. Since the current study investigates the knowledge representation of brain-inspired Spiking Neural Network architectures at different granularity levels, the above limitations restrict the ability to generalise the proposed approach to a broader analysis level. Therefore, the following source codes were implemented to address the above technical limitations.

Extracting brain coordinates from the Talairach brain atlas

The current study extracted brain-coordinates using the SPM12 (Statistical Parametric Mapping) Matlab toolbox (*SPM - Statistical Parametric Mapping*, n.d.). The different types of coordinates considered for this analysis, such as EEG channel locations, brain atlases usually follow different coordinate systems. They need to be transformed into a single coordinate system before mapping the EEG locations into the corresponding brain areas. There are tools such as Brainstorm(*Software*, n.d.) that supports these transformations. The Matlab source code presented in Appendix A.3.1 extracts brain coordinates from a given brain atlas, approximately maps a given set of EEG channel locations into the extracted brain coordinates and assign labels to associate anatomical information with the extracted coordinates.

For approximately map the extracted EEG channel locations with the brain coordinates extracted from a particular brain atlas, both coordinates should be first transformed into a common coordinate system. In this study, both EEG channel locations and brain coordinates extracted from the Talairach brain atlas was transformed into MNI coordinate system for this purpose using the Brainstorm Matlab software package (Wildetudor & Francois, 2014). The source code presented in Appendix A.3.2 implements this transformation and performs EEG mapping. The Euclidian distance between a particular EEG channel location and the extracted brain coordinates was first calculated, and the brain coordinate corresponds to the minimum Euclidian distance was selected as the corresponding 3-D coordinate of the EEG channel.

The coordinates were uploaded as a single CSV file to the Talairach client to assign the anatomical labels to the extracted brain coordinates. The Talairach client then retrieves the approximate brain regions corresponds to each 3-D coordinate. Appendix A.3.3 includes the Matlab source code implemented to convert the extracted nominal labels into numerical values.

Figure 7.3 depicts the initialisation of the experimental BI-SNN using the extracted 3-dimensional brain coordinates and their corresponding anatomical locations.

Since the EEG mapping of the NeuCube SNN architecture is based on the Talairach brain atlas, which contains the 3D coordinates of both cerebellum and cerebrum, the proposed Brain-Inspired Brain-Computer Interface architecture can represent both cerebrum and cerebellum activity together in the model. This architecture allows the BI-SNN model to utilise multiple brain networks that involve both the cerebrum and cerebellum.

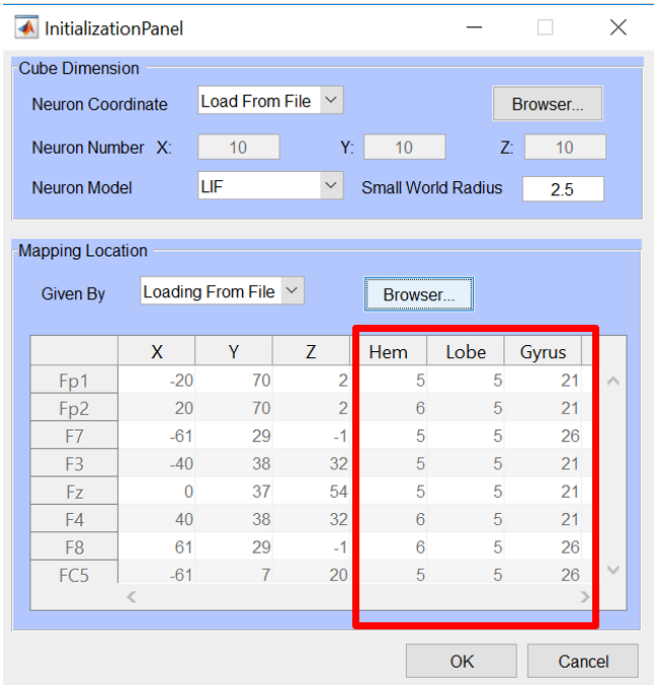

(a) Initialisation of the BCI

Hemisphere ID	Lobe ID	Gyrus ID	Tissue ID	Cell ID
1 LeftCerebellum	1 PosteriorLobe	1 InferiorSemiLunarLobule	1 GrayMatter	1 Brodmannarea20
2 RightCerebellum	2 Medulla	2 CerebellarTonsil	2 WhiteMatter	2 Brodmannarea38
3 LeftBrainstem	3 TemporalLobe	3 InferiorTemporalGyrus	3 CerebroSpinalFluid	3 Brodmannarea36
4 RightBrainstem	4 LimbicLobe	4 Uncus		4 Brodmannarea21
5 LeftCerebrum	5 FrontalLobe	5 MiddleTemporalGyrus		5 Brodmannarea28
6 RightCerebrum	. .	. .		. .
7 InterHemispheric	12 ParietalLobe	55 ParacentralLobule		71 Brodmannarea5

(b) Anatomical location identifiers for mapping 3-D coordinate

Figure 7.3: Initialisation of the NeuCube SNN using 3-D brain coordinates and mapping these coordinates with the anatomical locations of the brain using the Talairach brain atlas

7.3.2 Parameters for detecting active spatial clusters

Several parameters were introduced to quantify the activation level of an individual spiking neuron, a cluster of spiking neurons and its interaction with the other clusters as they evolve over time. They can be mainly divided into two categories as structural and functional parameters. The number of synapses of a certain neural cluster that shows a significant synaptic weight update during STDP learning was obtained as a measure of structural change as the SNN evolve over time. The spike rate of a spiking neuron and the average spike rate of a neural cluster during recalling were obtained as a measure of functional changes of the SNN.

7.3.3 Transition probability matrix

The probability of transitioning from one state to another in the state space created by different neural clusters was obtained using the above parameters that measure the activation level. This is a 3D matrix where each element represents the probability of transitioning from a particular state to another state at a certain time interval.

7.3.4 Neural trajectory

The significant neural trajectories were obtained using the transition probability matrix and visualised in the 3D space.

7.3.5 Knowledge granularity and representation

A spatial cluster of neurons associated with a specific functionality can be considered as a granule structure. A hierarchical structure can be formed through several levels where each level consists of granules at the same hierarchical level.

For instance, in a higher abstraction level, neuronal clusters spatially located in frontal and parietal lobes can be considered as two distinct granules. In terms of functionality of each granule structure, the frontal lobe is associated with motor functions and decision making while the parietal lobe is associated with sensory information processing. At a deeper level of the hierarchy, the primary motor cortex (Brodmann area 4) which is located in the frontal lobe can be identified as a separate granule structure. In terms of functionality, it is associated with planning and executing movement which is a more focused activity type related to movement execution. The brain-inspired NeuCube SNN framework presented in this chapter enables knowledge representation abstracted according to distinct spatial and temporal resolutions.

During training we use the algorithm 3 for extracting deep spatio-temporal rules using the Brain-inspired Spiking Neural Network.

7.4 Experimental Validation

The feasibility of obtaining the underlying neural trajectory during a cognitive task using the above describe framework was evaluated using a case study on Brain-Computer Interface. This case study examines the feasibility of extracting the dynamic interactions of distinct brain regions when grasping an object using the Brain-inspired Spiking Neural Network algorithms presented in section 3.11. Using the NeuCube algorithms from section 3.11, a BCI is created for analysing deep spatio-temporal patterns and knowledge extraction. The extracted dynamic patterns are presented as a set of spatio-temporal rules and applied to predict the onset of a grasping movement using the proposed BI-BCI framework.

Here an SNN architecture for BCI which consider the dynamics of the whole brain network in a spatio-temporal manner. The knowledge extracted indicates

Algorithm 3 Algorithm for Extracting Deep spatio-temporal Rules

Input: S_i, input signals (i.e. EEG); A_n, 3-D coordinates of the neurons in SNN; l_n, spatial cluster ids of each neuron in SNN; A_i, 3-D coordinates of each input channel

Parameters: th_{encode}, threshold for spike encode; d_{swr}, small world radius; $th_{cluster}$, threshold to select active spatial clusters; th_{rule}, threshold to select spatial clusters to generate spatio-temporal rules

Output: π, a set of deep spatio-temporal rules

Generic NeuCube process:

1: Encode input signals into spikes: $s_{input} = f_{encode}(S_{input}, th_{encode})$

2: Initialise SNN using 3-D coordinates of spiking neurons: $W_{init} = f_{init}(A_{hidden} = [x_n, y_n, z_n], d_{smr})$

3: Map input channel locations into 3-D space of SNN $A_{input} = min(d_{euclidean}([x_{hidden_i}, y_{hidden_i}, z_{hidden_i}], [x_{channel_j}, y_{channel_j}, z_{channel_j}]))$

4: Perform unsupervised learning in SNN using STDP learning rule

Extraction of deep spatio-temporal rules:

5: Get spike response of the leaky integrate and fire spiking neurons in the trained SNN for training spikes

6: Get activation state of of each spatial cluster in each time bin $q_{n,t} = f_{state}(\sum_{i=1}^{k} \frac{r_{n,i}}{k})$ where $r_{n,i}$ is the firing rate of the i^{th} neuron in the n^{th} spatial cluster during the time bin t; $f_{state}(x) = 1$ if $x >= th_{cluster}$ and $f_{state}(x) = 0$ otherwise

7: Get the probability of each spatial cluster being active at each time bin $P_{n,t} = \frac{k_{active}}{k_{active}+k_{inactive}}$ where k_{active} is the number of occurrences of n^{th} cluster being active at t^{th} time bin during all training samples and $k_{inactive}$ is the number of occurrences the same cluster not being active during the same time bin

8: Select spatial clusters $E_{event} \subseteq U$ using $n = f(P_{n,t} : \forall n, th_{rule})$ where t is the event onset time bin, $n \in E_{event}$ and $f(x) = \begin{cases} n & if\ x >= th_{rule} \\ \{\} & otherwise \end{cases}$

9: Generate a set of fuzzy/crisp rules for the event using E_{event}

where (space) and *when* (time) the activities take place and such knowledge can effectively be used in many BCI applications.

7.4.1 Description of the dataset

In this case study we have used the WAY-EEG-GAL (WAY: Wearable interfaces for hAnd function recovery, EEG: Electroencephalography, GAL: Grasp-And-Lift) dataset (Luciw et al., 2014a, 2014b). A detailed description of the dataset was presented in section 4.4.

7.4.2 Pre-processing

First, the EEG signals were filtered using a band-pass filter (low-pass cutoff: 12 Hz and high-pass cutoff: 30Hz) and encoded into spike trains using the Threshold-based encoding algorithm. These input spikes were then used to build the BI-BCI using the NeuCube spiking neural network architecture. Learning in the BCI was achieved using the Spike Time Dependent Plasticity learning rule. This rule quantifies the efficiency of transferring information from a presynaptic neuron to postsynaptic neuron based on the difference of spike timing of both neurons. The STDP learning results in evolving connections depending on the firing time of pre and postsynaptic neurons.

7.4.3 Data extraction

EEG samples of seven events that occur during a grasp-and-lift trial were extracted using the Electromyography, force, kinematics and status of the LED of each trial. The starting time of each event is detected using these behavioural signals as below.

1. Cue onset: 0s to 0.5s after the time the LED was switched on

2. Motor planning: 0.5s to 0s before the mean EMG signal from all EMG sensors exceed a threshold

3. Movement onset: 0.5s to 0s after the mean EMG signal from all EMG sensors exceed a threshold

4. First touch the object: 0s to 0.5s after the mean of the force signal exceeded a threshold

5. Hold object on air: 0.5s to 1s after the mean of the force signal exceeded a threshold

6. Release (movement offset): 0.5s to 0s before the mean EMG signal from all EMG sensors went below a threshold

7. Rest: 0s to 0.5s after the mean EMG signal from all EMG sensors went below a threshold

7.4.4 E3: Analysis and Knowledge Representation using BI-SNN framework

The input signals were then processed by the NeuCube BI-SNN framework. The dataset was divided 50:50 ratio as training:testing. The input signals were encoded into input spike trains using the modified threshold-based encoding algorithm. Then the BI-SNN was initialised using the 3D coordinates of spiking neurons with random initial synaptic connections as defined by the small-world radios. The input neurons were mapped to the 3D SNN cube using the EEG channel locations and the anatomical mapping was performed using the corresponding anatomical labels of the Talairach brain atlas. The spiking neuron with the shortest Euclidean distance to the actual EEG channel location in a common

3D coordinate system was selected as the input neuron of the input signal. For each one of the seven events extracted during the GAL task, deep unsupervised learning was performed using the same initial connection weights and the modified STDP learning algorithm using training data. The training input data was then propagated again on the trained BI-SNN to extract the polychronising spike patters. The synaptic connections and spike trains were analysed for knowledge extraction. Activation of slightly different clusters of neurons at slightly different times in their sequence forms a fuzzy/crisp rule. Thus, such a fuzzy rule allows for the event reach-to-grasp to be recognised. Finally, the extracted knowledge was evaluated by recalling the test input spike trains on the trained BI-SNN model.

7.5 Results and Discussion

The deep knowledge extracted from the BI-SNN represents an informative pattern of multi-modal and multi-dimensional data, deep in time and space. The knowledge is interpretable for a better understanding of the data and the processes that generated it. Here the deep knowledge is presented in two different forms. Firstly, the BI-SNN framework was used to represent knowledge of the functional organisation of neural clusters in the brain during the execution of a GAL movement. Secondly, we represent knowledge on the trajectories of synaptic evolution in sensory and motor areas of the brain during a GAL task.

7.5.1 Functional organisation of neural clusters

For each participant, a subset of brain areas that indicate a specific combination of activation level during each of the events was selected. This subset of brain areas forms a meta-state-space and was used to distinguish the events. The brain areas that form the meta-state-space which are common for a majority

of participants includes primary and secondary visual cortex, posterior parietal lobe that forms the dorsal pathway of vision, the inferior temporal area which forms the ventral pathway of vision, motor cortex and prefrontal cortex. However, since the organisation of the brain's neural network differ from person to person, it is difficult to find a common representation for all participants. Thus, the brain areas of the meta state which are common for more than three participants together with their order of being active over time are highlighted in figure 7.4. The temporal resolution for the analysis is 4bps (2-time bins for each sample).

Table 7.1 summaries the functional significance of the brain areas of the extracted elements of the meta-state observed in previous neuro-imaging literature.

The information obtained through the above spatio-temporal analysis is used to form deep knowledge and fuzzy/crisp rules were obtained. These rules are used by the inference engine for deducing information. Two different crisp rules that can be used for predicting movement intention can be written as follows.

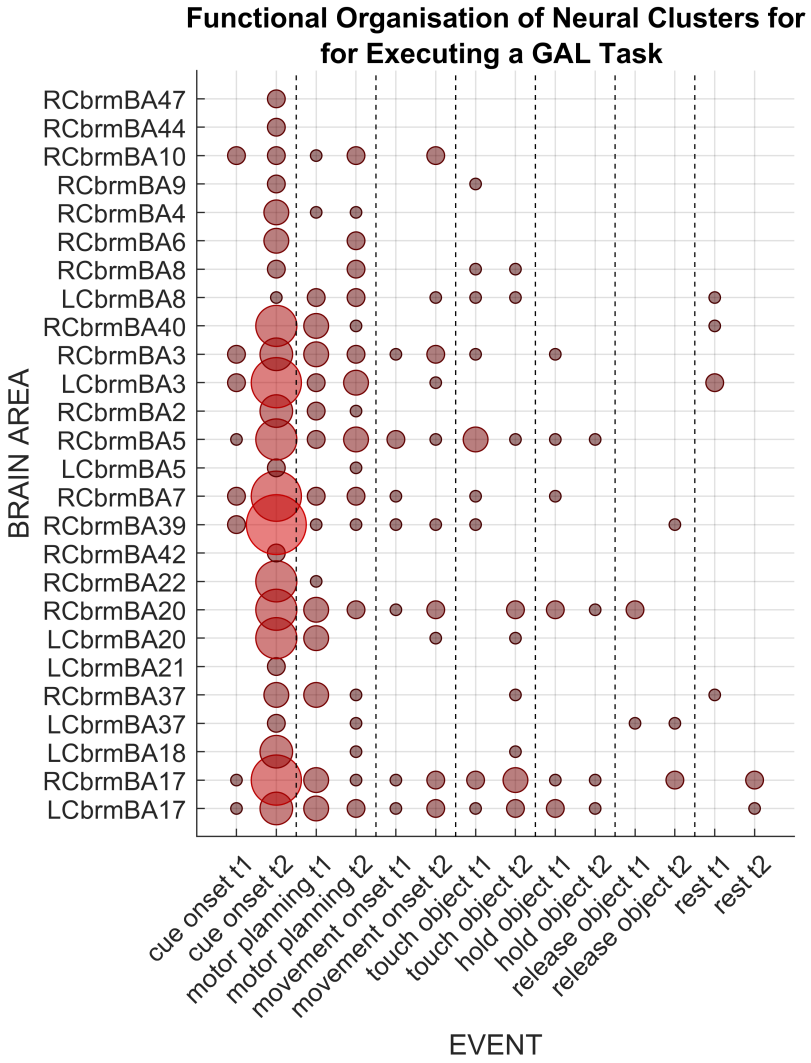

Figure 7.4: Functional organisation of different brain areas for executing a GAL task (number of participants = 12)

Table 7.1: Functional significance of the brain areas of the meta-state

Brodmann area	**Description**	**Functions**
BA17, 18	Occipital lobe - Primary (V1) and secondary (V2) visual cortex	*Vision:* Observe light intensity Goodyear and Menon (1998); Chen et al. (1998); Moradi et al. (2003), Monitor and discriminate colors Claeys et al. (2004), Visual memory and primingSlotnick and Schacter (2006), Visual attention Smith et al. (2006), Visuo-spatial information processing Waberski et al. (2008)
BA37, 20, 21	Temporal lobe - Middle and inferior temporal areas	*Memory:*Episodic encoding Leube et al. (2001), Visual fixation Richter et al. (2004) Attribution of intention Brunet et al. (2000), Attention to color Le et al. (1998)
BA22	Temporal lobe Superior temporal cortex (part of Wernicke's area)	*Sound:* Speech processing Brown et al. (2006), auditory attention and discrimination of voice Nakai et al. (2005)
BA42	Temporal lobe Primary auditory cortex	*Sound:* sense of hearing J. Upadhyay et al. (2008), sentence comprehension Tulving et al. (1994)
BA39	Parietal lobe Angular area (part of Wernicke's area)	*Attention:* Processing a sequence of actions Crozier et al. (1999), executive control Kübler et al. (2006)
BA7	Parietal lobe Somatosensory association cortex	*Attention:*manipulation and planning of goals Fincham et al. (2002), Visuospatial attentionMorton et al. (2009), visuo-motor coordination Ohgami et al. (2004), construct an understanding of the object being felt Reed et al. (2005); Caselli (1993)
BA5	Parietal lobe Somatosensory association cortex	*Somatosensory:*visuo-motor coordination Ohgami et al. (2004) tactile object recognition Reed et al. (2005); Caselli (1993) working memory Yoo et al. (2004)
BA3,2	Parietal lobe Primary somatosensory cortex	*Somatosensory:*Localize touch, vibration, pain and temperature Overduin and Servos (2004); Casey et al. (1996), Sense of body and fingers Overduin and Servos (2004), move hand Mima et al. (1999); Bernard et al. (2002)
BA40	Parietal lobe Inferior parietal lobule	*Attention:* visuomotor transformation Meister et al. (2004) somatosensory spatial discriminationAkatsuka et al. (2008); Milner et al. (2007), motor planning Fincham et al. (2002)

Continued over page ...

Table 7.1: Functional significance of the brain areas ... *(continued)*

Brodmann area	**Description**	**Functions**
BA8	Frontal lobe Supplementary motor area	*Motor:*voluntary movement intention, contributors to early stage pre-movement activity, preparation and readiness for voluntary movement (i.e. planning motor synergies)Cunnington et al. (2003); De Waele et al. (2001), visuospatial and visuomotor functions Cheng et al. (1995)
BA6	Frontal lobe Pre-motor cortex	*Motor:*Action planning Schubotz and von Cramon (2002); Bischoff-Grethe et al. (2004), Start movesDagher A and DJ (1999)
BA4	Frontal lobe Primary motor cortex	*Motor:* executing motor movementsA. Georgopoulos et al. (1982); Schwartz et al. (1988); A. Georgopoulos et al. (1988); Kettner et al. (1988), Move hands Nakayama (1997)
BA10	Frontal lobe anterior prefrontal cortex	*Executive functions:* working memory Pochon et al. (2002); J. Zhang et al. (2003) recognition and recall Ranganath et al. (2003)
BA44	Frontal lobe ventral premotor cortex (part of Broca's area)	*Executive functions:*working memory J. Zhang et al. (2003) object manipulation Binkofski et al. (1999)
BA47	Frontal lobe Inferior frontal area	*Executive functions:*working and episodic memory J. Zhang et al. (2003); Ranganath et al. (2003)

7.5.2 Trajectories of structural evolution

The trajectories of synaptic evolution for each participant were obtained after STDP learning. The activation level of a synaptic location was determined by the number of synapses with significant synaptic weight increase compared to the resting state. The probability of two synaptic locations on increasing the synaptic weight after one another (the trajectory of synaptic evolution) was obtained using the STDP connection weights of the 12 participants.

The analysis highlights synaptic evolution in the occipital, parietal, temporal and frontal areas of the brain. Synaptic evolution starts from the primary and secondary visual cortex in the occipital lobe after the cue is presented. This may influence synaptic evolution in the somatosensory and somatosensory association cortex in the parietal lobe, as well as the middle and inferior temporal areas of the temporal lobe. This corresponds to the dorsal (from occipital to parietal lobe) and ventral (occipital to temporal lobe) steams of visual information processing in the human brain. Similarly, observing the cue also influences synaptic evolution in the motor cortex, specifically in the supplementary motor cortex, premotor cortex and primary motor cortex. Figure 7.6 shows synaptic evolution of a single participant during the six events with respect to the resting state.

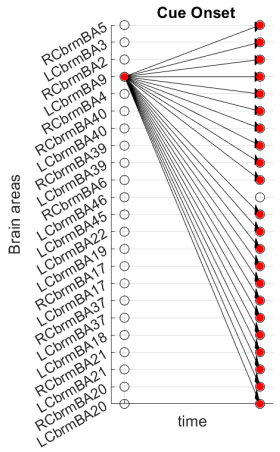

(a) Cue onset

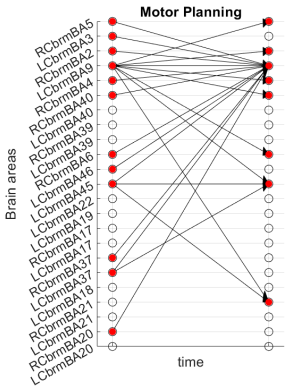

(b) Motor planning

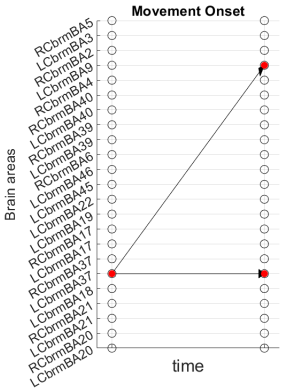

(c) Movement onset

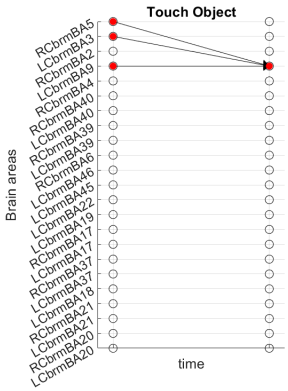

(d) Touching the object

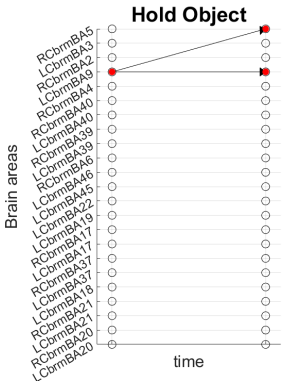

(e) Holding the object

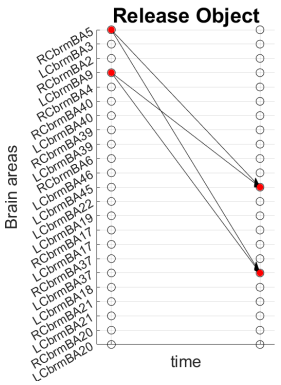

(f) Release object

Figure 7.5: Changes in activation level of the brain areas that form different microstates using the selected brain areas

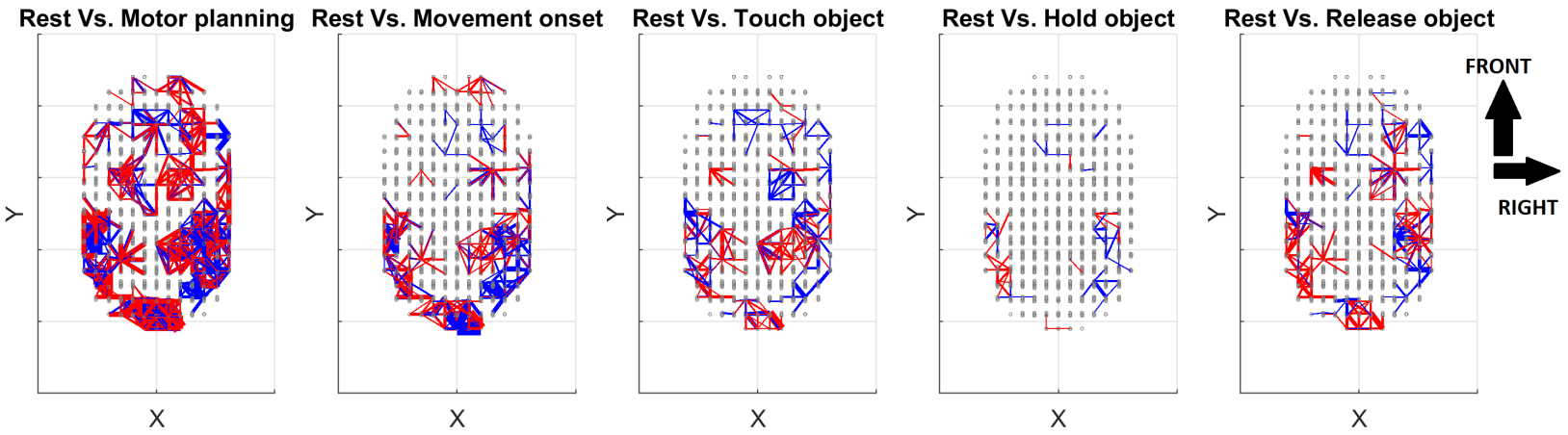

Figure 7.6: Synaptic connections during rest and rest vs other events during a GAL task

This knowledge can further be elaborated and converted into meaningful representations using the knowledge granularity permitted by the proposed BI-SNN framework. The knowledge extracted at different granularity levels improves event prediction from EEG signals in BI-BCI while revealing the underlying biological process that generated the signals. Among several important representations of knowledge, transfer of information from sensory areas to motor areas and vice versa as shown in figure 7.7 helps to improve the state-of-the-art in sensorimotor rhythm-based BCI.

In figure 7.7a BI-SNN reveals synaptic evolution observed in the ventral pathway ('what' pathway) of visual information processing which consists of the visual cortex, middle and inferior temporal areas and Wernicke's area. As summarised in table 7.1, these areas involve the recognition of the visual cue. Simultaneously, synaptic evolution along the dorsal pathway ('where' or 'how' pathway) of visual information processing was also highlighted. This includes the visual cortex, somatosensory association cortex and primary somatosensory cortex. In addition, synaptic evolution was also observed in the ventral pre-motor cortex (part of Broca's area). As stated in the 7.1, previous neuroimaging studies have found the involvement of these areas in motor planning. Only a subset of parietal areas such as primary somatosensory cortex was specifically reactivated when the object is touched.

Figure 7.7b highlights the trajectories of synaptic evolution in motor areas during the GAL task. These areas include the supplementary motor area, primary motor cortex and primary somatosensory cortex during motor planning and movement execution. In addition, synaptic evolution was also observed in the pre-motor cortex after the movement onset.

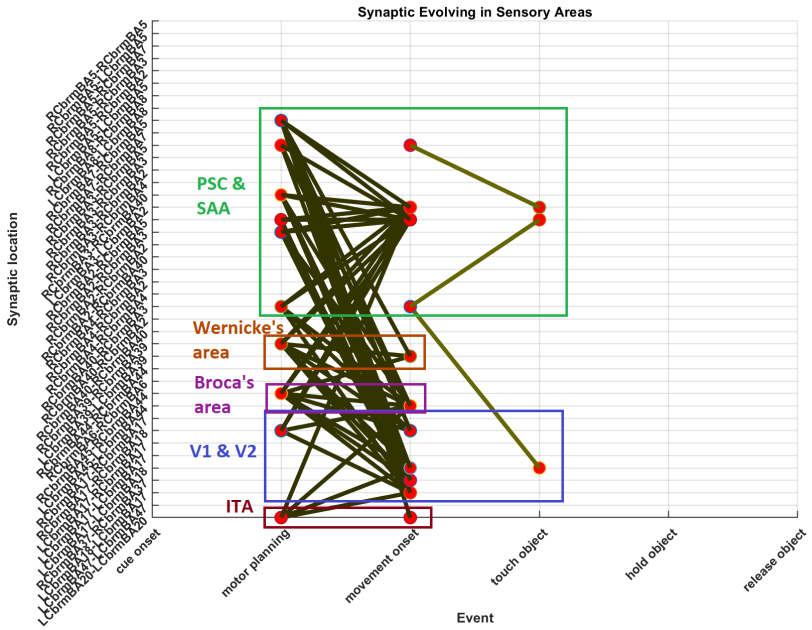

(a) Sensory

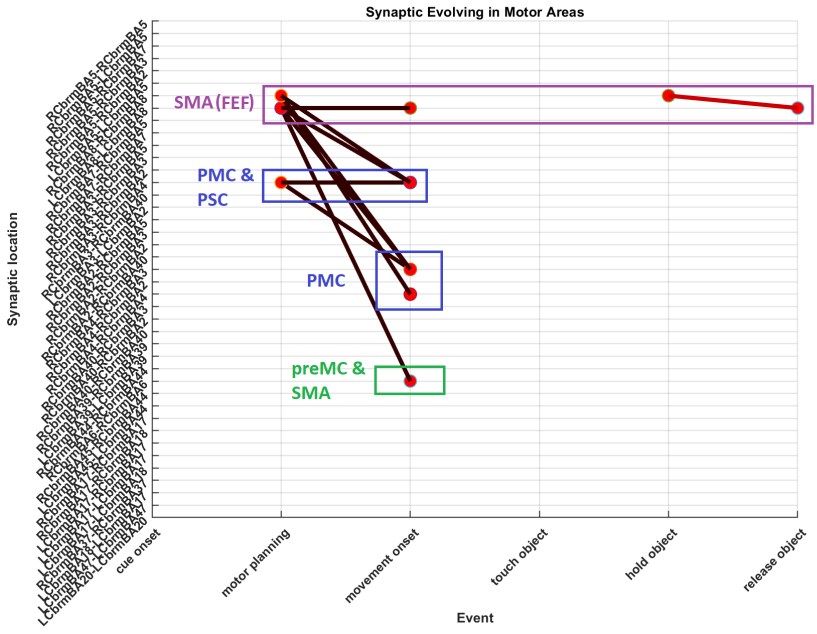

(b) Motor

Figure 7.7: Transfer of information from sensory to motor and vice versa (SMA: Supplementary Motor Area, PMC: Primary Motor Cortex, PSC: Primary Somatosensory Cortex, SAA: Somatosensory Association Area, V1: Primary Visual Cortex, V2: Secondary Visual Cortex, ITA: Inferior Temporal Area, WA: Wernicke's area, FEF: Frontal Eye Field)

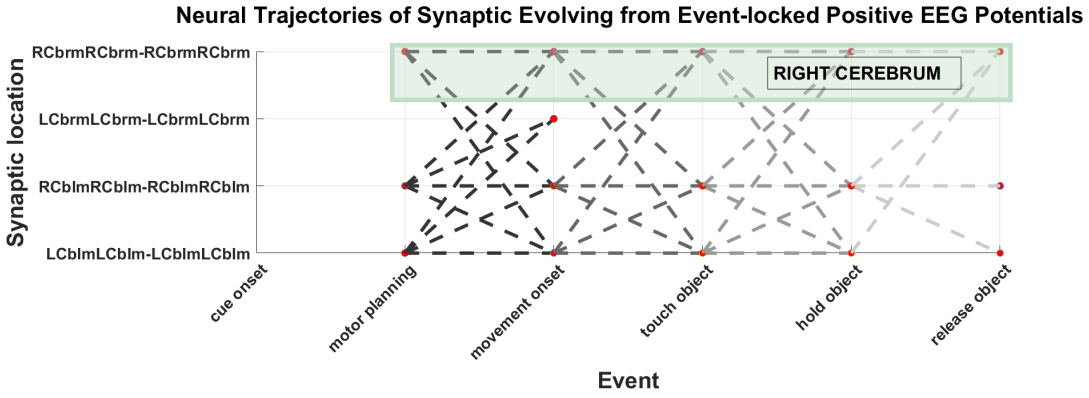

(a) Hemisphere

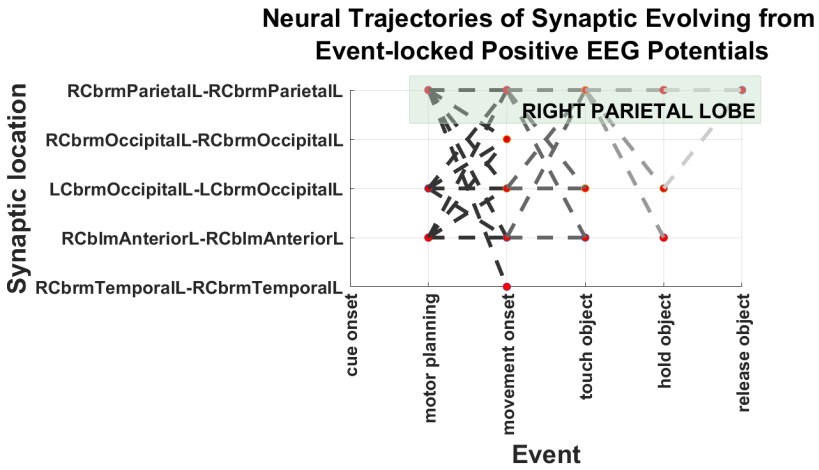

(b) Lobe

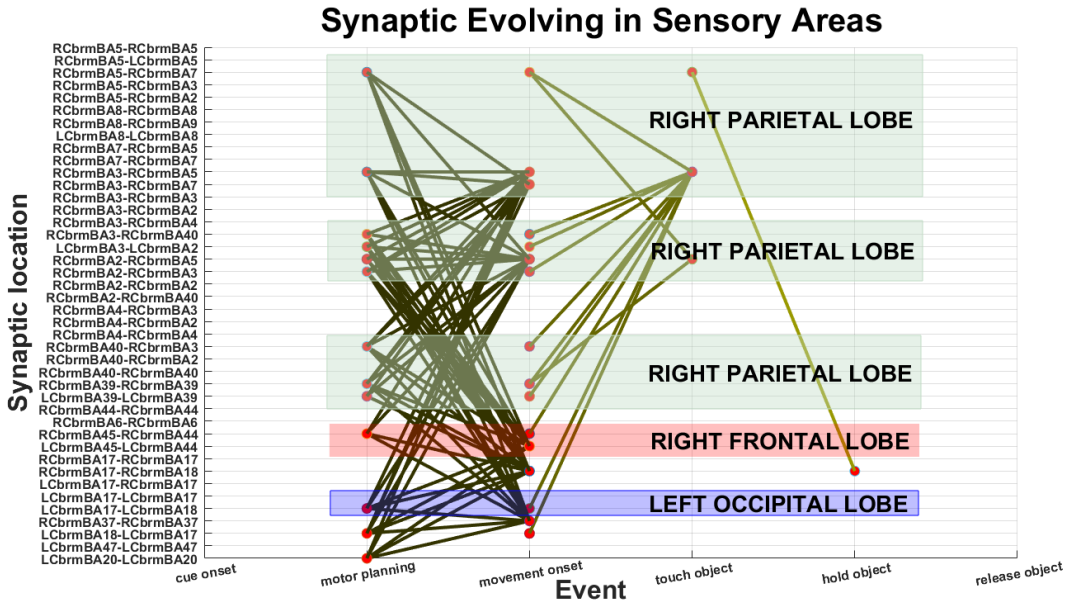

(c) Cellular

Figure 7.8: Granularity of knowledge in space

7.5.3 Granularity of knowledge

One of the promising features of the presented BI-SNN architecture is its ability to organise knowledge in a hierarchical order. Such hierarchy forms knowledge granules. Figure 7.8 highlights the significance of using the most suitable granularity level. It highlights that the neural clusters in the right parietal lobe that distinguish the subsequent events during a GAL task become prominent only at the cellular level, as shown in figure 7.8c, but not at the hemispheric (figure 7.8a) or lobe (figure 7.8b) levels. In addition, discriminating cluster activities such as the BA44 and BA45 (ventral pre-motor area) in the frontal lobe become apparent only at the cellular level. Therefore, finding the most informative granularity level is crucial for solving the problem as different features become significant in different granularity levels of the hierarchy.

7.5.4 Extraction of Fuzzy/Crisp rules

Activation of slightly different clusters of neurons at slightly different times in their sequence forms a fuzzy/crisp rule. A crisp rule common for all 12 participants is stated below.

Let the set of events during a GAL task $E = \{ E_{cue\text{-}onset}, E_{motor\text{-}planning}, E_{movement\text{-}onset}, E_{touch\text{-}object}, E_{hold\text{-}object}, E_{release\text{-}object}, E_{rest}\}$ and any arbitrary event E_i is represented as a function of $E_i = (F_i, S_i, T_i, P_i)$ where F_i is the function that generated the event, S_i is the brain areas involve in executing the event, T_i is the time of event onset and, P_i is the probability of the event. Bellow is the crisp rule obtained for participant 3 from the BI-SNN framework.

The elements of the meta-state of a GAL task can be denoted as, $S_{GAL} \subset S$ where S is the set of all brain areas in the corresponding spatial granularity level. For instance, S_{GAL} at the cellular level of the hierarchy can be represented using

the following subset of Brodmann areas.

$S_{\text{GAL}} = \{S_{\text{LBA18}}, S_{\text{LBA3}}, S_{\text{LBA47}}, S_{\text{LBA6}}, S_{\text{LBA8}}, S_{\text{RBA10}}, S_{\text{RBA19}}, S_{\text{RBA2}}, S_{\text{RBA21}},$

$S_{\text{RBA22}}, S_{\text{RBA3}}, S_{\text{RBA40}}, S_{\text{RBA47}}, S_{\text{RBA5}}, S_{\text{RBA6}}, S_{\text{RBA7}}, S_{\text{RBA9}}\}$

$\text{S}_{\text{cue-onset}}$, $\text{S}_{\text{motor-planning}}$, $\text{S}_{\text{movement-onset}}$, $\text{S}_{\text{touch-object}}$, $\text{S}_{\text{hold-object}}$, $\text{S}_{\text{release-object}}$ and S_{rest} are subsets of S_{GAL} where,

1. $S_{\text{cue-onset}} = \{S_{\text{LBA18}}, S_{\text{LBA3}}, S_{\text{LBA47}}, S_{\text{LBA6}}, S_{\text{LBA8}}, S_{\text{RBA10}}, S_{\text{RBA19}}, S_{\text{RBA2}}, S_{\text{RBA21}},$
   $S_{\text{RBA22}}, S_{\text{RBA3}}, S_{\text{RBA40}}, S_{\text{RBA47}}, S_{\text{RBA5}}, S_{\text{RBA6}}, S_{\text{RBA7}}, S_{\text{RBA9}}\}$
2. $S_{\text{motor-planning}} = \{S_{\text{LBA18}}, S_{\text{LBA6}}, S_{\text{LBA8}}, S_{\text{RBA10}}, S_{\text{RBA2}}, S_{\text{RBA21}},$
   $S_{\text{RBA3}}, S_{\text{RBA40}}, S_{\text{RBA47}}, S_{\text{RBA5}}, S_{\text{RBA6}}, S_{\text{RBA7}}, S_{\text{RBA9}}\}$
3. $S_{\text{movement-onset}} = \{S_{\text{LBA6}}, S_{\text{LBA8}}, S_{\text{RBA10}}, S_{\text{RBA21}},$
   $S_{\text{RBA3}}, S_{\text{RBA47}}, S_{\text{RBA5}}, S_{\text{RBA6}}\}$
4. $S_{\text{touch-object}} = \{S_{\text{LBA8}}, S_{\text{RBA5}}\}$
5. $S_{\text{hold-object}} = \{\}$
6. $S_{\text{release-object}} = \{S_{\text{RBA21}}\}$
7. $S_{\text{rest}} = \{S_{\text{LBA6}}, S_{\text{RBA5}}\}$

A crisp rule for predicting a GAL task for participant 3 can be written as,

IF$(E_{\text{cue-onset}} : F_{\text{cue-onset}},\ S_{\{\text{cue-onset}\}},\ t_{\text{cue-onset}},\ P_{>0.8})$

$AND(E_{\text{motor-planning}} : F_{\text{motor-planning}},\ S_{\text{motor-planning}},\ t_{\text{motor-planning}},\ P_{>0.8})$

$AND(E_{\text{movement-onset}} : F_{\text{movement-onset}},\ S_{\text{movement-onset}},\ t_{\text{movement-onset}},\ P_{>0.8})$

$AND(E_{\text{touch-object}} : F_{\text{touch-object}},\ S_{\text{touch-object}},\ t_{\text{touch-object}},\ P_{>0.8})$

$AND(E_{\text{hold-object}} : F_{\text{hold-object}},\ S_{\text{hold-object}},\ t_{\text{hold-object}},\ P_{>0.9})$

$AND(E_{\text{release-object}} : F_{\text{release-object}},\ S_{\text{release-object}},\ t_{\text{release-object}},\ P_{>0.8})$

$AND(E_{\text{rest}} : F_{\text{rest}},\ S_{\text{rest}},\ t_{\text{rest}},\ P_{>0.8})$

THEN$(Q = Q_{\text{grasp-and-lift}})$.

where $\text{S}_\text{i} = \{\ \text{S}_{\text{PosteriorLobe}},\ \text{S}_{\text{TemporalLobe}},\ \text{S}_{\text{LimbicLobe}},\ \text{S}_{\text{FrontalLobe}},\ \text{S}_{\text{AnteriorLobe}},\ \text{S}_{\text{OccipitalLobe}},\ \text{S}_{\text{Midbrain}},\ \text{S}_{\text{ParietalLobe}}\}$; then an informative pattern $\text{Q}_{\text{reach-to-grasp}}$ can be recognized and classified as below. A deep fuzzy rule related to the grasp and lift task as shown in the above neural activation pattern can be represented according to the following form.

7.5.5 Polychronising Neuronal Groups in the trained BI-SNN

Figure 7.7 depicts the polychronisation effect of the trained BI-SNN for unseen spike trains. Mean Peri Stimulus Time Histogram (PSTH) of each neural cluster of the meta-state was obtained to evaluate the ability of the trained BI-SNN to reproduce a known spike sequence when a similar unseen spike pattern is observed. The evaluation was performed using approximately 90 unseen testing samples per event (class) from each participant (90 x 7 =630 samples per participant).

Here we demonstrate the polychronisation effect of several neural clusters that

belong to the meta-state. Figure 7.9a shows the mean PSTH of the primary visual cortex. Approximately a similar mean PSTH was observed during all events of the GAL task from the Secondary Visual cortex (BA18). This indicates the constant involvement of the Secondary Visual Cortex during the entire GAL task. Increased PSTH in the Inferior Temporal Area when the participant was cued to start and stop the movement as per figure 7.9b indicates the involvement of ITA for identifying the visual cue. Figure 7.8c shows a peak spiking activity in the BA 8 (Supplementary Motor Area) after cue onset and during motor planning. Figure 7.7f depicts the involvement of the Primary Somatosensory Cortex for perception of the cue, planning and executing the movement. The peak PSTH values observed in the Somatosensory Association cortex (BA5 and 7), as indicated in figure 7.8d and 7.7e, highlight the neural clusters involved in processing the sensory information related to touch.

These findings show the ability of the presented BI-SNN architecture to extract polychronous neural clusters which can describe the complex brain dynamics that occur during a cognitive process. The trained BI-SNN exhibits reproducible time-locked firing sequences when a similar unseen spike pattern is presented to the network.

The brain-inspired SNN BCI framework presented in the chapter reveals essential patterns that characterise the dynamics of brain activity during a motor task and these patterns can be represented as knowledge representation, comprehensible by humans. The extracted knowledge can be presented in a form of deep fuzzy or crisp rules. Thus, the framework demonstrates manifest deep learning from brain data during such motor tasks. The extracted knowledge exhibits the following key features.

The knowledge is adaptable in an incremental, theoretically, ‘life-long’ knowledge and the knowledge is not restricted by fixed structures. Figure 7.8 depicts

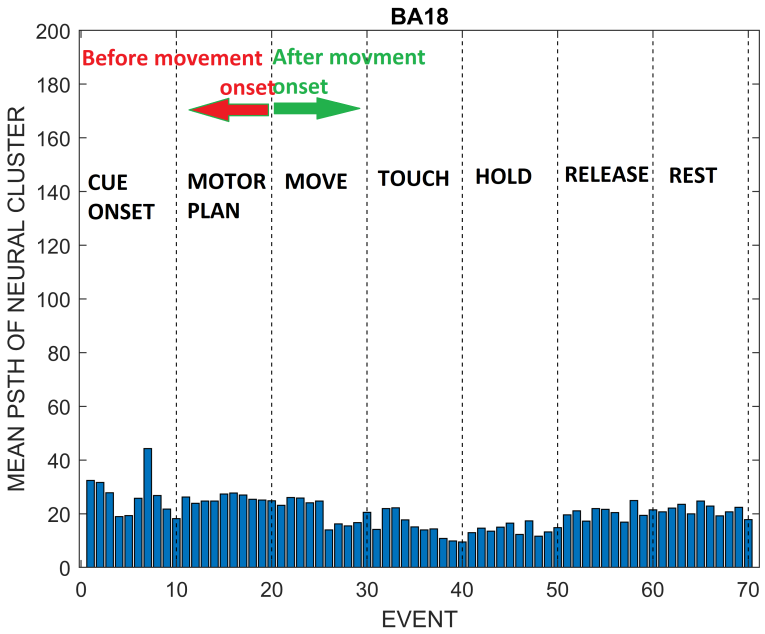

(a) Secondary Visual Cortex

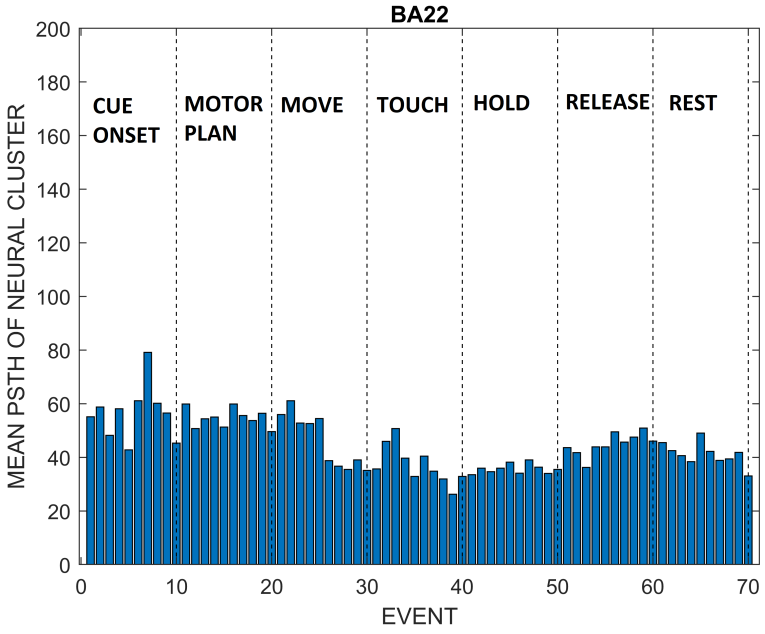

(b) Inferior Temporal Area

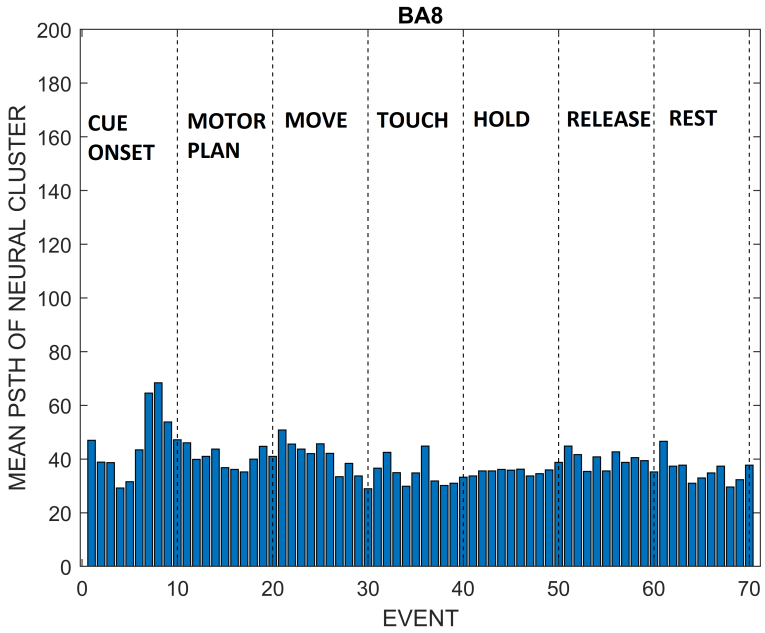

(c) Supplementary Motor Area

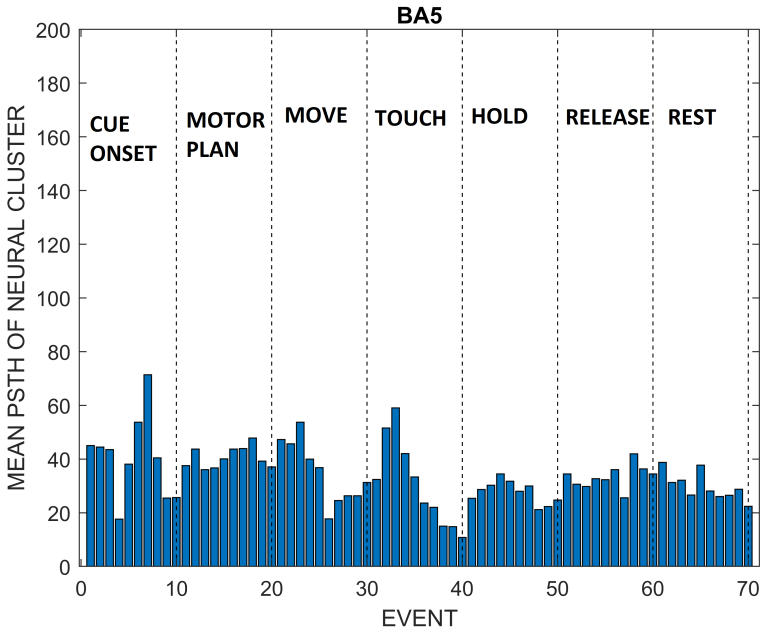

(d) Somatosensory Association Area (Brodmann area 5)

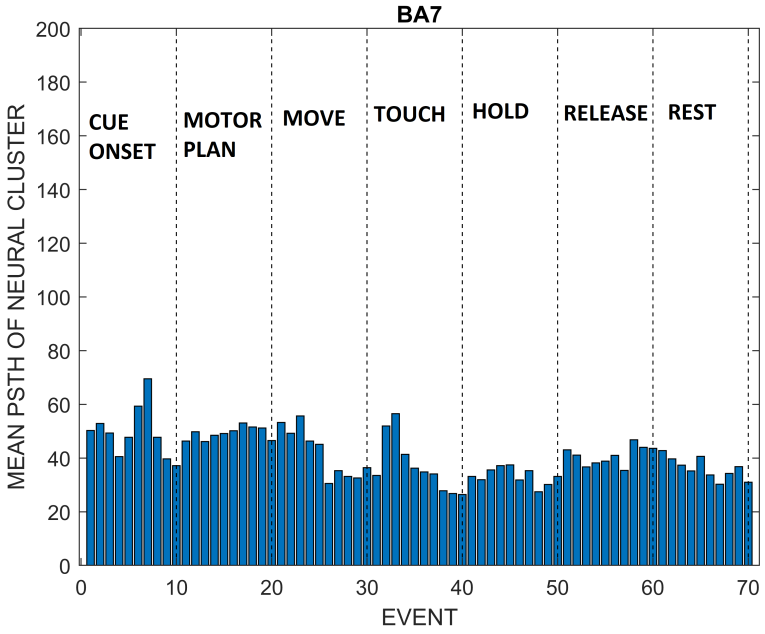

(e) Somatosensory Association Area (Brodmann area 7)

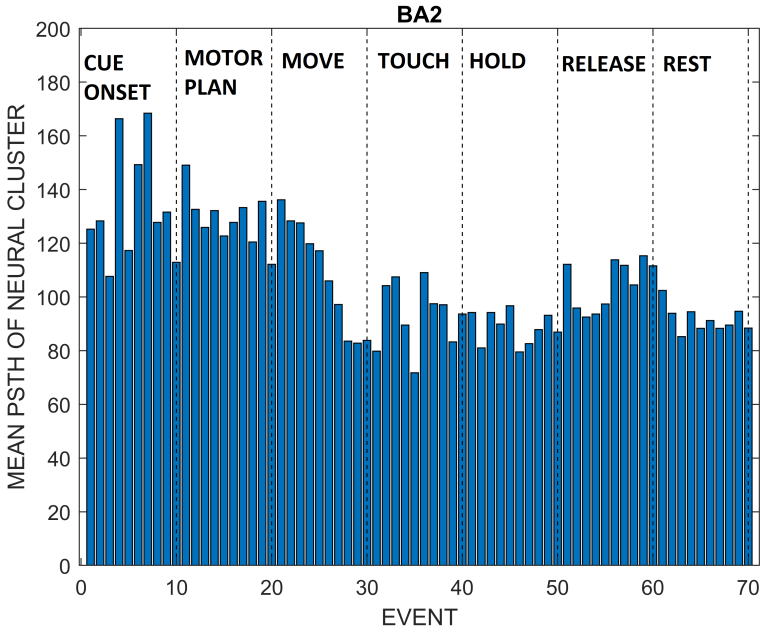

(f) Primary somatosensory cortex

Figure 7.7: Polychronisation of the meta-state brain areas for unseen spike trains

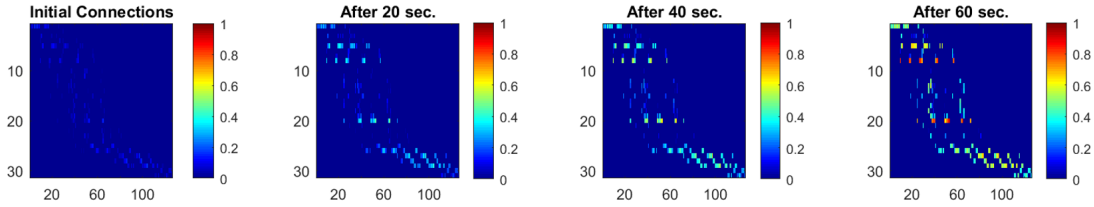

Figure 7.8: Evolving connection weights

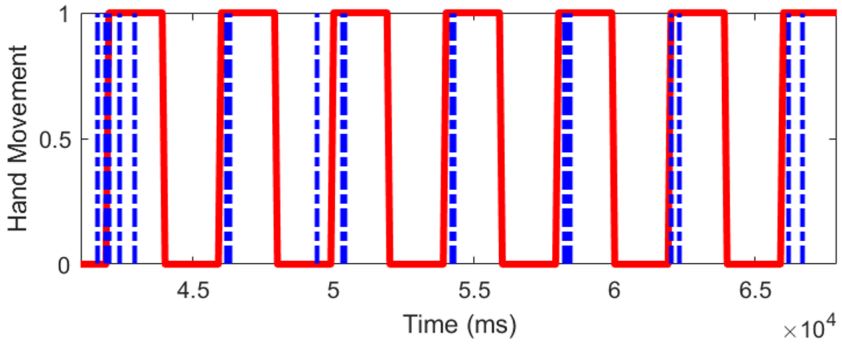

Figure 7.9: Predicted movement onset using the spike-trains of the test data using the crisp rules extracted in section 5

the connectivity matrix of the SNN BCI during different stages of learning. The connections evolve over time and indicate incremental and adaptive learning.

The deep knowledge is obtained in supervised-, unsupervised or semi-supervised modes and can be used for early and accurate future event prediction. The predicted movement onsets from continuous testing EEG samples at 10bps temporal resolution are depicted in figure 7.9.

7.6 Significance of the study

The human brain consists of a complex yet highly efficient network of neural clusters that collaborate together to perform a cognitive task. Understanding the complex spatio-temporal brain dynamics is important for improving many applications. This chapter proposed a Brain-Inspired Spiking Neural Network architecture which can learn and reveal deep in time-space functional and structural

patterns from spatio-temporal data. The chapter presented an algorithmic pipeline to explore the functional and structural interactions of brain networks in different granularity levels using the generic NeuCube SNN framework. The experimental validation shows the feasibility of creating a new type of BCI's called Brain-Inspired Brain-Computer Interfaces using the deep knowledge extracted from the BI-SNN architecture.

The approach could be used for the creation of a wider class of BI-BCI across different applications. Here it was applied to characterize the cortical activity during a cued grasp and lift movement. A sub-set of meaningful functional interaction patterns were obtained, and reasoning was performed using fuzzy/crisp rules by an inference engine. The results suggest that the BI-SNN architecture can extract polychronising neuronal groups that contribute to executing a GAL task. Further, the findings were compared with the previous neuroimaging studies and it is evident that the findings are in accordance with these physiological studies. The findings suggests that the proposed BI-SNN framework is able to unveil dynamic topological patterns of human brain networks and such knowledge can be effectively used to enhance the state-of-the-art in BCI. This knowledge representation framework will be used to extract spiking activity from different regions of interest in the brain to construct the proposed Brain-Inspired Brain-Computer Interface presented in chapter 9.

7.7 Summary of the chapter

This chapter proposed a spike-based generic algorithm for extracting deep spatio-temporal knowledge from Brain-Inspired Spiking Neural Network architectures. A theoretical framework, the corresponding algorithmic pipeline and the relevant source code segments for implementing the proposed algorithm were presented

in this chapter. The neural trajectories during grasp and lift movements were extracted by using the proposed knowledge representation algorithm. The analysis demonstrated the feasibility of revealing the topological patterns during a cognitive task such as grasp and lift movements. The proposed framework is a promising direction for building a new type of Brain-Computer Interface called Brain-Inspired Brain-Computer Interfaces. The next two chapters will describe the proposed Brain-Inspired Brain-Computer Interface system that integrates these generic methods for building a novel type of Brain-Computer Interface.

7.8 Contributions

- This study proposed a methodology for extracting deep knowledge from brain-inspired Spiking Neural Network architectures
- The research developed learning algorithm for knowledge extraction and implemented in Matlab
- The research extended the generic NeuCube framework by integrating the proposed knowledge representation algorithms to enhance the interpretability of the NeuCube SNN architecture
- The chapter presented an algorithmic pipeline to extract deep knowledge from SNNs
- The research experimentally validated the proposed knowledge representation framework through a case study on extracting deep knowledge of the spatio-temporal organisation of the brain's cortex during grasp and lift movements

7.9 Related publications

1. **Kumarasinghe, K.**, Kasabov, N., & Taylor, D. (2020). Deep learning and deep knowledge representation in Spiking Neural Networks for Brain-Computer Interfaces. Neural Networks, 121, 169-185.

Chapter 8

FaNeuRobot: A Framework for Robot and Prosthetics Control using the NeuCube Spiking Neural Network Architecture and Finite Automata Theory

"Science is magic that works."

Kurt Vonnegut - a writer

Chapter Overview

Previous chapters proposed two spike-based generic methods for constructing an interpretable machine learning model which could incrementally learn to predict complex spike sequences from stochastic data streams. These methods show the feasibility of constructing a novel Brain-Inspired Brain-Computer Interface

system which can effectively address several limitations of current restorative BCIs. This chapter presents a proof of concept on decoding hand movements from EEG signals using Spiking Neural Networks and evaluates the feasibility of the proposed SNN-based neural decoder to control a prosthetic hand. The proposed FaNeuRobot frameworks is a motor control framework for prosthetic control through Brain-Computer Interface that integrates a Finite Automata with the NeuCube evolving Spiking Neural Network architecture. This preliminary study investigates the feasibility of a cognitive computational model that is inspired by the muscle synergies for motor control in human upper limb to perform continuous control of the prosthetic hand through a non-invasive Brain-Computer Interface.

8.1 Introduction

The precise temporal activation of muscle synergies is an essential requirement for enabling object manipulation in humans. The intuitive manipulation of a prosthetic hand through a non-invasive neural interface such as a Brain-Computer Interface requires the computation of kinematics and kinetics of fingertips for achieving such a task through a BCI. Decoding such information from EEG useful for restorative non-invasive BCI is a challenging task.

A typical recording of an EEG electrode represents the accumulated activity from several thousands of neurons in the brain. The EEG channels which monitor the primary motor cortex sub-serving the hand muscles, receive a mixture of neural activity from several nearby neuron populations responsible for moving different parts of the body. The neural decoder should be able to extract brain activity correspond to the activation of specific muscle synergies which contribute to executing a certain movement. This is a challenging task as EEG suffers from poor spatial resolution and volume conductance effect (van den Broek et al., 1998; Edelman et al., 2016). Thus, distinguishing the activity of different forearm muscle synergies from EEG results in less accuracy.

Recent studies have investigated the feasibility of detecting different movements of the same limb from EEG signals. Simultaneous EEG-EMG was examined to discover specific neural-muscular interactions during movements (Artoni et al., 2016; Pirondini et al., 2017; Yoshimura et al., 2012, 2017). All of these studies report the results of the offline prediction of muscle synergies from EEG. This chapter presents a preliminary study that evaluates the feasibility of online control a prosthetic hand through a non-invasive BCI.

Previous studies have shown the feasibility of the NeuCube SNN framework for

controlling neurorehabilitation robots such as exoskeletons in patients with movement impairments (Taylor et al., 2014). The proposed FaNeuRobot framework is an SNN model that integrates finite automata with the brain-inspired NeuCube SNN architecture. The finite automata represent a simplified behavioural model of the forearm muscle synergies that enables hand opening and closing. The proposed framework was experimentally validated to prove its feasibility for voluntary object grasping through the non-invasive neural interface. Figure 8.1 depicts the basic architecture of the proposed approach. This chapter will address the following research question specific for non-invasive Brain-Computer Interfaces applied for motor recovery and restoration. The proposed neural interface shows the feasibility of such manipulation for transradial level prosthetics. Higher levels of control are also possible to achieve through a hierarchical multi-class BCI classifier.

- **RQ5: How can the NeuCube SNN architecture be improved in order to enable continuous control of a prosthetic hand from EEG signals?**

The research presented in this chapter is a collaborative work with Mahonri Owen and Chi Kit Au from The University of Waikato. The contributors of this joint work, Mahonri Owen and Chi Kit Au solely contributed to the development of the prosthetic hand used in this study. The development of the prosthetic hand was a part of Mahonri Owen's PhD research (Owen, 2019) and a detailed description of the prosthetic hand is available in (Owen, 2019; Kumarasinghe et al., 2018). Kaushalya Kumarasinghe, Denise Taylor and Nikola Kasabov solely contributed for the design and development of the proposed machine learning model for decoding neural activity from EEG signals. All collaborators jointly contributed to the development of the neural interface and controlling the prosthetic hand through the BCI.

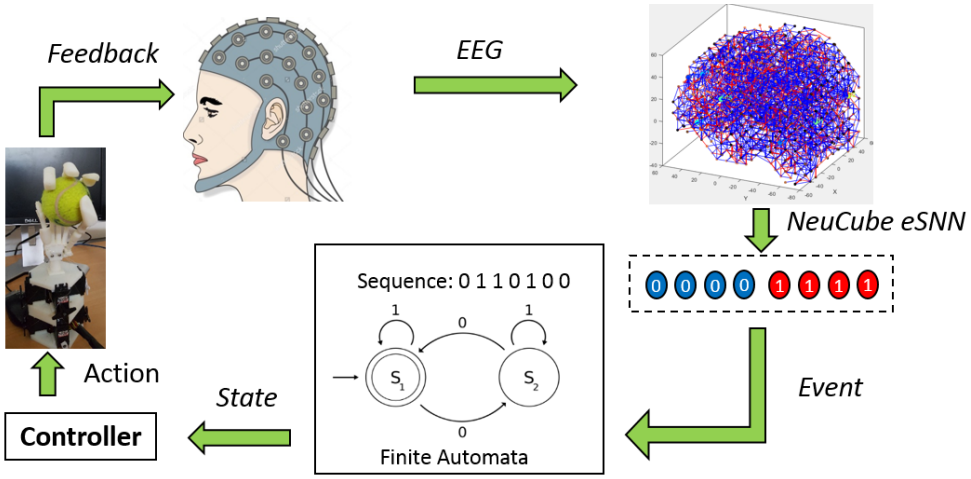

Figure 8.1: Proposed Brain-Computer Interface Framework for Prosthetic Control through Cognitive Computing and Automata Theory

8.2 FaNeuRobot Framework

The FaNeuRobot framework integrates a Finite State Machine with the generic NeuCube SNN architecture. The proposed brain state based SNN model contains a Finite State Machine which will act as a finite memory to the biologically plausible NeuCube SNN model. The SNN is trained to predict events from EEG, which can cause state transitions while the FSM then compute the final state based on the previous state and the decoded event. As a case study, the proposed model is validated on predicting the opening and closing of the right hand from EEG signals.

Learning in the proposed FaNeuRobot framework includes spike encoding, input mapping, network initialisation, unsupervised learning through Spike-Time Dependent Plasticity and supervised learning using the dynamic evolving Spiking Neural Network. A detailed description of the NeuCube SNN framework was presented in section 3.11. This section will describe the proposed FaNeuRobot framework which extends the generic NeuCube SNN framework for online classification of movements from EEG signals. Figure 8.2 depicts the integration of

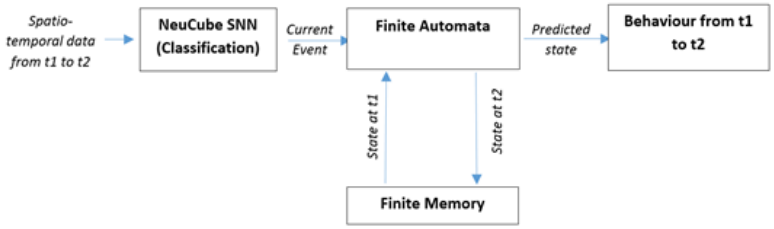

Figure 8.2: Integration of the Finite State Machine with the generic NeuCube SNN architecture - The NeuCube is trained to decode the event from time t1 to t2 using the spiking activity of the SNN reservoir. The model uses a finite memory to store the previous state. A Finite State Machine is integrated with the SNN to predict the new state using the event decoded by the SNN and the previous state stored in the memory.

the Finite State Machine with the SNN model for decoding state transitions over time.

Formally a Finite Automata M can be written using five elements,

$$M = (Q, \sum, \delta, q_0, F) \tag{8.1}$$

where Q is the set of states, $\sum$ is the alphabet, δ is the state transition function can be defined by a state transition table, q_0 is the set of initial states ($q_0 \in Q$) and F is a set of final states ($F \subseteq Q$).

- Set of States: Q

  Finite Automata contains two states, hand opened (S1) and hand closed (S2), S ={S1, S2}, triggered by the activation of flexor (M_{Ft}) and extensor (M_{Et}) muscles. To simplify, each forearm muscle (M_X) was considered as a binary unit that can either be contracted ($M_{Xt} = 1$) or relaxed ($M_{Xt} = 0$) at time t. i.e. $M_{Ft} = 1$ if the flexor muscle is contracted at time t and $M_{Ft} = 0$ if otherwise.

- Alphabet: $\sum$

  The model stores the state at time t_1=t and monitors the events happen

from t_1 to t_2=t+Δt.

e=$\{e_{11}, e_{22}, e_{12}, e_{21}\}$,

based on the muscle activation from t_1 to t_2, (M_{Xt}), as

e = {(M_{F1}=1&M_{E1}=0⇒ M_{F2}=1& M_{E2}=0),(M_{F1}=0& M_{E1}=1⇒ M_{F2}=0& M_{E2}=1),(M_{F1}=0& M_{E1}=1⇒M_{F2}=1&M_{E2}=0),(M_{F1}=1 &M_{E1}=0⇒M_{F2}=0&M_{E2}=1)}.

Considering the spiking activity of EEG, this event space was further generalized to

e= {e_1,e_2} = {(M_{F2}=M_{F1} & M_{E2} = M_{E1}), ($M_{F2}\neq M_{F1}$ & $M_{E2}\neq M_{E1}$)}.

- Transition function: δ

  The model predicts the new state using its current state and the events occurred from t_1 to t_2. The state transition function can be defined by a following state transition table.

Table 8.1: State transition table

State \ Event	e_1	e_2
S1	S1	S2
S2	S2	S1

- Initial state: q_0
- Final state: F

FSM contain two states, hand opened (S_1) and hand closed (S_2), $S = \{S_1, S_2\}$ triggered by the activation of flexor (M_F) and extensor (M_E) muscles. To simplify, each forearm muscle (M_x) was considered as a binary unit that can either be contracted (M_x = 1) or relaxed (M_x = 0). i.e. M_F = 1 if the flexor muscle is contracted and M_F = 0 if otherwise. The model stores the state at time $t_1 = t$

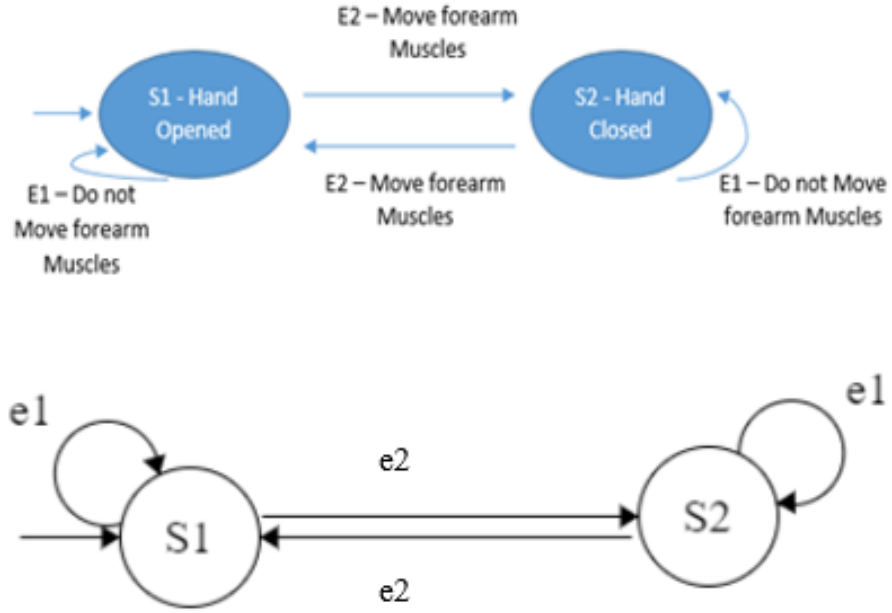

Figure 8.3: Finite Automata

and monitors the events happen from t_1 to $t_2 = t + \Delta t$. Four different events were observed, $e = (e_{11}, e_{22}, e_{12}, e_{21})$, based on the muscle activation from t_1 to t_2, (M_{XT}), as $e = \{(M_{F1} = 1 \& M_{E1} = 0 to M_{F2} = 1 \& M_{E2} = 0), (M_{F1} = 0 \& M_{E1} = 1 to M_{F2} = 0 \& M_{E2} = 1), (M_{F1} = 0 \& M_{E1} = 1 to M_{F2} = 1 \& M_{E2} = 0), (M_{F1} = 1 \& M_{E1} = 0 to M_{F2} = 0 \& M_{E2} = 1)\}$. Considering the spiking activity of EEG, this event space was further generalized to $e = \{e1, e2\} = \{(M_{F2} = M_{F1} \& M_{E2} = M_{E1}), (M_{F2} \neq M_{F1} \& M_{E2} \neq M_{E1})\}$. Simply, e1 keeps the hand in the same state (gesture) from t_1 to t_2 while e_2 alters the current state (either from S_1 to S_2 or S_2 to S_1). The SNN was trained to decode e_1 and e_2 from EEG. The model predicts the new state using its current state and the events occurred from t_1 to t_2. The model was applied for online control of a prosthetic arm through BCI. Figure 8.3 depicts the finite automata used by the FaNeuRobot framework. The SNN was trained to decode e_1 and e_2 from EEG.

8.3 Proof of concept

8.3.1 Rehabilitation device

An anthropomorphic transradial (below elbow) level upper-limb prosthesis was used as the rehabilitation device in this proof of concept. The prosthetic hand was on par with current electromechanical hands in terms of degrees of freedom and capability (Owen, 2019).

8.3.2 Subjects

EEG data from a healthy right-handed participant with no neurological impairment was used to evaluate the accuracy of prosthetic control through BCI.

8.3.3 Experimental protocol

EEG from a single healthy right-handed participant was collected for the preliminary analysis presented in this chapter. Twenty-two EEG channels placed on the frontal and central areas were collected while the participant was performing hand open and close movements. The researcher has collected her own EEG data for the experimental validation of this study. Therefore, the ethical approval was not required for the data collection. However, the participant was not novice to the intended cognitive task and it is a limitation of the current study. This limitation will be addressed in the next chapter which will present a comprehensive analysis on predicting grasp and lift movements from EEG signals using EEG data from twelve participants.

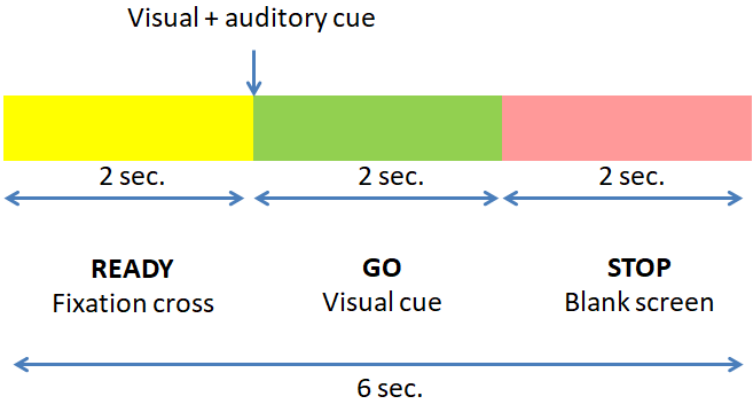

Figure 8.4: Timing of a single trial

8.3.4 Signal recording

EEG signals were collected using the Cognionics dry electrode EEG headset containing 32 channels (INC, n.d.). The Lab Streaming Layer (LSL) API which is a software framework for synchronizing data collection and devices (Kothe, n.d.) was used to stream EEG signals into the BCI application. A customized Matlab script was prepared to present audio and visual cues and to record EEG signals. According to the cue displayed on the computer screen, the subject was asked to perform four different right-hand movements; 1) move the five fingers from opened to closed position, 2) move the five fingers from closed to opened position, 3) remain in the closed position 4) remain in the opened position. Offline analysis was performed under two sessions on two days. Each session contained 40 trials executed within a single run. Timing of a single trial is presented in figure 8.4. 50% of samples from each session was used for training while the rest was used for testing.

8.4 Results

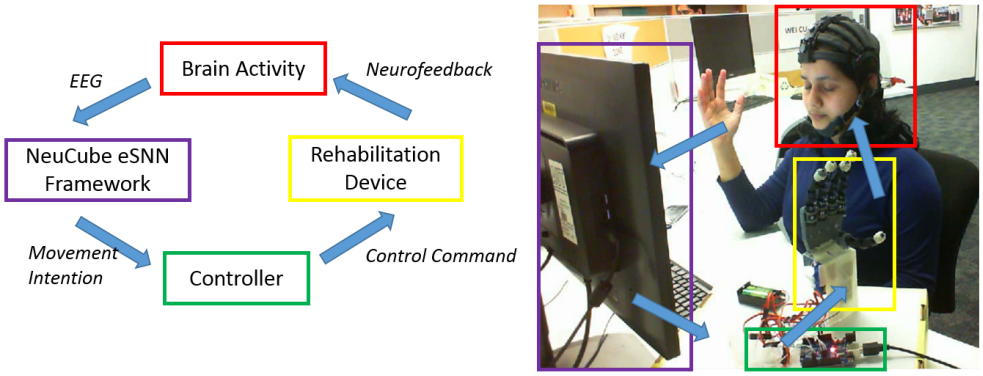

Figure 8.5: Prosthetic control through BCI

8.4.1 Online control of a prosthetic hand through the FaNeuRobot framework

A single healthy participants operated the BCI during multiple sessions. Each session contained six runs and each run contained four trials. The subject was instructed to perform the four hand gestures in a preferred order following the 'GO' cue. Due to constraints in processing time and eye movement-related artifacts, it was necessary to use the channels that are not often affected by eye movement-related contamination. Therefore, the current model utilised C3, C4 and Cz channels that monitor the primary motor cortex sub-serving the hand muscles.

The previous studies on Movement-Related Cortical Potentials have shown that the changes of EEG can be observed even before the onset of a voluntary movement. These EEG potentials are referred to as early Bereitschaftspotentials (early BP). Early BP may be common for both healthy people and amputees as they occur before the onset of movement. Table 8.2 indicates the prediction performance of the FaNeuRobot framework. The analysis was performed at two different EEG sample lengths. The 2s EEG segments contain EEG signals corresponds to 2 seconds of duration from the moment the participant was shown

the 'GO' cue. The 1s EEG segments contain EEG data corresponds to 1 second of duration from the moment the participant was shown the 'GO' cue. The study also evaluated the impact of three different model parameters, the threshold of the threshold-based encoding method, mod and drift parameters of the deSNN classifier. The model could achieve maximum overall accuracy of 90% by using 2s EEG sample segments. The feasibility of the early detection of a movement was evaluated using 1 second EEG segments from the 'GO' cue. The analysis shows that the model could achieve 80% overall accuracy only by using EEG signals corresponds to the 1-second duration from the cue onset.

The accuracy of the proposed motor control approach for BCI was compared with three other machine learning methods commonly used as classifiers in BCI - Support Vector Machine, Multi-Layer Perceptron, and Linear Discriminant Analysis. Each session contained 40 samples, ten samples for each event (S1 to S1, S1 to S2, S2 to S2 and S2 to S1). Table 8.3 presents a comparison of the classification accuracy by each machine learning method.

According to the experimental results, the proposed FaNeuRobot approach resulted in the highest classification accuracy compared to SVM, MLP and LDA methods.

Table 8.2: Performance of decoding hand open and close movements from EEG by the FaNeuRobot framework

Session	**Length of sample for classification (s)**	**Parameters**			**Accuracy (%)**		
		Threshold	**Mod**	**Drift**	**Overall**	**Class 1**	**Class 2**
1	2s (2s to 4s)	0.5	0.8	0.005	70	80	60
1	2s (2s to 4s)	0.5	0.7	0.5	85	100	70
1	2s (2s to 4s)	0.5	0.7	0.05	90	100	80
2	2s (2s to 4s)	0.3	0.9	0.005	90	80	100
2	1s (2s to 3s)	0.3	0.7	0.05	70	80	60
2	1s (2s to 3s)	0.3	0.6	0.05	80	90	70
2	1s (2s to 3s)	0.3	0.6	0.7	80	90	70

Table 8.3: Comparison-Offline Analysis

Accuracy	SVM	MLP	LDA	FANeuRobot
Session 1	55%	85%	65%	90%
Session 2	45%	75%	85%	95%
Average	50(+-7)%	80(+-7)%	75(+-14)%	92.5(+-3.5)%

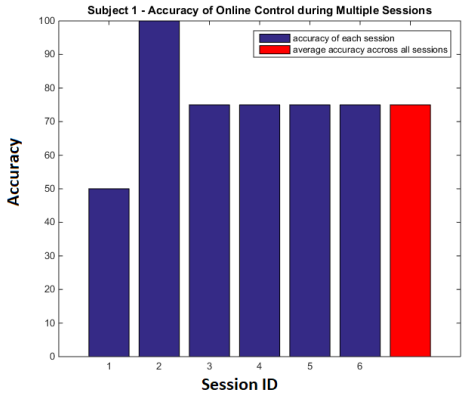

Figure 8.6: Accuracy of online control of the integrated system across multiple sessions

8.4.2 E4: Online control of the prosthetic hand through the proposed neural interface

This section presents the performance during online control of the integrated BCI-Prosthetic control system. Figure 8.5 depicts the experimental setup. Figure 8.6 depicts the classification accuracy across multiple sessions. The FaNeuRobot could achieve an average accuracy 75% for online prediction of hand opening and closing from EEG signals.

8.5 Discussion

This research have shown the feasibility of continuous voluntary control of a prosthetic hand through the FaNeuRobot framework. The current study has used dry electrodes for recording EEG signals which exhibits a low signal to noise ratio compared to the wet electrodes used in (Yoshimura et al., 2012, 2017; Pirondini et al., 2017; Artoni et al., 2016), and (Edelman et al., 2016). A video demonstration of the experiments is available from the following URL: https://www.youtube.com/watch?v=cLqtUoBjJWs&t=18s.

The neuro-muscular interactions through muscle synergies during hand movements can be modelled using a Finite State Machine. Among such behavioural models, the FSM used by the FaNeuRobot framework can estimate the dynamic state changes of the hand (from open to close and vice versa) only by detecting the activation of any muscle from the relevant agnostic-antagonistic muscle pair. It was not required to predict whether it is the activation of flexor muscle or the extensor muscle to estimate the dynamic state changes. This is in contrast to the recent studies on predicting muscle synergies from EEG such as (Yoshimura et al., 2012, 2017; Pirondini et al., 2017; Artoni et al., 2016) and (Edelman et al., 2016) which have not explored the importance of a behavioural model of the hand (i.e. automata) for improving the prediction accuracy. As the study was limited to a single healthy participant who is not a novice user to the motor task, the results do not fully confirm the applicability of this approach for prosthetic control by people with movement impairments. Further experiments are required to evaluate the feasibility of the proposed approach for voluntary prosthetic control by people with movement impairments.

This proof of concept study have shown the feasibility of the continuous voluntary control of a prosthetic hand through a non-invasive Brain-Computer Interface. The decoding of movements from EEG signals were performed by the FaNeuRobot framework. Non-invasive BCI is a potential approach for voluntary prosthetic control due to its low cost, low risk and high user preference due to its non-invasiveness. Further, it can support a large group of amputees as it extracts the motor commands from the brain. Proper positioning of fingers of the prosthetic hand is necessary for secure grasping of an object. However, decoding these finger kinematics from EEG is challenging for a non-invasive BCI decoder due to the poor spatial resolution and volume conductance effect of EEG. The research has shown that a simplified behavioural model which model the dynamic

behaviour of neuro-muscular synergies can reduce the computational complexity of the BCI decoder. Therefore, the classifier could improve the accuracy in decoding movements. It is equally important to choose the proper model from all possible behavioural models which will maximize the inter-class separability.

EEG signals were collected using the Cognionics 32 channel dry electrode EEG headset. Dry electrodes have a lower signal to noise ratio than the EEG signals recorded with wet electrodes. The lower signal to noise ratio can compromise the prediction accuracy. However, on the other hand, since the model works accurately with dry electrodes, it is more applicable for translational aspects of the proposed Brain-Inspired Brain-Computer Interface.

8.6 Summary of the chapter

This chapter presented the FaNeuRobot framework for decoding hand movements from Electroencephalography signals. FaNeuRobot is a framework which extends the generic NeuCube brain-inspired Spiking Neural Network architecture for facilitating online prosthetic control through a non-invasive Brain-Computer Interface. The study aimed at improving the SNN algorithm by integrating a Finite State Machine with the generic NeuCube SNN architecture and the development of prototype software that enabled online control of the prosthetic limb. The Finite State Machine modelled the behaviour of agnostic-antagonistic muscle pairs of the forearm that contribute for hand open and close. The chapter presented a preliminary study on evaluating the feasibility of the proposed FaNeuRobot framework for controlling an upper-limb prosthesis through a non-invasive Brain-Computer Interface. The next chapter will present the integration of the proposed spike-based learning algorithms for constructing the Brain-Inspired Brain-Computer Interface. A comprehensive analysis which will experimentally validate and benchmark the

performance of the proposed model will be presented in the next chapter.

8.7 Contributions

- This research designed and implemented the FaNeuRobot framework that extended the generic NeuCube framework.
- This chapter presented a preliminary analysis on decoding continuous movements from EEG signals through the FaNeuRobot framework.
- The research have shown that a simplified behavioural model which model the dynamic behaviour of neuro-muscular synergies can reduce the computational complexity of the BCI decoder.
- The current study showed the feasibility of controlling a prosthetic hand through the proposed FaNeuRobot framework.

8.8 Related publications

1. **Kumarasinghe, K.**, Owen, M., Taylor, D., Kasabov, N., & Kit, C. (2018, May). FaNeuRobot: A Framework for Robot and Prosthetic Control Using the NeuCube Spiking Neural Network Architecture and Finite Automata Theory. In 2018 IEEE International Conference on Robotics and Automation (ICRA). IEEE. doi:10.1109/ICRA.2018.8460197
2. A video demonstration on controlling a prosthetic hand described in the conference paper - 'FaNeuRobot: A Framework for Robot and Prosthetics Control Using the NeuCube Spiking Neural Network Architecture and Finite Automata Theory' presented at the IEEE International Conference on Robotics and Automation (ICRA) 2018 is available from the

following URL. https://www.youtube.com/watch?v=cLqtUoBjJWs&list=

PLwgHof7plcyU9m_scUqdFvA3lnpZbkkRD

Chapter 9

Brain-Inspired Spiking Neural Networks for Decoding and Understanding Muscle Activity and Kinematics

"Everything is theoretically impossible until it is done. "

Robert A. Heinlein - The 'dean of science fiction writers'

Chapter overview

Previous chapters proposed two spike-based generic methods for constructing an interpretable machine learning model which could incrementally learn to predict complex spike sequences from stochastic data streams. These methods show the feasibility of constructing a novel Brain-Inspired Brain-Computer Interface system which can effectively address several limitations of the current restorative BCIs. This chapter will describe the integration of the proposed generic methods with

the generic NeuCube SNN framework for developing the proposed Brain-Inspired Brain-Computer Interface system. BI-SNN can map spiking activity from input channels into a high dimensional source-space which will enhance the evolution of polychronising spiking neural populations. Here it will be applied to predict muscle activity and kinematics from electroencephalography signals during upper limb functional movements.

9.1 Introduction

This chapter presents a Brain-Inspired Spiking Neural Network (BI-SNN) model, which integrates the proposed spike-based generic learning algorithms with the NeuCube SNN framework to construct a novel type of Brain-Inspired Brain-Computer Interface. The proposed BI-SNN is a generic SNN architecture that can be applied for the predictive modelling of spatio-temporal data streams such as to predict muscle activity and kinematics from EEG during various human activities. This study shows that the proposed BI-SNN approach enhances the decoding of forearm muscle activity and kinematics from EEG during grasp and lift movements. The proposed BI-SNN is based on the two spike-based generic learning algorithms proposed in this thesis - the evolving Spike Pattern Association Neural Network (Kumarasinghe et al., 2019) learning model and the framework for deep knowledge representation in brain-inspired SNN architectures.

The primary goal of this study is to evaluate the feasibility of Brain-Inspired Spiking Neural Networks to construct a novel, interpretable neural decoder which can incrementally learn to predict an upcoming movement from EEG signals. The two main objectives of the study are to predict the onset and the trajectory of a movement from EEG signals. The EMG activity of the forearm muscles is used as the expected output to train the BI-SNN for decoding movement onset from EEG signals. The kinematic signals are used as the expected output from the BI-SNN for decoding the trajectory of a movement.

This chapter will address the following research questions.

- **RQ6: Does the Brain-Inspired Spiking Neural Network model that integrates the eSPANNet with the NeuCube SNN architecture result in higher prediction accuracy than the pure eSPANNet learning model for predicting continuous movements from EEG**

signals?

- **RQ7: How do the Brain-Inspired Spiking Neural Networks and the non-Brain-Inspired machine learning models compare in terms of their ability for sequence prediction, interpretability, and incremental learning to predict complex movements from EEG signals useful for motor recovery and restoration through Brain-Computer Interfaces?**

The study will evaluate four key aspects: how accurate the prediction is, the latency of the prediction, the training speed to reach an acceptable prediction, and the interpretability of the model (the degree to which a human can understand the cause of a decision made by the model). The correlation(Pirondini et al., 2017; Liang & Bougrain, 2012; Wang et al., 2011; Pistohl et al., 2008) between the actual and predicted motor signal is used as a measure of prediction accuracy. The average prediction latency per single time interval in a pseudo-online experimental setup is used to evaluate the prediction latency of the model. The machine learning models were trained by gradually increasing the training dataset size to evaluate the training speed. The performance of each model at a specific training dataset size was evaluated using the same test dataset, and the model performance corresponds to a particular training dataset size is used to compare the training speed. The interpretability of the BI-SNN model is evaluated using the connectivity patterns of each subject-specific BI-SNN model(Kumarasinghe et al., 2020).

The novelty of the BI-SNN approach is its ability to learn which area of the brain carry useful information for decoding a certain motor behaviour in an incremental and online manner. The brain-inspired architecture enhanced the ability to explain the reasons behind the model predictions in a form which is

comprehensible to human understanding. This study evaluated the performance of predicting the activity of the five muscle groups and twenty-four object and hand kinematic sensor recordings from EEG using the BI-SNN model and compared with the Generalised Linear Model approach. GLM is used in the analysis as the main baseline method for comparison as it has been the most popular method used in the literature so far for the task under consideration. While Recurrent Neural Networks is a popular method for solving other tasks, they lack interpretability and knowledge representation of the model, which is one of the main advantages of proposed BI-SNN, along with achieving higher accuracy. GLM still offer some limited interpretability, and this is another reason to use it as a benchmark method.

9.2 Deep learning in Brain-Inspired Spiking Neural Networks

This section presents a description of the BI-SNN model and the experimental procedure for validating and comparative analysis of the proposed BI-SNN. The previous chapters showed promising empirical results of the eSPANNet's performance on predicting different upper limb movements from invasive and non-invasive brain data. So far, eSPANNet was used as a sensor-space model as it directly used the encoded spike sequence from EEG channels to evolve the population vectors of spiking neurons. Given the feasibility of the NeuCube SNN architecture to map the spiking activity into the structural and functional regions of interest in the brain presented in chapter 7 (Kumarasinghe et al., 2020), it was hypothesised that the integration of eSPANNet as the output layer of the NeuCube would enable better detection of polychronising spiking neural populations. Figure 9.1

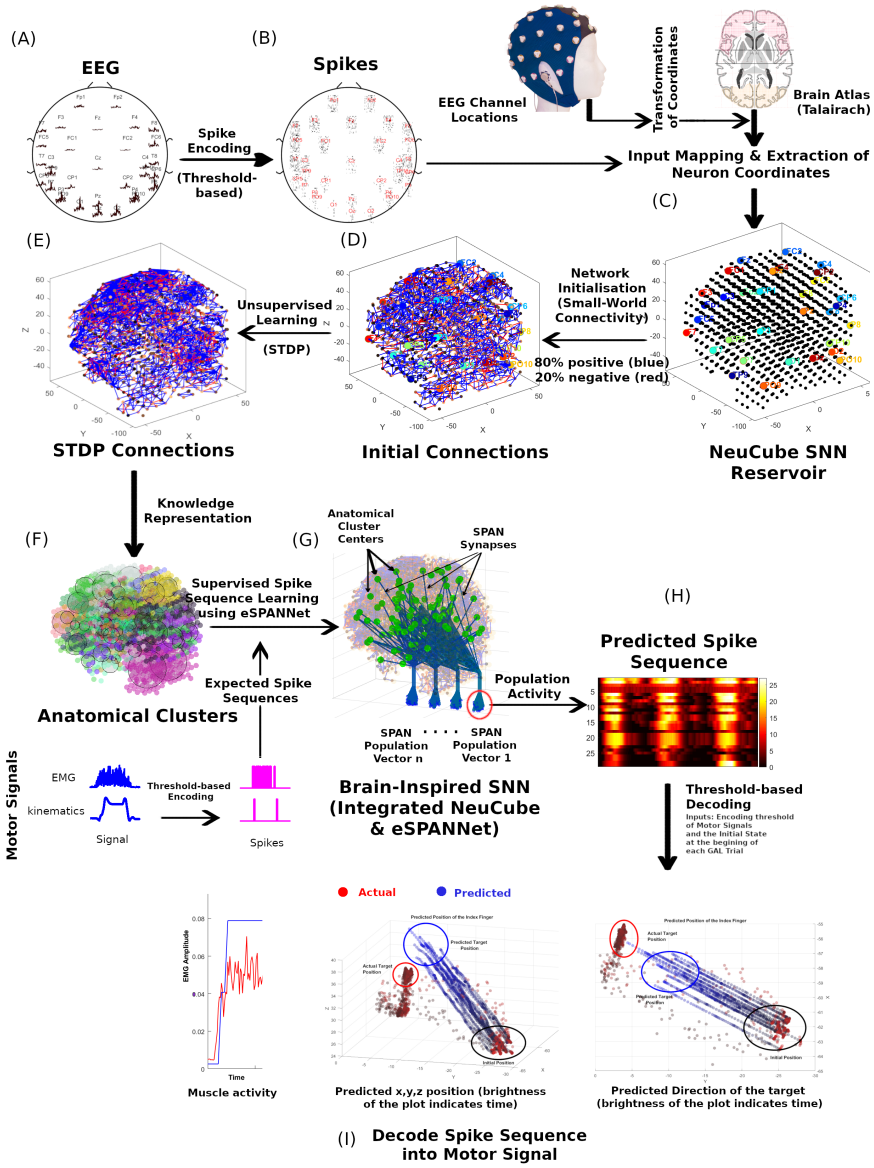

Figure 9.1: Integration of the eSPANNet with the NeuCube SNN architecture and major steps in training a BI-SNN model - A) Filtered EEG B) Spike encoding c) Extraction of brain coordinates from a brain template and mapping EEG channel locations D) Initialisation of the SNN based on the small-world connectivity principle E) Unsupervised Spike Time Dependent Plasticity learning F) Extraction of anatomical clusters G) Training population vectors using eSPANNet learning H) Predicted spike sequence by the SNN I) Decoding predicted spike sequences into muscle activity and kinematics using the threshold-based decoding

illustrates the architecture of BI-SNN, which integrates the proposed eSPANNet learning model and the deep knowledge representation framework with the generic NeuCube SNN architecture.

A detailed description of the NeuCube SNN framework was presented in chapter 3 (refer section 3.11 for further details). The details of the proposed eSPANNet learning model were discussed in chapter 5 and 6 while the proposed knowledge representation framework was presented in chapter 7. This chapter will present the integration of these learning algorithms for constructing the BI-SNN model.

Learning in BI-SNN includes spike encoding, input mapping, network initialisation, and unsupervised learning which are specific to modelling data using the NeuCube SNN framework. As shown in figure 9.1 A, the BI-SNN model considers the signals from the 32 EEG channels as the input to the model, and the EMG and kinematics signals as the expected outputs from the model. In the BI-SNN, the input signals are first encoded into spike sequences (figure 9.1 B) using a spike encoding algorithm. To model the motor behaviour in a spike-based interpretation, first, both input (EEG) and expected output (EMG and kinematic) signals were converted into spike sequences using the threshold-based encoding method.

A threshold-based encoding algorithm was used to encode EEG signals in the experimental validation of the study due to its less processing time for encoding spikes. The threshold-based encoding method forms one of the simplest forms of spike encoding approaches. As a result of this simplicity, its main advantage is the ability to deliver fast encoding, which fulfils one of the requirements for real-time information processing.

First, the temporal difference between the consecutive observations (d) in the input stream (x) is obtained to compute the encoding threshold (refer equation 3.13). The mean value ($mean$) and the standard deviation (std) of the computed temporal differences are calculated to compute the encoding threshold as per

equation 3.14 where c denotes a pre-defined variable called encoding factor. The sign of the threshold value can be used to form both positive (th_+) and negative (th_-) encoding thresholds. However, since the Spike Pattern Association Neuron can not be trained with both positive and negative spikes together at the same time, here the polarity of the spike train is not considered in the current analysis. Any temporal difference that reaches either the positive or negative threshold value is encoded as a positive spike event.

The NeuCube reservoir maps the encoded spiking activity from EEG channels into this 3D space through EEG mapping, as shown in figure 9.1 C. The initial synaptic connections in the SNN are initialised by assigning random weights using the small-world connectivity principle (Braitenberg & Schüz, 2013; Bullmore & Sporns, 2009)(figure 9.1 D).

Unsupervised learning in NeuCube applies spike-time based learning rules such as Spike-Time Dependent Plasticity on the input spike sequences received from input neurons. As the input spike trains are fed into this reservoir through input neurons, the SNN evolves based on the spike time of pre and post-synaptic neurons according to Spike-Time Dependent Plasticity learning (Gerstner et al., 1996; Markram & Tsodyks, 1996) (figure 9.1 E).

The STDP learning rule quantifies the synaptic weight update of the pre-synaptic neuron j, Δw_j according to the relative timing of the pre synaptic (i) spike arrival and the firing time of the post synaptic (j) spikes. The pre-synaptic spike arrival is denoted as t_j^f and the firing time of the post-synaptic neuron is indicated by t_i^n where $f = 1, 2, 3....$ The total synaptic weight update Δw_j is given by equation 3.29 where $W(x)$ denotes the STDP learning window given by the equation 3.30. The learning process results in evolving synaptic connections in the reservoir based on the relative timing of the spiking activity between pre and post-synaptic neurons. The STDP learning permits the spiking neurons in the

NeuCube reservoir to associate temporally correlated input spike sequences and then transform them into a meaningful output.

The spike response of the reservoir can be approximately mapped to different regions of interest in the brain through the knowledge representation framework of NeuCube (Kumarasinghe et al., 2020) presented in chapter 7. The BI-SNN will then cluster the spiking activity based on their anatomical locations (figure 9.1 F) the and apply supervised learning specific to eSPANNet, which will enable the SNN to incrementally learn the spatio-temporal association of spiking activity correspond to distinct brain regions (figure 9.1 G). The proposed BI-SNN replaces the deSNN classifier in the generic NeuCube framework by the evolving Spike Pattern Association Neural Network model. The eSPANNet learning model utilises the polychronisation effect of Spiking Neural Networks(Izhikevich, 2006) to decode neural activity from spatio-temporal brain data. It contains a network of Spike Pattern Association Neurons (SPAN), a spiking neuron model which can emit spikes at the desired time point (Mohemmed, Schliebs & Kasabov, 2011; Mohemmed, Schliebs, Matsuda & Kasabov, 2011; Mohemmed & Kasabov, 2012; Mohemmed, Lu & Kasabov, 2012; Mohemmed, Schliebs et al., 2012; Mohemmed et al., 2013). The integration of eSPANNet as the output layer of NeuCube SNN architecture enables incremental learning of spike sequences to associate temporally correlated spiking activity from distinct brain areas with the output neuron layer of the BI-SNN.

When the BI-SNN receives an input spike sequence corresponding to a particular event (i.e. flexion of the Flexor Digitorum muscle), the eSPANNet will first determine whether there is any SPAN in the corresponding population associated with that particular event. If there are no trained SPANs for the current event or if the trained SPANs can not produce the expected spike sequence, a new SPAN is initialised in the corresponding population vector and trained to emit

the expected spike sequence at the desired time point(s). As the SNN is exposed to continuous input spike sequences associated with distinct events, BI-SNN will incrementally evolve separate SPAN populations to associate the population activity of the NeuCube reservoir with the corresponding event. As the SPAN readout populations are evolved, each spiking neuron in the SPAN population is validated using their ability to emit spikes at desired time points for unseen input spike sequences. The BI-SNN only considers the spiking activity of the SPANs, which result in higher accuracy than a pre-defined threshold level. The threshold level is determined by the number of SPANs and the maximum prediction accuracy of the SPANs in a population. For each unseen input spike trains, the spike response of each SPAN population will be obtained to determine the corresponding class label. Different strategies, such as the average population activity or majority voting, can be followed to determine the class label of a particular input spike sequence.

Finally, the BI-SNN will extract the polychronising spiking neural clusters which can generate temporally associated spike sequences correlated with the predicted event as per figure 9.1 H. These predicted spike sequences are decoded back to signals for predicting different motor signals such as muscle activity and kinematics by using the encoding threshold values of each motor signal and the initial state of each motor signal at the beginning of the GAL trial as exemplified in figure 9.1 I.

9.3 Results

This chapter experimentally validated the BI-SNN model using the publicly available WAY-GAL-EEG (Wearable interfaces for hAnd function recovery Electroencephalography Grasp-And-Lift) dataset (Luciw et al., 2014a, 2014b). Since

this is a functional upper limb movement, the participants were gazing at the cue, hand, object, initial position and target position of the object. The participants demonstrated natural coordination among eye, hand, object and target position while performing the grasp and lift movement. A detailed description of the EEG dataset was presented in chapter 4 (refer section 4.4 for details).

The EEG signals were pre-processed to remove the EEG artefacts such as the eye blinks, vertical and horizontal eye movements and generic discontinuities using the ADJUST plugin(Mognon et al., 2011) of the EEGLab (Delorme & Makeig, 2004). The artefact-free EEG signal was then filtered using a band-pass filter to extract the alpha, beta and gamma frequency bands and then rectified and down-sampled to 100Hz. The training dataset contained approximately fifteen grasp-and-lift trials per participant and corresponded to a total duration of 12 minutes.

The performance of reconstructing twenty-nine motor signals was evaluated using the cross-correlation between the actual and predicted signals. The cross-correlation measured the similarity between the predicted and actual signals as a function of a short displacement of one signal relative to the other. Here the BI-SNN has used a time lag of 100 ms for calculating the cross-correlation. For each motor signal, the cross-correlation coefficients between the actual and the predicted activity using the BI-SNN, eSPANNet and GLM approaches were obtained. Each model was trained separately using alpha, beta and gamma frequency bands of the EEG signal. The maximum coefficient of the cross-correlation sequence returned from all three frequency bands by each approach was recorded. This maximum coefficient indicates the best fit between the actual and predicted signals within a short displacement permitted by the 100ms lag. The comparative analysis was performed using the maximum cross-correlation coefficient of each method. To interpret the results, the coefficients ($0 <= r <= 1$) were divided into four

ranges; 'high', 'moderate', 'weak' and 'very weak or no correlation' ('high': r>=0.7, 'moderate': 0.7 > r >= 0.5, 'weak': 0.5 > r >=0.3, and 'very weak': r<0.3).

9.3.1 Deep learning in BI-SNN enhances polychronisation of SNN

This experiment answers the RQ6 of the research.

- **RQ6: Does the Brain-Inspired Spiking Neural Network model that integrates the eSPANNet with the NeuCube SNN architecture result in higher prediction accuracy than the pure eSPANNet learning model for predicting continuous movements from EEG signals?**

The integration of eSPANNet with the NeuCube, which forms the BI-SNN model resulted in more strongly correlated population activity in comparison with the standalone eSPANNet model along with significant biofeedback generated by the trained 3D NeuCube SNN reservoir. BI-SNN demonstrated the feasibility of finding polychronising spiking neuron populations from different brain areas associated with the grasp and lift movement. The readout population activity in the BI-SNN was more temporally associated with muscle activity and hand kinematics than the pure eSPANNet. For the comparison, the normalised cross-correlation between each actual and predicted motor signal by all participants was obtained using BI-SNN, eSPANNet and GLM approaches. The average cross-correlation of each motor signal was computed using the maximum coefficient of the cross-correlation sequence correspond to each participant on that particular motor signal. Table 9.1 indicates the results of cross-correlation analysis using the BI-SNN ($\bar{r}_{\text{BI-SNN}}$), eSPANNet ($\bar{r}_{\text{eSPANNet}}$) and GLM ($\bar{r}_{\text{GLM}}$) approaches. The highest average correlation coefficient corresponds to each motor signal is highlighted

in bold text in table 9.1. The comparative analysis of BI-SNN, eSPANNet and GLM showed that BI-SNN resulted in the highest average correlation between the actual and predicted motor signals in twenty-three out of the twenty-nine motor signals. In contrast, eSPANNet corresponded to the highest average correlation in eight out of twenty-nine motor signals. BI-SNN resulted in the highest average correlation in the majority of the motor signals that correspond to executing a grasp and lift movement. The results suggest that the BI-SNN can predict each motor signal (muscle activity and joint kinematics) more accurately than the pure eSPANNet or GLM models.

Depending on when the spike sequence learning is applied on the spike trains, the SNN models discussed in this paper can be divided into two main categories as the 'sensor-space' spike sequence learning models and the 'source-space' spike sequence learning models. A sensor-space model directly uses the spike trains extracted from sensors, such as the data obtained from EEG channels, for learning the expected spike sequences. On the other hand, the source-space spike sequence learning model first maps the spiking activity extracted from sensor data into a 3D space that represents different regions of interest in the brain. The source-space model then applies the spike sequence learning algorithm on this approximated source data to learn the expected spike sequences. The eSPANNet learning model represents a sensor-space spike model as it directly uses the spike sequences extracted from EEG sensor data for spike sequence learning. In contrast, the BI-SNN represents a source-space model as it performs the spike sequence learning on the approximated source data using the method presented in (Kumarasinghe et al., 2020) for learning the expected spike sequence. The results show that BI-SNN, as a source-space SNN model, has the feasibility to find spiking neuron clusters that are more temporally associated with EMG activity and hand kinematics compared to the sensor-space eSPANNet model.

Table 9.1: Comparison of the average correlation coefficients between the actual and predicted motor signals by BI-SNN, eSPANNet and GLM (AD: Anterior Deltoid, B: Brachoradial, FD: Flexor Digitorum, CED: Common Extensor Digitorum, FDI: First Dorsal Interosseous)

Motor Signal	$\bar{r}_{\text{BI-SNN}}$	$\bar{r}_{\text{eSPANNet}}$	$\bar{r}_{\text{GLM}}$
Elevation of Object	**0.55**	0.54	0.25
Elevation of Index Finger	**0.56**	0.53	0.53
Elevation of Thumb	**0.57**	0.49	0.47
Elevation of Wrist	**0.58**	**0.58**	0.56
Roll of Object	**0.58**	0.55	0.54
Roll of Index Finger	**0.68**	0.65	0.67
Roll of Thumb	**0.6**	0.57	0.55
Roll of Wrist	**0.58**	0.52	0.53
Azimuth of Object	0.55	**0.57**	0.5
Azimuth of Index Finger	**0.7**	0.68	0.69
Azimuth of Thumb	**0.64**	0.62	0.59
Azimuth of Wrist	**0.61**	0.58	0.58
X-position of Object	**0.63**	0.62	0.56
X-position of Index Finger	**0.63**	0.6	0.55
X-position of Thumb	0.58	**0.59**	0.52
X-position of Wrist	**0.59**	0.58	0.53
Y-position of Object	**0.65**	0.63	0.59
Y-position of Index Finger	0.58	**0.59**	0.53
Y-position of Thumb	**0.58**	0.55	0.53
Y-position of Wrist	**0.58**	0.54	0.53
Z-position of Object	**0.6**	0.56	0.57
Z-position of Index Finger	**0.7**	0.68	0.66
Z-position of Thumb	0.67	**0.69**	0.64
Z-position of Wrist	**0.67**	0.66	0.64
Muscle-activity of AD	**0.74**	**0.74**	**0.74**
Muscle-activity of B	**0.7**	0.64	0.69
Muscle-activity of FD	0.69	**0.73**	0.67
Muscle-activity of CED	0.72	**0.73**	0.71
Muscle-activity of FDI	**0.67**	0.58	0.64

BI-SNN has the following features which contributed to the higher prediction accuracy by BI-SNN than the pure eSPANNet. BI-SNN has an additional hidden layer which is initially connected using the small-world connectivity principle and then evolved through STDP learning. This STDP layer enhances the evolution of polychronising spiking neural populations. In theory, it has been established that many of the functions will converge at a higher level of abstraction. So more layers will lead towards gaining better results.

Further, EEG mapping transforms the spiking activity into a high dimensional space, and this type of source localisation is more compatible with neuromorphic architectures compared to other source localisation methods. The eSPANNet only process temporal information while BI-SNN process both spatial and temporal information in the model. Spatio-temporal analyses have additional benefits over purely spatial or time-series analyses with its better interpretability in terms of capturing and explaining spatio-temporal patterns of brain activity.

The following series of experiments (E5.2 - E5.7) address the RQ7 of the research.

- **RQ7: How do the Brain-Inspired Spiking Neural Networks and the non-Brain-Inspired machine learning models compare in terms of their ability for sequence prediction, interpretability, and incremental learning to predict complex movements from EEG signals useful for motor recovery and restoration through Brain-Computer Interfaces?**

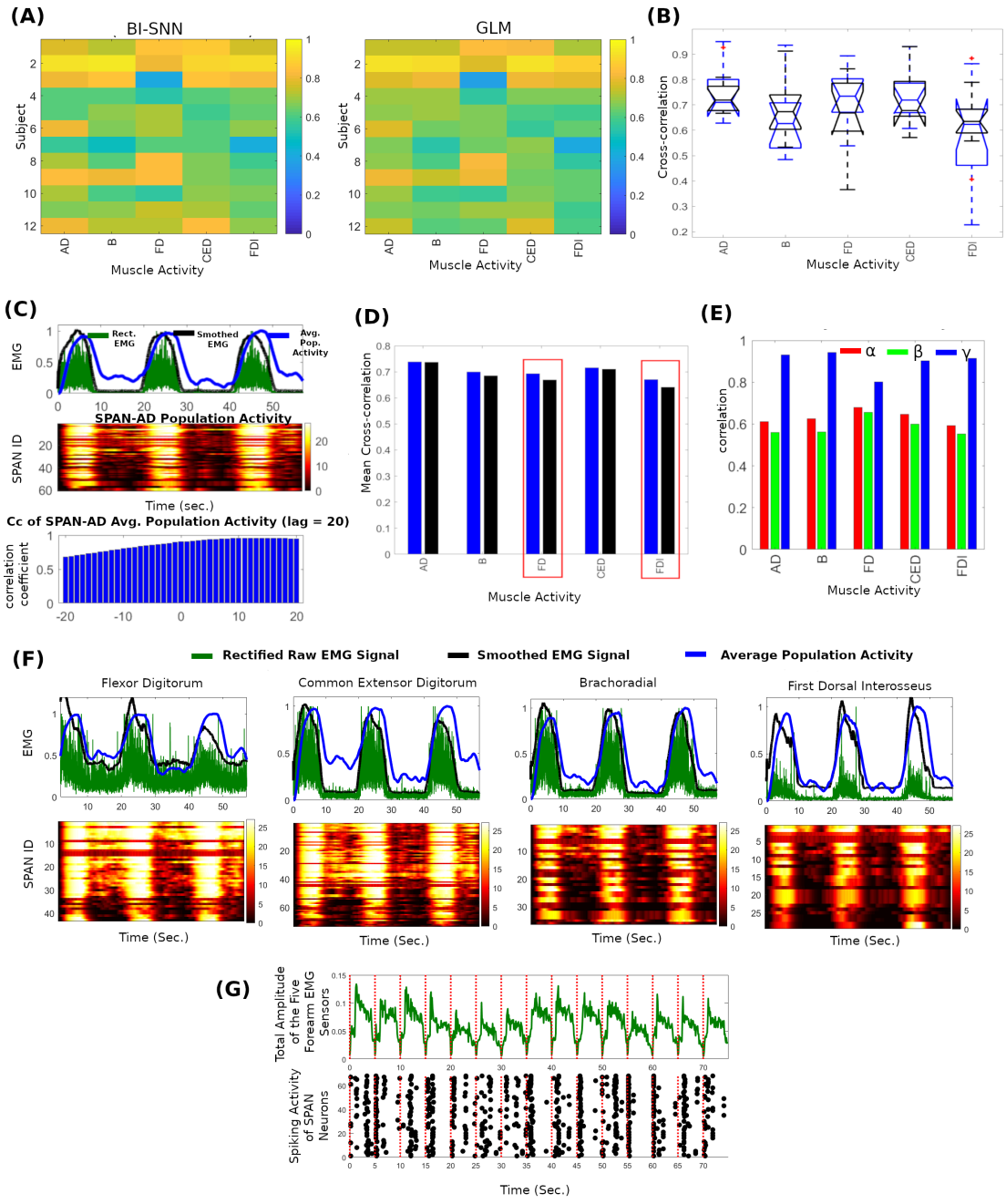

Figure 9.2: Comparative analysis of decoding muscle activity from EEG using BI-SNN and GLM approaches A) Normalised cross-correlation coefficients between the actual and predicted muscle activity B) Statistical distribution of the correlation coefficients by BI-SNN (blue) and GLM (black) C) Calculation of the normalised cross-correlation coefficients between EMG activity of AD muscle and SPAN_{AD} population activity D) Comparison of the mean cross-correlation coefficients E) Band-specific cross-correlation coefficients of participant 2 F) Actual muscle activity of B, FD, CED, FDI muscles and the response of corresponding SPAN population G) Population activity of $\text{SPAN}_{\text{movement-onset}}$ and the accumulated amplitude of the five EMG sensors.

9.3.2 E5.2: Decoding continuous muscle activity in BI-SNN

The cross-correlation between the actual and predicted EMG activity shows that the BI-SNN approach results in a 'high' cross-correlation in predicting muscle activity of the Anterior Deltoid (AD), Brachoradial (B), Flexor Digitorum (FD), Common Extensor Digitorum (CED) and First Dorsal Interosseous (FDI) muscles. The supplementary table 1 shows the comparative analysis of predicting EMG activity using BI-SNN and GLM methods. The participant-wise mean cross-correlation coefficients in predicting all muscle activity indicate that in nine out of twelve participants there was a 'high' mean correlation ($r >= 0.7$) while in the remaining three participants there was a 'moderate' mean correlation ($0.7 > r >= 0.5$). The BI-SNN delivered a 'high' mean cross-correlation in predicting all muscle activity. The AD muscle showed the highest average correlation of 0.74 of the group. The 'high' cross-correlation coefficients indicate a strong temporally associated relationship between the spiking activity of the corresponding spiking neuron population in the BI-SNN and the associated muscle activity. The cross-correlation measured the similarity between the actual and the predicted muscle activity as a function of 100ms displacement of the predicted signal relative to the actual signal. The high correlation suggests the feasibility of accurately decoding the muscle activity from EEG signals using the BI-SNN model.

Figure 9.2 A represents the cross-correlation coefficients between the actual and predicted muscle activity by the BI-SNN and GLM. The statistical distribution of the correlation coefficients within the participant group is presented in figure 9.2 B. Figure 9.2 C (Top: rectified (green) and smoothed (black) EMG signal from the AD muscle of participant 2, and the average convoluted spike sequence generated by the SPAN_{AD} (blue) population, middle: convoluted spike sequences emitted

by spiking neurons in $SPAN_{AD}$ population, bottom: normalised cross-correlation coefficients between the smoothed rectified EMG signal and the average $SPAN_{AD}$ convoluted population activity using cross-correlation lag of 200ms) compares the mean cross-correlation of each muscle by BI-SNN and GLM. Figure 9.2 C illustrates the effect of the change in the observed cross-correlation coefficient as a result of the permitted displacement between the two signals. A wider correlation lag of 200ms was used to illustrate the effect. However, all results reported in this paper utilised a cross-correlation lag of 100ms. The cross-correlation lag indicates how far the two time series are offset. The cross-correlation lag corresponds to the highest correlation coefficient represents the best fit between the two time series. At longer lags, the number of possible matches between the two signals can decrease as the longer lags increase the chance of not overlapping the two series. A short cross-correlation lag is preferred than a long lag as it indicates a shorter displacement between the signals. The shorter displacement is and an indication of the probability of detecting an event within a short delay.

The comparison indicates that BI-SNN results in higher mean correlation than GLM for all muscles (figure 9.2 D). Several participants such as participant 1, 2, and 3 exhibited notably higher correlation in a specific frequency band (figure 9.2 E). Although such a difference was not common for all participants in the considered frequency bands, this observation suggests that muscle activity related neural information may be prominent in certain subject-specific sub-frequency bands and needs to be further investigated. Figure 9.2 F depicts the muscle activity of the Brachoradial, Flexor Digitorum, Common Extensor Digitorum and First Dorsal Interosseous muscles of participant 2 and the population activity of the corresponding $SPAN_{B}$, $SPAN_{FD}$, $SPAN_{CED}$, and $SPAN_{FDI}$ neural populations. Figure 9.2 G shows the total amplitude of the smoothed EMG signals from the five muscles (top) and the spike response of the $SPAN_{movement\text{-}onset}$ population. The

$\text{SPAN}_{\text{movement-onset}}$ population was trained to produce spikes at the movement onset (bottom). In general, the $\text{SPAN}_{\text{movement-onset}}$ population activity was synchronised with movement onset events denoted by the muscle activity, and indicate the feasibility of detecting movement onset using the proposed BI-SNN approach. However, on certain occasions, the spiking events were not closely aligned with the movement onset moment. This inconsistency can be due to multiple reasons. In addition to the movement onset, spiking events were also observed when the participant releases the object. This may be due to the activation of the same fore-arm muscle synergies that involved on both occasions. The inconsistency may also be due to the variability of the motor planning time and effort as the person becomes familiar with the task after repeating multiple trials. In addition, noise and non-stationarity of EEG have also contributed to the uncorrelated spiking events. However, the spiking behaviour of the readout population was generally correlated with the movement onset time in many grasp and lift trials.

9.3.3 E5.3:Accurate decoding of kinematic signals in a BI-SNN

Twenty-four kinematic sensors monitored the x, y and z position as well as the elevation, roll and azimuth angles (orientation) of the object, thumb, index finger and wrist. The BI-SNN contained separate SPAN populations trained to emit spikes according to each kinematic signal. Figure 9.3 A and B graphically represents the cross-correlation coefficients between the actual and the predicted object and hand kinematics by the BI-SNN and GLM approaches, respectively.

BI-SNN resulted in a 'high' cross-correlation in predicting y coordinates of the object, z coordinates of the index finger, thumb and wrist and as well as the roll and azimuth angles of the index finger. A 'moderate' correlation was observed in

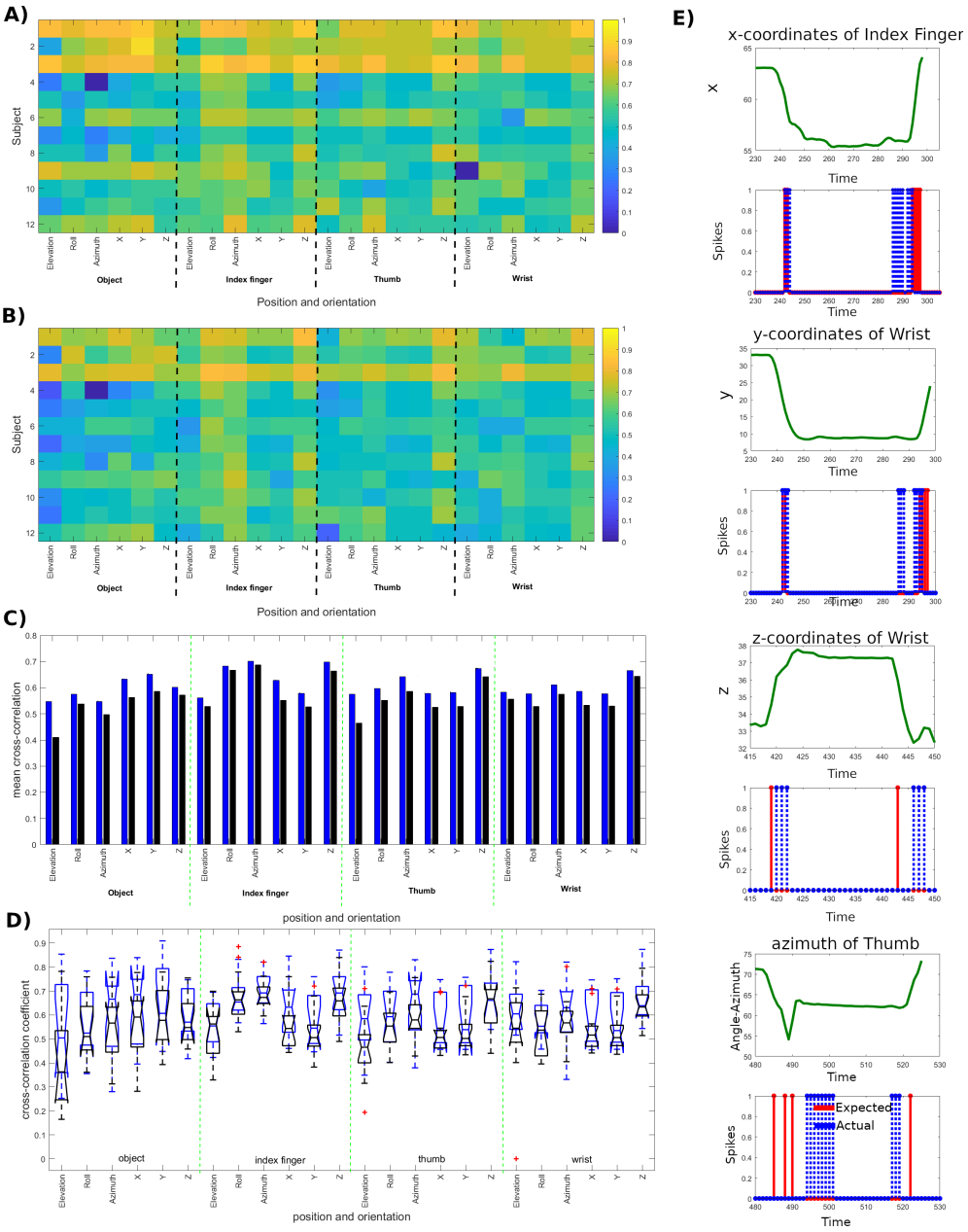

Figure 9.3: Results of predicting the object and hand kinematics using BI-SNN and GLM approaches. A) The maximum coefficient of the cross-correlation sequence between the actual and predicted kinematic signal by BI-SNN. B) The maximum cross-correlation coefficients between the actual and predicted kinematic signal by GLM C) Comparison between the BI-SNN and GLM methods on predicting the object and hand kinematics D) The statistical distribution of the cross-correlation coefficients within the participant group. The correlation analysis shows that the BI-SNN results in a 'moderate' to 'high' cross-correlation ($0.6 <= r <= 0.7$) in predicting x,y,z Cartesian coordinates. E) The actual kinematic signals and the spike response of a single neuron in $\text{SPAN}_{\text{index-x}}$, $\text{SPAN}_{\text{wrist-y}}$, $\text{SPAN}_{\text{wrist-z}}$ and $\text{SPAN}_{\text{thumb-azimuth}}$ populations during a Grasp-and-Lift trial

predicting x and z coordinates of the object, the x and y coordinates of the index finger, thumb and wrist, and as well as elevation, roll and azimuth of the object, thumb and wrist. Prediction of the azimuth angle and z position of the index finger showed the highest sensor-specific mean correlation (r = 0.7) within the twelve participants while participant 1 and 3 showed the highest participant-specific mean correlation of the twenty-four kinematics signals (r=0.8) using the BI-SNN.

Figure 9.3 C shows a comparison of the mean cross-correlation coefficients in predicting the object and hand position by both approaches. Figure 9.3 D shows the statistical distribution of the cross-correlation coefficients within the participant group. The comparison indicates that the BI-SNN results in a higher mean correlation compared to the GLM for all twenty-four kinematics signals. Figure 9.3 E exemplifies the predicted (blue dotted line) and actual (solid red line) spike sequences during a GAL trial.

9.3.4 E5.4: Prediction latency of the BI-SNN

Here the study reports the processing time of the two SNN models, BI-SNN and eSPANNet and show their feasibility in performing real-time and online predictions. The total pseudo-online prediction latency per each participant was divided by the number of data points in the test dataset to obtain the average prediction latency per single time interval. This latency is compared with the 10 ms delay between the two consecutive input data points of the SNN model as the input signals were sampled at 100Hz sampling rate. The experiments were performed using an ordinary PC (CPU: 2.6GHz, RAM: 16GB). The source code was written in Matlab and did not utilise any parallel processing features such as multi-threading, GPU (Graphical Processing Unit) or neuromorphic computing.

Figure 9.4 A shows the average prediction time of each subject-specific SNN

model to predict the spiking activity of the twenty-nine spiking neuron populations using a single input data point of the EEG signal. Figure 9.4 B shows the statistical distribution of the average prediction time by both methods within the group of twelve participants. The median prediction time of the twenty-nine behavioural spike sequences by BI-SNN and eSPANNet model corresponding to a single time interval is 3.5ms and 1ms, respectively. The current pseudo-online system is set up to receive EEG signal at a sampling rate of 100Hz. So, there is a 10 ms delay between two consecutive observations of the EEG in the current experimental setup. Therefore, a neural decoder which can predict the corresponding output of a single observation within this 10 ms lag will be able to perform real-time event predictions. As shown in the analysis, BI-SNN takes approximately 3.5ms to process a single observation in a particular EEG frequency band while eSPANNet takes about 1ms for the same task. Therefore, assuming that there are no other delays (i.e. delays in signal transmission), both spiking neuron models should be able to perform real-time predictions at a sampling rate of 100Hz.

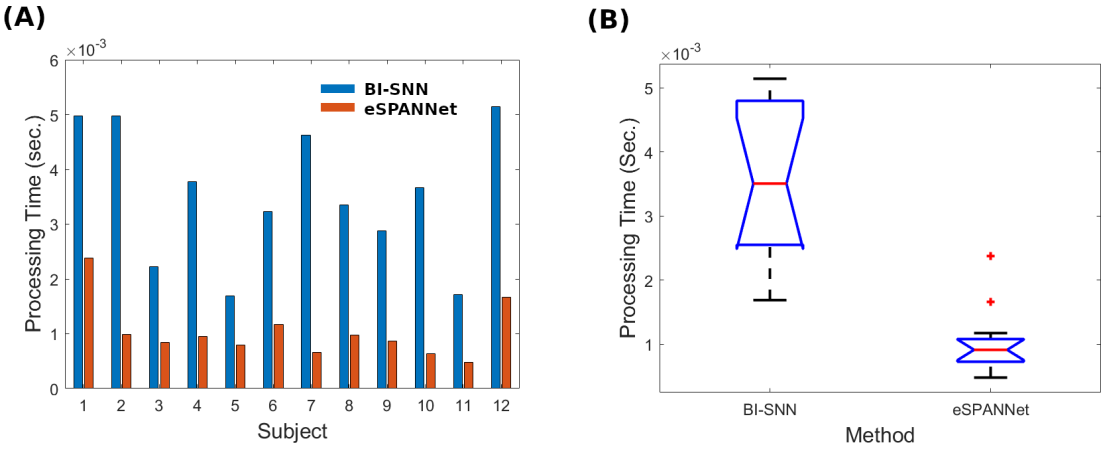

Figure 9.4: The feasibility of BI-SNN for real-time prediction A) The average prediction latency of a single time interval of the test EEG signal by each participant B) The statistical distribution of the average prediction latency within the participant group

Although the integration of eSPANNet with NeuCube has increased the processing time, it also has improved the prediction accuracy and interpretability of the neural decoder. The trade-off between the prediction accuracy and prediction latency in BCI is a common problem and optimisation of prediction accuracy without compromising the latency of prediction, and vice versa is a key challenge in BCI. The current implementations of the SNN models only utilise the sequential processing capabilities of an ordinary CPU. Such nature of processing limits the ability of real-time prediction as the spike response of each neuron is obtained sequentially. The implementation of the BI-SNN and eSPANNet models in a parallel processing computational platform will enable simultaneous prediction of spiking activity of all neurons at each time-interval. Both SNN models are based on the brain-inspired computational elements and will be compatible with neuromorphic computational platforms. The induction of an appropriate parallel processing approach, such as multi-threading, multi-core processing with GPU or implementation of the SNN models in a neuromorphic chip (i.e. SpiNNaker or IBM TrueNorth) will eliminate this limitation.

9.3.5 E5.5: BI-SNN performance with respect to training dataset size

The analysis of model performance with respect to the dataset size suggests that the two SNN models can learn using a lesser amount of training data than GLM. Figure 9.5 A and B exemplify the performance of the three machine learning models as a function of the training dataset size. In these two examples, the three models were able to achieve closely similar performance, and the analysis evaluated how quick each method could learn the temporal association from input spike sequences. The performance of predicting Flexor Digitorum muscle activity

is shown in figure 9.5 A. Figure 9.5 B shows the performance of predicting the orientation of the index finger. It was observed that the SNN models produce more strongly correlated output using a relatively smaller amount of training data than GLM. This ability of SNN may be due to the evolving connectionist nature of the SNN, which is also be seen in living nervous systems.

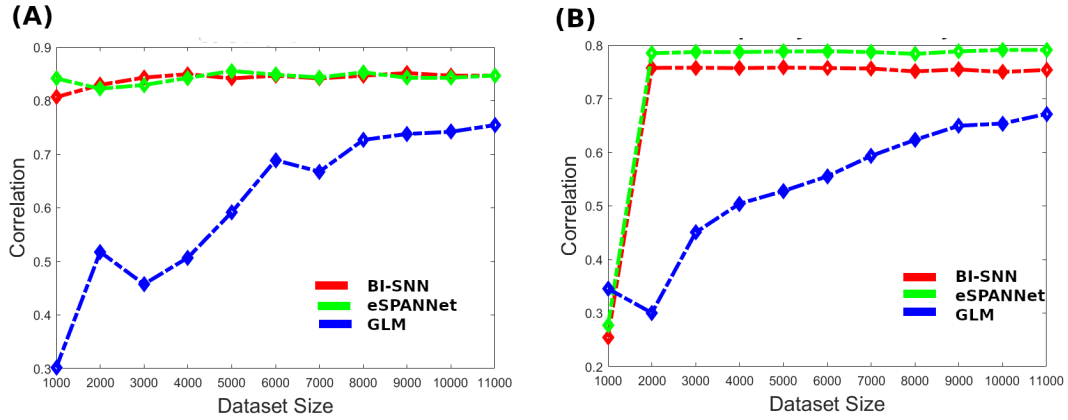

Figure 9.5: The feasibility of BI-SNN to learn from a smaller amount of training dataset A) Cross-correlation between the actual and predicted muscle activity of the Flexor Digitorum muscle activity with respect to the training dataset size B) Cross-correlation between the actual and predicted orientation of the index finger with respect to the training dataset size

9.3.6 E5.6: Interpretability of the BI-SNN as a neural decoder for BCI

The analysis of the connectivity in BI-SNN indicates that each SPAN population in the output layer is connected with brain areas that play a vital role in executing a grasp and lift movement. Figure 9.6 A and B illustrate the connectivity patterns extracted from BI-SNN models of participants 1 and 3, respectively. The connectivity of a single SPAN population in each model is highlighted as an exemplification. Figure 9.6 A shows the connectivity of the $\text{SPAN}_{\text{index-elevation}}$ population that predict the elevation of the index finger with spiking neurons

spatially located in brain regions corresponding to different Brodmann areas. Figure 9.6 B shows the connectivity of the SPAN_{CED}. The thickness of the line is proportional to the number of SPANs connected with the corresponding brain region. The connectivity pattern shows that the $\text{SPAN}_{\text{index-elevation}}$ and SPAN_{CED} are connected with different brain areas that contribute to executing the movement such as visual information processing by the primary and secondary visual cortex, and the inferior temporal gyrus, cognitive control by the anterior prefrontal cortex, spatial cognition and attention by angular gyrus, planning and executing movement by the motor cortex and the processing of somatosensory information by the somatosensory cortex. These visualisations suggest that the BI-SNN model can contribute to a better understanding of brain activity in neurofeedback rather than a 'black box' or less-interpretable model.

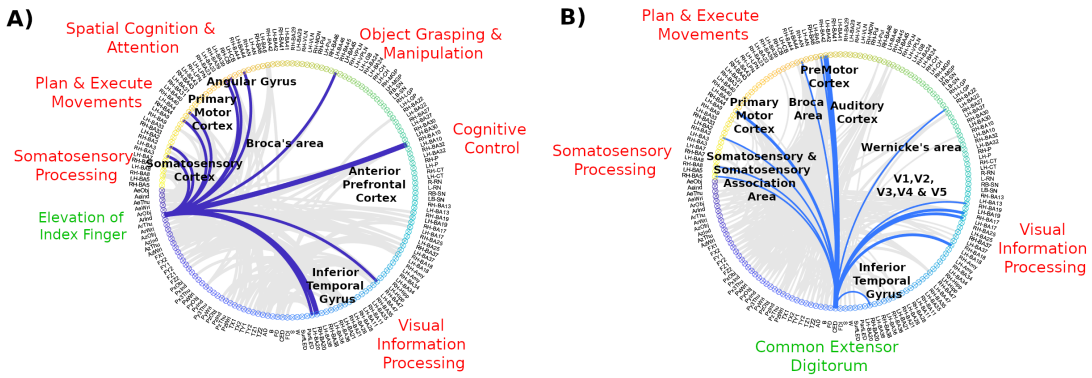

Figure 9.6: Interpretability of the subject-specific BI-SNN models A) The connectivity patterns of the BI-SNN trained using data from participant 1. The connectivity between the $\text{SPAN}_{\text{index-elevation}}$ population vector and the spiking neurons in the 3D NeuCube SNN reservoir corresponds to different brain regions are highlighted as an exemplification B) The connectivity patterns of the BI-SNN trained using data from participant 3. The connectivity between the SPAN_{CED} population vector and the spiking neurons in the 3D SNN reservoir corresponds to different brain regions are highlighted as an exemplification

9.4 Discussion

This paper presents a novel Brain-Inspired Spiking Neural Network model for the incremental learning of spike sequences. The proposed BI-SNN is a generic architecture that can be applied for the predictive modelling of spatio-temporal data. Here the study shows that BI-SNN enhances the decoding of continuous muscle activity and kinematics of upper-limb during grasp and lifting tasks. The comparative cross-correlation analysis suggests that 1) BI-SNN architecture enabled the evolution of polychronising neuron populations associated with different brain areas that contribute to the execution of the task better than the standalone sensor-space eSPANNet architecture, 2) BI-SNN reconstructed continuous muscle activity and kinematics better than the Generalised Linear Model. Further, BI-SNN demonstrated the feasibility of real-time prediction. BI-SNN achieved higher performance in reconstructing muscle activity and kinematics using less training data than GLM. The SNN models demonstrated the feasibility of incremental learning using the principles of evolving Connectionist Systems. BI-SNN is more interpretable for a better understanding of brain activity in neurofeedback than less-interpretable conventional machine learning models that behave as 'black boxes'.

The scope of this study was limited to offline analysis as it is based on a publicly available dataset. Our experiments show that the proposed method allows and supports online processing as it is one of its advantages, but its application for specific tasks would require specific considerations about how this generic method can be efficiently applied. An online analysis of any time-series data generally leaves limited opportunity to understand the model behaviour or evaluate the impact of different model parameters on its performance and to optimise them accordingly. While online prediction is our final goal due to its relevance

in rehabilitation interventions, to achieve that it is necessary to have a good understanding of the model behaviour. Prior knowledge of feature importance, parameters which can significantly affect the model performance, strategies for optimisation, understanding the extent to which the problem can be addressed by the proposed solution (whether it completely address the problem or if it cannot what it can and cannot achieve), the feasibility of real-time prediction, optimal sampling frequency and the interpretability of the model and its predictions are important aspects that need to be understood. This is even more challenging in single-trial event prediction from EEG signals due to the low signal-to-noise ratio and the non-stationarity of EEG. Conducting an offline analysis before the online analysis is helpful to gain a better understanding of the model parameters, their impact on model performance and the optimisation strategies. In addition, the offline analysis also lays the foundation for designing an effective data collection protocol. Therefore, the study presented in this manuscript is an offline analysis that uses a publicly available EEG dataset which is highly relevant to the specific application addressed by this research. Notwithstanding this limitation, the analysis was performed in a pseudo-online experimental setup meaning that the EEG signals were treated as they were streamed into the model for continuous and real-time prediction.

While this study did not fully confirm the possibility of real-time prediction, the average prediction time indicates that at the 100 Hz sampling rate; the SNN models can produce the corresponding output of a single input data point at a lower latency than the delay between two consecutive input data points. As we were not involved in data collection, the authors have limited knowledge about the quality of the recording.

The neural network architecture also has the following limitations. The BI-SNN utilised the Leaky Integrate and Fire (LIF) neuron model because of its

computational efficiency. However, the LIF neuron model does not attempt to model the shape and the biophysical mechanisms of a spike. It considers the generation of spikes as precisely-timed events that carry the information. The LIF model only represents the timing of the spikes but not it's shape. However, in order to accurately decode actions like reaching to grasp which occur within a very short period, the SNN should be able to represent both time and shape of a spiking event. Therefore, it would be more appropriate to use a spiking neuron model which can represent both timing and shape of a spike while keeping the computational efficiency such as the Izhikevich neuron model(Izhikevich, 2003) is more suitable than the Leaky Integrate and Fire neuron model.

The present study adds to the growing body of AI research that indicates the significance of brain-inspired models and has been one of the first attempts to examine the feasibility of finding neural correlates of muscle activity and kinematics non-invasively. The findings of the research influence the following future directions. Further studies may aim to implement the SNN models in neuromorphic processors. BI-SNN as an interpretable neural decoder, future research may investigate the feasibility of transferring the interpreted knowledge to reduce the BCI calibration time. The current study shows the importance of integrated spatial, temporal and spectral analysis of EEG to increase prediction accuracy. The proposed BI-SNN can be extended to process all three EEG bands in a single model which could be pursued in future research. The BI-SNN framework can be extended by integrating the three BI-SNN models that separately process each band-specific data in parallel where the connectivity of the SNN will guide each neuron population to receive spike sequences from a specific EEG frequency band. Future studies of the BI-SNN that utilise EEG data from motor-impaired people will support translating the technology to assistive and rehabilitation applications that improve the quality of life of motor-impaired people.

9.5 Summary of the chapter

This chapter described the integration of these generic methods in the NeuCube SNN framework for developing the proposed Brain-Inspired Brain-Computer Interface system. BI-SNN can map spiking activity from input channels into a high dimensional source-space which enhances the evolution of polychronising spiking neural populations. Here it is applied to predict muscle activity and kinematics from electroencephalography signals during upper limb functional movements. The findings suggest the feasibility of the proposed BI-SNN to construct an interpretable neural decoder that can incrementally learn complex movements from stochastic EEG signals for non-invasive Brain-Computer Interfaces.

9.6 Contributions

- This research presented a Brain-Inspired Spiking Neural Network model that extended the generic NeuCube framework by integrating the proposed spike-based learning algorithms
- The research enhanced the interpretability of the machine learning model by integrating the proposed knowledge representation algorithms with NeuCube
- The study demonstrated the feasibility of real-time movement prediction from EEG signal through the proposed Brain-Inspired Spiking Neural Network
- This research showed the feasibility of constructing a novel Brain-Inspired Brain-Computer Interface and experimentally validated its performance on predicting continuous muscle activity and hand kinematics from EEG signals

9.7 Publications

- **Kumarasinghe, K.**, Kasabov, N., & Taylor, D., Brain-Inspired Spiking Neural Networks for Decoding and Understanding Muscle Activity and Kinematics from Electroencephalography Signals during Hand Movements, Nature Scientific Reports (under review)

Chapter 10

Discussion and Conclusion

> "We will always have STEM with us. Some things will drop out of the public eye and will go away, but there will always be Science, Engineering, and Technology. And there will always, always be Mathematics.'
>
> *Katherine Johnson - one of the NASA's "human computers"*

Chapter overview

The previous five chapters of this thesis presented two generic spike-based methods and integrated them with the generic NeuCube SNN framework; for constructing the proposed Brain-Inspired Spiking Neural Network. The proposed BI-SNN is a promising direction for creating a novel type of a Brain-Inspired Brain-Computer Interface. This thesis presented a series of experiments that experimentally validated the proposed spike-based learning methods. This chapter will present a summary of these studies that supports the validation of the main hypothesis of this research. The chapter will begin by restating the aim and objectives of the research. Thus, a brief discussion on the significant findings, the limitations of each

experimental validation, and the approaches followed to address the limitations will be discussed. Furthermore, the chapter will examine how far the research questions have been answered through the proposed solutions. The implications of the research for the field of Deep Learning, Artificial Neural Networks, and Neurorehabilitation will be suggested, followed by several recommendations for future research.

10.1 Overview of the research

This thesis proposed a novel Brain-Inspired Spiking Neural Network model for incremental learning of spike sequences from stochastic data streams. It aimed at enabling synaptic learning of polychronising spiking neuron populations that produce spike trains that are correlated with the predicted event. The proposed BI-SNN is a generic SNN architecture that can be applied for predictive modelling of Spatio-temporal data streams. Here it was applied to construct an interpretable neural decoder which can incrementally learn spike sequences from non-stationary Electroencephalography signals. The thesis argued that the proposed Spiking Neural Network approach results in a better neural decoder compared to the traditional machine learning approaches that construct neural decoders for restorative BCI in various aspects. The thesis addressed seven research questions.

The research hypothesised that the proposed brain-inspired neural decoder would perform better than traditional neural decoders that use non-brain-inspired machine learning models to decode neural activity from EEG signals. It assumed that the following features of the proposed brain-inspired machine learning model would give rise to a better neural decoder than the traditional machine learning methods.

- The proposed BI-SNN utilises the principles of Evolving Connectionist Systems that feature the evolving, incremental, and theoretically life-long nature of learning. These features of BI-SNN will address the non-stationarity of EEG signals better than the traditional machine learning methods.
- As a source-space model, BI-SNN will address the less spatial resolution of EEG better than the traditional neural decoders
- The proposed knowledge representation framework integrated with the

BI-SNN will enhance the interpretability of the neural decoder

The thesis presented a detailed literature review on recent developments in machine learning methods that decode various human motor tasks from electroencephalography signals which are useful for constructing restorative Brain-Computer Interfaces for motor recovery and restoration. It highlighted the limitations of the current literature and the challenges in analysing EEG signals in the context of restorative BCI. Several future directions were outlined, and suggestions were proposed to improve the machine learning approach utilised to decode neural activity from EEG signals

10.2 Discussion of findings

The literature review emphasised the need for a brain-inspired computational approach to address the limitations in the existing neural decoders. The thesis provided an overview of brain-inspired computing, Spiking Neural Networks, and the NeuCube Spiking Neural Network architecture. The thesis proposed two spike-based generic learning algorithms to construct an interpretable machine learning model that can incrementally learn to predict events from temporal, Spatio-temporal, or spectro-temporal data streams. A series of experiments were conducted to validate the proposed spike-based learning methods.

10.2.1 Evolving Spike Pattern Association Neural Network for spike-based supervised and incremental learning

One of the objectives of the research was to develop a spike-based learning method for incremental learning of spike-sequences from electroencephalography signals for online event prediction. The research addressed the following research question

to achieve this objective.

RQ1: How can Spike Pattern Association Neuron be extended to develop incremental spike sequence learning model for online event prediction from spatio-temporal data streams?

The thesis proposed the evolving Spike Pattern Association Neural Network as a generic method to answer the above research question. The goal of eSPANNet was to utilise the polychronization effect of Spiking Neural Networks for spike sequence learning. The thesis described the design and development of the eSPANNet learning algorithm with relevant source code segments for implementing the proposed model as a software prototype. An initial proof of concept study that evaluated the feasibility of incremental learning and accurate event prediction of the eSPANNet learning model was presented in chapter 5 for answering this research question.

The classification (E1.1) and regression (E1.2) performance of eSPANNet was evaluated using a case study on finger flexion events prediction from Electrocoticography signals. The Electorcoticography exhibits a higher signal to noise ratio than the non-invasive Electroencephalography signals. An invasive signal was used for this preliminary analysis to reduce the impact of the non-stationarity and noise of the input data. E1.1 showed that the eSPANNet resulted in higher accuracy, sensitivity, and F1 score and lower FPR, FNR, and FDR than many other supervised learning methods (refer fig. 5.15 and 5.16). The eSPANNet marginally outperformed Liang and Bougrain (2012)(refer fig. 5.13) and demonstrated the feasibility of incremental learning.

Upon the promising preliminary results of the eSPANNet learning model for predicting finger movements from invasive Electrocoticography signals, the thesis then addressed the following research question to evaluate the performance of

eSPANNet for predicting movements from non-invasive EEG signals.

RQ2: How can the network architecture of the eSPANNet learning model be improved to enhance its convergence and the prediction accuracy when learning from non-stationary stochastic data streams such as Electroencephalography?

The proof of concept of the eSPANNet was limited to invasive ECoG signals which correspond to a higher signal to noise ratio than the non-invasive EEG signals. This limitation was addressed in E2.1 by performing the experimental validation of eSPANNet using non-invasive Electroencephalography signals. The preliminary study presented in E1.1 to E1.3 was limited to data from a single participant, and therefore, the findings could not be generalised to a broader group of people. The experimental validation of eSPANNet presented in E 2.1, 2.2, and 2.3 were performed using data from twelve participants to address this limitation. In the proof of concept, the performance of eSPANNet was compared only with traditional non-Brain-Inspired machine learning methods that were not based on Artificial Neural Networks. Therefore it was difficult to determine how the results support the main hypothesis of the research. This limitation was addressed in the experimental validation of eSPANNet by comparing eSPANNet with both brain-inspired methods such as Convolutional Neural Networks and Recurrent Neural Networks and as well as the non-brain-inspired machine learning methods such as Support Vector Machine, Decision trees, and Linear regression.

Chapter 6 presented a comparative analysis and benchmarked the performance of the eSPANNet learning model for online event prediction from EEG signals. The research question investigated how the network architecture of eSPANNet is to be improved to enhance the convergence and prediction accuracy when learning from stochastic data streams such as EEG. The eSPANNet was compared with

several brain-inspired and as well as the traditional non-brain-inspired machine learning methods. The statistical significance of the obtained results was evaluated using the Student's t-test and ANOVA.

The thesis proposed two network architectures of eSPANNet and analysed the performance of each architecture in predicting movement intentions from EEG signals. The experiment E2.1 compared the performance of single input synapse and multiple input synapse based eSPANNet architectures. The study showed a statistically significant improvement of the average correct rate by the single-input synapse-based eSPANNet than the multi-input synapse-based network architecture. The results empirically showed that the single input synapse based network architecture addressed the stochasticity of EEG signals better than the multiple input synapse based architecture. Table 10.1 summarises these studies that compare the proposed spike-based learning methods with other brain-inspired (ANN-based) and traditional machine learning models.

Table 10.1: A summary of experiments performed

Goal	**Task**	**Dataset**	**Sample size**	**Experiments**	**Performance measure**	**Stat.**	**Comparison**
Proof of concept of eSPANNet	predict finger flexion events from ECoG signals	BCI Competition IV dataset 4	1	E1.1: Evaluate and benchmark classification performance of eSPANNet (section 5.4.1)	Accuracy, sensitivity, Specificity, F1 score, FPR, FNR, FDR	-	SVM, DT, LDA, kNN, AdaBoost, RUSBoost, Bagging and Subspace
				E1.2: Valuate regression performance of eSPANNet (section 5.4.2)	Pearson correlation coefficients	-	Liang et al
				E1.3: Demonstrate the feasibility of incremental learning by eSPANNet (section 5.4.3)	Evolution of true positive rate and error rate	-	
Experimental validation of eSPANNet	Predict movement intention from EEG signals	WAYGAL-EEG	12	E2.1: Compare performance of single input synapse and multiple input synapse based eSPANNet architectures (section 6.5.1)	accuracy	t-test	Single input synapse and multiple input synapse based eSPANNet architectures
				E2.2: Compare performance of eSPANNet with multiple machine learning models that use static input features(section 6.5.2)	accuracy	One-way ANOVA	RNN, SVM
				E2.3: Compare the performance of eSPANNet with multiple sequence learning methods that use dynamic input features (section 6.5.3)	accuracy	One-way ANOVA	CNN, RNN, SVM, Decision tree, linear regression

Continued over page ...

Table 10.1: A summary of experiments performed ... *(continued)*

Goal	**Task**	**Dataset**	**Sample size**	**Experiments**	**Performance measure**	**Stat.**	**Comparison**
Experimental validation of the knowledge representation framework	Extract a set of fuzzy/crisp rules that represent brain activity during grasp and lift tasks from BI-SNN	WAY-GAL-EEG	12	E3: Feasibility of obtaining the topological patterns, and underlying neural trajectories from during grasp and lift movements using the above describe framework (section 7.4.4)	transition probability	-	-
Proof of concept of FaNeuRobot	Evaluate the feasibility of controlling a prosthetic hand through the FaNeuRobot framework	Dataset collected using the Cognionics 32 channel dry EEG headset at KEDRI EEG Lab	1	E4: Evaluate the feasibility of the FaNeuRobot to decode hand movements from EEG signals to construct a BCI and the feasibility of controlling a prosthetic hand through the BCI (section 8.4.2)	accuracy	-	SVM, MLP and LDA
Experimental validation of BI-BCI	Decode continuous muscle activity and joint kinematics of upper limb during grasp and lift movements	WAY-GAL-EEG	12	E5.1: Compare performance of eSPAN-Net and BI-BCI in predicting muscle activity and hand kinematics (section 9.3.1)	cross-correlation	correlation	GLM, eSPAN-Net
				E5.2: Evaluate the performance of approximating the activity of five EMG sensors that monitor the muscle activity of AD, B, FD, CED, and FDI muscles during grasp and lift movements (section 9.3.2)	cross-correlation	correlation	GLM

Continued over page ...

Table 10.1: A summary of experiments performed ... *(continued)*

Goal	**Task**	**Dataset**	**Sample size**	**Experiments**	**Performance measure**	**Stat.**	**Comparison**
				E5.3: Evaluate the performance of predicting kinematics of the object, index finger, thumb and wrist during GAL task (section 9.3.3)	cross-correlation	correlation	GLM
				E5.4: Evaluate and compare the prediction latency of BI-SNN and eSPANNet (section 9.3.4)	cross-correlation	-	eSPANNet
				E5.6: Evaluate the performance of BI-SNN, eSPANNet and GLM respect to the size of the training dataset (section 9.3.5)	cross-correlation	correlation	GLM, eSPANNet
				E5.6: Demonstrate the interpretability of the BI-SNN as a neural decoder for BCI (section 9.3.6)	population size, population connectivity and synaptic weight	-	-

However, the research did not present a theoretical proof on how single input synapse based eSPANNet architecture perform better than the multiple input synapse based eSPANNet architecture. This is a limitation of this research that can be addressed in future research. E2.2 and E2.3 compare the performance of eSPANNet with multiple machine learning models that use static and dynamic input features, respectively. The SVM and RNN models that used the spike rate marginally outperformed the performance of eSPANNet. However, this difference is not statistically significant, while the eSPANNet has some significant advantages, as discussed in section 6.5.2. E2.3 showed that eSPANNet resulted in the highest mean correct rate compared to the RNN, CNN, SVM, DT, and LR that used spike sequences for training the model. eSPANNet showed a statistically significant difference in mean correct rate compared to RNN, SVM, or DT. However, the difference in mean correct rate between eSPANNet and LR or CNN was statistically insignificant (refer fig. 6.6).

10.2.2 Knowledge representation framework for Spiking Neural Networks

The lower interpretability of the machine learning models is a limitation in Artificial Intelligence. eSPANNet also does not facilitate much provision for interpreting the decisions made by the model and the association of the existing neurological findings that can reveal complex brain dynamics with the behaviour of the eSPANNet learning model is challenging. Enhancing the interpretability of the proposed spike-based neural decoder was specifically addressed in studies E3 and E5.6. The proposed knowledge representation framework evaluated the feasibility of the NeuCube SNN architecture to map spiking activity from EEG sensor-space into the structural and functional regions of interest in the brain.

The research addressed the following research question to fulfil these objectives.

RQ3: Based on the abilities of SNN for deep learning, can SNNs be used to construct an interpretable machine learning model that represents deep knowledge as spatio-temporal rules?

This framework could be applied to extract neural trajectories from Brain-Inspired SNN architectures to improve the machine learning model's interpretability and increase the understanding of the information representation in the model as deep Spatio-temporal rules.

The proposed generic methods showed the feasibility of constructing a novel Brain-Inspired Brain-Computer Interface, which can effectively address several limitations of current restorative BCIs. This research extended the generic NeuCube SNN framework by integrating the proposed learning algorithms.

The experiment E3 was performed to determine the feasibility of obtaining the topological patterns, and underlying neural trajectories from BI-SNN during grasp and lift movements. The knowledge representation framework revealed common patterns in dynamic cortical activity of the brain that characterise the Spatio-temporal organisation of the brain's cortex to execute a grasp and lift task. These patterns could be represented as a set of crisp rules comprehensible by humans.

One of the limitations associated with the proposed knowledge representation framework was it required a set of predefined parameters such as the transition probability threshold, the spatial and temporal depth to extract the deep knowledge learned in a BI-SNN. The proposed spike-based supervised learning models were integrated with the BI-SNN to learn Spatio-temporal rules as presented in E4, E5.1 to E5.6 to address this limitation. Another limitation of the proposed framework was the lack of a solid mathematical foundation and appropriate definition of

optimal depth and length of knowledge representation. The development of a mathematical foundation and defining optimal depth and length parameters is proposed as future work of this thesis. The practical applicability of the model was evaluated in principle through E4, followed by a comprehensive analysis presented under E5.

10.2.3 Brain-Inspired Spiking Neural Networks for Brain-Inspired Brain-Computer Interfaces

The research also focused on developing prototype software and conducting proof-of-concept studies to demonstrate the applicability of the proposed learning algorithms in restorative BCI applications through multiple case studies.

The first case study evaluated and benchmarked the performance of the eSPANNet learning model for movement intention prediction from EEG signals. The case study answered the following research question.

RQ4: How does the eSPANNet learning model compare with the static rate-based machine learning methods (such as the Convolutional Neural Networks and Support Vector Machine) and as well as the sequence learning-based methods (such as the Recurrent Neural Networks, linear regression, and SVM-based regression) for predicting movement intention from EEG signals?

The next case study evaluated the feasibility of the generic NeuCube framework to decode movements from EEG signals. The study addressed the following research question.

RQ5: How can the NeuCube SNN architecture be improved in order to enable continuous control of a prosthetic hand from EEG signals?

The proposed FaNeuRobot framework integrated a finite automata with the generic NeuCube framework and showed the feasibility of decoding continuous hand movements from EEG signals. The finite automata represented a simplified behavioural model of muscle synergies that represent how the agonist and antagonist forearm muscle pairs contribute to a hand opening and closing. The NeuCube SNN was trained to decode events that could trigger a state change while the finite automata acted as a finite memory to the Spiking Neural Network. Therefore, the integrated model predicted the current state of the prosthetic hand based on the decoded event and the previous state of the BCI. This approach could increase the inter-class separability of the machine learning problem compared to the traditional approach that did not utilise finite automata.

The feasibility of controlling a prosthetic hand through the FaNeuRobot framework was evaluated principally through a laboratory-based study presented under E4. The dataset was collected using the Cognionics 32 channel dry EEG headset at KEDRI EEG Lab. The experiment E4 evaluated the feasibility of the FaNeuRobot to decode hand movements from EEG signals continuously. FaNeuRobot showed the feasibility of constructing a non-invasive BCI for prosthetic control. Although the study demonstrated accurate control of a prosthetic hand through the proposed SNN-based non-invasive BCI, this preliminary analysis had multiple limitations. The proof of concept of FaNeuRobot was limited to 1D control of a prosthetic hand by a healthy participant. The researcher collected her EEG data for the experiment, and therefore the participant was not naive to the task or the intention of the research.

The following experiments were conducted to address the limitations of this

preliminary analysis. A series of experiments using the proposed Brain-Inspired Spiking Neural Networks was performed to evaluate the performance of predicting the activity of five forearm muscles and the kinematics of four upper-limb joints which generally require the involvement of multiple muscle synergies. These SNN models could represent multiple upper limb muscle synergies that contribute to performing complex upper limb functional movements. Therefore, the experimental validation showed the feasibility of improving the degrees of freedom of the prosthetic hand. E5.1 to 5.6 was performed using a publicly available dataset that contains EEG signals from twelve novice participants. The empirical evaluation of multiple degrees of freedom control through the proposed BI-BCI was mentioned as possible future work of this research.

The following case study experimentally validated and benchmarked the performance of the proposed Brain-Inspired Spiking Neural Network model for decoding and understanding grasp and lift movements from EEG signals. The BI-BCI is based on the Brain-Inspired Spiking Neural Network model that integrates the proposed spike-based generic methods with the NeuCube SNN architecture. It was validated through a series of experiments mentioned from E5.1 to E5.6, which evaluated various features of the proposed BI-BCI. All these experiments were performed using the WAY-GAL-EEG dataset, and the goal was to decode continuous muscle activity and joint kinematics of the upper limb during grasp and lift movements. The case study addressed the following research questions.

RQ6: Does the Brain-Inspired Spiking Neural Network model that integrates the eSPANNet with the NeuCube SNN architecture result in higher prediction accuracy than the pure eSPANNet learning model for predicting continuous movements from EEG signals?

The thesis described integrating the proposed spike-based learning methods with the generic NeuCube SNN framework for developing the proposed Brain-Inspired Brain-Computer Interface system. The experiment E5.1 compared the cross-correlation of predicted muscle activity and hand kinematics by the eSPANNet and BI-BCI models. BI-SNN, as a source-space SNN model, showed the feasibility of finding spiking neuron clusters that are more temporally associated with the EMG activity and hand kinematics compared to the sensor-space eSPANNet model. The BI-SNN permitted the extraction of population activity from different regions of interest in the brain, while the integration of eSPANNet as the output layer of the NeuCube enabled incremental learning of these polychronising spiking neuron populations.

The thesis presented multiple studies that evaluated different aspects of the BI-BCI approach such as - how accurate the prediction is, the latency of the prediction, the training speed to reach an acceptable prediction, and the interpretability of the model. The research answered the following research question in order to achieve the above objective.

RQ7: How do the Brain-Inspired Spiking Neural Networks and the non-Brain-Inspired machine learning models compare in terms of their ability for sequence prediction, interpretability, and incremental learning to predict complex movements from EEG useful for motor recovery and restoration in Brain-Computer Interfaces?

E5.2 evaluated the performance of approximating the activity of five EMG sensors that monitor the muscle activity of AD, B, FD, CED, and FDI muscles during grasp and lift movements and compared with a Generalised Linear Model. The majority of participants showed a 'high' mean correlation using BI-SNN. E5.3 evaluated the performance of approximating the position and orientation of the object, index finger, thumb, and wrist during a GAL task.

E5.3 evaluated and compared the prediction latency of BI-SNN and eSPANNet models. The median prediction time of the twenty-nine behavioural spike sequences by BI-SNN and eSPANNet models correspond to a single time interval is 3.5 ms and 1 ms, respectively. The shorter prediction latencies by the spiking neuron models suggested the feasibility of real-time prediction at a sampling rate of 100Hz. E5.5 evaluated the performance of BI-SNN, eSPANNet, and GLM with respect to the size of the training dataset. It was observed that the SNN models produce a stronger correlated output using a relatively smaller amount of training data than GLM.

E5.6 demonstrated the interpretability of the BI-SNN as a neural decoder for BCI. The analysis of the connectivity in a trained BI-SNN indicated that each SPAN population in the output layer is connected with brain areas that play a vital role in executing a grasp and lift movement. The connectivity pattern showed that the spiking neuron populations of the BI-SNN are connected with different brain areas that contribute to executing the movement such as visual information

processing by the primary and secondary visual cortex, and the inferior temporal gyrus, cognitive control by the anterior prefrontal cortex, spatial cognition and attention by angular gyrus, planning and executing movement by the motor cortex and the processing of somatosensory information by the somatosensory cortex. These visualisations suggested that the BI-SNN model can contribute to a better understanding of brain activity in neurofeedback rather than a 'black box' or less-interpretable model. Table 10.2 summarises the major findings of each experiment that supported the validation of the hypothesis.

Table 10.2: A summary of results

Experiment	**Major findings**
E1.1: Evaluate and benchmark classification performance of eSPANNet (refer sec. 5.4.1)	eSPANNet showed higher in accuracy, sensitivity and f1 score and lower FPR, FNR, and FDR that the other methods (refer fig. 5.15 and 5.16)
E1.2: Evaluate regression performance of eSPANNet (sec. 5.4.2)	eSPANNet marginally outperformed Liang and Bougrain (2012)(refer fig. 5.13)
E1.3: Demonstrate the feasibility of incremental learning by eSPANNet (sec. 5.4.1)	eSPANNet showed the feasibility of incremental learning (refer fig. 5.14)
E2.1: Compare the performance of single input synapse and multiple input synapse based eSPANNet architectures	Statistically significant improvement of the average correct rate by the single-input synapse-based eSPANNet than the multi-input synapse-based network architecture (p=0.001).
E2.2: Compare the performance of eSPANNet with multiple machine learning models that use static input features	SVM and RNN with mean spike rate marginally outperformed the performance of eSPANNet. However, this difference is not statistically significant (p=0.87).
E2.3: Compare the performance of eSPANNet with multiple sequence learning methods that use dynamic input features	eSPANNet resulted in the highest mean correct rate and showed a statistically significant difference in mean correct rate than RNN, SVM or DT. The difference in mean correct rate between eSPANNet and LR or CNN was statistically insignificant (refer fig. 6.6)
E3: Feasibility of obtaining the topological patterns, and underlying neural trajectories during grasp and lift movements using the above describe framework from EEG signals	The knowledge representation framework revealed essential patterns that characterise the dynamics of brain activity during a grasp and lift task.
E4: Evaluate the feasibility of the FaNeuRobot to decode hand movements from EEG signals to construct a BCI and the feasibility of controlling a prosthetic hand through the BCI	FaNeuRobot showed the feasibility of constructing a non-invasive BCI for prosthetic control. The average accuracy of the subject across all sessions was 75%.
E5.1: Compare the performance of eSPANNet and BI-BCI in predicting muscle activity and hand kinematics	The BI-SNN permits the extraction of population activity from different regions of interest in the brain, while the integration of eSPANNet as the output layer of the NeuCube enabled incremental learning of polychronising spiking neuron populations.

Continued over page ...

Table 10.2: A summary of results ... *(continued)*

Experiment	**Major findings**
E5.2: Evaluate the performance of approximating the activity of five EMG sensors that monitor the muscle activity of AD, B, FD, CED, and FDI muscles during grasp and lift movements	Nine out of twelve participants showed a 'high' mean correlation, while the remaining three participants showed a 'moderate' mean correlation using BI-SNN.
E5.3: Evaluate the performance of approximating x,y,z position of the object, index finger, thumb and wrist during GAL task	BI-SNN results in a 'moderate' to 'high' cross-correlation ($0.6 <= r <= 0.7$) in predicting x,y,z Cartesian coordinates. The cross-correlation coefficients show that BI-SNN approach results in a 'moderate' to 'high' cross-correlation ($0.5 <= r <= 0.7$) in predicting elevation, roll and azimuth angles.
E5.4: Evaluate and compare the prediction latency of BI-SNN and eSPANNet	The median prediction time of the twenty-nine behavioural spike sequences by BI-SNN and eSPANNet models corresponding to a single time interval is 3.5 ms and 1 ms, respectively.
E5.6: Evaluate the performance of BI-SNN, eSPANNet and GLM respect to the size of the training dataset	It was observed that the SNN models produce more strongly correlated output using a relatively smaller amount of training data than GLM.
E5.6: Demonstrate the interpretability of the BI-SNN as a neural decoder for BCI	The analysis of the connectivity in BI-SNN indicates that each SPAN population in the output layer is connected with brain areas that play a vital role in executing a grasp and lift movement. The visualisations suggest that the BI-SNN model can contribute to a better understanding of brain activity in neurofeedback rather than a 'black box' or less-interpretable model.

10.2.4 BI-SNN for closed-loop prosthetic control

The human nervous system exhibits bi-directional information flow from the central nervous system to the periphery (feed-forward path) and the periphery to the central nervous system (backward path). Closed-loop BCI systems which consider both directions of information flow exhibits many advantages over conventional uni-directional (open-loop) BCI systems.

The neural decoder needs to consider the data flow in both forward and backwards directions into the model to enable the closed-loop control. Most studies on non-invasive Brain-Computer Interfaces have mainly focused on the feed-forward path and construct open-loop BCI control. They do not have a mechanism to incorporate and represent feedback information directly in the model. The brain-inspired network architecture of BI-SNN can establish closed-loop neuroprosthetic control through BCI in contrast to the traditional open-loop BCIs. The thesis has shown that BI-SNN can accurately predict muscle activity and joint kinematics from EEG signals. This aspect contributes to the feed-forward path of the closed-loop control. At the same time, the model can also utilise information travel from the peripheral to the central nervous system, such as the information from the sensory receptors (vision, sense of touch) and the neural signature of error processing in the brain (Error-related Potentials). These aspects contribute to establishing the feedback information flow of the closed-loop control. Therefore the proposed BI-SNN model shows the feasibility of closed-loop neuroprosthetic control compared to conventional open-loop BCI systems.

Since the EEG mapping of the NeuCube SNN architecture is based on the Talairach brain atlas, which contains the 3D coordinates of both cerebellum and cerebrum, the proposed Brain-Inspired Brain-Computer Interface architecture can represent both cerebrum and cerebellum activity together in the model. Therefore,

the BI-SNN supports the neural decoder to utilise information flow across various brain networks that interconnect the periphery, cerebrum, and cerebellum to predict different human activity.

10.2.5 Translation of BI-BCI from clinical into simple BCI systems

The thesis reports multiple experiments that used EEG data collected using both wet and dry electrodes. The case studies reported in chapter 6, 7 and 9 have used EEG data collected using the actiCAP (*actiCAP*, n.d.) which contains gel-based (Ag/AgCl) active EEG electrodes. The gel electrodes result in a lower noise level compared to dry EEG electrodes. The study presented in chapter 8 has utilised the Cognionics 32 channel dry electrode EEG headset. Dry electrodes are more likely to have a higher noise level than gel electrodes. The lower signal to noise ratio can compromise the prediction accuracy when using a dry electrode EEG headset. However, on the other hand, dry electrodes enhance the BCI's translational aspects, leading to portable home-based personalised BCI intervention protocols. Since the BI-BCI works accurately with EEG data collected using dry electrodes, which is more prone to noise, it is more applicable to the BCI's translational aspects. The BI-SNN have shown the feasibility of accurately decoding neural activity using both types of EEG electrodes.

10.2.6 Robustness of BI-BCI

Numerous factors can affect brain activity which gives rise to the non-stationarity of EEG signals. Different experimental conditions such as the participant's posture and whether the person was gazing or not gazing at their hand can affect EEG. Also, there are other reasons, such as medication, consumption of alcohol or

caffeine, which could change the statistical properties of EEG signals. Studies have shown that medication such as painkillers and antiepileptic drugs (Konishi et al., 1995) can affect brain activity. Some of the effects of drugs are an increase of beta and decrease of alpha brain activity (Banoczi, 2005). Studies have shown that caffeine which contained in ordinary beverages such as tea and coffee, can substantially reduce EEG power(Siepmann & Kirch, 2002). Other physiological factors such as mood, sleep, fatigue, and stress level can change EEG patterns at different BCI sessions. These factors cause the non-stationarity of EEG signals which is a considerable challenge for decoding neural activity for BCI.

The non-stationarity of EEG results in inconsistent subject-to-subject and session-to-session prediction performance either under the same or different experimental conditions. From the machine learning perspective, the neural decoder should be robust to the non-stationarity of EEG, and it is an essential requirement for non-invasive BCI. In addition, the ability to interpret machine learning model leaves an opportunity to perform post hoc analysis when predicting using non-stationary data if an abnormality is observed. The proposed BI-SNN have shown robust prediction performance under different experimental conditions through the case studies reported in the thesis. Also, it can interpret what has already been learnt by the model and the various features which contribute to model predictions in a way comprehensible to human understanding. In addition, the thesis has shown the feasibility of correlating such interpretations with findings of previous neuroscience studies. Therefore the proposed Brain-Inspired Brain-Computer Interface have demonstrated many advantages over the conventional non-brain-inspired machine learning approaches for addressing the non-stationarity of EEG.

10.3 Limitations of the research

The experimental validation of BI-BCI addressed several limitations of the state-of-the-art machine learning models commonly used in restorative Brain-Computer Interfaces. However, the proposed BI-BCI is constrained by the following limitations.

The performance of online event prediction of the BI-BCI was not evaluated as the experiments were performed using a publicly available dataset. Notwithstanding this limitation, the experiments were performed on a pseudo online experimental setup. The online prediction of the proposed BI-BCI was validated principally through this pseudo online experimental setup. Also, the ability to perform online predictions and enabling continuous control of a rehabilitation device was demonstrated principally through experiment E4.

In addition, the researcher (myself) did not contribute to the data collection process and therefore had a limited ability to comment on the data quality. Another limitation of the current analysis is that the experimental validation was limited to healthy participants. Movement prediction using EEG data from motor-impaired people through the proposed BI-BCI was identified as a future work of this research. Several recommendations will be proposed to develop an appropriate experimental protocol based on the observations and findings of the current research. The limitations of each experimental study are summarised in table 10.3.

Table 10.3: A summary of limitations

Goal	**Limitations**	**Approach for addressing the limitations**
Proof of concept of eSPANNet learning model	Used invasive ECoG signals which are less noisy than non-invasive EEG signals	Experimental validation of eSPANNet (E 2.1 - 2.3) was performed using non-invasive EEG signals
	Limited to data from a single participant. Therefore difficult to generalise the findings to a broader group of people	Experimental validation of eSPANNet (E 2.1 - 2.3) was performed using data from twelve participants
	The comparison was not performed on Brain-Inspired ML methods. Therefore it is difficult to determine how the results support the main hypothesis of the research.	Experimental validation of eSPANNet (E 2.1 - 2.3) compared eSPANNet with both brain-inspired (CNN and RNN) and non-brain-inspired (SVM, Decision tree, linear regression) ML methods
Experimental validation of eSPANNet	The study empirically confirms the ability of a single input synapse based network architecture to address the stochasticity of the signal. However, the research does not present a theoretical proof on how single input synapse based eSPANNet architecture perform better than the multiple input synapse based eSPANNet architecture	This limitation is mentioned as a limitation of the current research and proposed to be addressed in future research
	Difficult to interpret results and associate existing neurological findings in the literature with the machine learning model	The interpretability of the BI-SNN is addressed explicitly in studies E3 and E5.6
experimental validation of the knowledge representation framework	The framework only facilitates knowledge extraction using a set of predefined parameters such as the spatial or temporal depth and transition probability. The framework does not automatically learn to extract knowledge from a BI-SNN. The study lacks a suitable mathematical foundation an appropriate definition of optimal depth and length in both space and time for knowledge representation	Spike-based supervised learning models are integrated with the BI-SNN to learn spatio-temporal rules (E4 and E5.1 to E5.6). Development of mathematical foundation and defining optimal depth and length of knowledge representation are proposed as future research, practical applicability of the model was evaluated in principle through experiment 4 followed by a comprehensive analysis presented in experiment 5

Continued over page ...

Table 10.3: A summary of limitations ... *(continued)*

Goal	**Limitations**	**Approach for addressing the limitations**
proof of concept of controlling a prosthetic hand through FaNeuRobot	The current study was limited to 1D control of a prosthetic hand by a healthy participant	A series of experiments using the Brain-Inspired Spiking Neural Networks was performed to evaluate the performance of predicting the activity of multiple muscles, and the kinematics of multiple joints require the involvement of multiple forearm muscle synergies. The experimental validation showed the feasibility of improving the degrees of freedom of the prosthetic hand. The empirical evaluation of multiple degrees of freedom control through the proposed BI-BCI was mentioned as a future work of this research.
Experimental validation, comparative analysis and statistical validation of BI-BCI	The performance of online prediction of the BI-BCI was not evaluated as the experiments were performed using a publicly available dataset. The analysis was limited to healthy participants, The experimenter did not contribute to the data collection and therefore had a limited ability to comment on the data quality	The feasibility of online prediction was demonstrated in principle through the experiment 4. Movement prediction using EEG data from motor-impaired people through the proposed BI-BCI was identified as a future work of this research

10.4 Recommendations for future research

Overall, this study strengthens the idea that BI-SNN is a promising neural decoder for non-invasive BCI. The present study adds to the growing body of AI research that indicates the significance of brain-inspired models and has been one of the first attempts to examine the feasibility of finding neural correlates of muscle activity and kinematics non-invasively. The findings of the research influence the following future directions. Further studies may aim to implement the SNN models in neuromorphic processors. BI-SNN as an interpretable neural decoder, future research may investigate the feasibility of transferring the interpreted knowledge to reduce the BCI calibration time. Further analysis of EEG data from motor-impaired people will support translating the technology to assistive and rehabilitation applications that improve the quality of life of motor-impaired people.

10.5 Conclusion

A growing body of literature on non-invasive Brain-Computer Interfaces for motor recovery and restoration highlights the need for improving the machine learning methods that decode neural activity from EEG signals. These studies point out the low accuracy in decoding movements of the same limb, less biological plausibility, less interpretability, high prediction latency, low degree of freedom as the common significant drawbacks in existing machine learning models used for decoding movements useful for motor recovery and restoration through BCI from EEG. This research evaluated multiple aspects of the BI-SNN, including the accuracy, interpretability, prediction latency, and training speed, which strengthens

the idea that BI-SNN is a promising approach for decoding neural activity in non-invasive Brain-Computer Interfaces. This research has extended the current body of knowledge regarding the machine learning approaches for decoding movements from EEG.

- This thesis has demonstrated that the proposed eSPANNet learning algorithm can incrementally learn complex spike sequences from stochastic data streams. As a generative model, it does not require certain predefined parameters related to network architecture, such as the number of neurons in the hidden layer as it evolves neurons if needed. Its simple network architecture reduces the processing time during training and prediction.

- The thesis has developed a theoretical framework, algorithmic pipeline, and associated software for representing and extracting deep knowledge from Brain-Inspired Spiking Neural Network architectures for enhancing its interpretability.

- The thesis has demonstrated the applicability of the proposed learning algorithm in multiple case studies such as movement intention prediction from EEG, decoding hand movements from EEG, and controlling an upper limb prosthesis through the proposed Brain-Inspired Brain-Computer Interface.

- The thesis has empirically validated that the integration of eSPANNet with the NeuCube SNN architecture, which formed the proposed BI-SNN can gain a higher prediction accuracy than the standalone sensor-space eSPANNet architecture.

- The thesis has benchmarked the performance of the proposed SNN-based learning algorithms and showed that they could gain a statistically significant

improvement in terms of the prediction accuracy compared to several machine learning methods.

- The thesis has shown the feasibility of extracting neural information that contributes to controlling a wide range of motor parameters such as the activity of multiple forearm muscles and joint kinematics from EEG signals using the proposed Brain-Inspired Spiking Neural Network model in healthy people.

In conclusion, the proposed BI-SNN is a potential approach to construct an interpretable neural decoder that can incrementally learn to predict complex movements in real-time from Electroencephalography signals.

10.6 Summary of the chapter

This chapter presented a general discussion and outlook of the studies conducted throughout this thesis. It discussed the significant findings of each study that supported the validation of the main hypothesis of this research. The chapter also discussed the limitations of each study and the strategies employed in this research to address them. The conclusion and recommendations for future research are presented at the end of the chapter.

References

Abbott, L. F. & Nelson, S. B. (2000). Synaptic plasticity: taming the beast. *Nature neuroscience*, *3*(11), 1178–1183.

acticap. (n.d.). Retrieved from https://www.brainproducts.com/productdetails.php?id=4

Action potential. (2013, November). Wikimedia Foundation. Retrieved 02-09-2020, from https://en.wikipedia.org/wiki/File:Blausen_0011_ActionPotential_Nerve.png

Action potential. (2020, March). Wikimedia Foundation. Retrieved 02-09-2020, from https://en.wikipedia.org/wiki/File:Action_potential.svg

Adam Moser, K. R. & York, D. M. (2008). Design and validation of a real-time spiking-neural-network decoder for brain-machine interfaces. *Bone*, *23*(1), 1–7. doi: 10.1038/jid.2014.371

Akatsuka, K., Noguchi, Y., Harada, T., Sadato, N. & Kakigi, R. (2008). Neural codes for somatosensory two-point discrimination in inferior parietal lobule: an fmri study. *Neuroimage*, *40*(2), 852–858.

An, J. (2016). Hand Motion Identification of Grasp-and-Lift task from Electroencephalography Recordings using Recurrent Neural Networks. *2016 International Conference on Big Data and Smart Computing (BigComp)*, 427–429. doi: 10.1109/BIGCOMP.2016.7425963

Ang, K. K. & Guan, C. (2013). Brain-computer interface in stroke rehabilitation.

Ang, K. K. & Guan, C. (2015). Brain–computer interface for neurorehabilitation of upper limb after stroke. *Proceedings of the IEEE*, *103*(6), 944–953.

Ang, K. K. & Guan, C. (2016). Eeg-based strategies to detect motor imagery for control and rehabilitation. *IEEE Transactions on Neural Systems and Rehabilitation Engineering*, *25*(4), 392–401.

Ang, K. K., Guan, C., Chua, K. S. G., Ang, B. T., Kuah, C., Wang, C., ... Zhang, H. (2010). Clinical study of neurorehabilitation in stroke using eeg-based motor imagery brain-computer interface with robotic feedback. In *2010 annual international conference of the ieee engineering in medicine and biology* (pp. 5549–5552).

Anh, N. T. H., Hoang, T. H., Dung, D. T., Thang, V. T. & Bui, T. T. (2016). An Artificial Neural Network approach for electroencephalographic signal classification towards brain-computer interface implementation. *2016 IEEE RIVF International Conference on Computing and Communication*

Technologies: Research, Innovation, and Vision for the Future, RIVF 2016 - Proceedings, 205–210. doi: 10.1109/RIVF.2016.7800295

Anopas, D., Horapong, M. & Wongsawat, Y. (2013). Bci-based neurorehabilitation and prediction system for stroke patients. In *Proceedings of the 7th international convention on rehabilitation engineering and assistive technology* (p. 28).

Arieli, A., Sterkin, A., Grinvald, A. & Aertsen, A. (1996). Dynamics of ongoing activity: explanation of the large variability in evoked cortical responses. *Science*, *273*(5283), 1868.

Artoni, F., Pirondini, E., Panarese, A. & Micera, S. (2016). Exploring neuro-muscular synergies of reaching movements with unified independent component analysis. In *Engineering in medicine and biology society (embc), 2016 ieee 38th annual international conference of the* (pp. 3183–3186).

Azizi, S. A. (2013). "i think therefore i am": New prospects for neural prostheses. *Neuroscience Letters*, *538*, 1–2.

Bai, Z., Fong, K. N., Zhang, J. J., Chan, J. & Ting, K. (2020). Immediate and long-term effects of bci-based rehabilitation of the upper extremity after stroke: a systematic review and meta-analysis. *Journal of neuroengineering and rehabilitation*, *17*, 1–20.

Banoczi, W. R. (2005). How some drugs affect the electroencephalogram (eeg). *American journal of electroneurodiagnostic technology*, *45*(2), 118–129.

Barbosa, A. O. G., Diaz, D. R. A., Vellasco, M. M. B., Meggiolaro, M. A. & Tanscheit, R. (2009). Mental tasks classification for a noninvasive BCI application. *Lecture Notes in Computer Science (including subseries Lecture Notes in Artificial Intelligence and Lecture Notes in Bioinformatics)*, *5769 LNCS*(PART 2), 495–504. doi: 10.1007/978-3-642-04277-5_50

Bashashati, H., Ward, R. K., Bashashati, A. & Mohamed, A. (2017). Neural Network Conditional Random Fields for Self-Paced Brain Computer Interfaces. *2016 15th IEEE International Conference on Machine Learning and Applications (ICMLA)*, 939–943. doi: 10.1109/icmla.2016.0169

Bauer, R. & Gharabaghi, A. (2017). Constraints and adaptation of closed-loop neuroprosthetics for functional restoration. *Frontiers in Neuroscience*, *11*(MAR). (cited By 1) doi: 10.3389/fnins.2017.00111

Bernard, R., Goran, D., Sakai, S., Carr, T., McFarlane, D., Nordell, B., ... Potchen, E. (2002). Cortical activation during rhythmic hand movements performed under three types of control: an fmri study. *Cognitive, Affective, & Behavioral Neuroscience*, *2*(3), 271–281.

Bhagat, N. A., Venkatakrishnan, A., Abibullaev, B., Artz, E. J., Yozbatiran, N., Blank, A. A., ... others (2016). Design and optimization of an eeg-based brain machine interface (bmi) to an upper-limb exoskeleton for stroke survivors. *Frontiers in neuroscience*, *10*, 122.

Bhattacharyya, S., Clerc, M. & Hayashibe, M. (2016). A study on the effect of electrical stimulation during motor imagery learning in brain-computer interfacing. In *2016 ieee international conference on systems, man, and*

cybernetics (smc) (pp. 002840–002845).

Bi, G.-q. & Poo, M.-m. (2001). Synaptic modification by correlated activity: Hebb's postulate revisited. *Annual review of neuroscience*, *24*(1), 139–166.

Biasiucci, A., Chavarriaga, R., Hamner, B., Leeb, R., Pichiorri, F., Fallani, F. D. V., ... Millán, J. d. R. (2011). Combining discriminant and topographic information in bci: preliminary results on stroke patients. In *2011 5th international ieee/embs conference on neural engineering* (pp. 290–293).

Binkofski, F., Buccino, G., Stephan, K., Rizzolatti, G., Seitz, R. & Freund, H.-J. (1999). A parieto-premotor network for object manipulation: Evidence from neuroimaging. *Experimental Brain Research*, *128*(1-2), 210-213. (cited By 217) doi: 10.1007/s002210050838

Bischoff-Grethe, A., Goedert, K. M., Willingham, D. T. & Grafton, S. T. (2004). Neural substrates of response-based sequence learning using fmri. *Journal of Cognitive Neuroscience*, *16*(1), 127-138. Retrieved from https://doi.org/10.1162/089892904322755610 doi: 10.1162/089892904322755610

Bohte, S. M. (2004). The evidence for neural information processing with precise spike-times: A survey. *Natural Computing*, *3*(2), 195–206.

Bohte, S. M., Kok, J. N. & La Poutre, H. (2002). Error-backpropagation in temporally encoded networks of spiking neurons. *Neurocomputing*, *48*(1), 17–37.

Boi, F., Moraitis, T., Feo, V. D., Diotalevi, F., Bartolozzi, C., Indiveri, G. & Vato, A. (2016). A bidirectional brain-machine interface featuring a neuromorphic hardware decoder. *Frontiers in Neuroscience*, *10*(December), 1–15. doi: 10.3389/fnins.2016.00563

Braitenberg, V. & Schüz, A. (2013). *Cortex: statistics and geometry of neuronal connectivity*. Springer Science & Business Media.

Broccard, F. D., Mullen, T., Chi, Y. M., Peterson, D., Iversen, J. R., Arnold, M., ... others (2014). Closed-loop brain–machine–body interfaces for noninvasive rehabilitation of movement disorders. *Annals of biomedical engineering*, *42*(8), 1573–1593.

Brown, S., Martinez, M. J. & Parsons, L. M. (2006). Music and language side by side in the brain: a pet study of the generation of melodies and sentences. *European journal of neuroscience*, *23*(10), 2791–2803.

Brunet, E., Sarfati, Y., Hardy-Baylé, M.-C. & Decety, J. (2000). A pet investigation of the attribution of intentions with a nonverbal task. *Neuroimage*, *11*(2), 157–166.

Bullmore, E. & Sporns, O. (2009). Complex brain networks: graph theoretical analysis of structural and functional systems. *Nature Reviews Neuroscience*, *10*(3), 186.

Bundy, D. T., Wronkiewicz, M., Sharma, M., Moran, D. W., Corbetta, M. & Leuthardt, E. C. (2012). Using ipsilateral motor signals in the unaffected cerebral hemisphere as a signal platform for brain–computer interfaces in

hemiplegic stroke survivors. *Journal of neural engineering*, *9*(3), 036011.

Burle, B., Spieser, L., Roger, C., Casini, L., Hasbroucq, T. & Vidal, F. (2015). Spatial and temporal resolutions of eeg: Is it really black and white? a scalp current density view. *International Journal of Psychophysiology*, *97*(3), 210–220.

Canuet, L., Paúl, N. & Maestú, F. (2015). Neurorehabilitation in stroke: The role of functional connectivity. *Int J Neurorehabilitation*, *2*(172), 2376–0281.

Caselli, R. J. (1993). Ventrolateral and dorsomedial somatosensory association cortex damage produces distinct somesthetic syndromes in humans. *Neurology*, *43*(4), 762–762.

Casey, K. L., Minoshima, S., Morrow, T. J. & Koeppe, R. A. (1996). Comparison of human cerebral activation pattern during cutaneous warmth, heat pain, and deep cold pain. *Journal of neurophysiology*, *76*(1), 571–581.

Cella, M., Bishara, A., Medin, E., Swan, S., Reeder, C. & Wykes, T. (2014). Identifying cognitive remediation change through computational modelling - effects on reinforcement learning in schizophrenia. *Schizophrenia Bulletin*, *40*(6), 1422-1432. (cited By 8) doi: 10.1093/schbul/sbt152

Chadwick, E., Blana, D., Simeral, J., Lambrecht, J., Kim, S.-P., Cornwell, A., ... Kirsch, R. (2011). Continuous neuronal ensemble control of simulated arm reaching by a human with tetraplegia. *Journal of neural engineering*, *8*(3), 034003.

Chakraborty, S., Tomsett, R., Raghavendra, R., Harborne, D., Alzantot, M., Cerutti, F., ... others (2017). Interpretability of deep learning models: a survey of results. In *2017 ieee smartworld, ubiquitous intelligence & computing, advanced & trusted computed, scalable computing & communications, cloud & big data computing, internet of people and smart city innovation (smartworld/scalcom/uic/atc/cbdcom/iop/sci)* (pp. 1–6).

Chan, V., Liu, S.-C. & van Schaik, A. (2007). Aer ear: A matched silicon cochlea pair with address event representation interface. *IEEE Transactions on Circuits and Systems I: Regular Papers*, *54*(1), 48–59.

Chavarriaga, R. & Millán, J. d. R. (2010). Learning from eeg error-related potentials in noninvasive brain-computer interfaces. *IEEE transactions on neural systems and rehabilitation engineering*, *18*(4), 381–388.

Chen, W., Zhu, X.-H., Kato, T., Andersen, P. & Uğurbil, K. (1998). Spatial and temporal differentiation of fmri bold response in primary visual cortex of human brain during sustained visual simulation. *Magnetic resonance in medicine*, *39*(4), 520–527.

Cheng, K., Fujita, H., Kanno, I., Miura, S. & Tanaka, K. (1995). Human cortical regions activated by wide-field visual motion: an h2 (15) o pet study. *Journal of Neurophysiology*, *74*(1), 413–427.

Chou, T.-P., Wang, W.-R. & Chang, T. S. (2015). Low complexity real time bci for stroke rehabilitation. In *2015 ieee international conference on digital signal processing (dsp)* (pp. 809–812).

Chowdhury, A., Raza, H., Meena, Y. K., Dutta, A. & Prasad, G. (2017). Online

covariate shift detection-based adaptive brain–computer interface to trigger hand exoskeleton feedback for neuro-rehabilitation. *IEEE Transactions on Cognitive and Developmental Systems*, *10*(4), 1070–1080.

Cirstea, M. & Levin, M. F. (2000). Compensatory strategies for reaching in stroke. *Brain*, *123*(5), 940–953.

Claeys, K. G., Dupont, P., Cornette, L., Sunaert, S., Van Hecke, P., De Schutter, E. & Orban, G. A. (2004). Color discrimination involves ventral and dorsal stream visual areas. *Cerebral Cortex*, *14*(7), 803–822.

Collins, D. L. (1994). *3d model-based segmentation of individual brain structures from magnetic resonance imaging data* (Unpublished doctoral dissertation). McGill University.

Crozier, S., Sirigu, A., Lehéricy, S., van de Moortele, P.-F., Pillon, B., Grafman, J., ... LeBihan, D. (1999). Distinct prefrontal activations in processing sequence at the sentence and script level: An fmri study. *Neuropsychologia*, *37*(13), 1469–1476.

Cunnington, R., Windischberger, C., Deecke, L. & Moser, E. (2003). The preparation and readiness for voluntary movement: a high-field event-related fmri study of the bereitschafts-bold response. *Neuroimage*, *20*(1), 404–412.

Dagher A, B. H., Owen AM & DJ, B. (1999). Mapping the network for planning: a correlational pet activation study with the tower of london task. *Brain*.

Daly, I., Blanchard, C. & Holmes, N. P. (2018). Cortical excitability correlates with the event-related desynchronization during brain–computer interface control. *Journal of neural engineering*, *15*(2), 026022.

Daly, J. J. & Wolpaw, J. R. (2008). Brain–computer interfaces in neurological rehabilitation. *The Lancet Neurology*, *7*(11), 1032–1043.

Delorme, A. & Makeig, S. (2004). Eeglab: an open source toolbox for analysis of single-trial eeg dynamics including independent component analysis. *Journal of neuroscience methods*, *134*(1), 9–21.

Deng, L. (2018). Artificial intelligence in the rising wave of deep learning: The historical path and future outlook [perspectives]. *IEEE Signal Processing Magazine*, *35*(1), 180–177.

Dervin, J. (1990). Co-planar stereotaxic atlas of the human brain 3-dimensional proportional system: An approach to cerebral imaging 1988talairich j. and tournoux p. rayport mark georg thieme verlag. stuttgart, new york 3 13 711 701 1 price dm 268. pp. 122. illustrations 130. *The Journal of Laryngology & Otology*, *104*(1), 72–72.

De Waele, C., Baudonnière, P., Lepecq, J., Huy, P. T. B. & Vidal, P. (2001). Vestibular projections in the human cortex. *Experimental brain research*, *141*(4), 541–551.

Ding, S., Zhang, N., Xu, X., Guo, L. & Zhang, J. (2015). Deep Extreme Learning Machine and Its Application in EEG Classification. *Mathematical Problems in Engineering*, *2015*. doi: 10.1155/2015/129021

Djamal, Esmeralda Contessa and Suprijanto, Suprijanto and Setiadi, S. J. (2016).

Classification of EEG-based hand grasping imagination using autoregressive and neural networks. *Jurnal Teknologi*, *78*.

Doborjeh, Z. G., Kasabov, N., Doborjeh, M. G. & Sumich, A. (2018). Modelling peri-perceptual brain processes in a deep learning spiking neural network architecture. *Scientific reports*, *8*(1), 8912.

Duan, L., Bao, M., Miao, J., Xu, Y. & Chen, J. (2016). Classification Based on Multilayer Extreme Learning Machine for Motor Imagery Task from EEG Signals. *Procedia Computer Science*, *88*, 176–184. Retrieved from http://dx.doi.org/10.1016/j.procs.2016.07.422 doi: 10.1016/j.procs.2016.07.422

Duan, L., Zhong, H., Miao, J., Yang, Z., Ma, W. & Zhang, X. (2014). A Voting Optimized Strategy Based on ELM for Improving Classification of Motor Imagery BCI Data. *Cognitive Computation*, *6*(3), 477–483. doi: 10.1007/s12559-014-9264-1

Edelman, B. J., Baxter, B. & He, B. (2015). Eeg source imaging enhances the decoding of complex right-hand motor imagery tasks. *IEEE Transactions on Biomedical Engineering*, *63*(1), 4–14.

Edelman, B. J., Baxter, B. & He, B. (2016). Eeg source imaging enhances the decoding of complex right-hand motor imagery tasks. *IEEE Transactions on Biomedical Engineering*, *63*(1), 4–14.

Ethier, C., Gallego, J. & Miller, L. E. (2015). Brain-controlled neuromuscular stimulation to drive neural plasticity and functional recovery. *Current opinion in neurobiology*, *33*, 95–102.

Evans, A. C., Janke, A. L., Collins, D. L. & Baillet, S. (2012). Brain templates and atlases. *Neuroimage*, *62*(2), 911–922.

Farid, M., Rizkalla, N., Fahmy, M., Daoud, M. & El-Ayat, K. (2010). Neural prosthetic asynchronous control using eeg. In *Proceedings of the sixth iasted internationa conference* (Vol. 689, p. 195).

Faugeras, O., Touboul, J. & Cessac, B. (2009). A constructive mean-field analysis of multi population neural networks with random synaptic weights and stochastic inputs. *Frontiers in Computational Neuroscience*, *3*, 1. Retrieved from https://www.frontiersin.org/article/10.3389/neuro.10.001.2009 doi: 10.3389/neuro.10.001.2009

Fincham, J. M., Carter, C. S., Van Veen, V., Stenger, V. A. & Anderson, J. R. (2002). Neural mechanisms of planning: a computational analysis using event-related fmri. *Proceedings of the National Academy of Sciences*, *99*(5), 3346–3351.

Florian, R. V. (2007). Reinforcement learning through modulation of spike-timing-dependent synaptic plasticity. *Neural computation*, *19*(6), 1468–1502.

Formaggio, E., Masiero, S., Bosco, A., Izzi, F., Piccione, F. & Del Felice, A. (2016). Quantitative eeg evaluation during robot-assisted foot movement. *IEEE Transactions on Neural Systems and Rehabilitation Engineering*, *25*(9), 1633–1640.

Forney, E. M. & Anderson, C. W. (2011). Classification of EEG during imagined mental tasks by forecasting with Elman Recurrent Neural Networks. *Proceedings of the International Joint Conference on Neural Networks*(0208958), 2749–2755. doi: 10.1109/IJCNN.2011.6033579

Freeman, C. T. (2014). Electrode array-based electrical stimulation using ilc with restricted input subspace. *Control Engineering Practice*, *23*, 32–43.

Freeman, C. T. (2015). Upper limb electrical stimulation using input-output linearization and iterative learning control. *IEEE Transactions on Control Systems Technology*, *23*(4), 1546–1554.

Freeman, C. T., Rogers, E., Hughes, A. M., Burridge, J. H. & Meadmore, K. L. (2012, Feb). Iterative learning control in health care: Electrical stimulation and robotic-assisted upper-limb stroke rehabilitation. *IEEE Control Systems*, *32*(1), 18-43. doi: 10.1109/MCS.2011.2173261

Froemke, R. C. & Dan, Y. (2002). Spike-timing-dependent synaptic modification induced by natural spike trains. *Nature*, *416*(6879), 433–438.

Frolov, A. A., Mokienko, O., Lyukmanov, R., Biryukova, E., Kotov, S., Turbina, L., ... Bushkova, Y. (2017). Post-stroke rehabilitation training with a motor-imagery-based brain-computer interface (bci)-controlled hand exoskeleton: a randomized controlled multicenter trial. *Frontiers in neuroscience*, *11*, 400.

Furber, S. B. (2016). Brain-inspired computing. *IET Computers & Digital Techniques*, *10*(6), 299–305.

Furber, S. B., Galluppi, F., Temple, S. & Plana, L. A. (2014). The spinnaker project. *Proceedings of the IEEE*, *102*(5), 652-665.

Gandhi, V., Arora, V., Behera, L., Prasad, G., Coyle, D. H. & McGinnity, T. M. (2011). A Recurrent Quantum Neural Network model enhances the EEG signal for an improved Brain-computer interface. *IET Seminar Digest*, *2011*(13611). doi: 10.1049/ic.2011.0028

Gandhi, V., Prasad, G., Coyle, D., Behera, L. & McGinnity, T. M. (2014). Quantum neural network-based EEG filtering for a brain-computer interface. *IEEE Transactions on Neural Networks and Learning Systems*, *25*(2), 278–288. doi: 10.1109/TNNLS.2013.2274436

Gao, L., Wang, J., Li, J. & Zheng, Y. (2013). Design of bci based multi-information system to restore hand motor function for stroke patients. In *2013 ieee international conference on systems, man, and cybernetics* (pp. 4924–4928).

Georgopoulos, A., Kalaska, J., Caminiti, R. & Massey, J. (1982). On the relations between the direction of two-dimensional arm movements and cell discharge in primate motor cortex. *Journal of Neuroscience*, *2*(11), 1527-1537. Retrieved from https://www.scopus.com/inward/record.uri?eid=2-s2.0-0020401276&partnerID=40&md5=ced17579b25bf7877ca0f9a0524ae0f4 (cited By 1195)

Georgopoulos, A., Kettner, R. & Schwartz, A. (1988). Primate motor cortex and free arm movements to visual targets in three-dimensional space. ii. coding

of the direction of movement by a neuronal population. *Journal of Neuroscience*, *8*(8), 2928-2937. Retrieved from https://www.scopus.com/inward/record.uri?eid=2-s2.0-0023789678&partnerID=40&md5=79e72aee0da827ac2269eb08e0ed396e (cited By 522)

Georgopoulos, A. P., Caminiti, R., Kalaska, J. F. & Massey, J. T. (1983). Spatial coding of movement: a hypothesis concerning the coding of movement direction by motor cortical populations. *Experimental Brain Research*, *49*(Suppl. 7), 327–336.

Georgopoulos, A. P., Schwartz, A. B. & Kettner, R. E. (1986). Neuronal population coding of movement direction. *Science*, 1416–1419.

Gerstner, W., Kempter, R., Van Hemmen, J. L. & Wagner, H. (1996). A neuronal learning rule for sub-millisecond temporal coding. *Nature*, *383*(6595), 76–78.

Gerstner, W., Kistler, W. M., Naud, R. & Paninski, L. (2014). *Neuronal dynamics: From single neurons to networks and models of cognition*. Cambridge University Press.

Gerstner, W., Kreiter, A. K., Markram, H. & Herz, A. V. (1997). Neural codes: firing rates and beyond. *Proceedings of the National Academy of Sciences*, *94*(24), 12740–12741.

Gerstner, W. & Naud, R. (2009). How good are neuron models? *Science*, *326*(5951), 379–380. Retrieved from https://science.sciencemag.org/content/326/5951/379 doi: 10.1126/science.1181936

Gerstner, W., Sprekeler, H. & Deco, G. (2012). Theory and simulation in neuroscience. *science*, *338*(6103), 60–65.

Gharabaghi, A. (2016). What turns assistive into restorative brain-machine interfaces? *Frontiers in Neuroscience*, *10*(OCT). (cited By 3) doi: 10.3389/fnins.2016.00456

Goodale, M. A., Króliczak, G. & Westwood, D. A. (2005). Dual routes to action: contributions of the dorsal and ventral streams to adaptive behavior. In *Cortical function: a view from the thalamus* (Vol. 149, p. 269 - 283). Elsevier. Retrieved from http://www.sciencedirect.com/science/article/pii/S0079612305490196 doi: https://doi.org/10.1016/S0079-6123(05)49019-6

Goodfellow, I., Bengio, Y., Courville, A. & Bengio, Y. (2016). *Deep learning* (Vol. 1). MIT press Cambridge.

Goodyear, B. G. & Menon, R. S. (1998). Effect of luminance contrast on bold fmri response in human primary visual areas. *Journal of Neurophysiology*, *79*(4), 2204–2207.

Greig, L. C., Woodworth, M. B., Galazo, M. J., Padmanabhan, H. & Macklis, J. D. (2013). Molecular logic of neocortical projection neuron specification, development and diversity. *Nature Reviews Neuroscience*, *14*(11), 755–769.

Grimm, F., Naros, G. & Gharabaghi, A. (2016). Closed-loop task difficulty

adaptation during virtual reality reach-to-grasp training assisted with an exoskeleton for stroke rehabilitation. *Frontiers in Neuroscience*, *10*(NOV). (cited By 3) doi: 10.3389/fnins.2016.00518

Gutig, R. & Sompolinsky, H. (2006). The tempotron: a neuron that learns spike timing–based decisions. *Nature neuroscience*, *9*(3), 420–428.

Haas, L. F. (2003). Hans berger (1873–1941), richard caton (1842–1926), and electroencephalography. *Journal of Neurology, Neurosurgery & Psychiatry*, *74*(1), 9–9.

Hamedi, M., Salleh, S. H., Noor, A. M. & Mohammad-Rezazadeh, I. (2014). Neural network-based three-class motor imagery classification using time-domain features for BCI applications. *IEEE TENSYMP 2014 - 2014 IEEE Region 10 Symposium*(Mi), 204–207. doi: 10.1109/tenconspring.2014.6863026

Han, C.-H. & Im, C.-H. (2014). Data-driven user feedback: an improved neurofeedback strategy considering individual variability of eeg features. In *The 18th ieee international symposium on consumer electronics (isce 2014)* (pp. 1–2).

Han, C.-H., Kim, Y.-W., Kim, S. H., Nenadic, Z., Im, C.-H. et al. (2019). Electroencephalography-based endogenous brain–computer interface for online communication with a completely locked-in patient. *Journal of neuroengineering and rehabilitation*, *16*(1), 18.

Hashimoto, Y., Ota, T., Mukaino, M., Liu, M. & Ushiba, J. (2014). Functional recovery from chronic writer's cramp by brain-computer interface rehabilitation: a case report. *BMC neuroscience*, *15*(1), 103.

Hawkins, J., Lewis, M., Klukas, M., Purdy, S. & Ahmad, S. (2019). A framework for intelligence and cortical function based on grid cells in the neocortex. *Frontiers in neural circuits*, *12*, 121.

Hebb, D. O. (1949). *The organization of behavior: A neuropsychological approach*. John Wiley & Sons.

Hema C. R., Paulraj M. P., Nagarajan R. Sazali Yaacob, A. H. A. (2009). BRAIN MACHINE INTERFACE: A COMPARISON BETWEEN FUZZY AND NEURAL CLASSIFIERS Hema C. R., Paulraj M. P., Nagarajan R. Sazali Yaacob, A. H. Adom. *Information and Control*, *5*(7), 2009.

Hester, R., Foxe, J. J., Molholm, S., Shpaner, M. & Garavan, H. (2005). Neural mechanisms involved in error processing: a comparison of errors made with and without awareness. *Neuroimage*, *27*(3), 602–608.

Hires, S. A., Gutnisky, D. A., Yu, J., O'Connor, D. H. & Svoboda, K. (2015). Low-noise encoding of active touch by layer 4 in the somatosensory cortex. *Elife*, *4*, e06619.

Hodgkin, A. L. & Huxley, A. F. (1952). A quantitative description of membrane current and its application to conduction and excitation in nerve. *The Journal of physiology*, *117*(4), 500.

Holroyd, C. B., Nieuwenhuis, S., Mars, R. B. & Coles, M. G. (2004). Anterior cingulate cortex, selection for action, and error processing. *Cognitive*

neuroscience of attention, 219–231.

Hong, K., Zhang, L., Li, J. & Li, J. (2010). Multi-modal eeg online visualization and neuro-feedback. In *International symposium on neural networks* (pp. 360–367).

Hortal, E., Márquez-Sánchez, E., Costa, A., Pinuela-Martin, E., Salazar-Varas, R., Pérez-Nombela, S., ... Azorín, J. M. (2015). Starting and finishing gait detection using a bmi for spinal cord injury rehabilitation. In *2015 ieee/rsj international conference on intelligent robots and systems (iros)* (pp. 6184–6189).

Hsu, C.-C., Lee, W.-K., Shyu, K.-K., Chang, H.-H., Yeh, T.-K., Hsu, H.-T., ... Lee, P.-L. (2016). Study of repetitive movements induced oscillatory activities in healthy subjects and chronic stroke patients. *Scientific reports*, *6*, 39046.

Hussain, N., Alt Murphy, M. & Sunnerhagen, K. S. (2018). Upper limb kinematics in stroke and healthy controls using target-to-target task in virtual reality. *Frontiers in neurology*, *9*, 300.

Ibáñez, J., Monge-Pereira, E., Molina-Rueda, F., Serrano, J. I., Del Castillo, M. D., Cuesta-Gómez, A., ... others (2017). Low latency estimation of motor intentions to assist reaching movements along multiple sessions in chronic stroke patients: a feasibility study. *Frontiers in neuroscience*, *11*, 126.

INC, C. (n.d.). *Cognionics hd-72.* end2end-interest mailing list. Retrieved from http://www.cognionics.com/index.php/products/hd-eeg-systems/72-channel-system

Izhikevich, E. M. (2003). Simple model of spiking neurons. *IEEE Transactions on neural networks*, *14*(6), 1569–1572.

Izhikevich, E. M. (2004). Which model to use for cortical spiking neurons? *IEEE transactions on neural networks*, *15*(5), 1063–1070.

Izhikevich, E. M. (2006). Polychronization: computation with spikes. *Neural computation*, *18*(2), 245–282.

Izhikevich, E. M. (2007). Solving the distal reward problem through linkage of stdp and dopamine signaling. *Cerebral cortex*, *17*(10), 2443–2452.

Jagodnik, K., Thomas, P., Van Den Bogert, A., Branicky, M. & Kirsch, R. (2016). Human-like rewards to train a reinforcement learning controller for planar arm movement. *IEEE Transactions on Human-Machine Systems*, *46*(5), 723-733. (cited By 1) doi: 10.1109/THMS.2016.2558630

Jiang, S., Chen, L., Wang, Z., Xu, J., Qi, C., Qi, H., ... Ming, D. (2015). Application of bci-fes system on stroke rehabilitation. In *2015 7th international ieee/embs conference on neural engineering (ner)* (pp. 1112–1115).

Jochumsen, M., Niazi, I. K., Signal, N., Nedergaard, R. W., Holt, K., Haavik, H. & Taylor, D. (2016). Pairing voluntary movement and muscle-located electrical stimulation increases cortical excitability. *Frontiers in Human Neuroscience*, *10*, 482. Retrieved from

https://www.frontiersin.org/article/10.3389/fnhum.2016.00482 doi: 10.3389/fnhum.2016.00482

Jochumsen, M., Niazi, I. K., Taylor, D., Farina, D. & Dremstrup, K. (2015, aug). Detecting and classifying movement-related cortical potentials associated with hand movements in healthy subjects and stroke patients from single-electrode, single-trial EEG. *Journal of Neural Engineering*, *12*(5), 056013. Retrieved from https://doi.org/10.1088%2F1741-2560%2F12%2F5%2F056013 doi: 10.1088/1741-2560/12/5/056013

Johansson, R. & Westling, G. (1988a). Coordinated isometric muscle commands adequately and erroneously programmed for the weight during lifting task with precision grip. *Experimental brain research*, *71*(1), 59–71.

Johansson, R. & Westling, G. (1988b). Programmed and triggered actions to rapid load changes during precision grip. *Experimental brain research*, *71*(1), 72–86.

Kasabov, N. (2012). Evolving spiking neural networks and neurogenetic systems for spatio-and spectro-temporal data modelling and pattern recognition. In *Ieee world congress on computational intelligence* (pp. 234–260). doi: 10.1109/IS.2012.6335110

Kasabov, N. (2013). *Springer handbook of bio-/neuro-informatics*. Springer Science & Business Media.

Kasabov, N. & Benuskova, L. (2004). Computational neurogenetics. *Journal of Computational and Theoretical Nanoscience*, *1*(1), 47–61.

Kasabov, N. & Capecci, E. (2015). Spiking neural network methodology for modelling , classification and understanding of EEG spatio-temporal data measuring cognitive processes. *Information Sciences*, *294*, 565–575. Retrieved from http://dx.doi.org/10.1016/j.ins.2014.06.028 doi: 10.1016/j.ins.2014.06.028

Kasabov, N., Dhoble, K., Nuntalid, N. & Indiveri, G. (2013). Dynamic evolving spiking neural networks for on-line spatio-and spectro-temporal pattern recognition. *Neural Networks*, *41*, 188–201.

Kasabov, N., Scott, N. M., Tu, E., Marks, S., Sengupta, N., Capecci, E., ... others (2016). Evolving spatio-temporal data machines based on the neucube neuromorphic framework: design methodology and selected applications. *Neural Networks*, *78*, 1–14.

Kasabov, N., Zhou, L., Doborjeh, M. G., Doborjeh, Z. G. & Yang, J. (2017). New algorithms for encoding, learning and classification of fmri data in a spiking neural network architecture: A case on modeling and understanding of dynamic cognitive processes. *IEEE Transactions on Cognitive and Developmental Systems*, *9*(4), 293–303.

Kasabov, N. K. (2007). *Evolving connectionist systems: the knowledge engineering approach*. Springer Science & Business Media.

Kasabov, N. K. (2014). Neucube: A spiking neural network architecture for mapping, learning and understanding of spatio-temporal brain data. *Neural*

Networks, *52*, 62–76.

Kasabov, N. K. (2018). *Time-space, spiking neural networks and brain-inspired artificial intelligence*. Springer.

Kasabov, N. K., Hou, Z.-G., Feigin, V. & Chen, Y. (2016, 21 July). *Improved method and system for predicting outcomes based on spatio/spectro-temporal data* (Nos. WO2015/030606 A2, US2016/0210552 A1).

Kasahara, T., Terasaki, K., Ogawa, Y., Ushiba, J., Aramaki, H. & Masakado, Y. (2012). The correlation between motor impairments and event-related desynchronization during motor imagery in als patients. *BMC neuroscience*, *13*(1), 66.

Kasinski, A. & Ponulak, F. (2006). Comparison of supervised learning methods for spike time coding in spiking neural networks. *International Journal of Applied Mathematics and Computer Science*, *16*, 101-113.

Kempter, R., Gerstner, W. & Van Hemmen, J. L. (1999). Hebbian learning and spiking neurons. *Physical Review E*, *59*(4), 4498.

Kettner, R., Schwartz, A. & Georgopoulos, A. (1988). Primate motor cortex and free arm movements to visual targets in three-dimensional space. iii. positional gradients and population coding of movement direction from various movement origins. *Journal of Neuroscience*, *8*(8), 2938-2947. Retrieved from https://www.scopus.com/inward/record.uri?eid=2-s2.0-0023802612&partnerID=40&md5=b4b5b0da7c08339cff4efc6e379d6e3d (cited By 144)

Kim, H.-h. & Jeong, J. (n.d.). Representations of directions in EEG-BMI using Winner-take-all readouts ' Q. *2017 5th International Winter Conference on Brain-Computer Interface (BCI)*, 121–122. doi: 10.1109/IWW-BCI.2017.7858178

Klonowski, W. (2009). Everything you wanted to ask about eeg but were afraid to get the right answer. *Nonlinear Biomedical Physics*, *3*(1), 2.

Konishi, T., Naganuma, Y., Hongou, K., Murakami, M., Yamatani, M. & Okada, T. (1995). Effects of antiepileptic drugs on eeg background activity in children with epilepsy: initial phase of therapy. *Clinical Electroencephalography*, *26*(2), 113–119.

Koprinska, I. (2009). Feature selection for brain-computer interfaces. In *Pacific-asia conference on knowledge discovery and data mining* (pp. 106–117).

Kothe, C. (n.d.). *Lab streaming layer.* Retrieved 2010-09-30, from https://github.com/sccn/labstreaminglayer

Kottaimalai, R., Rajasekaran, M. P., Selvam, V. & Kannapiran, B. (2013). EEG signal classification using principal component analysis with neural network in brain computer interface applications. *2013 IEEE International Conference on Emerging Trends in Computing, Communication and Nanotechnology, ICE-CCN 2013*(Iceccn), 227–231. doi: 10.1109/ICE-CCN.2013.6528498

Kreuz, T. (2011). Measures of spike train synchrony. *Scholarpedia*, *6*(10), 11934.

(revision #190333) doi: 10.4249/scholarpedia.11934

Kübler, A., Dixon, V. & Garavan, H. (2006). Automaticity and reestablishment of executive control—an fmri study. *Journal of cognitive neuroscience*, *18*(8), 1331–1342.

Kumar, S., Sharma, A., Mamun, K. & Tsunoda, T. (2017). A Deep Learning Approach for Motor Imagery EEG Signal Classification. *Proceedings - Asia-Pacific World Congress on Computer Science and Engineering 2016 and Asia-Pacific World Congress on Engineering 2016, APWC on CSE/APWCE 2016*, 34–39. doi: 10.1109/APWC-on-CSE.2016.017

Kumarasinghe, K., Kasabov, N. & Taylor, D. (2020). Deep learning and deep knowledge representation in spiking neural networks for brain-computer interfaces. *Neural Networks*, *121*, 169–185.

Kumarasinghe, K., Owen, M., Taylor, D., Kasabov, N. & Kit, C. (2018). FaNeuRobot : A Framework for Robot and Prosthetics Control using the NeuCube Spiking Neural Network Architecture and Finite Automata Theory. *2018 IEEE International Conference on Robotics and Automation (ICRA)*, 1–8. doi: 10.1109/ICRA.2018.8460197

Kumarasinghe, K., Taylor, D. & Kasabov, N. (2019). espannet: Evolving spike pattern association neural network for spike-based supervised incremental learning and its application for single-trial brain computer interfaces. In *2019 international joint conference on neural networks (ijcnn)* (pp. 1–8).

Lan, T., Erdogmus, D., Black, L. & Van Santen, J. (2010). A comparison of different dimensionality reduction and feature selection methods for single trial erp detection. In *2010 annual international conference of the ieee engineering in medicine and biology* (pp. 6329–6332).

Le, T. H., Pardo, J. V. & Hu, X. (1998). 4 t-fmri study of nonspatial shifting of selective attention: cerebellar and parietal contributions. *Journal of neurophysiology*, *79*(3), 1535–1548.

LeCun, Y., Bengio, Y. & Hinton, G. (2015). Deep learning. *nature*, *521*(7553), 436.

Lee, Y., Kim, J., Lee, S. & Lee, M. (2010). Characteristics of motor imagery based eeg-brain computer interface using combined cue and neuro-feedback. In *2010 annual international conference of the ieee engineering in medicine and biology* (pp. 4238–4241).

Legenstein, R., Pecevski, D. & Maass, W. (2008). A learning theory for reward-modulated spike-timing-dependent plasticity with application to biofeedback. *PLoS Comput Biol*, *4*(10), e1000180.

Lei, X., Wang, L., Kong, W., Peng, Y., Hu, S., Zeng, H., ... Tong, S. (2017). Identification of eeg features in stroke patients based on common spatial pattern and sparse representation classification. In *2017 8th international ieee/embs conference on neural engineering (ner)* (p. 114-117).

Leube, D. T., Erb, M., Grodd, W., Bartels, M. & Kircher, T. T. (2001). Differential activation in parahippocampal and prefrontal cortex during word and face encoding tasks. *Neuroreport*, *12*(12), 2773–2777.

Leuthardt, E. C., Schalk, G., Roland, J., Rouse, A. & Moran, D. W. (2009). Evolution of brain-computer interfaces: going beyond classic motor physiology. *Neurosurgical Focus FOC*, *27*(1), E4. Retrieved from https://thejns.org/focus/view/journals/neurosurg-focus/27/1/article-pE4.xml

Li, M., Liu, Y., Wu, Y., Liu, S., Jia, J. & Zhang, L. (2014). Neurophysiological substrates of stroke patients with motor imagery-based brain-computer interface training. *International Journal of Neuroscience*, *124*(6), 403–415.

Li, M., Zhang, M., Luo, X. & Yang, J. (2016). Combined long short-term memory based network employing wavelet coefficients for MI-EEG recognition. *2016 IEEE International Conference on Mechatronics and Automation, IEEE ICMA 2016*, 1971–1976. doi: 10.1109/ICMA.2016.7558868

Li, N., Daie, K., Svoboda, K. & Druckmann, S. (2016). Robust neuronal dynamics in premotor cortex during motor planning. *Nature*, *532*(7600), 459.

Li, T., Hong, J. & Zhang, J. (2013). Brain – machine interface control of a manipulator using small-world neural network and shared control strategy. (November 2018). doi: 10.1016/j.jneumeth.2013.11.015

Liang, N. & Bougrain, L. (2012). Decoding finger flexion from band-specific ecog signals in humans. *Frontiers in neuroscience*, *6*.

Lisi, G., Rivela, D., Takai, A. & Morimoto, J. (2018). Markov switching model for quick detection of event related desynchronization in eeg. *Frontiers in neuroscience*, *12*, 24.

Liu, J., Cheng, Y. & Zhang, W. (2015). Deep learning EEG response representation for brain computer interface. *Chinese Control Conference, CCC*, *2015-September*, 3518–3523. doi: 10.1109/ChiCC.2015.7260182

Liu, Y.-H., Huang, C.-W. & Hsiao, Y.-T. (2013). Comparsion of methods for a motor imagery-based two-state self-paced brain-computer interface. In *2013 international conference on advanced robotics and intelligent systems* (pp. 174–178).

Liyanage, S. R., Xu, J. X., Guan, C., Ang, K. K., Zhang, C. S. & Lee, T. H. (2009). Classification of self-paced finger movements with EEG signals using neural network and evolutionary approaches. *2009 IEEE International Conference on Control and Automation, ICCA 2009*, 1807–1812. doi: 10.1109/ICCA.2009.5410152

Luciw, M. D., Jarocka, E. & Edin, B. B. (2014a). Multi-channel eeg recordings during 3,936 grasp and lift trials with varying weight and friction. *Scientific data*, *1*, 140047.

Luciw, M. D., Jarocka, E. & Edin, B. B. (2014b). *Multi-channel eeg recordings during 3,936 grasp and lift trials with varying weight and friction.* FigShare. doi: http://dx.doi.org/10.6084/m9.figshare.988376

Maass, W., Natschläger, T. & Markram, H. (2002). Real-time computing without stable states: A new framework for neural computation based on perturbations. *Neural computation*, *14*(11), 2531–2560.

Mahadevappa, M., Shendkar, C., Lenka, P., Biswas, A. & Kumar, R. (2013).

Modelling a bci system to estimate fes stimulation intensity for individual stroke survivors in foot drop cases. *Biomedical Engineering/Biomedizinische Technik*, *58*(SI-1-Track-A).

Mainen, Z. F. & Sejnowski, T. J. (1995). Reliability of spike timing in neocortical neurons. *Science*, *268*(5216), 1503–1506.

Mak, J. N. & Wolpaw, J. R. (2009). Clinical applications of brain-computer interfaces: current state and future prospects. *IEEE reviews in biomedical engineering*, *2*, 187–199.

Mao, Z., Yao, W. X. & Huang, Y. (2017). EEG-based biometric identification with deep learning. *International IEEE/EMBS Conference on Neural Engineering, NER*, 609–612. doi: 10.1109/NER.2017.8008425

Markram, H. (2006). The blue brain project. *Nature Reviews Neuroscience*, *7*(2), 153–160.

Markram, H. (2012). The human brain project. *Scientific American*, *306*(6), 50–55.

Markram, H., Lübke, J., Frotscher, M. & Sakmann, B. (1997). Regulation of synaptic efficacy by coincidence of postsynaptic aps and epsps. *Science*, *275*(5297), 213–215.

Markram, H. & Sakmann, B. (1995). Action potentials propagating back into dendrites trigger changes in efficacy of single-axon synapses between layer v pyramidal neurons. In *Soc. neurosci. abstr* (Vol. 21, p. 2007).

Markram, H. & Tsodyks, M. (1996). Redistribution of synaptic efficacy between neocortical pyramidal neurons. *Nature*, *382*(6594), 807–810.

Marshall, J. C. & Fink, G. R. (2003). Cerebral localization, then and now. *Neuroimage*, *20*, S2—-S7.

Martišius, I., Šidlauskas, K. & Damaševičius, R. (2013). Real-time training of Voted Perceptron for classification of EEG data. *International Journal of Artificial Intelligence*, *10*(13 S), 41–50.

Mashford, Benjamin S and Yepes, A Jimeno and Kiral-Kornek, Isabell and Tang, Jianbin and Harrer, S. (2017). Neural-network-based analysis of EEG data using the neuromorphic TrueNorth chip for brain-machine interfaces. *IBM Journal of Research and Development*, *61*, 7—-1.

Masquelier, T., Guyonneau, R. & Thorpe, S. J. (2009). Competitive stdp-based spike pattern learning. *Neural computation*, *21*(5), 1259–1276.

Mattia, D., Astolfi, L., Toppi, J., Petti, M., Pichiorri, F. & Cincotti, F. (2016). Interfacing brain and computer in neurorehabilitation. In *2016 4th international winter conference on brain-computer interface (bci)* (pp. 1–2).

Meadmore, K. L., Exell, T. A., Hallewell, E., Hughes, A.-M., Freeman, C. T., Kutlu, M., ... Burridge, J. H. (2014). The application of precisely controlled functional electrical stimulation to the shoulder, elbow and wrist for upper limb stroke rehabilitation: a feasibility study. *Journal of neuroengineering and rehabilitation*, *11*(1), 105.

Meister, I. G., Krings, T., Foltys, H., Boroojerdi, B., Müller, M., Töpper, R. & Thron, A. (2004). Playing piano in the mind—an fmri study on music

imagery and performance in pianists. *Cognitive Brain Research*, *19*(3), 219–228.

Merolla, P. A., Arthur, J. V., Alvarez-Icaza, R., Cassidy, A. S., Sawada, J., Akopyan, F., ... Modha, D. S. (2014). A million spiking-neuron integrated circuit with a scalable communication network and interface. *Science*, *345*(6197), 668–673. Retrieved from https://science.sciencemag.org/content/345/6197/668 doi: 10.1126/science.1254642

Miller, K. J. & Schalk, G. (2008). Prediction of finger flexion: 4th brain-computer interface data competition. *BCI Competition IV*, *1*, 1–2.

Milner, T. E., Franklin, D. W., Imamizu, H. & Kawato, M. (2007). Central control of grasp: manipulation of objects with complex and simple dynamics. *Neuroimage*, *36*(2), 388–395.

Mima, T., Ikeda, A., Yazawa, S., Kunieda, T., Nagamine, T., Taki, W. & Shibasaki, H. (1999). Somesthetic function of supplementary motor area during voluntary movements. *Neuroreport*, *10*(9), 1859–1862.

Mognon, A., Jovicich, J., Bruzzone, L. & Buiatti, M. (2011). Adjust: An automatic eeg artifact detector based on the joint use of spatial and temporal features. *Psychophysiology*, *48*(2), 229–240.

Mohemmed, A. & Kasabov, N. (2012). Incremental learning algorithm for spatio-temporal spike pattern classification. In *Neural networks (ijcnn), the 2012 international joint conference on* (pp. 1–6).

Mohemmed, A., Lu, G. & Kasabov, N. (2012). Evaluating span incremental learning for handwritten digit recognition. In *International conference on neural information processing* (pp. 670–677).

Mohemmed, A., Schliebs, S. & Kasabov, N. (2011). Span: A neuron for precise-time spike pattern association. In *Neural information processing* (pp. 718–725).

Mohemmed, A., Schliebs, S., Matsuda, S. & Kasabov, N. (2011). Method for training a spiking neuron to associate input-output spike trains. *Engineering Applications of Neural Networks*, 219–228.

Mohemmed, A., Schliebs, S., Matsuda, S. & Kasabov, N. (2012). Span: Spike pattern association neuron for learning spatio-temporal spike patterns. *International Journal of Neural Systems*, *22*(04), 1250012.

Mohemmed, A., Schliebs, S., Matsuda, S. & Kasabov, N. (2013). Training spiking neural networks to associate spatio-temporal input–output spike patterns. *Neurocomputing*, *107*, 3–10.

Moradi, F., Liu, L., Cheng, K., Waggoner, R. A., Tanaka, K. & Ioannides, A. A. (2003). Consistent and precise localization of brain activity in human primary visual cortex by meg and fmri. *Neuroimage*, *18*(3), 595–609.

Morales-Flores, E., Ramírez-Cortés, J. M., Gómez-Gil, P. & Alarcón-Aquino, V. (2013). Mental tasks temporal classification using an architecture based on ANFIS and recurrent neural networks. *Studies in Computational Intelligence*, *451*, 135–146. doi: 10.1007/978-3-642-33021-6_11

Morrison, A., Diesmann, M. & Gerstner, W. (2008). Phenomenological models of synaptic plasticity based on spike timing. *Biological cybernetics*, *98*(6), 459–478.

Morton, J. B., Bosma, R. & Ansari, D. (2009). Age-related changes in brain activation associated with dimensional shifts of attention: an fmri study. *Neuroimage*, *46*(1), 249–256.

Moubayed, N. A. & Mcgough, A. S. (2017). Enhanced Detection of Movement Onset in EEG through Deep Oversampling. In *International joint conference on neural networks (ijcnn)* (Vol. 44).

Müller, K.-R., Tangermann, M., Dornhege, G., Krauledat, M., Curio, G. & Blankertz, B. (2008). Machine learning for real-time single-trial eeg-analysis: from brain–computer interfacing to mental state monitoring. *Journal of neuroscience methods*, *167*(1), 82–90.

Müller, P., Balligand, C., Seel, T. & Schauer, T. (2017). Iterative learning control and system identification of the antagonistic knee muscle complex during gait using functional electrical stimulation. *IFAC-PapersOnLine*, *50*(1), 8786–8791.

Müller-Putz, G. R., Scherer, R., Pfurtscheller, G. & Rupp, R. (2006). Brain-computer interfaces for control of neuroprostheses: from synchronous to asynchronous mode of operation/brain-computer interfaces zur steuerung von neuroprothesen: von der synchronen zur asynchronen funktionsweise. *Biomedical Engineering/Biomedizinische Technik*, *51*(2), 57–63.

Muñoz, J. E., Chavarriaga, R. & Lopez, D. S. (2014). Application of hybrid bci and exergames for balance rehabilitation after stroke. In *Proceedings of the 11th conference on advances in computer entertainment technology* (pp. 1–4).

Muralidharan, A., Chae, J. & Taylor, D. (2011). Extracting attempted hand movements from eegs in people with complete hand paralysis following stroke. *Frontiers in neuroscience*, *5*, 39.

Nakai, T., Kato, C. & Matsuo, K. (2005). An fmri study to investigate auditory attention: a model of the cocktail party phenomenon. *Magnetic Resonance in Medical Sciences*, *4*(2), 75–82.

Nakayama, K. (1997). Localization of the cortical motor area by functional magnetic resonance imaging with gradient echo and echo-planar methods, using clinical 1.5 tesla mr imaging systems. *Osaka city medical journal*, *43*(1), 29-48. Retrieved from https://www.scopus.com/inward/record.uri?eid=2-s2.0-0031158663&partnerID=40&md5=587964ba4b7bde7c9d526b76b4b41533 (cited By 0)

Nakayama, K., Horita, H. & Hirano, A. (2010). A BCI system based on orthogonalized EEG data and multiple multilayer neural networks in parallel form. *Lecture Notes in Computer Science (including subseries Lecture Notes in Artificial Intelligence and Lecture Notes in Bioinformatics)*, *6352 LNCS*(PART 1), 205–210. doi: 10.1007/978-3-642-15819-3_27

Narejo, S., Pasero, E. & Kulsoom, F. (2016). EEG based eye state classification using deep belief network and stacked autoencoder. *International Journal of Electrical and Computer Engineering*, *6*(6), 3131–3141. doi: 10.11591/ijece.v6i6.12967

Neuromodulation. (2021, Jun). Wikimedia Foundation. Retrieved from https://en.wikipedia.org/wiki/Neuromodulation

Neuron. (2012, October). Wikimedia Foundation. Retrieved 2-09-2020, from https://en.wikipedia.org/wiki/Neuron#/media/File:Smi32neuron.jpg

Nguyen, J. & Duong, H. (2019). Neurosurgery, sensory homunculus. In *Statpearls [internet].* StatPearls Publishing.

Niazi, I. K., Jiang, N., Tiberghien, O., Nielsen, J. F., Dremstrup, K. & Farina, D. (2011). Detection of movement intention from single-trial movement-related cortical potentials. *Journal of neural engineering*, *8*(6), 066009.

Noda, T., Sugimoto, N., Furukawa, J., Sato, M.-a., Hyon, S.-H. & Morimoto, J. (2012). Brain-controlled exoskeleton robot for bmi rehabilitation. In *2012 12th ieee-ras international conference on humanoid robots (humanoids 2012)* (pp. 21–27).

Nuntalid, N., Dhoble, K. & Kasabov, N. (2011). Eeg classification with bsa spike encoding algorithm and evolving probabilistic spiking neural network. In *International conference on neural information processing* (pp. 451–460).

Nurse, E., Mashford, B. S., Yepes, A. J., Kiral-Kornek, I., Harrer, S. & Freestone, D. R. (2016). Decoding EEG and LFP signals using deep learning: heading TrueNorth. In *Proceedings of the acm international conference on computing frontiers* (pp. 259–266).

Ochoa, J. F., Ascencio, J. L. & Suárez, J. C. (2014). Application of advanced neuroimaging in motor rehabilitation. *Biomédica*, *34*(3), 330–339.

Ohgami, Y., Matsuo, K., Uchida, N. & Nakai, T. (2004). An fmri study of tool-use gestures: body part as object and pantomime. *Neuroreport*, *15*(12), 1903–1906.

Ortner, R., Irimia, D., Scharinger, J. & Guger, C. (2012). Brain-computer interfaces for stroke rehabilitation: evaluation of feedback and classification strategies in healthy users. In *2012 4th ieee ras & embs international conference on biomedical robotics and biomechatronics (biorob)* (pp. 219–223).

Osuagwu, B. C., Wallace, L., Fraser, M. H. & Vuckovic, A. (2015). Brain-computer interface and functional electrical stimulation for neurorehabilitation of hand in sub-acute tetraplegic patients-functional and neurological outcomes. In *Neurotechnix* (pp. 15–23).

Overduin, S. A. & Servos, P. (2004). Distributed digit somatotopy in primary somatosensory cortex. *Neuroimage*, *23*(2), 462–472.

Owen, M. W. (2019). *Mana motuhake ringa: The non-invasive neural interface based artificial hand* (Unpublished doctoral dissertation). The University of Waikato.

Özdenizci, O., Yalçın, M., Erdoğan, A., Patoğlu, V., Grosse-Wentrup, M. &

Çetin, M. (2017). Electroencephalographic identifiers of motor adaptation learning. *Journal of Neural Engineering*, *14*(4), 046027.

Park, W., Kang, J.-H., Kwon, G., Kim, L. & Kim, S.-P. (2013). Sample-by-sample detection of movement intention from eeg using a classifier with optimized decision parameters. In *Converging clinical and engineering research on neurorehabilitation* (pp. 653–658). Springer.

Paugam-Moisy, H., Martinez, R. & Bengio, S. (2006). *A supervised learning approach based on stdp and polychronization in spiking neuron networks* (Tech. Rep.). IDIAP.

Paulun, L., Wendt, A. & Kasabov, N. K. (2018). A retinotopic spiking neural network system for accurate recognition of moving objects using neucube and dynamic vision sensors. *Frontiers in Computational Neuroscience*, *12*, 42.

Perrin, X., Chavarriaga, R., Colas, F., Siegwart, R. & Millán, J. d. R. (2010). Brain-coupled interaction for semi-autonomous navigation of an assistive robot. *Robotics and Autonomous Systems*, *58*(12), 1246–1255.

Petro, B., Kasabov, N. & Kiss, R. M. (2020). Selection and optimization of temporal spike encoding methods for spiking neural networks. *IEEE Transactions on Neural Networks and Learning Systems*, *31*(2), 358-370.

Pichiorri, F., Morone, G., Pisotta, I., Secci, M., Cincotti, F., Paolucci, S., ... Mattia, D. (2013). Randomized controlled trial to evaluate a bci-supported task-specific training for hand motor recovery after stroke. In *Converging clinical and engineering research on neurorehabilitation* (pp. 501–505). Springer.

Pirondini, E., Coscia, M., Minguillon, J., Millán, J. d. R., Van De Ville, D. & Micera, S. (2017). Eeg topographies provide subject-specific correlates of motor control. *Scientific reports*, *7*(1), 1–16.

Pistohl, T., Ball, T., Schulze-Bonhage, A., Aertsen, A. & Mehring, C. (2008). Prediction of arm movement trajectories from ecog-recordings in humans. *Journal of neuroscience methods*, *167*(1), 105–114.

Plechawska-Wojcik, M., Wolszczak, P., Cechowicz, R. & Lygas, K. (2016). Construction of neural nets in brain-computer interface for robot arm steering. *Proceedings - 2016 9th International Conference on Human System Interactions, HSI 2016*, 348–354. doi: 10.1109/HSI.2016.7529656

Pochon, J., Levy, R., Fossati, P., Lehericy, S., Poline, J., Pillon, B., ... Dubois, B. (2002). The neural system that bridges reward and cognition in humans: An fmri study. *Proceedings of the National Academy of Sciences of the United States of America*, *99*(8), 5669-5674. (cited By 303) doi: 10.1073/pnas.082111099

Popov, E. & Fomenkov, S. (2016). Classification of hand motions in EEG signals using recurrent neural networks. *2016 2nd International Conference on Industrial Engineering, Applications and Manufacturing, ICIEAM 2016 - Proceedings*, 1–4. doi: 10.1109/ICIEAM.2016.7911620

Prathibha, R., Swetha, L. & Shobha, K. (2017). Brain computer interface:

Design and development of a smart robotic gripper for a prosthesis environment. In *2017 international conference on networks & advances in computational technologies (netact)* (pp. 278–283).

Ranganath, C., Johnson, M. & D'Esposito, M. (2003). Prefrontal activity associated with working memory and episodic long-term memory. *Neuropsychologia*, *41*(3), 378-389. (cited By 278) doi: 10.1016/S0028-3932(02)00169-0

Rao, R. P. & Sejnowski, T. J. (2001). Spike-timing-dependent hebbian plasticity as temporal difference learning. *Neural computation*, *13*(10), 2221–2237.

Reardon, S. (2016). Faster higher stronger: the cybathlon is a cyborg olympics that will help disabled people to navigate the most difficult course of all: the everyday world. *Nature*, *536*(7614), 20–23.

Reed, C. L., Klatzky, R. L. & Halgren, E. (2005). What vs. where in touch: an fmri study. *Neuroimage*, *25*(3), 718–726.

Reimann, M. W., Nolte, M., Scolamiero, M., Turner, K., Perin, R., Chindemi, G., ... Markram, H. (2017). Cliques of neurons bound into cavities provide a missing link between structure and function. *Frontiers in computational neuroscience*, *11*, 48.

Remsik, A., Young, B., Vermilyea, R., Kiekhoefer, L., Abrams, J., Evander Elmore, S., ... others (2016). A review of the progression and future implications of brain-computer interface therapies for restoration of distal upper extremity motor function after stroke. *Expert review of medical devices*, *13*(5), 445–454.

Ren, Y. & Wu, Y. (2014). Convolutional deep belief networks for feature extraction of EEG signal. *Proceedings of the International Joint Conference on Neural Networks*, 2850–2853. doi: 10.1109/IJCNN.2014.6889383

Ribeiro, M. T., Singh, S. & Guestrin, C. (2016). " why should i trust you?" explaining the predictions of any classifier. In *Proceedings of the 22nd acm sigkdd international conference on knowledge discovery and data mining* (pp. 1135–1144).

Richter, H. O., Costello, P., Sponheim, S. R., Lee, J. T. & Pardo, J. V. (2004). Functional neuroanatomy of the human near/far response to blur cues: eye-lens accommodation/vergence to point targets varying in depth. *European Journal of Neuroscience*, *20*(10), 2722–2732.

Roberts, P. D. (1999). Computational consequences of temporally asymmetric learning rules: I. differential hebbian learning. *Journal of computational neuroscience*, *7*(3), 235–246.

Roland, P. (1984). Organization of motor control by the normal human brain. *Human neurobiology*, *2*(4), 205–216.

Rossiter, H. E., Boudrias, M.-H. & Ward, N. S. (2014). Do movement-related beta oscillations change after stroke? *Journal of neurophysiology*, *112*(9), 2053–2058.

Rossum, M. v. (2001). A novel spike distance. *Neural computation*, *13*(4), 751–763.

Roy, K., Jaiswal, A. & Panda, P. (2019). Towards spike-based machine intelligence with neuromorphic computing. *Nature*, *575*(7784), 607–617.

Roy, R., Konar, A., Tibarewala, D. N. & Janarthanan, R. (2012). EEG driven model predictive position control of an artificial limb using neural net. *2012 3rd International Conference on Computing, Communication and Networking Technologies, ICCCNT 2012*(July), 1–9. doi: 10.1109/ICCCNT.2012.6395913

Rutkove, S. B. (2007). Introduction to volume conduction. In *The clinical neurophysiology primer* (pp. 43–53). Springer.

Sakhavi, S., Guan, C. & Yan, S. (2015). Parallel convolutional-linear neural network for motor imagery classification. *2015 23rd European Signal Processing Conference, EUSIPCO 2015*, 2736–2740. doi: 10.1109/EUSIPCO.2015.7362882

Sampson, P., Freeman, C., Coote, S., Demain, S., Feys, P., Meadmore, K. & Hughes, A.-M. (2016). Using functional electrical stimulation mediated by iterative learning control and robotics to improve arm movement for people with multiple sclerosis. *IEEE Transactions on Neural Systems and Rehabilitation Engineering*, *24*(2), 235–248.

Sanchez, J. C., Gunduz, A., Carney, P. R. & Principe, J. C. (2008). Extraction and localization of mesoscopic motor control signals for human ecog neuroprosthetics. *Journal of neuroscience methods*, *167*(1), 63–81.

Sánchez-Cossío, G. I., Alonso-Valerdi, L. M., de Jesús Soto-Ortiz, R. & Ramírez-Mendoza, R. A. (n.d.). Practical and meaningful feedback method for training users of motor imagery based brain-computer interfaces.

Savic, A., Lontis, R., Malesevic, N., Popovic, M., Jiang, N., Dremstrup, K., ... Mrachacz-Kersting, N. (2014). Feasibility of an asynchronous event related desynchronization based brain switch for control of functional electrical stimulation. In *Dgbmt jahrestagung, bmt* (Vol. 59).

Savić, A. M., Malešević, N. B. & Popović, M. B. (2013). Motor imagery driven bci with cue-based selection of fes induced grasps. In *Converging clinical and engineering research on neurorehabilitation* (pp. 513–516). Springer.

Schalk, G., Kubanek, J., Miller, K., Anderson, N., Leuthardt, E., Ojemann, J., ... Wolpaw, J. (2007). Decoding two-dimensional movement trajectories using electrocorticographic signals in humans. *Journal of neural engineering*, *4*(3), 264.

Scherer, R., Faller, J., Balderas, D., Friedrich, E. V., Pröll, M., Allison, B. & Müller-Putz, G. (2013). Brain-computer interfacing: More than the sum of its parts. *Soft Computing*, *17*(2), 317–331. doi: 10.1007/s00500-012-0895-4

Schrauwen, B., D'Haene, M., Verstraeten, D. & Van Campenhout, J. (2007). Compact hardware for real-time speech recognition using a liquid state machine. In *2007 international joint conference on neural networks* (pp. 1097–1102).

Schrauwen, B. & Van Campenhout, J. (2003). Bsa, a fast and accurate spike train encoding scheme. In *Proceedings of the international joint conference*

on neural networks, 2003. (Vol. 4, p. 2825-2830 vol.4).

Schrauwen, B. & Van Campenhout, J. (2003). Bsa, a fast and accurate spike train encoding scheme. In *Proceedings of the international joint conference on neural networks* (Vol. 4, pp. 2825–2830).

Schreiber, S., Fellous, J.-M., Whitmer, D., Tiesinga, P. & Sejnowski, T. J. (2003). A new correlation-based measure of spike timing reliability. *Neurocomputing*, *52*, 925–931.

Schubotz, R. I. & von Cramon, D. (2002). A blueprint for target motion: fmri reveals perceived sequential complexity to modulate premotor cortex. *NeuroImage*, *16*(4), 920 - 935. Retrieved from http://www.sciencedirect.com/science/article/pii/S1053811902911833 doi: https://doi.org/10.1006/nimg.2002.1183

Schwartz, A., Kettner, R. & Georgopoulos, A. (1988). Primate motor cortex and free arm movements to visual targets in three-dimensional space. i. relations between single cell discharge and direction of movement. *Journal of Neuroscience*, *8*(8), 2913-2927. (cited By 330)

Scott, S. H. (2004). Optimal feedback control and the neural basis of volitional motor control. *Nature reviews. Neuroscience*, *5*(7), 532.

Sengupta, N. (2018). *Neuromorphic computational models for machine learning and pattern recognition from multi-modal time-series data* (Unpublished doctoral dissertation). Auckland University of Technology. (http://hdl.handle.net/10292/11646)

Sengupta, N. & Kasabov, N. (2017). Spike-time encoding as a data compression technique for pattern recognition of temporal data. *Information Sciences*, *406*, 133–145.

Siepmann, M. & Kirch, W. (2002). Effects of caffeine on topographic quantitative eeg. *Neuropsychobiology*, *45*(3), 161–166.

Sironi, V. A. (2011, aug). Origin and evolution of deep brain stimulation. *Frontiers in integrative neuroscience*, *5*, 42. Retrieved from https://pubmed.ncbi.nlm.nih.gov/21887135https://www.ncbi.nlm.nih.gov/pmc/articles/PMC3157831/ doi: 10.3389/fnint.2011.00042

Sjöström, J. & Gerstner, W. (2010). *Spike-timing dependent plasticity. scholarpedia 5, 1362.*

Skomrock, N. D., Schwemmer, M. A., Ting, J. E., Trivedi, H. R., Sharma, G., Bockbrader, M. A. & Friedenberg, D. A. (2018). A characterization of brain-computer interface performance trade-offs using support vector machines and deep neural networks to decode movement intent. *Frontiers in neuroscience*, *12*, 763.

Slotnick, S. D. & Schacter, D. L. (2006). The nature of memory related activity in early visual areas. *Neuropsychologia*, *44*(14), 2874–2886.

Smith, A. T., Cotillon-Williams, N. M. & Williams, A. L. (2006). Attentional modulation in the human visual cortex: the time-course of the bold response and its implications. *Neuroimage*, *29*(1), 328–334.

Soekadar, S. R., Birbaumer, N., Slutzky, M. W. & Cohen, L. G. (2015).

Brain–machine interfaces in neurorehabilitation of stroke. *Neurobiology of disease*, *83*, 172–179.

Software. (n.d.). Retrieved from https://neuroimage.usc.edu/brainstorm/Introduction

Soltic, S. & Kasabov, N. (2010). Knowledge extraction from evolving spiking neural networks with rank order population coding. *International Journal of Neural Systems*, *20*(06), 437–445.

Sorbello, R., Tramonte, S., Giardina, M. E., La Bella, V., Spataro, R., Allison, B., ... Chella, A. (2017). A human–humanoid interaction through the use of bci for locked-in als patients using neuro-biological feedback fusion. *IEEE Transactions on Neural Systems and Rehabilitation Engineering*, *26*(2), 487–497.

Spm - statistical parametric mapping. (n.d.). Retrieved from https://www.fil.ion.ucl.ac.uk/spm/

staff, S. X. (2018, Jul). *Why are neuron axons long and spindly? study shows they're optimizing signaling efficiency.* Medical Xpress. Retrieved 02-09-2020, from https://medicalxpress.com/news/2018-07-neuron-axons-spindly-theyre-optimizing.html

Stroke Foundation NZ. (n.d.). *Facts about stroke in New Zealand.* Retrieved from https://www.stroke.org.nz/facts-and-faqs

Sun, H., Xiang, Y. & Yang, M. (2011). Neurological rehabilitation of stroke patientsviamotor imaginary-based brain-computer interface technology. *Neural Regeneration Research*, *6*(28), 2198–2202.

Suri, R. E. & Schultz, W. (2001). Temporal difference model reproduces anticipatory neural activity. *Neural computation*, *13*(4), 841–862.

Tabar, Yousef Rezaei and Halici, U. (2016). A novel deep learning approach for classification of EEG motor imagery signals. *Journal of neural engineering*, *14*.

Talairach daemon. (n.d.). Retrieved from http://www.talairach.org/daemon.html

Tan, H. G., Shee, C. Y., Kong, K. H., Guan, C. & Ang, W. T. (2011). Eeg controlled neuromuscular electrical stimulation of the upper limb for stroke patients. *Frontiers of Mechanical Engineering*, *6*(1), 71–81.

Tan, P., Sa, W. & Yu, L. (2016). Applying Extreme Learning Machine to classification of EEG BCI. *6th Annual IEEE International Conference on Cyber Technology in Automation, Control and Intelligent Systems, IEEE-CYBER 2016*, 228–232. doi: 10.1109/CYBER.2016.7574827

Tavella, M., Leeb, R., Rupp, R. & Millán, J. d. R. (2010). Towards natural non-invasive hand neuroprostheses for daily living. In *2010 annual international conference of the ieee engineering in medicine and biology* (pp. 126–129).

Tayeb, Z., Ercelik, E. & Conradt, J. (2017). Decoding of motor imagery movements from EEG signals using SpiNNaker neuromorphic hardware. *International IEEE/EMBS Conference on Neural Engineering, NER*,

263–266. doi: 10.1109/NER.2017.8008341

Taylor, D., Niazi, I., Signal, N., Jochumsen, M., Demstrup, K. & Farina, D. (2015). A brain computer interface (bci) intervention to increase corticomotor excitability in the lower limb in people with stroke. *Physiotherapy*, *101*, e1495.

Taylor, D., Scott, N., Kasabov, N., Capecci, E., Tu, E., Saywell, N., ... Hou, Z.-G. (2014). Feasibility of neucube snn architecture for detecting motor execution and motor intention for use in bciapplications. In *Neural networks (ijcnn), 2014 international joint conference on* (pp. 3221–3225).

Tessadori, J., Bisio, M., Martinoia, S. & Chiappalone, M. (2012). Modular neuronal assemblies embodied in a closed-loop environment: toward future integration of brains and machines. *Frontiers in neural circuits*, *6*.

The Internet Stroke Center. (n.d.). *Stroke Statistics.* Retrieved from http://www.strokecenter.org/patients/about-stroke/stroke-statistics/

Thorpe, S. & Gautrais, J. (1998). Rank order coding. In *Computational neuroscience* (pp. 113–118). Springer.

Trofimov, A., Skrugin, V. & Rodriguez, A. H. (2012). Extraction and recognition of electroencephalogram dynamic patterns for brain-computer interfaces. In *2012 xxxviii conferencia latinoamericana en informatica (clei)* (pp. 1–9).

Tu, E., Kasabov, N. & Yang, J. (2017). Mapping temporal variables into the neucube for improved pattern recognition, predictive modeling, and understanding of stream data. *IEEE transactions on neural networks and learning systems*, *28*(6), 1305–1317.

Tudor, M., Tudor, L. & Tudor, K. I. (2005). *Hans Berger (1873-1941)–the history of electroencephalography.*

Tulving, E., Kapur, S., Markowitsch, H. J., Craik, F., Habib, R. & Houle, S. (1994). Neuroanatomical correlates of retrieval in episodic memory: auditory sentence recognition. *Proceedings of the National Academy of Sciences*, *91*(6), 2012–2015.

Tung, S. W., Guan, C., Ang, K. K., Phua, K. S., Wang, C., Kuah, C. W. K., ... Chew, E. (2015). A measurement of motor recovery for motor imagery-based bci using eeg coherence analysis. In *2015 10th international conference on information, communications and signal processing (icics)* (pp. 1–5).

Turnip, A., Hong, K. S. & Ge, S. S. (2010). Backpropagation neural networks training for single trial EEG classification. *Proceedings of the 29th Chinese Control Conference, CCC'10*, 2462–2467.

Upadhyay, J., Silver, A., Knaus, T. A., Lindgren, K. A., Ducros, M., Kim, D.-S. & Tager-Flusberg, H. (2008). Effective and structural connectivity in the human auditory cortex. *Journal of Neuroscience*, *28*(13), 3341–3349.

Upadhyay, R., Kankar, P. K., Padhy, P. K. & Gupta, V. K. (2013). Feature extraction and classification of imagined motor movement electroencephalogram signals. *International Journal of Biomedical Engineering and Technology*, *13*(2), 133–146.

van den Broek, S. P., Reinders, F., Donderwinkel, M. & Peters, M. (1998). Volume conduction effects in eeg and meg. *Electroencephalography and clinical neurophysiology*, *106*(6), 522–534.

van Polanen, V. & Davare, M. (2015). Interactions between dorsal and ventral streams for controlling skilled grasp. *Neuropsychologia*, *79*, 186–191.

Vargic, R., Chlebo, M. & Kacur, J. (2015). Human computer interaction using bci based on sensorimotor rhythm. In *2015 ieee 19th international conference on intelligent engineering systems (ines)* (pp. 91–95).

Vasilaki, E., Frémaux, N., Urbanczik, R., Senn, W. & Gerstner, W. (2009, 12). Spike-based reinforcement learning in continuous state and action space: When policy gradient methods fail. *PLOS Computational Biology*, *5*(12), 1-17. Retrieved from https://doi.org/10.1371/journal.pcbi.1000586 doi: 10.1371/journal.pcbi.1000586

Verplaetse, T., Sanfilippo, F., Rutle, A., Osen, O. & Bye, R. T. (2016). On usage of eeg brain control for rehabilitation of stroke patients. In *30th european conference on modelling and simulation, regensburg germany, may 31st–june 3rd, 2016.*

Verstraeten, D., Schrauwen, B., Stroobandt, D. & Van Campenhout, J. (2005). Isolated word recognition with the liquid state machine: a case study. *Information Processing Letters*, *95*(6), 521–528.

Victor, J. D. & Purpura, K. P. (1996). Nature and precision of temporal coding in visual cortex: a metric-space analysis. *Journal of neurophysiology*, *76*(2), 1310–1326.

Vidal, J. J. (1973). Toward direct brain-computer communication. *Annual review of Biophysics and Bioengineering*, *2*(1), 157–180.

Waberski, T. D., Gobbelé, R., Lamberty, K., Buchner, H., Marshall, J. C. & Fink, G. R. (2008). Timing of visuo-spatial information processing: electrical source imaging related to line bisection judgements. *Neuropsychologia*, *46*(5), 1201–1210.

Wairagkar, M., Zoulias, I., Oguntosin, V., Hayashi, Y. & Nasuto, S. (2016). Movement intention based brain computer interface for virtual reality and soft robotics rehabilitation using novel autocorrelation analysis of eeg. In *2016 6th ieee international conference on biomedical robotics and biomechatronics (biorob)* (pp. 685–685).

Wang, Z., Miller, K. J., Schalk, G. et al. (2011). Prior knowledge improves decoding of finger flexion from electrocorticographic signals. *Frontiers in Neuroscience*, *5*, 127.

Wei, L., Yue, H., Jiang, X., Xi, C. & Xiaojun, W. (2009). The assessment of eeg in patients with spinal cord injury to movements. In *2009 third international symposium on intelligent information technology application workshops* (pp. 74–77).

Westlake, K. P. & Nagarajan, S. S. (2011). Functional connectivity in relation to motor performance and recovery after stroke. *Frontiers in systems neuroscience*, *5*.

Westling, G. & Johansson, R. (1984). Factors influencing the force control during precision grip. *Experimental brain research*, *53*(2), 277–284.

WHO. (2017). *WHO methods and data sources for global burden of disease estimates 2000-2015* (Tech. Rep. No. WHO/HIS/IER/GHE/2017.1). Department of Information, Evidence and Research WHO, Geneva: World Health Organization - Global Health Estimates Technical Paper.

Wildetudor & Francois. (2014, Aug). *Converting 10-20 system locations to (average) mni template coordinates.* Retrieved from https://neuroimage.usc.edu/forums/t/converting-10-20-system-locations-to-average-mni-template-coordinates/1352

Wright, J., Macefield, V. G., van Schaik, A. & Tapson, J. C. (2016). A review of control strategies in closed-loop neuroprosthetic systems. *Frontiers in Neuroscience*, *10*, 312. Retrieved from https://www.frontiersin.org/article/10.3389/fnins.2016.00312 doi: 10.3389/fnins.2016.00312

Wysoski, S. G., Benuskova, L. & Kasabov, N. (2010). Evolving spiking neural networks for audiovisual information processing. *Neural Networks*, *23*(7), 819–835.

Xiao, Z. G., Elnady, A. M., Webb, J. & Menon, C. (2014). Towards a brain computer interface driven exoskeleton for upper extremity rehabilitation. In *5th ieee ras/embs international conference on biomedical robotics and biomechatronics* (pp. 432–437).

Xie, X. & Seung, H. S. (2004). Learning in neural networks by reinforcement of irregular spiking. *Physical Review E*, *69*(4), 041909.

Xu, R., Jiang, N., Mrachacz-Kersting, N., Dremstrup, K. & Farina, D. (2016). Factors of influence on the performance of a short-latency non-invasive brain switch: Evidence in healthy individuals and implication for motor function rehabilitation. *Frontiers in neuroscience*, *9*, 527.

Xu, R., Jiang, N., Mrachacz-Kersting, N., Lin, C., Prieto, G. A., Moreno, J. C., ... Farina, D. (2014). A closed-loop brain–computer interface triggering an active ankle–foot orthosis for inducing cortical neural plasticity. *IEEE Transactions on Biomedical Engineering*, *61*(7), 2092–2101.

Yilmaz, O., Oladazimi, M., Cho, W., Brasil, F., Curado, M., Cossio, E. G., ... Ramos-Murguialday, A. (2013). Movement related cortical potentials change after eeg-bmi rehabilitation in chronic stroke. In *2013 6th international ieee/embs conference on neural engineering (ner)* (pp. 73–76).

Ying, S. H., Newman, G. I., Choi, Y.-S., Kim, H.-N., Presacco, A., Kothare, M. V. & Thakor, N. V. (2011). Cerebellar ataxia patients are able to use motor imagery to modulate mu-band power in a pilot study of eeg-based brain-computer interface control. In *2011 5th international ieee/embs conference on neural engineering* (pp. 192–195).

Yoo, S.-S., Paralkar, G. & Panych, L. P. (2004). Neural substrates associated with the concurrent performance of dual working memory tasks. *International Journal of Neuroscience*, *114*(6), 613–631.

Yoshimura, N., DaSalla, C. S., Hanakawa, T., Sato, M.-a. & Koike, Y. (2012). Reconstruction of flexor and extensor muscle activities from electroencephalography cortical currents. *Neuroimage*, *59*(2), 1324–1337.

Yoshimura, N., Tsuda, H., Kawase, T., Kambara, H. & Koike, Y. (2017). Decoding finger movement in humans using synergy of eeg cortical current signals. *Scientific Reports*, *7*(1), 11382.

Yoshioka, M., Zhu, C., Yoshikawa, Y., Nishikawa, T., Shimazu, S., Imamura, K., ... Yan, Y. (2011). Construction of real-time bmi control system based on motor imagery. In *2011 ieee international conference on robotics and biomimetics* (pp. 198–203).

Zhang, J., Leung, H.-C. & Johnson, M. (2003). Frontal activations associated with accessing and evaluating information in working memory: An fmri study. *NeuroImage*, *20*(3), 1531-1539. (cited By 103) doi: 10.1016/j.neuroimage.2003.07.016

Zhang, Y., Liu, B., Ji, X. & Huang, D. (2017). Classification of eeg signals based on autoregressive model and wavelet packet decomposition. *Neural Processing Letters*, *45*(2), 365–378.

Zhang, Y., Prasad, S., Kilicarslan, A. & Contreras-Vidal, J. L. (2017). Multiple kernel based region importance learning for neural classification of gait states from eeg signals. *Frontiers in neuroscience*, *11*, 170.

Zhao, X., Chu, Y., Han, J. & Zhang, Z. (2016). Ssvep-based brain–computer interface controlled functional electrical stimulation system for upper extremity rehabilitation. *IEEE Transactions on Systems, Man, and Cybernetics: Systems*, *46*(7), 947–956.

Appendix A

Source Code

A.1 Segments of source code used for implementing the eSPANNet learning model presented in Chapter 5

A.1.1 Matlab source code for obtaining the membrane potential of a Leaky Integrate and Fire neuron

```
%% function lif_model
%   INPUT(S) :
%       time_vector: time intervals of the spike train
%       synaptic_current: pre-synaptic input current
%       membrane_time_constant: time constant that characterises the timing
%       of this exponential decay of membrane potential
%   OUTPUT(S):
%       output_spike: output spike sequence of the LIF
%       membrane_potential: membrane potential of the LIF
%       membrane_potential_for_visualize: membrane potential of the LIF
%       marked with spiking events
%   REFERENCE:
%       http://neuroscience.ucdavis.edu/goldman/Tutorials_files/Integrate%26Fire.pdf
%       with some modifications to replace the loops by vectors to speed-up the calculations
%   AUTHOR: Kaushalya Kumarasinghe
%   DATE  : 10/09/2020
%%

```

```
function [output_spike, membrane_potential, membrane_potential_for_visualize] = lif_model(
    time_vector, synaptic_current, membrane_time_constant)

    %Define parameters
    dt = 1; %time step [ms]
    t_end = size(time_vector,2)-1; %total time of run [ms]
    n_neurons = size(synaptic_current,1);
    E_L = repmat(-70, n_neurons, 1); %resting membrane potential [mV]
    V_th = repmat(100, n_neurons, 1); %spike threshold [mV]
    V_reset = -75; %value to reset voltage to after a spike [mV]
    V_spike = 1000; %value to draw a spike to, when cell spikes [mV]
    R_m_val = 0.001;
    R_m = repmat(R_m_val, n_neurons, 1); %membrane resistance [MOhm]
    tau = repmat(membrane_time_constant, n_neurons, 1); %membrane time constant [ms]

    %DEFINE INITIAL VALUES AND VECTORS TO HOLD RESULTS
    V_vect = zeros(n_neurons,length(time_vector)); %initialize the voltage vector
    I_e_vect = synaptic_current./1000;
    % plot(I_e_vect)

    V_plot_vect = zeros(n_neurons,length(time_vector)); %pretty version of V_vect to be
        plotted, that displays a spike
    i = 1; % index denoting which element of V is being assigned
    V_vect(:,i)= E_L; %first element of V, i.e. value of V at t=0
    V_plot_vect(:, i) = V_vect(:, i); %if no spike, then just plot the actual voltage V

    output_spike = zeros(n_neurons, size(time_vector,2));

    for t=dt:dt:t_end %loop through values of t in steps of dt ms
        firing_neurons = zeros(n_neurons, 1);
        V_inf = E_L + I_e_vect(:, i).*R_m; %value that V_vect is exponentially
        %decaying towards at this time step
        %next line does the integration update rule
        V_vect(:, i+1) = V_inf + (V_vect(:, i) - V_inf).*(exp(-dt./tau));

        % find the indexes of neurons reaching the threshold
        firing_neurons(V_vect(:, i+1) > V_th) = 1;
        % set membrane potential of firing neurons to its resting potential
        current_potentials = V_vect(:, i+1);
        current_potentials(firing_neurons==1) = V_reset;
        V_vect(:, i+1) = current_potentials;

        % membrane potential with spike for plotting
        current_potentials_plot = V_plot_vect(:, i+1);
        current_potentials_plot(firing_neurons==1) = V_spike;
        current_potentials_plot(firing_neurons==0) = current_potentials(firing_neurons==0);
        V_plot_vect(:, i+1) = current_potentials_plot;
        output_spike(:, i+1) = firing_neurons;

        i = i + 1; %add 1 to index, corresponding to moving forward 1 time step
    end

    membrane_potential_for_visualize = V_plot_vect;
    membrane_potential = V_vect;
```

```
71
72 end
```

A.1.2 Matlab source code for spike convolution using the α-kernel

```
1  %% function alpha_kernel
2  %  INPUT(S) :
3  %       * time_vector1: time intervals of the spike sequence
4  %       * tf_vector: firing time of the spike train
5  %       * time_constant: time constant that characterises the timing of the
6  %       exponential decay of a convoluted spike
7  %  OUTPUT(S):
8  %       * conv_all_spikes: convoluted spike sequence
9  %
10 %  AUTHOR: Kaushalya Kumarasinghe
11 %  DATE  : 10/09/2020
12 %%
13 function conv_all_spikes = alpha_kernel(time_vector1, tf_vector, time_constant)
14     % number of spiking events in the current input spike train
15     n_spikes = size(tf_vector,2);
16     % number of time intervals of the input spike train
17     n_time_points = size(time_vector1, 2);
18
19     time_vector1_for_all_spikes = repmat(time_vector1, n_spikes, 1);
20     % firing time of spike sequence
21     tf_vector_for_all_spikes = repmat(tf_vector', 1, n_time_points);
22
23     % compute t - t_f
24     t_tf_for_all_spikes = time_vector1_for_all_spikes - tf_vector_for_all_spikes;
25     exp_p1_vector = repmat(exp(1), size(time_vector1_for_all_spikes));
26     time_constant_vector = repmat(time_constant^(-1), size(time_vector1_for_all_spikes));
27     % compute e^-(t-tf)/time_constant
28     exp_p2_vector = exp_p1_vector.^(-(t_tf_for_all_spikes./time_constant));
29     % apply heaviside step function
30     heaviside_vector = heaviside(t_tf_for_all_spikes);
31
32     % compute spike convolution
33     conv_per_tf = exp_p1_vector'.*time_constant_vector'.*t_tf_for_all_spikes'.*exp_p2_vector
           '.*heaviside_vector';
34
35     % combine each convoluted individual spike sequence into a single
36     % convoluted spike sequence
37     conv_all_spikes = sum(conv_per_tf, 2)';
38
39     % plot convoluted spike sequence
40     plot(conv_all_spikes')
41
42 end
```

A.1.3 Matlab source code for calculating the SPAN synaptic weight update

```
%% span_multiple_desired_spikes
%   INPUT(S):
%       * input_spike_time: timing of the input spike events
%       * expected_spike_time: timing of the expected spike events
%       * actual_spike_time: timing of the actual spike events
%       * error: Difference between expected and actual spike time
%       * membrane_time_constant: time constant that characterises the timing
%       of the exponential decay of membrane potential
%       * learning_rate: Learning rate of SPAN
%   OUTPUT(S): weight_change = calculated synaptic weight update as per the
%   SPAN learning rule
%   AUTHOR: Kaushalya Kumarasinghe
%   DATE  : 10/09/2020
%%

function weight_change = span_multiple_desired_spikes(input_spike_time, expected_spike_time,
     actual_spike_time, error, membrane_time_constant, learning_rate)
    % number of spikes in input, desired and actual spike sequences
    n_g = size(expected_spike_time, 2);
    n_f = size(input_spike_time, 2);
    n_h = size(actual_spike_time, 2);

    % compute [t_(input,f) - t_(desired,g)] where f and g are indeces of
    % input and desired spikes
    rep_input_for_desired = repmat(input_spike_time', n_g,1);
    rep_desired_for_input = repmat(expected_spike_time, n_f,1);
    input_desired_vector = horzcat(rep_input_for_desired, rep_desired_for_input);

    % compute [t_(input,f) - t_(out,h)] where f and h are indeces of
    % input and actual spikes
    rep_input_for_actual = repmat(input_spike_time, n_h,1);
    rep_input_for_actual_reshaped = reshape(rep_input_for_actual, size(rep_input_for_actual
         ,1)*size(rep_input_for_actual,2),1);
    rep_actual_for_input = repmat(actual_spike_time', n_f,1);
    input_actual_vector = horzcat(rep_input_for_actual_reshaped, rep_actual_for_input);

    % define parameters
    td = input_desired_vector(:,2);
    ti_desired = input_desired_vector(:,1);
    lr = learning_rate;
    tau = membrane_time_constant;
    tau_desired_vector = repmat(tau, size(ti_desired,1), 1);

    % compute synaptic weight of the current iteration
    if(~isempty(input_actual_vector))
        ta = input_actual_vector(:,2);
        ti_actual = input_actual_vector(:,1);
        tau_actual_vector = repmat(tau, size(ti_actual,1), 1);
        sum_ta_ti = sum((abs(ta-ti_actual)+tau_actual_vector).*(exp(-abs(ta-ti_actual)./
             tau_actual_vector)), 1);
```

```
48      else
49          sum_ta_ti = 0;
50      end
51      sum_td_ti = sum((abs(td-ti_desired)+tau_desired_vector).*(exp(-abs(td-ti_desired)./
            tau_desired_vector)), 1);
52
53      % compute synaptic weight update
54      weight_change = (lr*(exp(1)/membrane_time_constant)^2)*(sum_td_ti-sum_ta_ti);
55  end
```

A.1.4 Matlab source code for eSPANNet incremental learning

```
fprintf('Train SPAN Population Vector on NeuCube Spike States \n');
if(current_timebin > span_parameters.length_per_sample_ds && current_timebin < dataset.
    training_time_length-span_parameters.length_per_sample_ds)
    % get input spike segment
    ch_data = spike_state_all(:,current_timebin-span_parameters.length_per_sample_ds+1:
        current_timebin);

    % detect if there are any target event
    if(mean(sample_events_per_timebin_all(current_timebin-wait_duration, 1:end))>0)
        event_channel_id = (sample_events_per_timebin_all(current_timebin-wait_duration, :)
            ~=0);
        ch_labels = 1:size(event_channel_id,2);
        event_channel_id = ch_labels(1,event_channel_id==1);
        n_current_events = size(event_channel_id,2);

        isCorrectResponseFromCurrentPopulation = false;
        current_readout_neurons_of_event = [];

        % for the current event (any) onset, get the response of the current population
            vector
        % find the corresponding populations of current event
        if(~isempty(readout_population))
            current_readout_event_ids = readout_population(3,:);
            current_anatomical_cluster_ids = readout_population(2,:);
            current_readout_weights = readout_population(1,:);
            current_readout_ids = readout_population(4,:);

            % find neurons in the current population vector that
            % are trained to emit spikes
            if(ismember(event_channel_id, current_readout_event_ids))
                % for each current event
                for e_id = 1:size(event_channel_id, 2)
                    % update the relavent population vector
                    current_readout_neurons_of_event = horzcat(
                        current_readout_neurons_of_event, readout_population(:,
                        current_readout_event_ids==event_channel_id(e_id)));
                end
            end

            % if there are no trained neurons for the current event using current anatomical
                cluster in
            % the readout population
            if(isempty(current_readout_neurons_of_event))
                isCorrectResponseFromCurrentPopulation = false;
            else
                % get the response of this neuron population for the current spike sequence
                    neuron ids
                ids_of_trained_readouts = current_readout_neurons_of_event(4,:);
```

```
41                  readout_population(5,(readout_population(4,ids_of_trained_readouts))) =
                        readout_population(5,(readout_population(4,ids_of_trained_readouts))) +
                        ones(size(readout_population(5,(readout_population(4,
                        ids_of_trained_readouts)))));% recording the number of times the neurons
                        is exposed to similar events
42                  channel_ids_of_trained_neurons = current_readout_neurons_of_event(2,:);
43                  sample_ch_for_all_spans = ch_data(channel_ids_of_trained_neurons, :);
44                  [state_value, error_vector, class_label, neuron_vote, n_active_votes,
                        n_rest_votes, n_spikes, post_synaptic_spike_pattern_readout,
                        span_response] = get_actual_spike_time_with_readout(
                        sample_ch_for_all_spans', n_channels, span_parameters.interval,
                        span_parameters.time_constant, current_readout_neurons_of_event(1,:),
                        span_parameters.expected_spike_time);
45
46                  % compute the error
47                  [span_id, spike_time_of_span] = find(span_response==1);
48                  if(size(span_id,1)>1)
49                      span_spiketime_map = unique([span_id spike_time_of_span], 'rows');
50                  else
51                      span_spiketime_map = unique([span_id' spike_time_of_span'], 'rows');
52                  end
53
54                  if(~isempty(span_spiketime_map))
55                      [~, time_of_first_spike_idx] = unique(span_spiketime_map(:, 1), 'rows');
56                      time_of_first_spike = span_spiketime_map(time_of_first_spike_idx, 2);
57                      expected_spike_time_rep = repmat(span_parameters.expected_spike_time,
                            size(time_of_first_spike, 1), 1);
58                      current_span_readout_error = abs(time_of_first_spike-
                            expected_spike_time_rep);
59                      n_correct_predictions = find(current_span_readout_error<=span_parameters.
                            max_error);
60                      neuron_ids = current_readout_neurons_of_event(4, span_spiketime_map(
                            time_of_first_spike_idx, 1)');
61                      readout_population(6,neuron_ids) = readout_population(6,neuron_ids) +
                            ones(size(readout_population(6,neuron_ids)));
62                      if(n_correct_predictions>0)
63                          % correct responses from current readout population
64                          fprintf('*** %5.0f current SPAN population can produce precise spike
                                response for the evnet \n', point)
65                          isCorrectResponseFromCurrentPopulation = true;
66                      else
67                          % otherwise set isCorrectResponseFromCurrentPopulation to false, to
                                train a new SPAN
68                          fprintf('---%5.0f current SPAN population can not produce precise
                                spike response for the evnet. Training a new SPAN. \n', point)
69                          isCorrectResponseFromCurrentPopulation = false;
70                      end
71                  end
72              end
73          else
74              isCorrectResponseFromCurrentPopulation = false;
75          end
76
```

```
77          % if 1) there are no neurons in the corresponding population vector or 2)there is no
                accurate response from the existing population
78          % vector train a new SPAN and assign to the corresponding
79          % population vector
80          if(isCorrectResponseFromCurrentPopulation == false)
81              % train new spans for each channel
82              n_channels_all = size(ch_data,1);
83              for ch_id = 1:n_channels_all
84                  sample_ch = ch_data(ch_id, :);
85                  if(sum(sample_ch)~=0)
86                      % class label of the current sample
87                      population_vector_id = event_channel_id;
88                      n_channels = 1;
89                      initial_input_synaptic_weights = repmat(0.001, n_channels, 1);
90                      [trained_weight_vector, error, membrane_potential_for_visualize_history]
                            = get_span_connection_weights(sample_ch', n_channels,
                            initial_input_synaptic_weights, span_parameters.time_vector,
                            span_parameters.interval, span_parameters.time_constant,
                            span_parameters.n_time_points, span_parameters.n_epochs,
                            span_parameters.expected_spike_time, span_parameters.learning_rate,
                            span_parameters.max_error, population_vector_id);
91
92                      % if the trained SPAN can produce spike closer to
93                      % the desired time
94                      if(error<=span_parameters.max_error)
95                          % add the trained SPAN to the current population
96                          % readout population rows: raw 1 - synaptic weight, raw 2 -
                                anatomical cluster id, 3 - event id, 4 - number of validations
                                using future events, 5 - number of correct predictions for the
                                futre events
97                          readout_population = horzcat(readout_population, horzcat(repmat(
                                trained_weight_vector, n_current_events, 1), repmat(ch_id,
                                n_current_events, 1), population_vector_id', [neuron_id:1:(
                                neuron_id+n_current_events)-1]', zeros(n_current_events, 1),
                                zeros( n_current_events, 1))');
98                          neuron_id = neuron_id+n_current_events;
99                      end
100                 end
101             end
102         end
103     end
104 end
```

A.1.5 Matlab source code for network validation

```
%% function network_validation
% AUTHOR: Kaushalya Kumarasinghe
% DATE  : 10/09/2020
%
% description of the variables -
%   readout_population(6, :) = number of correct predictions for the future events
%   readout_population(6, :) = number of total events
%%
responsiveness_of_neurons_weighted = (readout_population(6, :)./readout_population(5, :));
readout_population = vertcat(readout_population, responsiveness_of_neurons_weighted);
readout_population_sorted = sortrows(readout_population', [3 7], 'descend')';

acc_threshold = 0.85;
n_neurons_threshold = 0.75;
selected_readout_population_all = [];
for trained_population_id=1:size(sample_events,2)
    % select neuron of the current population
    current_population = readout_population_sorted(:, readout_population_sorted(3,:)==
        trained_population_id);
    max_current_population_acc = max(current_population(7, :));
    max_current_population_n_neurons = max(current_population(5, :));
    % define the acc cut off limit using acc threshold and
    % max acc of the population
    acc_cutoff = max_current_population_acc*acc_threshold;
    n_neurons_cutoff = max_current_population_n_neurons*n_neurons_threshold;
    if(acc_cutoff>0)
        % select population
        selected_current_population = current_population(:, (current_population(7, :)>
            acc_cutoff)&(current_population(5, :)>n_neurons_cutoff));
        selected_readout_population_all = horzcat(selected_readout_population_all,
            selected_current_population);
    end
end

% validated population vector
espannet.population_vector = selected_readout_population_all;
```

A.1.6 Matlab source code for eSPANNet spike response prediction and determination of class labels

```
%% Function test_espannet
%   AUTHOR: Kaushalya Kumarasinghe
%   DATE  : 10/09/2020
%%
% extract current window of the input data stream
span_spike_sample = SPAN_activity_all(end-span_parameters.n_time_points+1:end, :);
% get the spike respnse of each SPAN in the validated eSPANNet model
[state_value, error_vector, class_label, neuron_vote, n_active_votes, n_rest_votes, n_spikes,
      post_synaptic_spike_pattern_readout, span_response] = get_actual_spike_time_with_readout
     (span_spike_sample, n_channels, span_parameters.interval, span_parameters.time_constant,
     SPAN_population_vector_connection_weights, span_parameters.expected_spike_time);
% get spike count at the duration of expected spike time +- max_error
span_response_at_expected_duration = sum(span_response(:, span_parameters.expected_spike_time
     -span_parameters.max_error:span_parameters.expected_spike_time+span_parameters.max_error)
     ,2);
% if there is any spiking activity, set span response at expected spike time 1
span_response_at_expected_duration(span_response_at_expected_duration~=0) = 1;

% record predicted output sequence
if(is_first_prediction==true)
    espannet_output = vertcat(espannet_output, zeros(size(readout_expected_events, 1)-1, size
         (readout_expected_events,2)), span_response_at_expected_duration');
    is_first_prediction = false;
else
    espannet_output = vertcat(espannet_output, span_response_at_expected_duration');
end
```

A.2 Segments of source code used for the experimental validation of the eSPANNet learning model presented in Chapter 6

Matlab source code of the Convolutional Neural Network for movement intention prediction used in the comparative analysis

```
%% Load dataset
% https://au.mathworks.com/help/deeplearning/ug/create-simple-deep-learning-network-for-classification.html
% Load spike raster plots for training
datasetPath_train = fullfile('data','image', strcat('s',num2str(subject_id)), 'train');
train_data = imageDatastore(datasetPath_train,...
    'IncludeSubfolders',true,'LabelSource','foldernames');
% Load spike raster plots for testing
datasetPath_test = fullfile('data','image', strcat('s',num2str(subject_id)), 'test');
test_data = imageDatastore(datasetPath_test,...
    'IncludeSubfolders',true,'LabelSource','foldernames');
XTrain = train_data;
YTrain = categorical(target_value_for_training);

XTest = test_data;
YTest = categorical(target_value_for_validation);

%% Set parameters
numObservations = numel(train_data);
numFeatures = 32;
numHiddenUnits = 1000;
numClasses = 2;
numOfDataPointsPerSample = 255;
maxEpochs = 1000;

%% Define network architecture of the Convolutional Neural Network
layers = [
    imageInputLayer([numOfDataPointsPerSample numFeatures 1])
    convolution2dLayer(4,16,'Padding',1)
    batchNormalizationLayer
    reluLayer
    maxPooling2dLayer(2,'Stride',2)
    convolution2dLayer(3,32,'Padding',1)
    batchNormalizationLayer
    reluLayer
    maxPooling2dLayer(2,'Stride',2)
    convolution2dLayer(3,64,'Padding',1)
```

```
    batchNormalizationLayer
    reluLayer
    fullyConnectedLayer(numClasses)
    softmaxLayer
    classificationLayer];

%% Set training options
options = trainingOptions('sgdm',...
    'MaxEpochs',maxEpochs, ...
    'Verbose',false,...
    'Plots','training-progress');

%% Train CNN
net = trainNetwork(XTrain, YTrain, layers, options);

%% Classify test data
YPred = classify(net,XTest);

%% Calculate prediction accuracy
acc = sum(YPred == YTest)./numel(YTest);
```

Matlab source code of the Long-Short Term Memory Recurrent Neural Network for movement intention prediction used in the comparative analysis

```
%% Load spike sequences for training and validation
train_data = spike_state_for_training;
test_data = spike_state_for_validation;
X = train_data;
Y = categorical(target_value_for_training);
XTest = test_data;
YTest = categorical(target_value_for_validation);

%% Set parameters for training
numObservations = numel(train_data);
numFeatures = 32;
numHiddenUnits = 1000;
numClasses = 2;

%% Define network architecture of the Long-Short Term Memory network
layers = [ ...
    sequenceInputLayer(numFeatures)
    lstmLayer(numHiddenUnits,'OutputMode','last')
    fullyConnectedLayer(numClasses)
    softmaxLayer
    classificationLayer];

%% Define training options
maxEpochs = 1000;
miniBatchSize = 27;
shuffle = 'never';
% https://au.mathworks.com/help/deeplearning/ug/classify-sequence-data-using-lstm-networks.
    html
% https://au.mathworks.com/help/deeplearning/ug/long-short-term-memory-networks.html
options = trainingOptions('sgdm', ...
    'MaxEpochs',maxEpochs, ...
    'MiniBatchSize',miniBatchSize, ...
    'Shuffle', shuffle);

%% Train LSTM
net = trainNetwork(X,Y,layers,options);

%% Predict movement intention accuracy
YPred = classify(net,XTest, ...
    'MiniBatchSize',miniBatchSize);
acc = sum(YPred == YTest)./numel(YTest);
```

Matlab source code for determining the statistical significance through One-way ANOVA

```
function statistical_testing
    %% Load results of comparative analysis
    data = csvread('results-comparison-sequencebased.csv');
    %% Perform one way ANOVA
    [~,~,stats] = anova1(data);
    set(findobj(gca,'type','line'),'linew',2)
    xticklabels({'eSPANNet', 'RNN-LSTM', 'SVMr', 'DTr', 'LR', 'CNN'})
    xlabel('Prediction Method')
    ylabel('Mean Correct Rate')

    %% Perform pairwise comparison
    figure
    multcompare(stats);
    set(findobj(gca,'type','line'),'linew',2)
    yticklabels(flip({'eSPANNet', 'RNN-LSTM', 'SVMr', 'DTr', 'LR', 'CNN'}))
    ylabel('Prediction Method')
    xlabel('Mean Correct Rate')
    title('Pair-wise Comparison')
end
```

A.3 Matlab source code segments used for implementing the knowledge representation framework presented in Chapter 7

A.3.1 Matlab source code for extracting the neuron coordinates correspond to different anatomical locations

```
%% Function get_coordinates_hierarchy
% first extracts brain coordinates from a given brain atlas then assigns anatomical labels
% and finally, mapps the EEG channel locations corresponds to the extracted
% coordinates
function get_coordinates_hierarchy
    file_cnt = 1; lobe_id = []; lobe_start_neuron_id = [];
    coordinates_mni_space = []; coordinates_talairach_space = [];
    side_id = []; % 1 = left, 2 = right, 3 = mid
    sidelobe_start_neuron_id = []; cnt = 1;cnt_pre = 0;

    %% Extract coordinates from the Talairach template
    % Read Neuroimaging Data into the Matlab workspace using the SPM
    % toolbox (https://www.fil.ion.ucl.ac.uk/spm/software/spm12/)
    % for each .nii file
    for file_id = 1:file_cnt
        % read the header information for the file
        V=spm_vol(strcat(num2str(file_id), '.nii'));
        % using the header information, read neuroimaging data and
        % import into the current Matlab workspace
        img=spm_read_vols(V);
        lobe_start_neuron_id(file_id, 1) = cnt;
        % Extract coordinates from the loaded image volumes
        % Here the coordinates are extracted at a 1cm3 resolution
        % (distance between the x,y and z coordinates of two adjcent neurons is 1cm).
        % This resolution can be adusted by changing the value of
        % coordinate_resolution varible.
        coordinate_resolution = 10; % resolution of extracted brain template
        for i=1:coordinate_resolution:size(img, 1)
            for j = 1:coordinate_resolution:size(img, 2)
                for k=1:coordinate_resolution:size(img, 3)
                    if(img(i, j, k) > 0)
                        coordinates_mat = [i, j, k, 1];
                        % get mm coordinates
                        coordinates_mat = transpose(coordinates_mat);
                        coordinates_mm = transpose(V.mat *coordinates_mat);
                        coordinates_talairach_space(cnt, :) = coordinates_mm(1, 1:3);
                        % convert Talairach coordinates into MNI
```

```
                        % coordinates for EEG mapping
                        coordinates_mm = tal2mni(coordinates_mm(1, 1:3));
                        coordinates_mni_space(cnt, :) = coordinates_mm(1, 1:3);
                        % get mm coordinates end

                        % Assign labels according to left hemisphere, right
                        % hemisphere and the inter hemispheric area
                        if(coordinates_mni_space(cnt, 1)<0)
                            side_id(cnt, 1) = 1;
                        elseif(coordinates_mni_space(cnt, 1)>0)
                            side_id(cnt, 1) = 2;
                        elseif(coordinates_mni_space(cnt, 1)==0)
                            side_id(cnt, 1) = 3;
                        end
                        lobe_id(cnt, 1) = file_id;
                        cnt = cnt + 1;
                    end
                end
            end
        end

    end
    csvwrite('side_id.csv', side_id);
    fprintf('coordinates cnt %d lobe_id cnt %d lobe_start_neuron_id cnt %d\n', size(
        coordinates_mni_space, 1), size(lobe_id, 1), size(lobe_start_neuron_id, 1));

    csvwrite('lobe_id.csv', lobe_id);
    csvwrite('lobe_start_neuron_id.csv', lobe_start_neuron_id);

    %% Load EEG channel locations for EEG mapping
    % Either use the available EEG mapping coordinates(commented) or
    % use the convert_eeg_channel_locations_to_MNI function to extract
    % and transform EEG channel locations correspond to different
    % coordinate systems, conventions, or EEG caps using the functions
    % provided by the Brainstrome tool (https://neuroimage.usc.edu/brainstorm/Introduction)
    %channel_locations = csvread('eeg_mapping.csv');
    %channel_locations = round(channel_locations);
    [channel_names, channel_locations_mni_space, selected_location_idx] =
        convert_eeg_channel_locations_to_MNI(coordinates_mni_space,
        coordinates_talairach_space); %%plot_electrode_locations();

    % for each channel location - find the closest brain coordinates from
    % the talairach atlas
    channel_locations = channel_locations_mni_space;

    csvwrite('eeg_mapping_mni_space.csv', channel_locations_mni_space);
    csvwrite('brain_coordinates_mni_space.csv', coordinates_mni_space);
    csvwrite('brain_coordinates_talairach_space.csv', coordinates_talairach_space);

    %% get location labels for eeg channel locations
    %brain_coordinates_with_location_labels = csvread('brain_coordinates_with_location_labels
        .csv');
    brain_coordinates_with_location_labels = get_neumarical_labels(coordinates_mni_space);
```

```
87      eeg_channel_with_location_labels = horzcat(channel_locations_mni_space,
            brain_coordinates_with_location_labels(selected_location_idx,4:end));
88      eeg_channel_with_location_labels = round(eeg_channel_with_location_labels);
89      csvwrite('eeg_mapping_with_location_labels.csv', eeg_channel_with_location_labels);
90
91      fileID = fopen('feature_names_eeg.txt','w');
92      fprintf(fileID,'%s\r\n',channel_names{:,1});
93      fclose(fileID);
94  end
```

A.3.2 Matlab source code for map EEG channel locations into the extracted brain coordinates

```
%% This function converts the EEG channel locations into MNI coordinate space
function [channel_names, channel_locations_mni_space, selected_location_idx] =
    convert_eeg_channel_locations_to_MNI(brain_coordinates_mni, brain_coordinates_talairach)
    % In Brainstorm
    % 1. Create a new subject, using the default anatomy
    % 2. Create a condition, right-click on it > Use default EEG cap > Colin27 > 10-20 (19)
    % 3. Right-click on the channel file > Export to Matlab > ChannelMat
    % 4. Right-click on the MRI file > File > Export to Matlab > sMri
    load('ChannelMat.mat'); load('sMri.mat');
    channel_names = {}; channel_locations = [];
    for i=1:65%size(ChannelMat.Channel,1)
        xyz_scs = ChannelMat.Channel(i).Loc';
        xyz_mri = cs_scs2mri(sMri, xyz_scs' .* 1000)';
        xyz_mni = cs_mri2mni(sMri, xyz_mri')' ;%./ 1000;
        xyz_mni(:,1) = xyz_mni(:,1).*(80/100);
        xyz_mni(:,2) = xyz_mni(:,2).*(90/100);
        xyz_mni(:,3) = xyz_mni(:,3).*(70/100);
        channel_locations = vertcat(channel_locations, xyz_mni);
        channel_names = vertcat(channel_names, ChannelMat.Channel(i).Name);
    end
    % Obtain Euclidean distance and select the neuron location with minimum ED
    [channel_locations_mni_space, selected_location_idx] = find_nearest_coordinates(
        channel_locations, brain_coordinates_mni, brain_coordinates_talairach)
end

function [selected_location_mni, selected_location_idx] = find_nearest_coordinates(
    channel_locations, brain_coordinates, brain_coordinates_talairach)
    % for each channel
    selected_location_mni = []; selected_location_idx = [];
    for channel_id = 1:size(channel_locations,1)
       % for eaach brain coordiantes
        dist_all = [];
        for brain_coordinate_id = 1:size(brain_coordinates,1)
           % calculate ED
            v    = brain_coordinates(brain_coordinate_id,:) - channel_locations(channel_id,:);
            dist = sqrt(sum(v .^ 2));
            dist_all = vertcat(dist_all,dist);
        end
       % select brain location which has minimum distance
        [val,idx]= min(dist_all);
        selected_location_mni = vertcat(selected_location_mni,brain_coordinates(idx,:))
        selected_location_idx = vertcat(selected_location_idx,idx)
    end
end
```

A.3.3 Matlab source code for assigning anatomical labels to 3-D brain coordinates

```
%% Source code for assigning anatomical labels to extracted brain coordinates
function coordinate_labels_neumaric = get_neumarical_labels(brain_coordinates_mni)
    %input('if any change to brain_coordinates (i.e change of resolution), then update the
        brain_coordinates_labels.txt first before proceeding further')
    reply = input('any change to brain_coordinates (i.e change of resolution)? [y/n]:','s');
    if strcmp(reply,'y')
      return;
    end

    fileID = fopen('brain_coordinates_labels.txt','r');   % exported file from EEG Lab
        Software
    formatSpec = '%d%d%d %s %s %s %s %s';
    coordinate_labels = textscan(fileID,formatSpec);
    coordinate_labels_neumaric = zeros(size(coordinate_labels{1, 1},1), size(
        coordinate_labels,2));
    coordinate_labels_neumaric(:,1:3)=brain_coordinates_mni(:,1:3);

    % for each level
    for level_id=1:5
        level_labels_text = coordinate_labels(:,3+level_id);
        level_labels_text = level_labels_text{1, 1};
        % load ids of the level
        level_label_id_file = strcat('labels_level', num2str(level_id),'.txt');
        label_id_map = textscan(fopen(level_label_id_file),'%d %s');
        % for each label id
        for label_id=1:size(label_id_map{1, 2},1)
           % find indexes of coordinates of the current label
            current_label_to_check = label_id_map{1, 2}{label_id, 1}  ;
            current_label_neumaric_id = label_id_map{1, 1}(label_id,1)  ;
            brain_coordinates_of_current_level = level_labels_text;
            coordinate_idx_of_label = find(strcmp(current_label_to_check,
                brain_coordinates_of_current_level)==1);
            coordinate_labels_neumaric(coordinate_idx_of_label,3+level_id) =
                current_label_neumaric_id;
        end
    end
    coordinate_labels_neumaric = round(coordinate_labels_neumaric);
    coordinate_labels_neumaric_sorted = [];

    %% sort coordinates according to anatomical labels
    for level_id=4:4
        sorted_coordinates_level1 = sortrows(coordinate_labels_neumaric,level_id);
        % for each label in the current level
        label_id_val =unique(sorted_coordinates_level1(:,level_id));
        for label_id = 1:size(label_id_val,1)
           % find all coordinates belong to the current label
            sorted_coordinates_level2 = sorted_coordinates_level1(sorted_coordinates_level1(:,
                level_id)==label_id_val(label_id,1),:);
            % sort coordinates according to level 2 labels
            sorted_coordinates_level2 = sortrows(sorted_coordinates_level2,level_id+1);
```

```
45            label_id_val_level2 =unique(sorted_coordinates_level2(:,level_id+1));
46            % for each label in level 2
47            for level2_label_id = 1:size(label_id_val_level2,1)
48                 % find all coordinates belong to the current label
49                 sorted_coordinates_level3 = sorted_coordinates_level2(
                        sorted_coordinates_level2(:,level_id+1)==label_id_val_level2(
                        level2_label_id,1),:);
50                 % sort coordinates according to level 3 labels
51                 sorted_coordinates_level3 = sortrows(sorted_coordinates_level3,level_id+2);
52                 % find labels of level 3
53                 label_id_val_level3 =unique(sorted_coordinates_level3(:,level_id+2));
54                 % for each label in level 3
55                 for level3_label_id = 1:size(label_id_val_level3,1)
56                     % find all coordinates belong to the current label
57                     sorted_coordinates_level4 = sorted_coordinates_level3(
                            sorted_coordinates_level3(:,level_id+2)==label_id_val_level3(
                            level3_label_id,1),:);
58                     % sort coordinates according to level 3 labels
59                     sorted_coordinates_level4 = sortrows(sorted_coordinates_level4,level_id
                            +3);
60                     % find labels of level 4
61                     label_id_val_level4 =unique(sorted_coordinates_level4(:,level_id+3));
62                     % for each label in level 4
63                     for level4_label_id = 1:size(label_id_val_level4,1)
64                         % find all coordinates belong to the current label
65                         sorted_coordinates_level5 = sorted_coordinates_level4(
                                sorted_coordinates_level4(:,level_id+3)==label_id_val_level4(
                                level4_label_id,1),:);
66                         % sort coordinates according to level 3 labels
67                         sorted_coordinates_level5 = sortrows(sorted_coordinates_level5,
                                level_id+4);
68                         coordinate_labels_neumaric_sorted = vertcat(
                                coordinate_labels_neumaric_sorted,sorted_coordinates_level5);
69                     end
70                 end
71            end
72        end
73    end
74    csvwrite('brain_coordinates_with_location_labels.csv', coordinate_labels_neumaric);
75    csvwrite('brain_coordinates_with_location_labels_sorted.csv',
          coordinate_labels_neumaric_sorted);
76 end
```

Appendix B

Permission for Reusing Third-party Copyright Materials

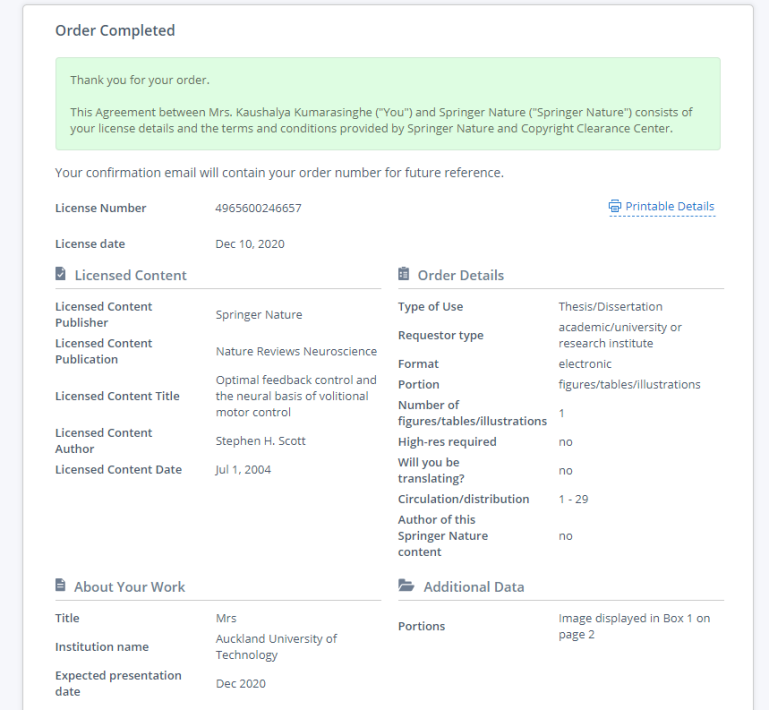

Order Completed

Thank you for your order.

This Agreement between Mrs. Kaushalya Kumarasinghe ("You") and Springer Nature ("Springer Nature") consists of your license details and the terms and conditions provided by Springer Nature and Copyright Clearance Center.

Your confirmation email will contain your order number for future reference.

Printable Details

License Number	4965600246657
License date	Dec 10, 2020

Licensed Content

Licensed Content Publisher	Springer Nature
Licensed Content Publication	Nature Reviews Neuroscience
Licensed Content Title	Optimal feedback control and the neural basis of volitional motor control
Licensed Content Author	Stephen H. Scott
Licensed Content Date	Jul 1, 2004

Order Details

Type of Use	Thesis/Dissertation
Requestor type	academic/university or research institute
Format	electronic
Portion	figures/tables/illustrations
Number of figures/tables/illustrations	1
High-res required	no
Will you be translating?	no
Circulation/distribution	1 - 29
Author of this Springer Nature content	no

About Your Work

Title	Mrs
Institution name	Auckland University of Technology
Expected presentation date	Dec 2020

Additional Data

Portions	Image displayed in Box 1 on page 2

Figure B.1: Copyright permission of (Scott, 2004)